1993

Kinetics Of Growth And Ice Nucleation Activity Of Pseudomonas Syringae

Amarjeet Singh Bassi

KINETICS OF GROWTH AND ICE NUCLEATION ACTIVITY OF *Pseudomonas syringae*

by

Amarjeet Singh Bassi

Department of Chemical and Biochemical Engineering

Submitted in partial fulfilment
of the requirements for the degree of
Doctor of Philosophy

Faculty of Graduate Studies
The University of Western Ontario
London, Ontario
June, 1993

ISBN 0-315-83988-0

ABSTRACT

Pseudomonas syringae causes freezing of supercooled water at temperatures close to 0° C. In this study, the growth kinetics and ice nucleation activity (INA) of the bacterium P. syringae cit 7 were investigated under a variety of culture conditions as well as in batch and continuous bioreactors. The "drop freezing assay" technique used for measurement of INA was first investigated and the effect of several variables on this assay was examined. When P. syringae cit 7 was cultured aerobically in a medium consisting of sucrose, peptone, K_2HPO_4, KH_2PO_4, and $MgSO_4.7H_2O$ (pH 7.0) at 25° C for 48 h, the highest INA was detected at -2.5° C. The INA expressed by the bacteria was independent of cooling rate at cooling rates less than 0.2° C/min. Cell growth at temperatures exceeding 25° C led to a decrease in INA expression of cells. Similarly, cell growth at pH of 8.0 also decreased the INA of the bacteria. Microaerophylic conditions during cell growth also decreased INA in the P. syringae cit 7 bacteria. In a 1 L bioreactor, the optimum cell growth temperature P. syringae cit 7 was found to be 28° C. INA of the cells developed in the lag as well as log phase of growth. The maximum INA in the bioreactor was obtained at the end of the exponential phase of growth at each temperature investigated. In the bioreactor growth at temperatures greater than 25° C led to a significant decrease in INA. Batch cell growth kinetics in the 15 L bioreactor followed a similar trend to the 1 L bioreactor.

Under continuous cultivation in a 1 L bioreactor at 25° C, and pH 7.0, the INA of P. syringae decreased with an increase in dilution rate. A maximum specific

growth rate of 0.08 h^{-1}, and a K_s of 0.21 g/L were obtained under these conditions. Under continuous conditions, cell productivity reached a maximum at a dilution rate of 0.054 h^{-1} and then continuously decreased. A mechanistic, unstructured model describing the batch growth kinetics in the 1 L bioreactor was found to adequately represent the growth and INA in the bioreactor. The results of this investigation can be applied towards large scale production of P. syringae bacteria for snow making applications.

ACKNOWLEDGEMENTS

I express my deepest appreciation and thanks to my Ph.D thesis supervisor, Dr. Argyrios Margaritis, Professor and Chairman, Department of Chemical and Biochemical Engineering for suggestion of the research topic, persistent encouragement and enthusiastic guidance, keen interest and constructive criticism throughout the course of this project and also for reviewing my thesis and for his suggestions for modifications and corrections. His tremendous enthusiasm and insight for biotechnology research and development and his ability to allow independence in others was an inspiring experience.

Financial support for this project came from NSERC Operating Grant #OGP4388 awarded to Dr. A. Margaritis. The support of the Ontario Ministry of Education through the Ontario Graduate Scholarship, the Faculty of Graduate Studies at the University of Western Ontario for the Graduate Entrance Scholarship, and the Graduate Research Fellowship, and the Department of Chemical and Biochemical Engineering at the University of Western Ontario for the Ivan Malek Scholarship in Biochemical Engineering and the E.G.D. Murray Award in Biochemical Engineering is truly appreciated.

Last but not least, to my wonderful wife and daughters, and my parents thank you for your support, love, affection and strong encouragement to pursue my doctoral studies.

TABLE OF CONTENTS

Page

Page

Page

Page

LIST OF TABLES

LIST OF FIGURES

APPENDIX FIGURES

LIST OF APPENDICES

LIST OF PHOTOGRAPHIC PLATES

NOMENCLATURE

Symbol	Description	Units
A°	Arrhenius constant	h^{-1}
B	substrate utilized per g cells	g/g
Bi	Biot number	
ce^2	strain energy due to lattice mismatch	erg
CSTBR	Continuous Stirred Tank Bioreactor	
D	dilution rate	h^{-1}
E	activation energy or temperature characteristic	
E_a	activation energy (cell growth)	cal/g
e	strain	
f	fraction of drops freezing in the temperature range 0° C to - θ° C	
$f(\sigma,\gamma)$	function of interfacial energy and the shape factor	
Δg	activation energy for self diffusion of a water molecule	erg
ΔG^{*}	critical free energy for ice nucleation	erg
ΔG	free energy change due to nucleation	kcal
ΔG_p	free energy change per unit	
	volume between water and ice	$kcal/m^3$
h	Plank's constant	joule.s
h	heat transfer coeffcient	btu/sq. ft/h/° F
INA	ice nucleation activity	ice nuclei/L
IN	ice nucleating	

Symbol	Description	Units
INP	ice nucleation protein	
INS	ice nucleation site	
J	rate of ice nucleation by a suspended particle	s^{-1}
k	Boltzmann constant	joule/° K
$k(\theta)$	fraction of active ice nuclei	
	per unit volume per unit temperature	$L^{-1}.C^{1}$
K	reaction rate	gmol/L.s
K_s	substrate limitation constant	g/L
$K(\theta)$	cumulative ice nuclei	
	concentration	cumulative no. of ice nuclei/L
KBA	King's Medium B agar	
L	latent heat of fusion	$kcal/m^3$
m	cell maintenance coefficient	h^{-1}
m	g dry weight mass per cell	
n	number of cells in a drop of volume V	
n_c	number of water molecules per unit particle surface area	
$\bar{n}(\theta)$	average fraction of ice nuclei active at a temperature θ	
N_0	initial total number of drops	
N_θ	number of drops unfrozen at time θ	

Symbol	Description	Units
dN	fraction of drops frozen in interval dθ	
ΔN	finite number of drops freezing	
P(1,2...)	probability of finding one or more ice nuclei active in a given drop	
P(dθ)	probability of freezing of one drop containing ice nuclei	
P(y)	probability of finding y ice nuclei active in a given drop	
P	ice nuclei concentration	ice nuclei/L
PI	phosphatidylinositol	
q_x	volumetric bioreactor cell productivity	g DW cell/L/h
q_p	specific INA productivity	ice nuclei/g DW cell/h
q_v	volumetric bioreactor INA productivity	ice nuclei/L/h
R	gas constant	1.987 cal/g • K
r	radius of a spherical ice particle formed during nucleation	m
r^*	critical radius of spherical particle for nucleation	m
S	limiting substrate (sucrose) concentration	g/L
SPM	sucrose peptone medium	
SSQ	sum of squares	
t	growth time	h
T	nucleation temperature	• C
T_{sat}	saturation freezing temperature at x_{sat}	• C
T_E	freezing point	• C

Symbol	Description	Units
T_{het}	heterogeneous nucleation temperature	°C
ΔT	degree of supercooling	°C
V	drop volume	mL
X	cell concentration	g cell DW/L
X_{exp}	experimental values of cell concentration	g cell DW/L
X_f	final cell concentration	g cell DW/L
X_{sm}	simulated values of cell concentration	g cell DW/L
x_{sat}	saturation cell concentration	no. of viable cells/mL
y	number of ice nucleation sites of the same activity in a drop	
$Y_{x/s}$	cell yield coefficient, g cell DW formed per g substrate consumed	
$Y_{p/x}$	product formed per g cells formed	g/g
$Y_{p/s}$	product formed per g substrate consumed per g of substrate consumed	g/g
$Y'_{p/x}$	ice nuclei yield coefficient used in modelling	ice nuclei/g cell DW
z	average fraction of ice nuclei active at a temperature θ	

Greek letters

γ_i	number of ice nuclei per cell	
η	experimentally measured ice nuclei per g cell DW	

Symbol	Description	Units
η_{max}	maximum INA in the 1 L bioreactor	ice nuclei/g cell DW
θ	temperature	°C
$d\theta$	infinitesimal temperature interval	°C
$\Delta\theta$	finite temperature interval	°C
θ_{th}	threshold temperature at which one or more drops freeze	°C
θ_1	temperature at which all drops of test sample froze	°C
μ	specific growth rate of cells	h^{-1}
μ_{max}	maximum specific growth rate	h^{-1}
σ	interfacial energy per unit area	$kcal/m^2$

Subscripts

exp	experimental
sm	simulated
max	maximum
1,2,3	different products, e.g., ice nucleation protein, CO_2 etc.

CHAPTER 1

INTRODUCTION

"Supercooling" is the process by which water can be cooled below its freezing point (0° C) and still remains a liquid. The introduction of an "ice nucleus" into the supercooled state of water, however, triggers the rapid chain reaction of ice formation.

Of major concern to farmers and agricultural scientists is ice nucleation on the surface of plants. Frost damage has been a leading hazard to agricultural production throughout the world. As early as 1954 (Lucas, 1954) it was suggested that atmospheric nuclei were the source of ice nucleation on plants. Although the atmosphere contains abundant ice nuclei which are active at -20° C, the number of airborne ice nuclei active at -5° C or warmer were found to be very low (Bigg and Miles, 1964). Most common sources of ice nuclei, e.g, dust particles, mineral clays, organic crystals could also be discounted as these were active at temperatures below -10° C.

Soulage (1957) was among the first to suggest that bacteria could serve as ice nucleating agents. Indeed, it was soon discovered that the principal cause of frost damage to plants was the presence of highly potent ice nucleation bacteria which inhabited the leaf surface and possessed ice nucleation activity (INA) in the range of 0 to -5° C. These bacteria were identified as certain, aerobic, Gram negative strains belonging to the genera Pseudomonas, Erwinia, or Xanthomonas. Recently, the phenomenon of bacterial ice nucleation has been extensively

reviewed by a number of researchers (Margaritis and Bassi, 1991; Lindow, 1983; Hirano, 1987; Warren, 1987; Wolber and Warren, 1989).

This "negative" property of bacterial ice nucleation which is responsible for frost damage, is being exploited in beneficial ways in important, commercial uses. Currently, bacterial ice nuclei play a key role in the production of "artificial" snow in ski-hills and skating rinks. The microorganism currently utilized in this application is Pseudomonas syringae. Other potential uses include the production and texturing of frozen foods, immuno-assays, and cloud seeding. In addition, the prevention of ice nucleation protects crops and fruit trees from frost damage.

The latter has been achieved by displacing the natural, ice nucleating bacterial populations from leaf surfaces by recombinant DNA "ice-minus" bacteria. The ice-minus bacteria are exactly identical to the former, except in one respect. They lack the gene responsible for ice nucleation. This technique has been successfully applied in the U.S. and elsewhere to prevent frost damage to crops and fruit trees.

Two interesting questions surround this unique phenomenon of bacterial ice nucleation:

(a) What is the genetic basis of bacterial ice nucleation? Information available at this time reveals that the ice nucleation phenotype is provided by one structural gene in the ice nucleation active (INA) bacteria. The product of this gene expression is a membrane bound protein, which interacts with membrane lipids to provide an active site ("ice nucleus") for ice formation.

(b) How can the ice nucleation phenotype of the INA bacteria be manipulated?

Being a protein, the INA phenotype is a function of conditions existing during growth of the cells, e.g., pH, temperature, medium composition etc.

In commercial and potential applications mentioned above, sound engineering principles and practices are needed in order to make the production of bacterial ice nuclei economically viable and attractive. The focus of much current research has been the biochemistry of the ice nucleation site, i.e., the size, structure, exact location of the protein and its in vitro isolation. While these areas are of fundamental importance, very little research has been directed at optimizing environmental conditions to produce efficient bacterial ice nuclei.

Most research of this nature has been limited to a few commercial companies and is therefore of a proprietary nature. A large amount of work still remains to be done towards scaling up production of bacterial ice nuclei.

A systematic perusal of the literature revealed that very little information is available on the kinetics of growth and INA of Pseudomonas syringae. The main objective of this thesis research was to carry out original, fundamental studies on the factors which control the kinetics of cell growth and INA of P. syringae.

Shake-flask experiments as well as batch and continuous studies in a 1 L bioreactor and batch growth in a 15 L bioreactor were carried out. A mechanistic, unstructured mathematical model was proposed and tested against the available data to describe the growth and INA kinetics of P.syringae cit 7 cells.

The information obtained in this study, including kinetic models and kinetic parameters may be useful, not only in bioreactor and process design of ice nucleation bacteria, but also in scale-up and control of processes employing them.

CHAPTER 2

REVIEW OF LITERATURE

2.1. Structure of Ice and Water

The water molecule has a structure which consists of extensively hydrogen bonded networks in which a tetrahedral coordination predominates (Figure 2.1). In water each oxygen atom is surrounded on an average by four other oxygen atoms, placed at, or close to, the vertices of a regular tetrahedron (as seen in Figure 2.1) with a hydrogen atom placed along each O-O axis. In the case of the solid, ice, this arrangement is regular with O-O distances of 0.275 nm and H-O-H angles corresponding to those of a regular tetrahedron, 109° 28'. In liquid water these distances and angles suffer a considerable distortion. However, previous studies suggest that the essentially 4-coordinated molecular distribution, characteristic of ice, is maintained in the liquid (Franks, 1985). The molecules of the liquid are subject to rapid diffusional motion, so that the term "structure" for liquid water means a time-averaged distribution of molecules.

2.2 The Process of Freezing

The equilibrium freezing point of water is 0° C (273.16 K); it is the temperature at which liquid water and ice coexist in equilibrium at atmospheric pressure and is denoted by T_f. In practice, when liquid water is cooled it does not spontaneously freeze at T_f, but at some lower temperature. Undercooling

Figure 2.1. Crystal Structure of Ice. The regular hexagonal lattice of oxygen atoms (dark circles) is shown with one hydrogen atom (light circle) lying on each O-O axis. Each oxygen atom is thus hydrogen bonded to four other oxygen atoms, placed at the vertices of a regular tetrahedron (Franks, 1985).

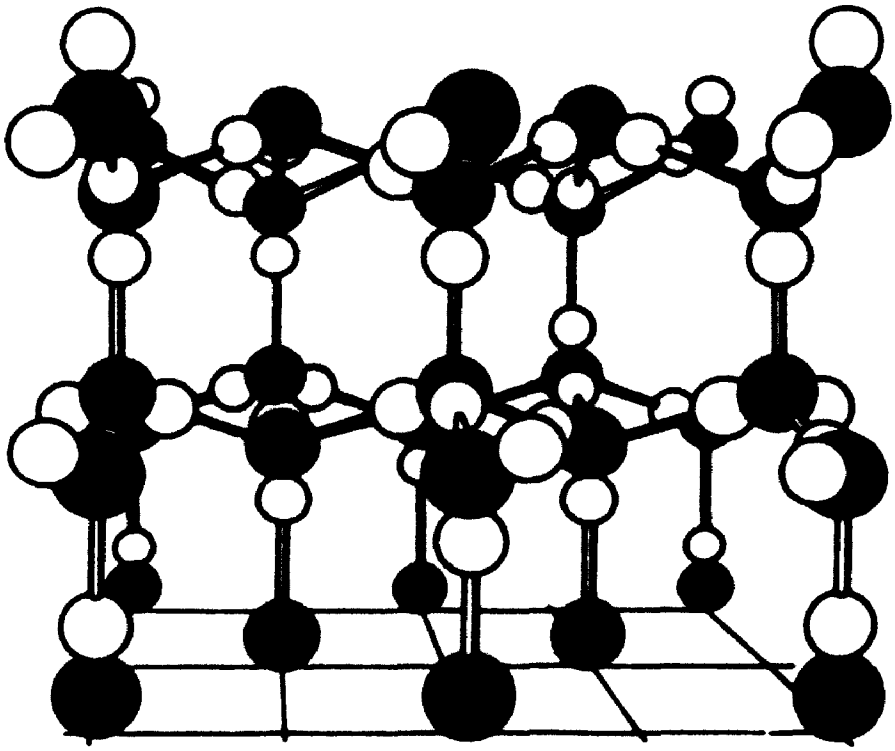

(or supercooling) is a common feature of liquids and is of great relevance to the phenomenon of biolcgical freeze resistance.

Nucleation can be defined as a process which generates within a metastable mother phase (e.g., the supercooled state of water), the initial fragments of a more stable phase. These fragments then spontaneously develop into gross fragments and the phase change is then complete. An effective nucleus consists of a group of molecules which can be 'recognized' by other, diffusing molecules as a structure resembling that of the solid phase. Such clusters of molecules can arise spontaneously by random density fluctuations within the body of the liquid; they have a finite lifetime which depends on the self-diffusion rate and eventually they dissociate.

On the other hand, such nuclei may occur in the form of heterogeneous impurities, such as dust particles or microcrystallites, which are able to absorb water molecules and thus facilitate the nucleation process.

2.2.1 Homogeneous Nucleation

Nucleation which takes place in pure systems (i.e. pure ice and water) is referred to as homogeneous nucleation. Only extremely pure water nucleates in this manner but the probability is zero that pure water will nucleate homogeneously at 0° C (Fletcher, 1970). As tiny droplets of pure water (less than 1 μm in diameter) are decreased in temperature, the probability of freezing approaches 1 at -41° C. A temperature of -41° C is usually accepted as a limit to which water can be supercooled (Fletcher, 1970).

For pure water, the energy barrier which exists for nucleation to occur can be explained on the basis of free energy changes that accompany nucleation (Lamer, 1952) as in equation 2.1:

$$\Delta G = \frac{4}{3} \pi r^3 \Delta G_p + 4 \pi r^2 \sigma \qquad (2.1)$$

where:

ΔG = Free energy change due to nucleation resulting in the formation of a spherical ice particle of radius, r, (kcal)

ΔG_p = Free energy change per unit volume between liquid water and solid ice during the formation of a spherical ice particle of radius r, ($kcal/m^3$)

σ = The interfacial energy per unit area between the two phases of water and ice at the given temperature, ($kcal/m^2$)

r = Radius of a spherical ice particle formed during nucleation (m)

The first term on the right is always negative and becomes increasingly so as r increases. This term relates to free energy release during hydrogen bond formation during the association of water molecules into an ordered

structure. The second term is always positive as r increases. This term relates to energy required to form the ice-water interface. When r is small, the surface energy term predominates. However, as r increases, the first term becomes more significant and a plot of ΔG versus r will pass through a maximum (Fennema et al., 1973) (Figure 2.2). This maximum represents the free energy of activation for nucleation at the temperature under consideration. A particle with a size corresponding to the maximum ΔG is said to have a critical radius, r^*, because any radius greater or smaller than r^* would lead to a decrease in free energy. Particles less than r^* will disintegrate while particles greater than r^* will grow. The critical radius is dependent on the degree of supercooling. The magnitude of the critical radius, r^*, is influenced by the interfacial free energy per unit area, σ, the solid liquid equilibrium temperature T_E, the latent heat of fusion, L, and the degree of supercooling, $\Delta T = (T_E - T)$ where T is the system temperature. The above discussion implies a pure water-ice system.

For homogeneous nucleation, the critical radius, r^*, is given by equation 2.2, assuming an incompressible, spherical solid and ΔH and ΔS independent of temperature (Fennema et al., 1973).

$$r^* = \frac{2 \sigma T_E}{L \Delta T} \qquad (2.2)$$

where:

r^* = critical radius of spherical particle (m)

Figure 2.2. Change in Free Energy During Nucleation (r^* = critical radius) (Fennema et al., (1973)

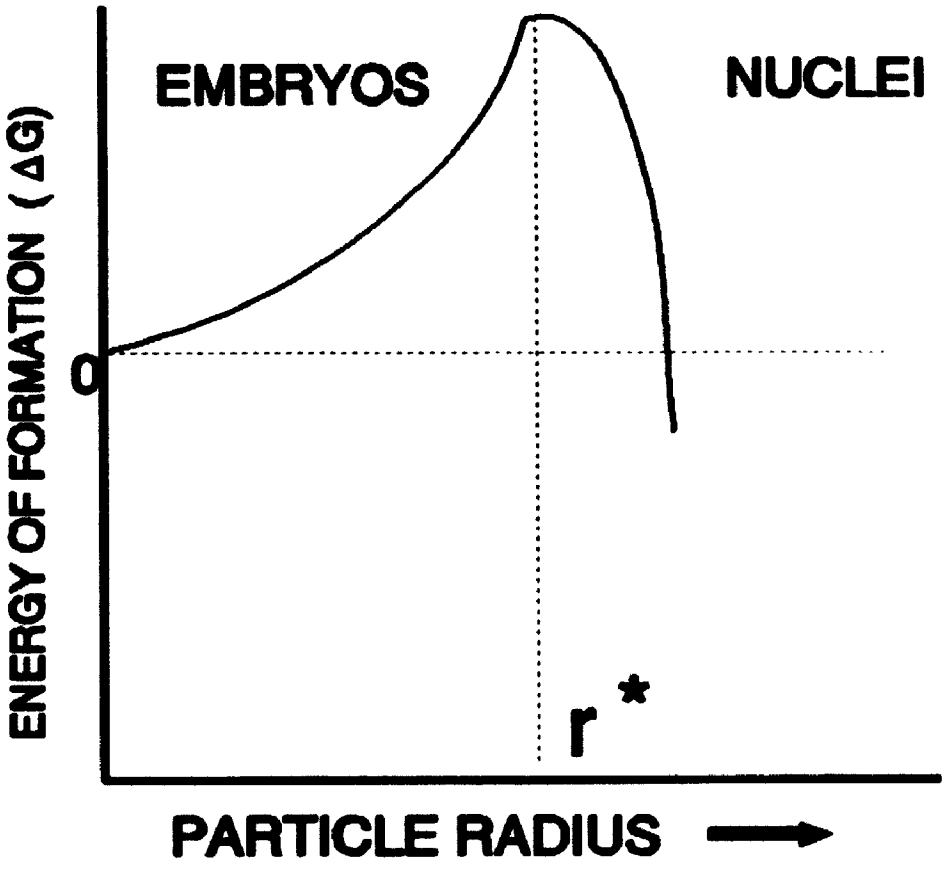
EMBRYOS
NUCLEI
ENERGY OF FORMATION (ΔG)
0
r *
PARTICLE RADIUS

L = latent heat of fusion (kcal/m^3)

ΔT = degree of supercooling (° C)

T_E = freezing point (° C)

Since σ, T_E and L are constant at constant pressure and do not vary greatly with temperature, then r^* becomes inversely proportional to the degree of supercooling, ΔT, as shown by equation 2.3:

$$r^* \propto \frac{1}{\Delta T} \qquad (2.3)$$

2.2.2 Heterogeneous Nucleation

This type of nucleation occurs in impure water when molecules of water aggregate in a crystalline arrangement on nucleating agents such as suspended foreign bodies, surface films or walls of containers (Turnbull and Vonnegut, 1952). This kind of nucleation is the predominant form of ice nucleation. Heterogeneous nucleation may involve fewer water molecules and a lower activation energy than homogeneous nucleation but the phenomenon is not well understood nor mathematically well characterized. The indications are that the heterogenous nucleation temperature, T_{het}, depends on the surface characteristics and dimensions of the nucleating particle in question (Fletcher, 1970).

Studies have been conducted which show that nucleating agents for ice formation are diverse and widespread. They include substances such as silver

iodide, α-phenazine, phloroglucinol dihydrate, metaldehyde, various silicates of clay and mica (kaolinite, covellite, magnetite), steroids (cholesterol), amino acids, proteins, lectins, bacteria and lichen (Fukuta and Mason, 1963; Head, 1961; Garten and Head, 1965; Mason, 1961; Head, 1962; Bigg, 1953; Power and Power, 1970; Barthakur and Maybank, 1963; Kozloff et al., 1983). Table 2.1 lists natural and artificial ice nucleating agents ranked in decreasing order of threshold temperature, i.e., the temperature at which the nuclei are most active in ice nucleation. The table lists both naturally occurring atmospheric dusts and some crystalline substances, all of which are effective ice nuclei between 0° C and -14° C.

Using this information the various ice nuclei may be grouped into specific threshold temperature ranges over which they may be most active. Such a classification is presented in Table 2.2. From Table 2.2, it can be seen that INA bacteria are amongst the most active ice nuclei known with threshold temperatures which compare with crystalline particles, e.g., silver iodide.

The development of new and better ice nucleating agents is an on-going field of research. Recently, a new ice nucleating aerosol has been developed which is a mixture of AgI and BiI_3 and provides closest possible match to the ice lattice (Scott, 1988). However, the threshold temperature at which this aerosol is active in nucleating ice formation has not been reported.

2.2.3 Theoretical Modelling of Heterogeneous Ice Nucleation

In the case of heterogeneous nucleation of ice, the nucleation capability

Table 2.1. Natural and Artificial Ice Nucleating Agents (Head, 1962)

Substance	Crystal Form	Threshold Temperature, θ_{th} (° C)
Ice crystal	Hexagonal	0
Silver Iodide	Hexagonal	-4
Covellite	Hexagonal	-5
Lead Iodide	Hexagonal	-6
Cupric Sulfide	Hexagonal	-6
BetaTridymite	Hexagonal	-7
Magnetite	Cubic	-8
Mercuric Iodide	Tetragonal	-8
Silver Sulfide	Monoclinic	-8
Kaolinite	Triclinic	-9
Ammonium fluoride	Hexagonal	-9
Hematite	Hexagonal	-10
Silver Oxide	Cubic	-11
Cadmium Iodide	Hexagonal	-12
Vanadium Pentoxide	OrthoRhombic	-14
Iodine	OrthoRhombic	-14

Threshold temperature: the temperature at which the nuclei effect the first onset of freezing

TABLE 2.2: Classification of Ice Nuclei and Ice Nucleation Mechanism Based on Temperature Range of Most Activity

Ice Nucleation Agent	Mechanism of Ice Nucleation	Threshold Temperature, θ_{th}, (° C)	Reference
Crystalline particles, lichen, ice nucleating bacteria	Heterogeneous	-2 to -10	Mason (1961) Kozloff et al. (1983) Kieft (1988)
Dust or pollen	Heterogeneous	-10 to -15	Lindow (1983a)
Mineral particles of meteoric origin	Heterogeneous	-15 or lower	Lindow (1983a)
None	Homogeneous	-35 or lower	Fletcher (1970)

of an ice nucleating site depends on lattice match and symmetry, water solubility, size of the nucleating site, polarizability, hydrophobicity, surface charge, and the number and strength of surface sites capable of absorbing water molecules. These include sites provided by foreign atoms or ions behaving like hydrophilic centers on a relatively hydrophobic surface. Silver iodide, having a low water solubility and a crystal lattice that closely resembles that of ice, has an unexpectedly poor ice nucleating ability when in the highly purified state compared to silver iodide containing impurity atoms. When a water insoluble particle is submerged in water, it is surrounded by a large number of water molecules. If the surface of the submerged solid particle is generally hydrophobic, but contains hydrophilic sites, water molecules are preferentially adsorbed at these sites (Thangaraj et al., 1988). In this case the hydrophilic sites may also be provided by foreign atoms or ions on the surface of the immersed particle. Thangaraj and co-workers (1988) have presented a model to calculate the critical free energy needed to form an ice nucleus and the nucleation rate. Thus the authors reported that the critical free energy required for the formation of an ice nucleus could be written as in equation 2.4 below:

$$\Delta G^{*} = \frac{16\pi}{3} \frac{f(\sigma,\gamma)}{(\Delta G_{v} + c\sigma^{2})^{2}} \qquad (2.4)$$

where $f(\sigma, \gamma)$ is a function of interfacial free energies and the shape of the

embryo, e is the strain, and ce^2 is the strain energy due to lattice mismatch, where c is a constant depending on the linear elastic constants of ice.

The rate at which a particle suspended in water nucleates can be written as in equation 2.5.

$$J = \frac{kT}{h} n_c 4\pi r^2 \exp(\frac{-\Delta g}{kT}) \exp(\frac{-\Delta G^*}{kT}) \qquad (2.5)$$

where k and h are Boltzmann and Plank's constants, T, the nucleation temperature, r is the radius of the nucleating particle suspended in water, and n_c the number of water molecules in contact with a unit area of the surface of the particle. Δg is the activation energy for self-diffusion in liquid or more precisely across the liquid-solid boundary. ΔG^* is the critical free energy from equation 2.4. The preexponential term in 2.5 takes care of the size of the nucleating particle, the number of water molecules on the surface and the frequency per unit area with which the molecules of the right type jump into the surface of the cluster. However, this expression in equation 2.5 should be modified to include the number of active sites capable of adsorbing water molecules. This modified form is shown in equation 2.6.

$$J' = \frac{kT}{h} 4\pi r^2 n_c n' \exp(\frac{\Delta g}{kT}) \exp(-\frac{\Delta G^*}{kT}) \qquad (2.6)$$

where n' is the number of sites which nucleate corresponding to a critical free

energy ΔG^*. The factor n' depends on the total number of active sites available, which can be the total number of ice nucleation protein molecules on the surface of the bacterium or the number of foreign atoms on the surface of the nucleating particle,e.g., silver iodide. Such theoretical considerations have been applied by Thangaraj et al. (1988) to ice nucleation by silver iodide and silver bromide.

Burke and Lindow (1990) have used heterogeneous ice nucleation theory to calculate the ice nucleation probability of bacterial ice nuclei at various supercooling temperatures assuming various surface properties, shapes, and sizes of heterogeneous nucleating particles. These were then compared with experimentally measured sizes of the bacterial ice nucleators of P. syringae and other INA bacteria. Good fit was obtained for particles (spheres, cylinders, and disks) which had surface tension identical to that of ice.

2.3 Occurrence and Properties of Psuedomonas syringae

P. syringae was first isolated as a bacterial pathogen of lilac (Syringa vulgaris) in 1902 and it has since been isolated from several plant species (Hirano et al., 1982). Included are patho-types pathogenic to citrus, beans, cherry, pear, almond, raspberry, pea, soyabean, blackberry, apple, tobacco, tomato, delphinium, passion flower, ash, sunflower, apricots, onion, cucumber, wheat, oat, corn, sorghum, and many others. The Eigth Edition of Bergey's Manual lists all phytopathogenic, oxidase negative, fluorescent pseudomonads under the species name P. syringae. This bacterium is Gram negative, rod

shaped, and motile (with one or two polar flagella) (Breed et al., 1948). The bacterium is a facultative aerobe, and produces fluorescent pigments on media low in iron (Breed et al., 1948). Energy yielding pathways in the bacterium are respiratory and not fermentative. P. syringae has 41 pathovars or subgroups, all pathovars do not possess ice nucleating activity (Dye et al., 1980). Various properties of this bacterium are summarized in Table 2.3.

P. syringae is usually differentiated from other pseudomonads by its negative reaction in the oxidase and arginine tests (Breed et al., 1948). Another identifying property of this bacterium is the production of a hypersensitive response on tobacco (Atkinson and Bakur, 1987). P. syringae has been found to be widely distributed throughout the world. Diseases caused by pathovars of P. syringae include foliar blight on snap beans, tomato, and wheat, blossom blight on pear, and canker formation on olive trees. Its toxic actions are attributed to several reasons it produces a plant toxin called syringomycin (Seemüller and Arnold, 1983), non-toxic to humans, and also produces lipases and ammonia. All the plant pathogenic actions caused by this bacterium have not been identified. P. syringae is also widespread on healthy host and non-host plants, surviving as an epiphyte e.g., on peach, almond, orchard weeds, apricot, and olives (Lindow et al., 1978). The widespread occurrence of P. syringae as an epiphyte has obvious implications for potential sources of primary inoculum for infection of host plants. This bacterium has been widely implicated in frost injury and infection to host plants (Lindow et al., 1978). Thus the reason for its ubiquity as an epiphyte.

Table 2.3. Summary of Phenotypic Characteristics of *P. syringae*

Phenotypic Characteristics of *P. syringae* bacteria
Phytopathogenic
Oxidase negative
Arginine negative
Production of fluorescent pigment
Gram negative
Rod shaped
Motile
One or two polar flagella
Facultative aerobe
Respiratory pathways (TCA cycle)
41 pathovars or sub-groups
Produces hypersensitive response on tobacco

P. syringae lives on the leaf surface and also invades tissues of the plant. A recent study has found that the motility of this bacterium confers on it epiphytic fitness advantage (Haefele and Lindow, 1987). This bacterium has also been found to be present in aerosols (Lindemann et al., 1982) and seeds (Neegaard, 1977). The bacterium can grow rapidly with 30 to 150 fold increase in 24 h (Hirano, 1987).

2.4 Bacterial Ice Nucleation

Ice nucleation initiated by microorganisms was first reported by Schnell and Vali (1973) when they discovered that decaying tree leaves were an important source of ice nucleating particles. Later Maki et al. (1974) isolated Pseudomonas syringae bacteria from decayed alder leaves. These isolates were found to be highly active in initiating ice formation at temperatures in the range of -2 to -5° C (Table 2.2). Since those findings, several strains of this bacterium and of at least five other bacteria have been identified as efficient ice nucleating agents. Strains of Erwinia herbicola (Kozloff et al., 1983), Erwinia ananas (Arai and Watanabe, 1986), Pseudomonas fluorescens (Maki and Willoughby, 1978), Pseudomonas viridiflava (Lindow et al., 1983), Xanthomonas campestris (Kim et al., 1987), and recombinant Escherchia coli (Orser et al., 1985) have been shown to possess ice nucleating activity. The question as to why bacteria possess INA is still open to speculation. The INA phenotype may confer an advantage on bacteria which express it; e.g., since these bacteria are epiphytic, ice nucleation and subsequent frost damage to the leaf surface on

which these bacteria reside may allow access to nutrients within the leaf tissues. It has also been suggested that the bacteria may participate in rain precipitation (Sands et al., 1987; Hirano, 1987).

Yankofsky et al., (1981) have compared INA bacteria from different parts of the world. Various strains of P. syringae, P. fluorescens were obtained from various North American habitats or Western Asia. Differences were found in terms of the highest temperature at which a given species could act and the stability of ice nuclei. They found that whole cells were more efficient than fragmented cells in expressing ice nucleation. Thus whole cells of the most efficient strain produced nuclei active at temperatures ranging from -2° C to -10° C, whereas fragments from these cells exhibited activity only at -8° C to -10° C. They found that the frequency of active cells in a population was low (1 in 10^4 cells at -2° C to -4° C) for all cases considered. They also found that the bacterial INA was a function of the cell's physiological state.

It has been convincingly demonstrated that the freezing nuclei of fluorescent INA bacteria are located on cells (Maki et al., 1974; Maki and Willoughby, 1978). At that time, the nature of the substance(s) responsible for ice nucleation activity (INA) in these bacteria was not known. However, nucleation activity was evidently localized on the outer membrane (Sprang and Lindow, 1981). The material nucleating at -5° C was found to be unstable and activity was lost following treatment of cells with respiratory inhibitors, sonication, solubilization with detergents such as SDS, phage lysis, or at extremes of pH (greater than pH 9.0 or less than pH 4.0) (Kozloff et al., 1983;

Lindow et al., 1978; Maki et al., 1974; Yankofsky et al., 1981). After these findings, extensive work followed on the biochemical basis of ice nucleation, which is discussed below.

2.5 Molecular Biology of the Ice Nucleation Site

In this section the molecular biological aspects of the bacterial ice nucleation site are reviewed. Different factors involved in the make-up of the ice nucleation activity of bacteria are also discussed.

2.5.1 The Ice Nucleation Genotype and its Translational Product

Membrane isolates from both P. syringae and E. herbicola were found to contain protease sensitive nucleating material (Sprang and Lindow, 1981). The nucleating material was also found susceptible to protein denaturing agents, including sulfhydryl reagents (Kozloff et al., 1983) which suggested that a protein was involved. Borate compounds and certain lectins, which are known to react with carbohydrates, also reduced the ice nucleation activity of both P. syringae and E. herbicola. Thus both protein and carbohydrate were implicated. Research into the white flounder antifreeze compound, the antithesis of ice nucleation, found it to be a glycoprotein with a very regular primary sequence (Feeney and Yeh, 1978).

Orser et al. (1983, 1984, 1985) devised a strategy to identify the ice-nucleation genes from P. syringae, E. herbicola. This involved the isolation of deficient (ice-minus) mutants and to screen cloned sequences for

complementation of the mutations. The gene coding for the ice nucleation protein in P. syringae, E. herbicola, and P. fluorescens was then identified as a small region on the chromosomal DNA of the bacteria (Orser et al., 1983, 1984; Corroto et al., 1986). The deletion of this gene completely abolished ice nucleation activity (Warren et al., 1987). The genes of the various bacteria were purified after cloning and overexpression in E. coli. The cloned genes were found to impart ice nucleation activity to the host E. coli and the level of activity in the transformant was found to correlate with the level of protein expression (Orser et al., 1984). A 4.5 kb fragment of DNA from P. syringae and a 5.7 kb fragment from E. herbicola conferred the INA phenotype on E. coli.

Green and Warren (1985) determined the nucleotide sequence of the ice nucleation genes of P. syringae and P. fluorescens. In each case this sequence (termed inaZ in P. syringae or inaW in P. fluorescens) was found to contain a single long open reading frame which indicated a single gene (Warren et al., 1986). The inaZ gene from P. syringae was substantially similar to the inaW gene from P. fluorescens. Orser et al.(1985) have shown using Southern blots that the ice nucleation gene from P.syringae has homology to the INA conferring region in E. herbicola.

The homology obtained between the inaZ and inaW genes indicates that the retention of similarities is due to the selection of a common function. A striking feature observed in these genes was a complex periodicity in their central regions. Each gene had about 120 contiguous repeats of an eight codon motif. A 16 codon periodicity was further superimposed throughout the

region of the eight codon periodicity. Another 48 codon periodicity was superimposed on the first two orders in two regions in each gene. A noticeable degree of sequence reiteration with a 24 base periodicity was observed in this reading frame. The consensus repeat sequence noted was GCCGGTTATGGCAGCACGCTGACC.

The authors found that the predicted translational product contained 1200 amino acids with a molecular weight of approximately 120 kD. Exactly 122 contiguous repeats of the consensus octapeptide:- Ala-Gly-Tyr-Gly-Ser-Thr-Leu-Thr could be recognized in it.

A partial sequence of the protein of E. herbicola has also been predicted by nucleotide sequencing of the corresponding genes (Phelps, 1987). The nucleotide sequence for the ice nucleation gene, inaX, from the bacterium X. campestris pv. translucens has also been determined (Zhao and Orser, 1990). The ice nucleation gene sequence from P. viridiflava, and E. ananas have not yet been reported.

The various ice nucleation proteins from the different INA bacteria have closely related structures. This has been determined based on two strong pieces of evidence: (i) the genes can be transferred to E. coli and do not lose the ice nucleation phenotype; and (ii) antibodies raised against the inaW protein, i.e., the product of the ice nucleating gene of P. fluorescens can recognize the inaZ protein from P. syringae after protein isolation from an E. coli clone (Deninger et al., 1988). Thus it has been concluded that the genes are homologous and their action is host independent.

Wolber and Warren (1989) have described the primary structure of the bacterial ice nucleation proteins. The majority of the amino acid sequence of each ice nucleating protein (81%) was found to be a complex repeating domain which could be further subdivided into three regions (Figure 2.3). The first two regions repeat with a high fidelity with period of 48 residues. Each of these 48-mer units in the first two repeating regions consisted of three 16-mer units with medium-fidelity repeats. The 16-mer units were themselves composed of two repeating 8-mer units of low fidelity repeats, which means that only two positions out of eight were strongly conserved. The third repeating section only consisted of 8-mer repeating units.

While the majority of the ice nucleation protein was a central repeating region as described above, 15% of the sequence was a unique N-terminal domain and 4% formed a C-terminal domain unique to each protein from the three different bacteria. The N-terminal domain was found to be relatively hydrophobic which would indicate membrane localization while the C-terminal domain was relatively hydrophilic.

Deletion mutations of the inaZ gene, in which the remaining sequences were in frame were used to probe the function of the ice-nucleation protein (Green et al., 1988). Removal of the N-terminal unique domain caused the ice nucleation activity of the P. syringae bacteria to decrease with threshold temperatures lower than -5° C. Removal of the C-terminal unique domain caused a total loss of ice nucleation activity while successive deletions in the repeating domain caused a corresponding decrease in ice nucleation tempera-

Figure 2.3. A Simplified Representation of the Primary Structure of the Ice Nucleation Protein. The top shows that the protein consists of N-unique and C-unique terminals and a central repeating region. The first two sections of the central repeating region have three orders of periodicity as depicted below the cartoon of the entire sequence: a primary repetitive sequence of 8 amino acid residues, superimposed by 16-mer repeats and 48-mer repeats (Adapted from Wolber and Warren, 1989)

First order of periodicity

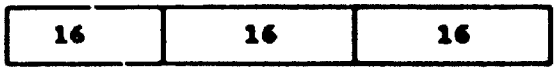

Second order of periodicity

Third order of periodicity

tures.

The secondary structure of the protein is thought to be a ß pleated sheet, punctuated by 5-6 turns per 48 amino acid sequence. The repeated unit is hydrophilic and particularly rich in serine and threonine. Based on this information, Wolber and Warren (1986) have presented structural models of the ice nucleation protein (INP) and suggest that the INP may mimic the ice lattice (Figure 2.4). The INP may provide a template for ice formation. Structural characterization is still too incomplete to supply an adequate working model, due undoubtedly to the complexity and size of the nuclei.

2.5.2 Additional Factors in Bacterial Ice Nucleation

Kozloff et al. (1984) have presented evidence that a lipid phosphatidyl-inositol (PI) is a component of the ice nucleation site. They originally hypothesized the involvement of the PI molecule based on the observation that another carbohydrate, mesoinositol, can form a structure highly compatible with the hexagonal lattice of ice and thus could be the sugar component of the nucleating site. Inositol , in PI, is a relatively rare component of the cell walls of the Gram negative bacteria and has been reported in the cell wall of P. syringae (McElroy, 1992).

PI was shown to cause haemagglutination of the lectins which had previously been shown to inhibit ice nucleation (Kozloff et al., 1984). It is therefore possible that PI may be the target of these lectins. The presence of PI on the surface of these cells was further examined by treating the cells with a

Figure 2.4. Structural Models in which the INA Protein Displays a Symmetry Related to that of Ice. Drawings are not to scale. (A) symmetry of ice illustrated by the spatial arrangement of water molecules (left), the symmetry of this structure (centre), and the way the symmetry becomes extended as more water is added (right); (B) triangular model for INA protein; (C) antiparallel double helix model (Wolber and Warren, (1986)

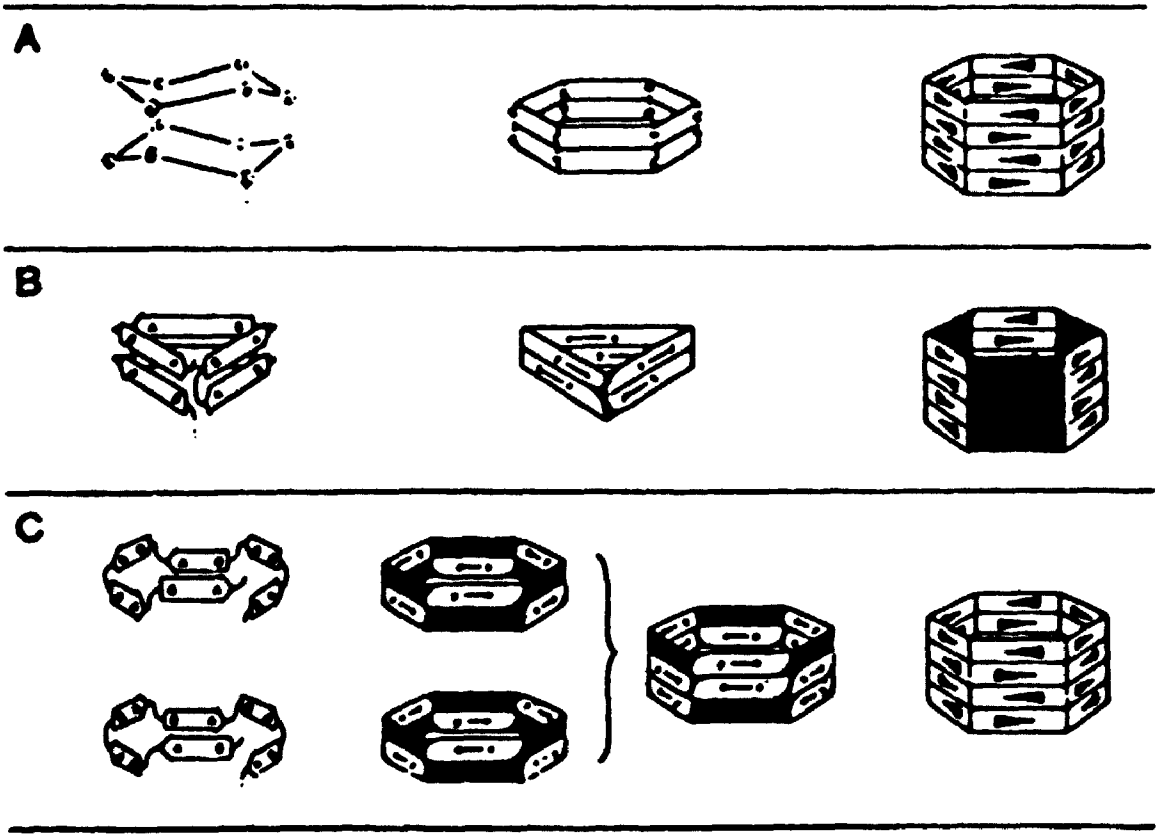
A
B
C

PI-specific hydrolase (a C_{11} lipase). This enzyme was purified by Kozloff and co-workers (1984) from the supernatant of broth cultures of Bacillus cereus (ATCC 10876). The hydrolase treatment inhibited or decreased INA in both P. syringae and E. herbicola.

Govindarajan and Lindow (1984, 1988a) also showed a relationship existed between loss of membrane lipids and corresponding loss in ice nucleation activity. These authors found that the delipidation of partially purified outer membranes of the bacterium by various delipidating agents led to a significant loss in INA. Both phospholipid content and ice nucleation activity of membranes were decreased by a similar fractional amount after treatment with phospholipases, sodium cholate and sodium dodecyl sulfate (SDS). The ice nucleation activity of delipidated outer membranes was restored by reconstitution with various phospholipids in a cholate dialysis procedure. Lipid classes differed in their ability to restore ice nucleation activity to sodium cholate treated outer membranes. These results suggested that a hydrophobic environment produced either by lipids or certain detergent micelles is required for proper assembly and organization of an oligomeric ice protein complex.

Another possible role that has not been investigated at all is the possibility of PI acting as a cell surface anchor for the protein. Low (1989) has reviewed this aspect in terms of the general functional role of glycosyl-phosphatidylinositol (GPI) as a dynamic and versatile anchor for cell surface proteins. The involvement of phosphatidylinositol in attaching proteins to membranes was first suspected when it was observed that a number of cell

surface enzymes could be released from the membrane by treatment with phospatidylinositol-specific phospholipases.

2.5.3 Localization of Bacterial Ice Nucleation Activity

Sprang and Lindow (1981) have shown that ice nuclei were present in cell membranes and found that eighty percent of the ice nuclei were associated with the outer membrane fraction. Phelps et al. (1986) showed that growing cultures of ice nucleating E. herbicola shed ice nuclei into the medium. Evidence indicated that the shed nuclei were associated with membrane vesicles which were shed under the same conditions as the nuclei. The shedding of the membrane vesicles also occurred in "ice minus" (ice gene deletion mutant) strains of E. herbicola.

Lindow et al. (1989) have quantified the ice nucleation activity in different sub-cellular fractions of the P. syringae and in E. coli containing the ice nucleation gene. For both the microorganisms, the ice nuclei were found to be localized in cell envelopes. The ice nucleation activity measured at -9° C in various sub-cellular fractions is shown in Table 2.4. Ice nucleation activity was found in Triton-X-100 insoluble membrane fragments as well as in slowly sedimenting high density membrane fragments. The outer membrane of these Gram negative bacteria had nearly all the ice nucleation activity associated with it. No ice nucleation was detected in any soluble cell fractions.

Table 2.4. The Ice Nucleation Activity in Various Sub-Cellular Fractions of P. syringae Cit 7 (Lindow et al. , 1989)

Cellular Fraction	Ice Nuclei Recovered (X 10^{10}) at -9° C
Starting cell suspension	10.6
Spheroplasts	14.1
Disrupted spheroplasts	13.6
Membrane vesicles and soluble cell contents	10.1
Soluble cell contents	0.001
Total membranes	1.90

2.5.4 Sensitivities of the Bacterial Ice Nucleation Sites

Consistent with the other evidence for the involvement of a protein, proteases cause the loss of INA in cell free preparations from E. herbicola (Phelps et al., 1986). Ice nucleation sites extracted from lichen are also susceptible to proteolysis (Kieft, 1988) but the sites contained by intact bacteria are not affected by exogenous proteases. Surfactants, most notably certain quaternary ammonium compounds, destroy bacterial ice nucleation sites, again suggesting an obligatory association with the membrane (Watanabe et al., 1988).

2.5.5 Measurement of Size of Membrane Bound Ice Nuclei

To circumvent the necessity of extraction and purification, Govindarajan and Lindow (1988b) employed gamma radiation target analysis to measure the in situ size of ice nucleation sites in strains of P. syringae, E. herbicola, and r-DNA E. coli cells containing the ice gene. The minimal size of a functional ice nucleus active below -10° C was about 1.5 X 10^6 daltons for all strains. The size of the ice nuclei increased logarithmically with activity at increasing nucleation temperatures from -12° C to -2° C where the estimated molecular weight was 1.9 X 10^7 daltons (Figure 2.5). The authors concluded that the ice nucleating site may be an oligomeric structure which can self-associate to assume many possible sizes.

Figure 2.5. Molecular Mass of Ice Nucleation Sites of Different Strains of Ice Nucleation Active Bacteria as a Function of Temperature (T) of Expression of Ice Nucleation Activity Estimated by Sensitivity to Gamma Radiation: P. syringae strain 31R1 (■), P. syringae strain cit7 (o), E. herbicola strain 26SR6-2 (□), and E. coli HB101 (●) (Govindarajan and Lindow, 1988b).

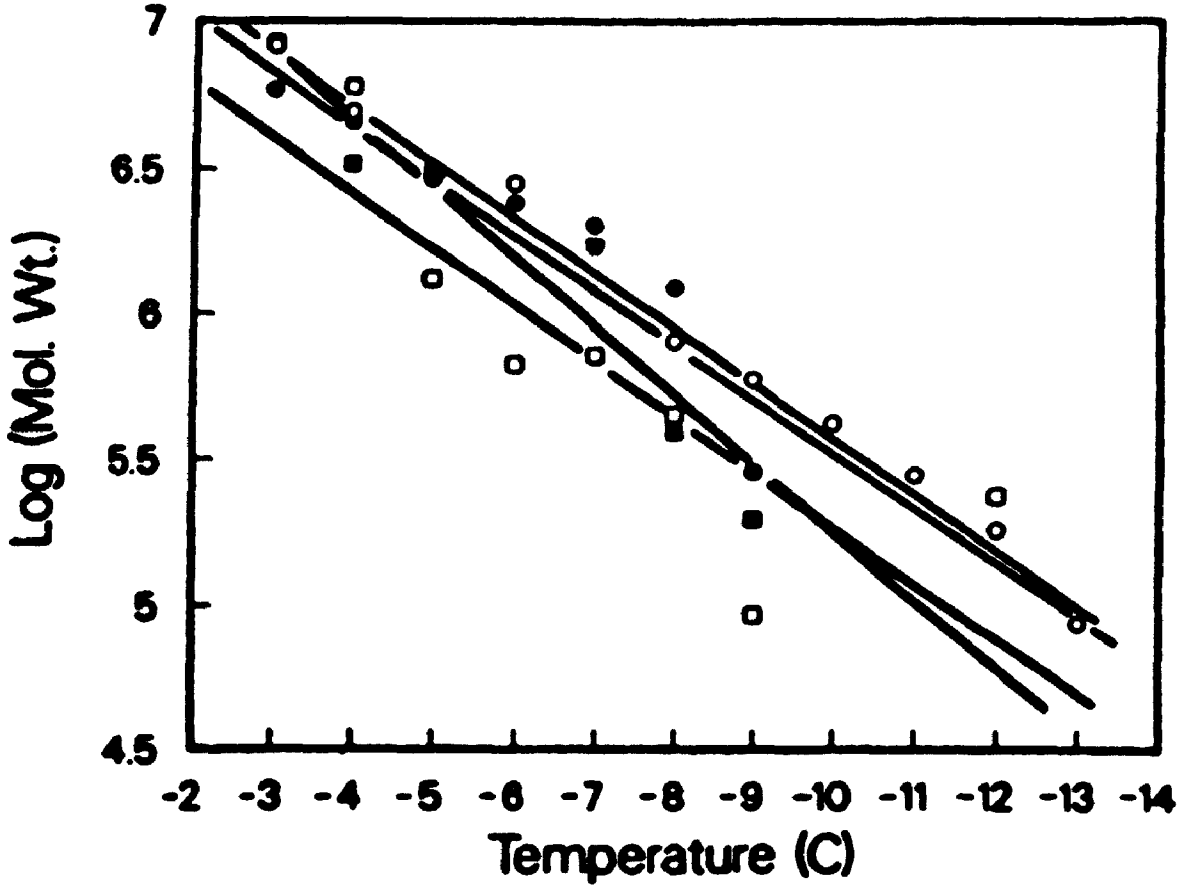
7
6.5
6
5.5
5
4.5
Log (Mol. Wt.)
-2 -3 -4 -5 -6 -7 -8 -9 -10 -11 -12 -13 -14
Temperature (C)

2.5.6 Utilization of the Isolated Ice Nucleation Protein

No studies have been published so far which report the utilization of the isolated ice nucleation protein in its native form. The protein fractions have been isolated and characterized as described by Deninger et al. (1988), Wolber et al. (1986) and others (Duman et al., 1984).

2.6 Environmental Manipulation of Bacterial Ice Nucleation Activity

A systematic perusal of the literature revealed that despite the potential commercial importance of Pseudomonas syringae as an efficient ice nucleation agent, very little research has been published on the environmental factors which affect its cell growth and INA. The INA expressed by bacteria is a function of the strain genotype, pH, temperature, composition of the growth medium and aeration. Bacteria grown on a solid medium may express different levels of INA than those cultured in the liquid broth.

Pooley and Brown (1991) cultured P. syringae 1105 (National Collection of Plant Pathogenic Bacteria, Harpenden, U.K) originally isolated from Pyrus communis in 250 mL flasks containing (i) 100 mL of Luria broth (LB); (ii) LB supplemented with 0.1% D-glucose (LBG); (iii) nutrient broth (NB) or (iv) Koser citrate broth at 25° C, 200 RPM and uncontrolled pH. Cell suspensions in deionized water were kept at 4° C for 1 h before determination of ice nucleation characteristics. Cells grown in KCB showed higher INA at -5° C (215 ice nuclei/10^9 cells) compared to zero activity at -5° C for the other three media. Results at -8° C also indicated that KCB was a better medium for INA than the

other three media tested. Cultures grown into the late exponential phase seemed to possess higher INA and cells grown on KCB agar plates were found to be more active than corresponding broth cultures.

Rogers et al. (1987) found that keeping INA bacterial cultures of E. herbicola at 5° C for approximately 1 h (low temperature conditioning) apparently increased their ice nuclei content. Obata et al. (1987) studied the INA characteristics of P. fluorescens as a function of growth media. Glucose, glycerol, and sodium citrate were good substrates yielding cells with high ice nucleating activity. Ammonium salts were good nitrogen sources also yielding cells with high INA. Heat treatment at 50° C for 30 min significantly reduced INA while heating at 90° C for 10 min completely eliminated INA. A pH of between 5.5 and 8.0 did not influence the ice nuclcation characteristics of P. fluorescens. All studies by these authors were conducted in 500 mL flasks containing 50 mL of medium.

Maki et al. (1974) identified ice nucleation bacteria from decayed tree leaves as P. syringae. The authors found that INA was found in intact cells and associated with the cell wall. Cetyl-pyridinium chloride, dyes, and physical disruption (sonic disintegration) destroyed INA. Certain antibiotics, notably, streptomycin and polymyxin B, killed the cells without destroying activity. Lack of oxygen inhibited activity of the cells.

Kozloff et al. (1983) found that exposure of P. syringae cells to metal chelating compounds did not influence INA. Borate compounds inhibited INA of the cells. Treatment with N-ethylmaleimide, p-hydroxymercuribenzoate, or

iodoacetamide irreversibly inhibited INA by 99%.

O'Brien and Lindow (1988) investigated the influence on the expression of INA of 15 P. syringae strains during growth on leaf surfaces of bean, pea, tomato, cucumber, oat, corn, and potato plants. Due to the complexity of environment, individual parameters affecting INA could not be identified and interactions among variables frequently occurred. Generally bacterial INA for species on leaf surfaces of various plants was found to be higher than that of bacteria in culture. Variations in INA on plant surfaces could be attributed to differences in strain identity, plant species, light intensity and humidity.

2.7 Applications of Ice Nucleating (Ice-Plus) and Ice Gene Deficient (Ice-Minus) P. syringae Bacteria

In this section various applications of the ice nucleating bacteria as well as ice minus bacteria are discussed. Only some applications of the INA bacteria are included as this a new and rapidly developing area of research.

2.7.1 Ice-Minus Bacteria

Frost control by ice-minus bacteria involves the displacement of the ice-plus (ice nucleating) P. syringae populations in their natural habitat on plants with ice-minus r-DNA P. syringae bacteria popu..tions (Cody et al.,1987, Lindow, 1982, 1983b, 1985). Since the two types of bacteria are exactly identical except for the ice nucleating ability, the problems of host specificity and adaptation to plant surface do not arise. The ice-minus bacteria would have to

be sprayed on plant surfaces before ice-plus populations develop and would need to grow to a sufficient numbers to prevent the latter from colonizing the plant surface. Thus this was a simple and effective means of frost control. The release of ice-minus bacteria into the environment has been the subject of debate (Van Brunt, 1987).

Four experiments, conducted independently by Advanced Genetic Sciences (AGS) and by S.Lindow of University of California (Berkeley) were carried out to evaluate the dispersal, environmental fate, colonization potential, and competition between ice-plus and ice-minus strains under actual field conditions with prior approval from the U.S. federal environmental agency.

AGS carried out field testing of the ice-minus bacteria in small field trials on 2500 strawberry plants. The results were found to be encouraging and larger field trials were then conducted on 17400 plants in 1988 (Biotechnology news report, 1988). Lindow's tests used potato as the model system to compare the competitive ability of ice-minus relative to the ice-plus P. syringae strain. The data on all these tests are available (Environment Protection Agency reports, 1988). It was found that blossoms and fruits treated with the ice minus bacteria had a significantly reduced probability of freezing between -2.5° C and -4.0° C.

Lindemann and Suslow (1987) carried out controlled laboratory tests in order to determine the probability of environmental risk associated with the release of ice-minus P. syringae and P. fluorescens deletion mutant strains into the environment for frost control applications. The survival of the ice-minus strains in the soil and on the roots of actively growing strawberry plants was

first considered. Three weeks after inoculation, populations of the ice-minus strains declined to undetectable levels while the ice-plus strains on control soil and plants only decreased ten-fold. P. syringae and P. fluorescens ice-minus strains were found to grow rapidly on blossoms of strawberry, almond, pear, cherry, and blackberry (populations greater than 10^7 cfu per blossom). Established populations of ice-plus cells however inhibited the ice-minus strains. A number of other variables were also investigated by the authors. These included dissemination during spray inoculation, dissemination by insects and effect of freezing and thawing on survival of ice-minus strains in vivo. Based on these studies, the authors concluded that the ice minus deletion mutants expressed no competitive advantage over the ice-plus strain and exhibited only a limited survival capability in the environment.

2.7.2 Food Industry Applications

While ice-minus bacteria are being tested in frost control, researchers elsewhere are considering alternative uses for ice nucleating bacteria. Watanabe and Arai (1987) have studied the application of ice nucleating Erwinia ananas in the efficient freeze drying of foods. The use of these bacteria raised the supercooling temperatures with savings in refrigeration cost. The process led to shortening of freezing times and efficient formation of products. Arai and Watanabe (1986) studied the freeze texturing of food materials using ice nucleating E. ananas. The bacterial cells, when added to isotropic aqueous dispersions or hydrogels of proteins and polysaccaharides, converted the bulk

water into directional ice crystals at subzero temperatures not lower than - 5° C with anistropically textured products. Raw egg white, bovine blood, soyabean curd, milk curd, aqueous dispersions or slurries of soyabean protein isolate were successfully tested.

The use of ice nuclei in the food industry requires that they be robust and environmentally safe. They must also be non-toxic, non-pathogenic and palatable. These criteria are best met by preparations in which the ice nuclei have been extracted and purified away from their bacterial source. Cell-free preparations are also likely to be accepted by national regulatory agencies. This involves the development of high levels of ice nucleation protein in the bacteria, then its purification and concentration in an active form. Such a development is yet to reach a commercial scale.

2.7.3 Artificial Snow Production

Since its invention in the early 50', artificial snow production has been enhancing ski conditions at a growing number of ski areas, and is considered a necessity for many ski areas. Most small ski areas operate 10-30 snow guns (nozzles) but larger ski areas may operate hundreds of snow guns. The snow guns are usually run all night, and handle between 10 to 100 gallons per minute of water along with several hundred standard cubic feet of compressed air. The process of snow making is very energy intensive and even a small improvement in efficiency can translate into considerable savings in energy costs.

The snow making process is essentially a spray freezing operation.

Water is mixed with compressed air and forced through an internal mixing nozzle (snow gun) from which it expands into the ambient air causing it to atomize and cool simultaneously. Under typical snow making conditions, the cooling provided by the free jet is small compared to the ambient cooling. The role of the compressed air is mainly to atomize the water droplets.The engineering considerations involved in a typical snow making process have been outlined by Liao and Ng (1990). Several variables can affect the process. These include water temperature and pressure, flow rate, droplet diameter, the ice nuclei present and the nucleation temperature. Chen and Kevorkian (1971) have identified certain requirements for successful artificial snow manufacture. These are:

1. The water spray must have droplets of certain diameter (220-700 μm).
2. The water droplets must be seeded with ice nuclei.
3. The droplets should have sufficient residence time in the ambient air to be able to convert to snow.

Recognizing the key role of ice nuclei, Eastman Kodak in collaboration with AGS has patented a product called Snomax (freeze dried P. syringae) used in artificial snow manufacture (Kocak and Van Gemert, 1988). This product is used for ski slopes and skating rinks and where snow is used as a construction material, e.g., in the arctic. Kocak and Van Gemert (1988) have patented a process for the manufacture of snow. A schematic is shown in Figure 2.5. Pure

Figure 2.6. Schematic Diagram for Producing Snow Inducing Bacteria (Kocak et al., 1988)

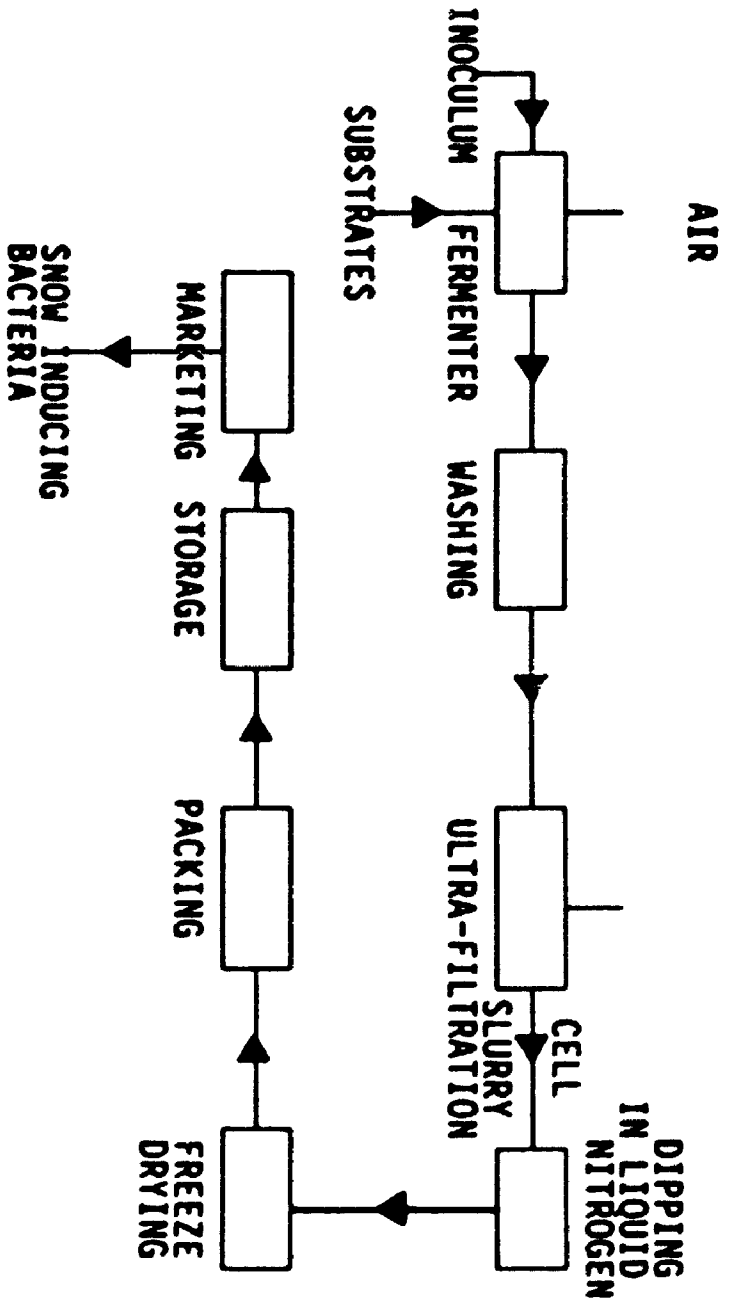
AIR
INOCULUM
SUBSTRATES
FERMENTER
WASHING
ULTRA-FILTRATION
SLURRY
CELL
DIPPING IN LIQUID NITROGEN
FREEZE DRYING
PACKING
STORAGE
MARKETING
SNOW INDUCING BACTERIA

P. syringae culture is ultra-filtered to form a slurry which is then dipped in liquid nitrogen to form pellets. The pellets are freeze dried and bagged. The product is marketed as Snomax snow inducer. Each pack contains 300 g of material which dissolves in 400 L of water. The solution is then injected into snow making water supply. The environmental effects of such snow have reportedly been investigated by the authors but the results of such investigations have not been described. Suslow et al, (1987) have also investigated the use of ice nucleation bacteria in air:water systems. The use of the INA bacteria led to an enhancement of snow production in such systems.

2.7.4 Other Current and Potential Applications

A patent has recently appeared on the application of bacterial ice nuclei in immunoassays (Warren and Wolber, 1989). The use of the INA bacteria in improving the efficiency during thermal storage in air conditioning and refrigeration systems has also been considered (Stewert and Bear, 1988). The nucleation of ice in such systems at higher temperatures increases system efficiency and reduces energy consumption. This becomes increasingly important with increasing volume and larger loads.

A novel and important application which has been developed is the BIND (bacterial ice nucleation assay) test (Worthy, 1991, Wolber and Green, 1990). This assay is used as a rapid test for food poisoning bacteria. For applications to the testing of Salmonella, first a Salmonella specific bacteriophage is incorporated with the gene coding for the ice nucleation protein. The

bacteriophage reagent is then added to test samples of food which may contain Salmonella, together with a green fluorescent dye. Any Salmonella present are infected with the bacteriophage. The test samples are then incubated at 37° C to allow the formation of the ice nucleation protein. The test samples are chilled to -5° C. If the bacteria are present, the samples freeze and the green dye becomes dark red and non-fluorescent. Samples which lack the bacteria and control samples without the bacteriophage do not freeze and remain bright green and fluorescent. The total time for the assay is 2-6 h compared to currently available Salmonella tests which take 2-5 days.

Freeze concentration is used in the chemical processing industry as a process for concentrating dilute streams by refrigeration techniques (Chowdhury, 1988). Currently, it is being utilized in the treatment of hazardous wastes, concentrating fruit juices and food freezing, and purifying organic chemicals. This is a potential area where bacterial ice nuclei may be successfully applied (Ryder, 1987). By using bacteria, supercooling to very low temperatures can be prevented with savings in energy costs. Supercooling to low temperatures also leads to rapid freezing and thus formation of impure ice crystals which trap the solute. Ice formation at warmer temperatures is slower and purer ice crystals are produced.

The potential of using P. syringae as a grain protectant has been discussed by Fields (1991). A common grain infesting insect is Cryptolestes ferrugineus. Adults of this species when exposed to grain treated with ice nucleating P. syringae had increased mortality than those exposed to untreated

controls at -10° C. The use of the INA bacteria lowered the freezing temperature of insect pests in the grain from -17° C to -10° C and thus prevented insect over wintering survival capacities.

2.8 Kinetics and Modelling

When a suitable quantity of living cells is added to a liquid solution of essential nutrients at a suitable temperature and pH, the cells will grow. A growing cell population interacts with the environment in a complicated way. Cells consume nutrients and convert substrates in the environment to products. The cells generate heat and, in turn the medium temperature sets the temperature of the cells. Mechanical interactions occur through hydrostatic pressure and flow effects from the medium to the cells and from changes in medium viscosity due to the accumulation of cells and cellular metabolic products.

When a microbial culture is grown in a batch mode, it passes through several phases of growth. Initially, when the inoculum is introduced into the system, there is a lag phase when the cells adapt to the new environment. This is followed by the exponential or log phase of growth where the specific growth rate, μ, (growth rate per unit biomass) is maximum and constant. When the growth limiting substrate is exhausted in the system, the cells go into maintenance mode in the stationary phase. In this phase, the cell population is constant. Gradually, the cell population starts to decrease in the death phase due to an accumulation of toxins and/or starvation of nutrients.

In each growing culture, there is a maximum specific growth rate (μ_{max}). This is the maximum possible rate of growth per unit of biomass with unlimited nutrients in the given environment.

The interpretation of batch culture kinetic data is a problem that arises frequently in many biochemical engineering studies, ranging from basic research on microbial kinetics to process development and scale-up. Mathematical modelling of bioprocesses is an important quantitative tool for optimization and prediction of product profiles. It can also be used to probe and provide an insight into process mechanisms. With rapid advancements in computer process control, mathematical models have become essential components of any on-line control strategy.

A kinetic model is a simplified and useful representation of cell population kinetics. With respect to the environment, it is common practice to formulate the growth medium so that all components but one are present at sufficiently high concentrations that change in their concentration does not change the overall fermentation rate. Such a system can be modelled by unstructured models, where only a single component is growth limiting. (a) Structured or segregated models , e.g., models based on intra-cellular components. These models require highly accurate and reliable estimates of intra-cellular components which may be present in insignificant amounts. The advantage is a more accurate and detailed representation of the bioprocess. (b) Unstructured models, e.g., models based on gross components, e.g., cell, substrate, and product concentration. The advantage of such models are simplicity of operation, and a

fewer number of parameters which are required. Two other kinds of models are mechanistic and empirical models. Empirical models cannot be generalized or used for prediction (extrapolation) of data. Mechanistic models are the models of choice for process control applications.

Cellular representations which are multi-component are called structured models. Also, if the average properties of a cell population are considered, an unsegregated model is formed. Consideration of discrete, heterogeneous cells constitutes a segregated viewpoint. The actual situation in a fermentation is a segregated and structured one, but an unsegregated, unstructured approach is easier to use and often a good representation of cellular kinetics. Various types of models are shown in Table 2.5.

One simple kinetic model which assumes that the rate of increase of cell mass is a function of cell mass only is Malthus' Law (Bailey and Ollis, 1986):

$$f(x) = \mu x \qquad (2.7)$$

with μ as a constant. This model does not take into account lag or death phases in a microorganism and assumes unrestricted growth in the cells. Hence, this is not at all a useful representation of cell kinetics.

Slater (1985) describes the logistic equation of cell growth which relates the specific growth rate, μ, to the cell mass concentration X, the maximum specific growth rate μ_{max}, and the final population size X_f. This equation is shown below (Equation 2.9).

Table 2.5. Various Models for Cell Kinetics

Population	Cell components	
	Unstructured	Structured
Distributed	Cells are represented by a single component which is uniformly distributed throughout the culture	Multiple cell components, uniformly distributed throughout the culture and interacting with each other
Segregated	Cells are represented by a single component, but they form a heterogeneous mixture	Cells are composed of multiple components and form a heterogeneous mixture

$$\mu = \mu_{max}\left(1 - \frac{X}{X_f}\right) \qquad (2.8)$$

This is an empirical model and has been found to approximate cell growth in a batch culture reasonably well. A serious drawback of the logistic equation is its lack of flexibility to represent the lag or stationary phases of cell growth.

A semi-empirical equation which has been found very useful in representing cell growth kinetics is the Monod equation (Monod, 1942; Bailey and Ollis, 1986). If the concentration of one essential constituent is limiting, the cell growth is given by:

$$\mu = \frac{\mu_{max} S}{K_s + S} \qquad (2.9)$$

here μ_{max} is the maximum specific growth of cells achievable when $S >> K_s$ and the concentration of all other nutrients is unchanged. K_s is the substrate limitation constant or the value of the limiting nutrient concentration at which the specific growth rate is half its maximum value.

Other related forms of specific growth rate dependence have been

proposed which may give a better fit to certain experimental data. Bailey and Ollis (1986) list the following models:

$$\mu = \mu_{max} (1 - e^{-S/K_s}) \tag{2.10}$$

$$\mu = \mu_{max}(1 + K_s S^{-\delta})^{-1} \tag{2.11}$$

$$\mu = \mu_{max} \frac{S}{BX + S} \tag{2.12}$$

2.9 Temperature Effects on Cell Processes

Temperature affects cell processes in various ways. The most obvious effects are cell death at high temperatures and freezing at lower temperatures. Microrganisms are classified according to the temperature range within which their optimum growth rate occurs. The general optimal temperature ranges applied are 55 - 75° C for thermophiles, 30 - 45° C for mesophiles and 15 to 30° C for psychrophiles (Stanier et al.,1976). Mammalian cells and plant cells are generally mesophillic. Among bacteria, fungi, and yeasts however all groups exist. Pseudomonas is classified as psychrophillic (Breed et al., 1948). Chemical reaction rates are related to temperature by the Arrhenius equation:

$$K = A e^{-E/RT} \qquad (2.13)$$

where K is the reaction rate, R is the gas constant, T is the absolute temperature, A is a constant dependent on the frequency of formation of activated complexes of the reactants and E is a constant known as "activation energy" or "temperature characteristic". From Equation 2.13, we have:

$$\ln K = \ln A - E/RT \qquad (2.14)$$

Hence a plot of log K against 1/T should be a straight line with slope, E/RT. If we substitute the specific growth rate, μ, for the reaction rate, K, in equation 2.14, straight line relationships are obtained for ln μ versus 1/T. At higher temperatures, the specific growth rate, μ, of microrganisms may abruptly decrease due a disruption in metabolic regulation or cell death. The death rate may become dominant at high temperatures if the activation energy for death exceeds that for growth.

CHAPTER 3

THEORETICAL CONSIDERATIONS

3.1 Introduction

In this chapter, first the theory of ice nucleation by bacteria is reviewed in section 3.2. In sections 3.3 and 3.4, a theoretical analysis of the method of ice nucleation measurement, i.e., the drop freezing assay, is undertaken. Section 3.5 describes a mathematical model of batch growth and ice nucleation activity (INA) in a 1 L bioreactor. In section 3.6, theoretical concepts of continuous cultivation of microorganisms are discussed.

3.2 The Nucleation of Ice by Bacteria

This section describes the theoretical background of ice nucleation by P. syringae bacteria. This description is then used as a basis for the theoretical derivation for the method of measurement of bacterial INA.

Figure 3.1 depicts a schematic cross section of the cell wall of any Gram negative bacterium, such as P. syringae. On the basis of the literature surveyed, the following hypothetical location is shown in Figure 3.1 for the ice nucleation protein (INP) - phosphatidylinositol (PI) complex which together form the ice nucleation site in P. syringae (Warren, 1987; Govindarajan and Lindow, 1988a). It has been earlier shown that one end of the ice nucleation protein is hydrophobic (Wolber and Warren, 1989). Therefore, in Figure 3.1, the INP's hydrophobic terminal is shown to be combined with the PI and buried in the outer membrane

Figure 3.1. Schematic Diagram of the Cell Envelope of a Gram Negative Ice Nucleating Bacterium. The hypothesized location of the ice nucleation site consisting of the ice nucleation protein (INP) - phosphatidyl-inositol (PI) complex is shown.

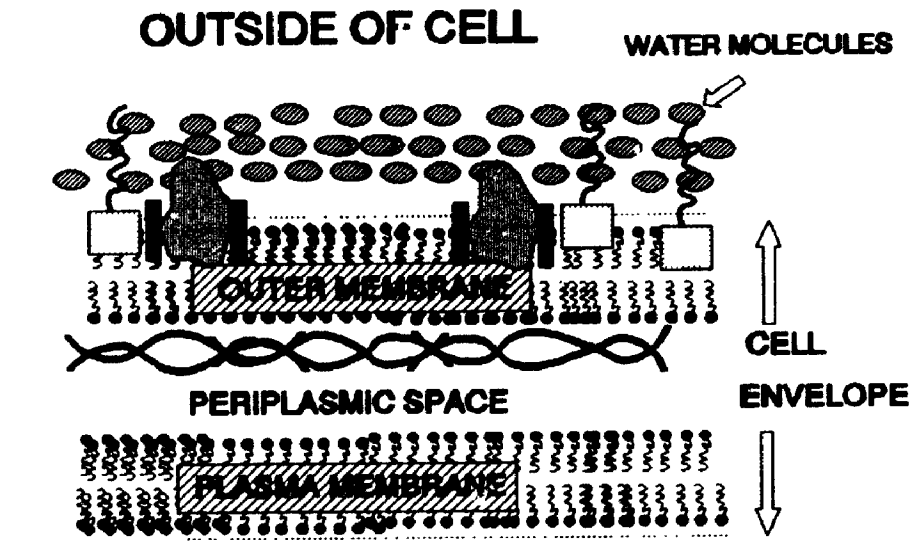
OUTSIDE OF CELL
WATER MOLECULES
OUTER MEMBRANE
CELL
ENVELOPE
PERIPLASMIC SPACE
PLASMA MEMBRANE
INSIDE OF CELL

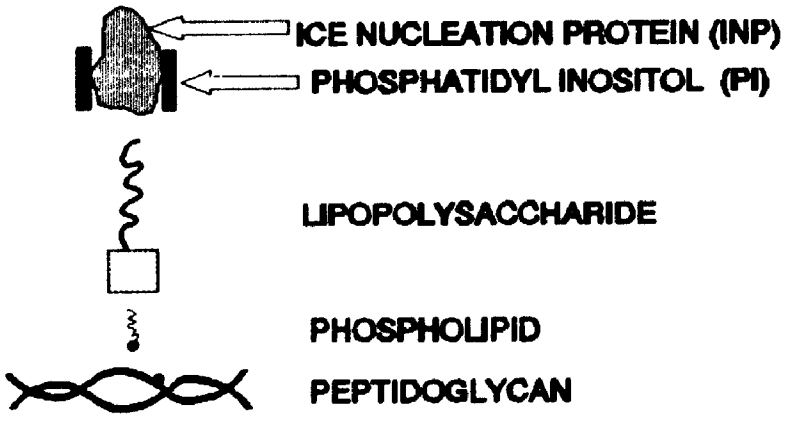
ICE NUCLEATION PROTEIN (INP)
PHOSPHATIDYL INOSITOL (PI)
LIPOPOLYSACCHARIDE
PHOSPHOLIPID
PEPTIDOGLYCAN

of the bacterium. The other end of the protein is hydrophillic and in contact with surrounding water molecules.

The first step in the activation of the ice nucleation site is the assembly of surrounding water molecules by hydrogen bonding to the protein residues. This is followed by rearrangement of the randomly moving water molecules into an ordered structure which physically resembles the ice lattice.

If the freezing temperature is higher, e.g. -3° C, water molecules possess greater kinetic energy and are moving much more rapidly than water molecules at lower freezing temperatures, e.g., -9° C. Thus at higher temperatures, more active sites are required in order to bring some of the water molecules into an ordered arrangement. Thus, higher temperatures tend to favour supercooling.

Figure 3.2 is a schematic diagram of a single water drop containing cells of ice nucleating bacteria with the ice nucleation sites. In the figure, the INP distribution per cell surface may vary widely, with some cells having more INP than others. This has been recently proven by the use of monoclonal antibodies raised against ice nucleation(IN) proteins from Pseudomonas species using Western blots (Mueller et al., 1990). In immunofluorescent staining of whole bacteria, the antibodies revealed the location of the INP in clusters, as indicated by patches of intense fluorescence in Escherichia coli heterologously expressing Pseudomonas genes. The abundance, size, and brightness of the INP clusters varied from cell to cell which may explain the variability in INA among a given population of bacterial cells.

In figure 3.2, for any cell i, present within the drop, the number of ice nuclei

Figure 3.2. Schematic Representation of a Water Drop Containing Ice Nucleating Bacteria showing the Ice Nucleation Protein (INP) Sites on the Bacterial Surface. The INP site distribution per cell surface varies.

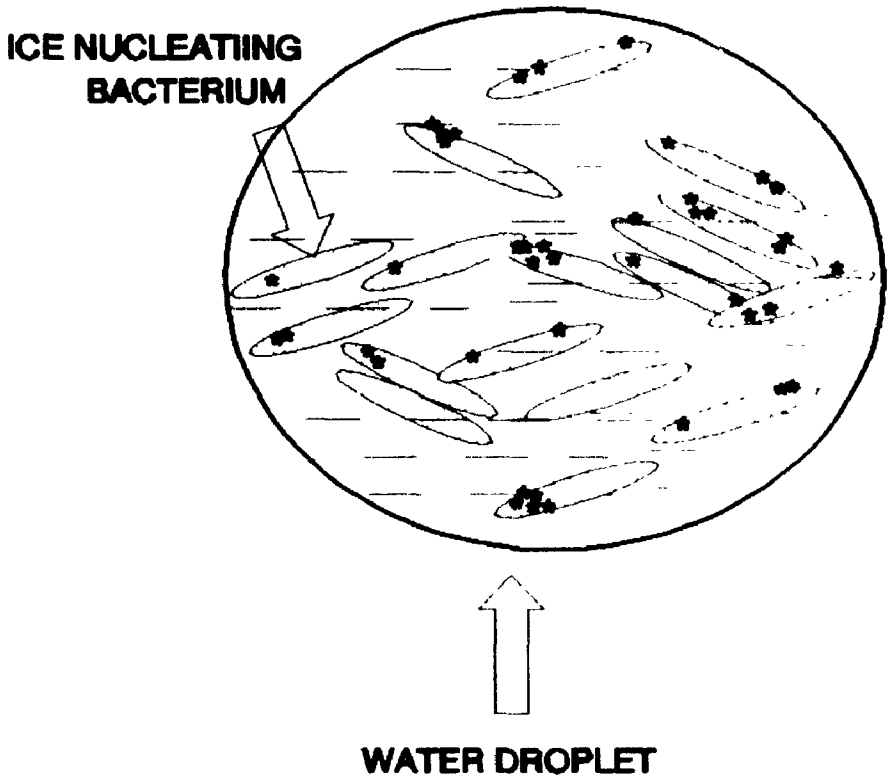

* ICE NUCLEATION PROTEIN (INP)

per cell can be denoted by γ_i, and γ_i varies from cell to cell as explained previously. Thus there is a distribution of γ_i in the total cell population.

The total number of ice nuclei present in a water drop of volume V and containing n cells, is given by equation 3.1.

$$\textit{Total no. of ice nuclei} = \sum_{i=1}^{n} \gamma_i = \gamma_1 + \gamma_2 + \gamma_3 \ldots \gamma_n \qquad (3.1)$$

Let n = the total number of cells in a drop of volume V

Let m = g dry weight mass per cell

Let X = cell concentration within the drop of volume V

Therefore, X = n.m/V (g cell DW/L)

The number of ice nuclei/g cell DW within the drop, is given by equation 3.2.

$$\textit{Total no. of ice nuclei per g cell DW} = \frac{\sum_{i=1}^{n} \gamma_i}{n.m} \qquad (3.2)$$

For ice nucleation to occur at a given freezing temperature for a given cell population within the water drop, we need at least one active ice nucleation site (INS) which will initiate the freezing process followed by very rapid propagation

until the whole water drop freezes. This ice formation can be observed by the opaque colour of the drop.

3.3 Measurement of Ice Nucleation Activity of Water Samples containing Ice Nucleation Active Bacteria by Observing the Freezing of a Collection of Drops

The following section describes an adaptation of the equation originally developed by Vali (1971) for measurement of INA in rain-drops containing heterogeneous ice nuclei. The technique used by Vali was based on the cooling of a number of small drops of equal volume to temperatures below 0° C and observing the freezing pattern of the drops with decrease in temperature.

Experiments have shown that the individual freezing temperatures of a collection of drops of supercooled water are spread over several degrees (Bigg, 1953). Two hypotheses have been advanced to explain this phenomenon:

1. The process of ice nucleation is stochastic i.e., freezing of the drops occurs in a random fashion. This hypothesis is favoured during the process of homogeneous nucleation where impurity nuclei are absent and the supercooled water is essentially pure.
2. For heterogeneous systems, it is known that impurities contribute in the ice nucleation process. Each impurity may be defined as having a characteristic temperature at which it is "active", i.e., causes nucleation to occur in the drop containing it. Therefore the distribution of freezing events in the population of drops with decrease in temperature is directly related to the

distribution of impurity nuclei with their characteristic temperatures. This is the so called "singular" hypothesis: every drop would freeze at a temperature characteristic of the most "active" nucleus in the drop.

Stansbury, (1961) reported that both the stochastic and the singular hypotheses could be applied to describe the behaviour of the freezing of drops of supercooled water. However, Vali and Stansbury (1966) concluded based on their observations that for heterogeneous ice nucleation, the singular hypothesis was more representative of the actual phenomena and the stochastic hypothesis was of secondary importance. Based on these studies, Vali (1971) developed a quantitative measure of the ice nuclei content of a given sample. This technique is the so called "drop freezing assay". It has been applied by all previous researchers on ice nucleation bacteria, and it is also applied in this thesis to measure INA.

The following assumptions have been used by Vali (1971) in the drop freezing assay:

(1) Each particular freezing nucleus becomes active at its characteristic temperature - "singular" hypothesis

(2) The nucleation events are independent of the time rate of change of temperature.

3.4 Derivation of Vali's Equation for Measurement of Bacterial Ice Nucleation Activity

Let k(θ) be the fraction of active ice nuclei present per unit volume of sample containing P. syringae cells, within a unit temperature interval about the temperature θ. Let $\bar{n}(\theta)$ be the average fraction of active nuclei present in the water drop of volume V per unit temperature interval θ, then n(θ) is given by equation 3.3.

$$\bar{n}(\theta) = k(\theta)V \qquad (3.3)$$

If we lower the temperature by d θ, i.e. from θ to (θ - d θ), then the fraction of active ice nuclei per drop of volume V is given by equation 3.4 which is the result of multiplying both sides of equation 3.3 by d θ.

$$\bar{n}\,(\theta)\; d\,\theta = k(\theta)\; V\, d\,\theta \qquad (3.4)$$

The fraction of active ice nuclei, $\bar{n}(\theta)$, by definition can vary from 0 to maximum 1. Equation 3.4 also represents the probability of the presence of fraction of active ice nuclei in a drop of volume V for a given temperature interval d θ. This probability function $\bar{n}(\theta)$, can vary from zero (no active ice nuclei) to 1 when all ice nuclei present in the drop of volume V are active. Therefore, for values of n(θ) d

θ smaller than one, equation 3.4 represents the probability that a given drop of volume V will contain an active ice nucleus within the specified temperature interval $d\theta$.

Let N_0 be the total number of water drops of volume V each, which are being tested for freezing. Out of the total number of drops N_0, let N_θ be the number of drops which are still unfrozen at a freezing temperature θ. Therefore ($N_0 - N_\theta$) is the number of drops which are frozen at temperature θ. If we lower the freezing temperature by $d\theta$, i.e., from θ to $\theta - d\theta$, the additional number of drops freezing is dN. Therefore the fraction of drops which froze within temperature $d\theta$, is given by dN/N_θ. This fraction dN/N_θ also represents the empirical probability of freezing $Pd\theta$, for one of the unfrozen drops and is given by equation 3.5.

$$P(d\theta) = d\frac{N}{N_\theta} \qquad (3.5)$$

In freezing experiments please note that both N_θ and θ decrease with time and therefore both $d\theta$ and dN are negative. Therefore the probability $Pd\theta$ can be evaluated from the observable experimental variables dN, and N_θ that are measured during the freezing of water drops. The probability $Pd\theta$ is also the probability of finding an ice nucleation site active within the freezing temperature range θ to ($\theta - d\theta$) in any one of the total number of original water drops N_0, which is based on the assumption that all drops have an equal chance of

containing an ice nucleation site. Therefore, the empirical probability of freezing, Pd θ, given by equation 3.5 which is calculated from observable quantities of unfrozen drops N_θ, can also be equated to the expected value of probability $\bar{n}(\theta)$ shown in equation 3.4.

$$P\, d\theta = \bar{n}(\theta).d\theta \tag{3.6}$$

or

$$\frac{dN}{N_\theta} = k(\theta).V.d\theta \tag{3.7}$$

$$k(\theta) = \frac{dN}{d\theta}.\frac{1}{N_\theta.V} \tag{3.8}$$

From equation 3.8 we have an expression for k(θ), which is the fraction of active ice nuclei per unit volume. The function k(θ) is also known as the differential form of INS spectrum per unit volume per unit temperature with units of $L^{-1}.\,^{\circ}C^{-1}$.

Equation 3.8 shows that because of infinitesimal decreases in temperature d θ, this implies that no more than one ice nucleation site was responsible for the observed freezing of water drops, and therefore, the probability of finding two or

more ice nucleation sites of the same activity in the same drop becomes negligible. This is based on the application of Poisson's Probability function (Hoel, 1962) which gives the probability P(y) for finding y number of ice nucleation sites of the same activity in the same water drop as shown in equation 3.9.

$$P(y) = \frac{e^{-z} \cdot z^{y}}{y!}, \quad z>0, \quad y = 0,1,2,3,... \qquad (3.9)$$

where $z = \bar{n}(\theta)\, d\theta$, and y = number of ice nucleation sites of the same activity in the same water drop. For example, for y = 1,2,3, we have according to equation 3.9, $P(1) = e^{-z}.z^{1}/1!$; $P(2) = e^{-z}.z^{2}/2!$, $P(3) = e^{-z}.z^{3}/3!$. Therefore, the probability of finding 1, 2, 3 ice nucleation sites of the same activity, in the same drop are proportional to z, $z^2/2$, $z^3/6$.... respectively. For an infinitesimal change in freezing temperatures $d\theta$, the number z is also infinitesimal, and therefore the terms of z with higher powers, i.e., $z^2/2$, $z^3/6$... etc. are also negligible. This proves that the probability of finding two or more ice nucleation sites of the same activity in the same water drop is negligible. However, because we use finite measurements of temperature and number of frozen drops, i.e., $\Delta\theta$ and ΔN respectively, we need to account for all infinitesimal probabilities (equation 3.9). This means that there may be one or more active ice nucleation sites per water drop over a finite freezing temperature change $\Delta\theta$. Let P(0) be the probability of finding zero number ice nucleation sites per water drop, and P(1,2,3) be the probability of finding 1,2,3 or

more ice nucleation sites per drop. Therefore the total probability for a given water drop is given by equation 3.10.

$$P(1,2,3....) + P(0) = 1.0 \qquad (3.10)$$

From Poisson distribution equation 3.9 for active ice nucleation sites we have:

$$P(0) = e^{-z}.(1)/1 \qquad (3.11)$$

Therefore:

$$P(1,2,3...) = 1 - e^{-z} \qquad (3.12)$$

where z is now defined on a difference basis, i.e., $z = \bar{n}(\theta).\Delta\theta$. Since P(1,2,3...) is equal to $(\Delta N)/N_0$ then:

$$\frac{\Delta N}{N_0} = 1 - e^{-(n(\theta).\Delta\theta)} \qquad (3.13)$$

Since $\bar{n}(\theta) = k(\theta).V$ (equation 3.3), therefore:

$$\frac{\Delta N}{N_0} = 1 - \exp(-k(\theta).V.\Delta\theta) \qquad (3.14)$$

Solving for $k(\theta).\Delta\theta$ we get:

$$\ln(1 - \frac{\Delta N}{N_0}) = -k(\theta).V.\Delta\theta \qquad (3.15)$$

or:

$$k(\theta) = -\frac{\ln[1 - \frac{\Delta N}{N_0}]}{V.\Delta\theta} \qquad (3.16)$$

Equation 3.16 can be used to calculate $k(\theta)$ from measurable experimental parameters N_0, ΔN, over temperature range $\Delta\theta$ of a water drop of fixed volume V. It is also important to calculate the cumulative ice nucleation active sites concentration $K(\theta)$, over the freezing range zero to any lower freezing temperature θ. This can be done by integrating the differential definition of $k(\theta)$ shown in

equation 3.7 over the entire temperature range from 0 to -θ (i.e., at θ = 0, N = N_0, and at θ = θ, N = N_θ assuming a drop of constant volume V). This is shown below.

$$\int_0^{-\theta} k(\theta).d\theta = K(\theta) = \frac{1}{V}\int_{N_0}^{N_\theta}\frac{dN}{N_\theta} \qquad (3.17)$$

or:

$$K(\theta) = \frac{1}{V}[\ln N_\theta]_{N_0}^{N_\theta} \qquad (3.18)$$

Therefore:

$$K(\theta) = \frac{1}{V}(\ln N_0 - \ln N_\theta) \qquad (3.19)$$

Further modification to equation 3.19 results in equation 3.20.

$$K(\theta) = \frac{\ln(\frac{N_0}{N_\theta})}{V} \qquad (3.20)$$

where:

$K(\theta)$ = cumulative concentration of ice nucleation active sites per L of water drop over the freezing temperature range 0 to $-\theta$. (Units of $K(\theta)$: L^{-1})

N_0 = total number of initial (unfrozen) drops at 0° C

N_θ = number of water drops remaining unfrozen at freezing temperature $-\theta$° C.

Let:

$$N_f = N_0 - N_\theta = \textit{no. of drops frozen} \qquad (3.21)$$

and

$$f = \frac{N_f}{N_0} \qquad (3.22)$$

where f is the fraction of drops frozen over the temperature range 0° C to $-\theta$° C.

Rearranging equation 3.20, we have:

$$K(\theta) = \frac{1}{V}.\ln[\frac{1}{1 - f}] \qquad (3.23)$$

Equation 3.23 is used in this thesis to calculate K(θ) by measuring V (which was kept constant at 9.75 μL per drop, and also kept constant was the initial no. of drops, N_0 = 30 drops of equal volume), number of drops frozen N_t over the range 0 to -θ° C using a constant temperature bath. An alternative way to express K(θ) per g cell DW of ice nucleating P. syringae is to divide both sides of equation 3.23 by cell concentration X in the water drop which is given by Equation 3.24:

$$\eta = \frac{1}{V.X}.\ln[\frac{1}{1 - f}] \qquad (3.24)$$

where: η = K(θ)/X, cumulative concentration of ice nucleation active sites per g dry weight of cells of P. syringae over the freezing temperature range from 0° C to -θ° C, units of η = cumulative no. of ice nuclei per g DW cells.

We also define, the threshold temperature θ_{th}, as the freezing temperature at which the first freezing of one or more water drops starts. In addition to measuring the cumulative number of frozen drops over a temperature range, we also measured the freezing temperature θ_1, at which all 30 drops froze, i.e., at θ_1, f = 1.

The observed spread in the freezing of drops, i.e., a plot of f versus θ, is

known as the droplet freezing spectrum, and it has a range from θ_{th} to θ_1. Thus, η, θ_{th}, θ_1, or the droplet freezing spectrum, are indications of bacterial INA of a given sample.

3.5 Mathematical Modelling of Growth of Pseudomonas syringae and its INA

In this investigation, an attempt was made to develop a suitable, mathematical model of growth kinetics and cellular INA of P. syringae cit 7 bacteria grown in the 1 L bioreactor. This is the first reported effort, and no previous models were available describing growth and INA of P. syringae. In this section, an unstructured, mechanistic model has been developed to represent P. syringae cell growth and INA production.

3.5.1 Model Development

In order to develop a mathematical representation of bacterial INA, it is helpful to visualize its physical basis. INA is provided by a membrane protein which exists as clusters on the bacterial surface (Mueller et al., 1990). Batch growth and INA data of P. syringae cells in the bioreactor at different temperatures seemed to indicate that INA was produced during the lag and the growing phase of the cells and not as a secondary metabolite. A model describing such a condition is shown in Equation 3.25.

$$\frac{dP}{dt} = Y'_{p/x}\,\mu\,X \qquad (3.25)$$

where P is the product concentration measured as ice nuclei per L; t is growth time, h; $Y'_{p/x}$ is a yield constant, ice nuclei per g cell DW; μ is specific growth rate

of cells, h-1; and X is cell concentration, g cell DW/L. It should be noted here that $Y'_{p/x}$ is not identical with η, (cumulative number of ice nuclei per g cell DW) which is a variable. The symbol P is identical to $K(\theta)$ defined earlier in Section 3.4. However, the notation P is used for the purpose of modelling.

Let us assume that under constant conditions of temperature and pH, P. syringae cit 7 cells produce a constant amount of ice nucleation protein (INP). Thus at any given time, the concentration of the INP is directly proportional to the cell concentration. However, Southworth et al. (1988) reported that the activity of the INP increased as the 2nd to 3rd power of the protein concentration. This is because when a substantial number of INP clusters are present on the bacterium, a large increase in INA is observed in the bioreactor due to synergistic interaction between the INP clusters. Therefore, Equation 3.25 which assumes that the product formation is directly proportional to the cell concentration needs to be modified.

Due to the non-linear relationship between bacterial INA and cell concentration, it was found that predicted values of P obtained by model simulations using Equation 3.25 with a single constant value of $Y'_{p/x}$ did not represent the actual, experimental data of P versus time. Several non-linear modifications to equation 3.25 were also unsuccessfully attempted.

This problem was resolved by assuming that Y'p/x was constant but with different values over different phases of cell growth. Therefore, constant but different values of Y'p/x were assumed for lag phase, early exponential, late exponential, and stationary phases of cell growth. Various values of $Y'_{p/x}$ were

obtained from experimental data at different growth temperatures by successive curve fitting during the model simulations. The values of $Y'_{p/x}$ used in the model simulations are shown in Table 3.1.

3.5.2 Model Assumptions

1. P. syringae cells are represented by a single component X, g cell dry weight per L of bioreactor volume.
2. The population of cellular mass is homogeneously distributed throughout the culture and the heterogeneous nature of cells is neglected.
3. Besides the assumptions for the cells, the medium is formulated so that only one component (the concentration of sucrose, S g/L) is reaction rate limiting with all other components are at sufficiently high concentrations, so that minor changes do not significantly affect the reaction rate.
4. The bioreactor is operated under controlled conditions of pH, temperature, and dissolved oxygen levels greater than the critical requirements for the microorganisms.
5. Product formation occurs during the lag and log phase of cell growth.
6. The product yield constant, Y'p/x, is represented as previously described.

3.5.3 Description of Equations for Batch Growth

Mass balances were made on the substrate (S, g/L), product (P, ice nuclei per L) and the cells (X, g cell dry weight per L) for P. syringae growth in the

bioreactor. Based on the mass balances, a set of differential equations was developed. The set of differential equations which describe the batch cultivation in the 1 L bioreactor are:

(CELL BALANCE)

$$\frac{dX}{dt} = \mu X \qquad (3.26)$$

Equation 3.26 relates the accumulation of cells in the bioreactor to the specific growth rate of cells. Here X is the cell concentration, g cell DW/L; t is the growth time, h; μ is the specific growth rate of cells in the bioreactor, h-1. A model which describes cell growth kinetics for P. syringae is the Monod equation (Equation 3.27).

(MONOD MODEL FOR CELL GROWTH)

$$\mu = \frac{\mu_{max} S}{K_s + S} \qquad (3.27)$$

where μmax is the maximum specific growth rate of cells under given conditions (h^{-1}); S is the limiting substrate (sucrose) concentration, g/L; and K_s is the

substrate limitation constant, g/L. This model is valid in the absence of substrate or product inhibition of cell growth, which is the case for P. syringae cultivation.

(PRODUCT BALANCE)

$$\frac{dP}{dt} = Y'_{p/x} \mu X \qquad (3.28)$$

Equation 3.28 relates the change in ice nuclei concentration in the bioreactor to the concentration of the growing cells of P. syringae. The assumption is that the product, ice nuclei/L are produced during the lag and log phases of cell growth.

(SUBSTRATE MASS BALANCE)

$$-\frac{dS}{dt} = B \mu X + m X \qquad (3.29)$$

Equation 3.29 is the substrate mass balance and relates the change in substrate concentration with time in the bioreactor to the substrate utilization for cell growth, product formation and cell maintenance. Previously, models reported in literature have only accounted for one or two products formed. These could be the products of interest or the major products formed. Thus substrate was considered to be utilized only for cell growth, cell maintenance and one or two products. In a bio-

process however, cell kinetics is the result of a complex network of biochemical reactions and transport phenomena which involves multiple phases and multi-component systems. During the course of growth, the heterogeneous mixture of young and old cells is continuously changing in physical and chemical conditions. Numerous metabolic products are being formed. Thus the mass balance on the substrate cannot be considered completely "closed" since all products are not accounted for. With these considerations in mind, the term B in Equation 3.29 above was defined as follows in Equation 3.30:

$$B = \left(\frac{1}{Y_{x/s}} + \left(\frac{Y_{p/x}}{Y_{p/s}}\right)_1 + \left(\frac{Y_{p/x}}{Y_{p/s}}\right)_2 + \left(\frac{Y_{p/x}}{Y_{p/s}}\right)_3 + \ldots.\right) \qquad (3.30)$$

Here $Y_{x/s}$ is the cell growth yield or g cell DW formed per substrate consumed. $Y_{p/x}$ is g product formed per g DW of cells and $Y_{p/s}$ is g of product formed per g substrate consumed. The subscripts 1, 2, 3 refer to different products, i.e., ice nucleation protein, carbon dioxide, other products including acids etc. Thus the term B may be defined as a general substrate utilization constant (g of substrate consumed per g of cell DW). A second reason for choosing B over other constants listed in Equation 3.30, was to minimize the number of constants in the model. The evaluation of individual constants of Equation 3.30 would require a detailed analytical study and is included as a recommendation for future work.

The above equations (Eq. 3.26 to 3.29) were solved using a fourth order

Runge-Kutta algorithm for the discretization of the derivative terms in the time domain. A flow chart for this method is shown in Figure 3.3. The complete computer program is included in Appendix C.

3.5.4 Parameter Estimation

There are 5 constants in the above equations. These are μ_{max}, K_s, m, B, and $Y'_{p/x}$. During exponential growth:

$$\frac{dX}{dt} = \mu_{max} \cdot X \qquad (3.31)$$

Thus a plot of ln X versus time t is a straight line during exponential growth phase with slope μmax. The maximum specific growth rate, μ_{max}, was obtained from the experimental data of the cell concentration versus time at different growth temperatures. The values of $Y'_{p/x}$ were also determined by trial and error from experimental plots of η (ice nuclei per g cell DW) versus cell growth temperature, T (° C). These values are reported in Table 3.1. The values of the remaining parameters were estimated by successive curve fitting and multiple non-linear regression of batch data. The response test variable used was the measured concentration of biomass in the bioreactor. The sum of squares, SSQ, was then given by:

Figure 3.3. Flow Chart for Numerical Simulation of Simultaneous Differential Equations of the Model using Fourth Order Runge-Kutta Method

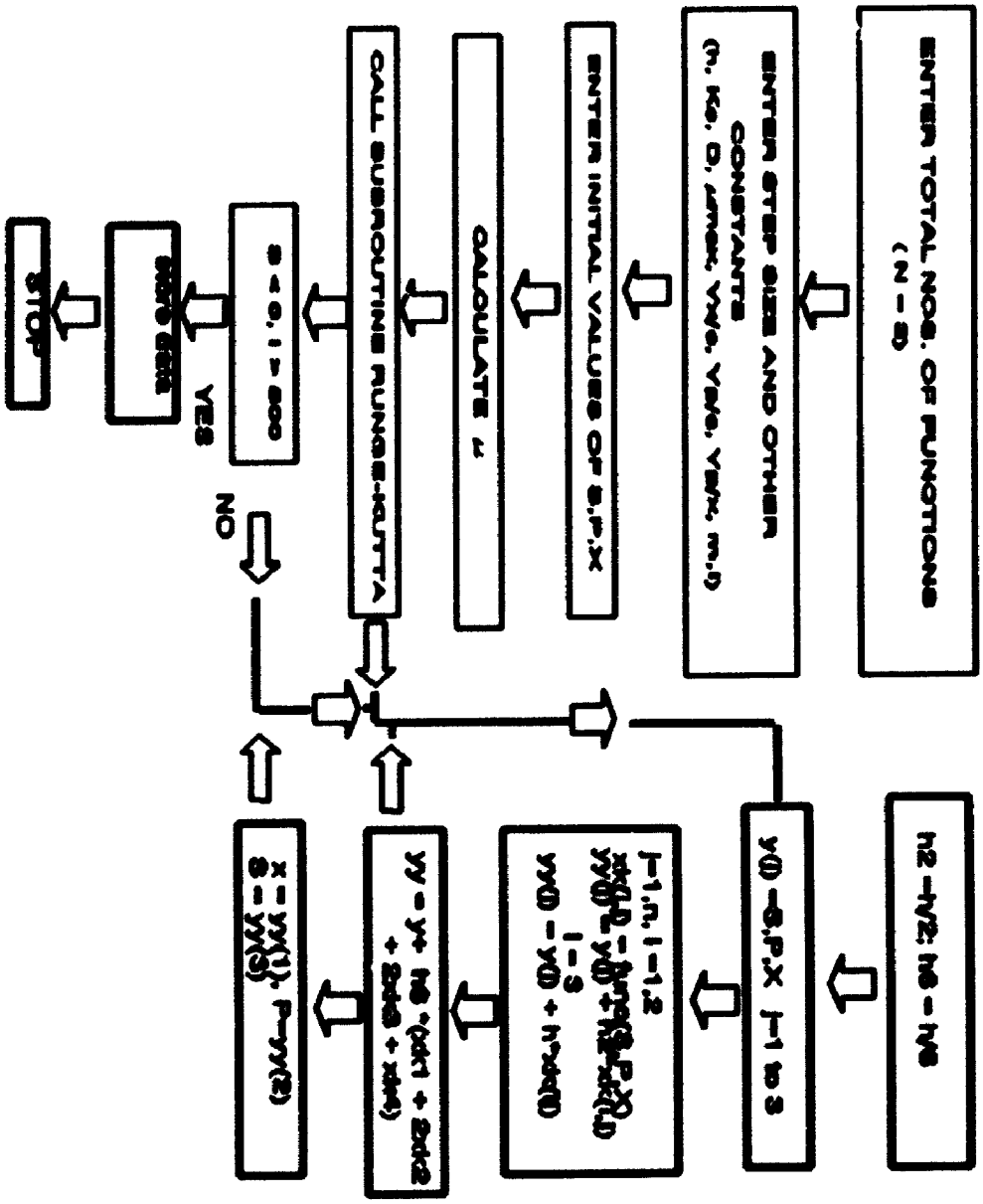
ENTER TOTAL NOS. OF FUNCTIONS
(N = 5)
ENTER STEP SIZE AND OTHER
CONSTANTS
(h, Ka, D, Amax, Ymin, Ymax, Yerr, m)
ENTER INITIAL VALUES OF S,P,X
CALCULATE a
CALL SUBROUTINE RUNGE-KUTTA
S = 0, 1 TO 500
YES
NO
STOP
h2 =h/2; h6 = h/6
Y(I) =S,P,X I=1 to 3
I=1,n, I =1,2
Y(I) = Y(I) + h/6 *(xk1 + 2xk2
+ 2xk3 + xk4)
x = Y(1), P=Y(2)
S = Y(3)

Table 3.1. Values of the Constant $Y'_{p/x}$ from Equation 3.25 Used for Model Simulations in Various Phases of Cell Growth

CELL GROWTH TEMPERATURE (° C)	$Y'_{P/X} \times 10^6$			
	LAG	EARLY EXPON-ENTIAL	LATE EXPON-ENTIAL	STATIONARY
5.5	0.01	0.05	0.50	34.0
10.0	4.50	80.0	100.0	100.0
15.0	.002	0.05	0.50	950.0
20.0	.002	45.0	60.0	550.0
25.0	.002	.002	200.0	250.0
28.0	60.0	300.0	850.0	850.0
35.0	100.0	100.0	250.0	150.0

$$SSQ = \sum_{0}^{t} [(X_{exp} - X_{sm})^2] \qquad (3.32)$$

The particular technique used to evaluate the model parameters in this analysis was Marquardt's method (Marquardt, 1944; Himmelblau, 1970). Marquardt's method is a compromise procedure which combines the method of steepest descent and the Gauss linearization method (Himmelblau, 1970). This procedure uses the steepest descent approach at the outset and the linearization in the final stages of computation. This algorithm almost always converges and often at a faster rate than either of the two procedures alone. The computer program used was a non-linear regression analysis package in Fortran using Marquardt's method called UWHAUS (Jutan, 1987). The exact procedure followed for the estimation of model parameters is outlined in steps as follows:

Step 1: The initial estimates for the parameters were identified using initial guesses as described earlier.

Step 2: The set of coupled equations (Equations 3.25 to 3.28) were solved numerically using these initial estimates along with specified initial values of substrate, cells, and product. Fourth Order Runge Kutta method was used as described earlier.

Step 3: Initially, the response test variable used was the sum of three response variables S, X, and P. However, this procedure was not found to be very effective, therefore only the cell concentration X

was used as the test variable to compare the experimental data.

Step 4: Using Marquardt's method, the parameter estimates were revised and using these revised estimates, the procedure was repeated from Step 2.

Step 5: This iterative procedure was continued until the sum of squares converged to its minimum value.

A set of parameter values was thus obtained from each of 7 batch runs at different growth temperatures.

3.6 Continuous Cultivation of Microorganisms

In this section, the principles of continuous, steady state cultivation of microrganisms in a bioreactor are considered. The continuous cultivation of a culture of bacteria is carried out in the chemostat or the continuous, stirred tank bioreactor (CSTBR). A schematic representation of the principle of continuous cultivation of microrganisms is shown in Figure 3.4. In the CSTBR, the liquid (culture) volume is always kept constant at V_L. Fresh medium consisting of a limiting substrate, S (g/L) and other essential nutrients, is continuously introduced into the CSTBR at a constant feed rate F (L/h). The inlet feed rate is also equal to the rate of removal of cells from the CSTBR. The cell concentration in the CSTBR is denoted by X (g/L). In the inlet stream to the CSTBR, X = 0, and S = S_0 is constant.

A mass balance on the cells in the CSTBR yields:

$$\textit{Net increase of cells} = \textit{growth} - \textit{output} \qquad (3.33)$$

Or this can be written as:

$$V_L \cdot \frac{dX}{dt} = V_L \cdot \mu \cdot X - F \cdot X \qquad (3.34)$$

Figure 3.4. Schematic Diagram of the Continuous Stirred Tank Bioreactor System (CSTBR). The cell and growth limiting substrate concentrations are shown by symbols X and S respectively. The culture volume is denoted by V_L, which is held constant. The constant volumetric feed rate of the fresh medium into the CSTBR is F which is equal to the rate of removal of culture from the bioreactor vessel.

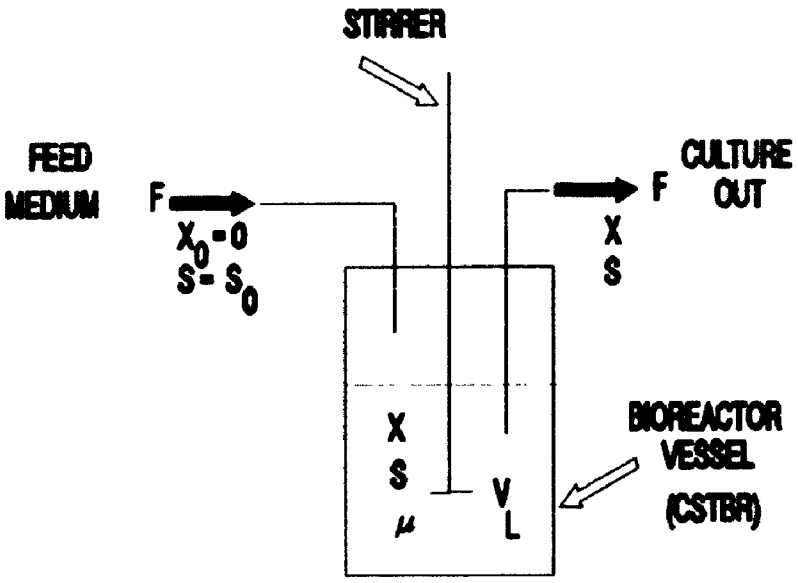
STIRRER
FEED
MEDIUM
F
$X_0 = 0$
$S = S_0$
F
CULTURE
OUT
X
S
X
S
μ
V
L
BIOREACTOR
VESSEL
(CSTBR)

We define the dilution rate, D (h^{-1}) as the ratio of feed rate F (L/h) to the bioreactor volume, V_L, or $D = F/V_L$. Thus dividing both sides of Equation 3.34 by V_L, and replacing F/V_L by the dilution rate, D, we get Equation 3.35.

$$\frac{dX}{dt} = (\mu - D).X \qquad (3.35)$$

Under steady flow conditions, there is no change in cell concentration X with time t in the bioreactor. Hence the L.H.S of equation 3.35 is zero. Therefore equation 3.35 becomes:

$$\mu = D \qquad (3.36)$$

Thus under steady state conditions, the dilution rate equals the specific growth rate of the cells. By increasing D, therefore, μ can be increased. However, since μ cannot be increased beyond the maximum specific growth rate of the cells, μ_{max}, for a given inlet substrate concentration S_0, a value of D higher than μ_{max} will make the L.H.S. of equation 3.35 negative. The cell concentration will then decrease to zero. This condition, i.e., $D > \mu_{max}$ will therefore lead to a condition known as "washout" of cells.

Making a mass balance on the limiting substrate, S we have:

$$\begin{matrix}\textit{net decrease}\\ \textit{of}\\ \textit{limiting substrate}\end{matrix} = \textit{input} - \textit{output} + \textit{consumption} \qquad (3.37)$$

Or:

$$\frac{dS}{dt} = D.S_0 - D.S - \frac{\mu X}{Y_{x/s}} \qquad (3.38)$$

Here $Y_{x/s}$ is the cell yield coefficient, g cells formed/ g substrate consumed. In Equation 3.38, substrate utilization for product formation is not accounted for. However, equation 3.38 may be easily modified to also include terms for product formation. Under steady state conditions, the L.H.S of equation 3.38 is zero, therefore:

$$D(S_0 - S) - \frac{\mu . X}{Y_{x/s}} = 0 \qquad (3.39)$$

Thus equations 3.36 and 3.39 define steady state conditions in the CSTBR.

CHAPTER 4

MATERIALS AND METHODS

4.1 Bacteria

Pseudomonas syringae pv. syringae cit 7 was obtained from our culture collection in the laboratory. The culture was originally obtained from Dr. S.E. Lindow, Department of Plant Pathology, University of California, Berkeley. Three other P. syringae strains named PDDCC461, 5D19, and 5D4132 were kindly provided by Dr. D. Cuppels, Agriculture Canada Research Centre, London, Ontario. Table 4.1 lists the origin of these strains of P. syringae. The cultures were revived by incubation in 50 mL of nutrient broth (SIGMA Chemicals, St. Louis, Mo.) supplemented with 2.5% glycerol at 25° C and 200 RPM for 48 h. Absence of contamination was confirmed by microscopic observation as well as by nutrient agar-glycerol (NAG) streak plates (nutrient agar, Sigma Chemicals, St. Louis, Mo., + 2.5% glycerol). The strains were stored as lyophilized cultures at room temperature, or on King's Medium B agar (KBA) Petri plates or slants at 4° C. Table 4.2 lists the medium composition of King's Medium B (King et al., 1954). A loopful of cells from the master culture prepared as above was aseptically transferred to a 500 mL flask containing 100 mL of King's Medium B broth. The composition in listed in Table 4.2 was used except no agar was added during the preparation of the medium. This was then incubated for 48 h at 25° C and 200 RPM. The grown culture was used to streak 15 slants and 5 Petri plates. These slants were prepared in 15 X 30 mL, borosilicate, screw-cap test-tubes which

Table 4.1. Origin of *P. syringae* Strains Used in this Study

P. syringae strain	Habitat	Obtained from
PDDCC 461	Plum	ACRC, London
5D19	Cherry	ACRC, London
5D4132	Apricot	ACRC, London
cit 7	Orange	UC Berkeley

Table 4.2. Composition of King's Agar Medium B (KBA) (King et al., 1954)

Component	g/L
Proteose Peptone	20.0
Bactoagar	20.0
Glycerol	10.0
K_2HPO4	1.5
$MgSO_4.7H_2O$	1.5

contained 15 mL of slanted KBA medium. The slants (or plates) were incubated at 25° C for 3 days and kept in the refrigerator at 4° C until needed for inoculum development. Absence of contamination was confirmed by microscopic observation or NAG streak plates.

4.2 Medium Preparation

For routine propagation of cultures, King's Medium B agar (KBA) was used (composition in Table 4.2). Except in medium composition studies or unless otherwise indicated, a chemically defined medium comprising of sucrose (SIGMA) 5 g/L, ammonium phosphate 2.5 g/L, K_2HPO_4 3.5 g/L, KH_2PO_4 1 g/L, and $MgSO_4.7H_2O$ 0.1 g/L (pH 7.0) was used as the standard culture medium in the bioreactor. Aerobic shake flask studies were conducted with various carbon and nitrogen sources as described later. The medium used in all other shake-flask studies was composed of sucrose (SIGMA) 5 g/L, peptone (DIFCO) 1 g/L, K_2HPO_4 3.5 g/L, KH_2PO_4 1.0 g/L, and $MgSO_4.7H_2O$ 0.1 g/L (SPM medium).

For comparing ice nucleation activity of P. syringae cit 7 cells grown on agar plates versus cells grown in broth culture, the following procedure was adopted: a volume of four hundred mL of SPM medium was distributed into 4 X 300 mL Erlenmeyer flasks in 100 mL aliquots and sterilized. Two percent agar was added to another 100 mL of this medium. This latter mixture was then sterilized and poured into Petri plates to make solid media for cell growth.

For cell growth studies in the 1 L bioreactor a chemically defined medium was used, i.e., sucrose 5 g/L, ammonium phosphate 2.5 g/L, K_2HPO_4 3.5 g/L,

KH_2PO_4 1.0 g/L, $MgSO_4.7H_2O$ 0.1 g/L. These components were dissolved in deionized, distilled water. One L of this cell growth medium was made in a 2 L Erlenmeyer, conical flask and the pH of the growth medium was then adjusted to 7.0 with 1 N HCl or 1 N NaOH.

For cell growth in the 15 L bioreactor, ten L of standard culture medium of composition sucrose 5 g/L, ammonium phosphate 2.5 g/L, K_2HPO_4 3.5 g/L, KH_2PO_4 1.0 g/L, $MgSO_4.7H_2O$ 0.1 g/L, were dissolved in deionized, distilled water and the pH adjusted to 7.0. The medium was placed in a 20 L polythene bottle and autoclaved at 121° C for 90 min. The medium was then cooled and aseptically transferred into the 15 L bioreactor.

4.3 Cell Growth Studies

First investigations were conducted in aerobic, shake flasks. Then P. syringae cit 7 cells were cultivated in the 1 L bioreactor under batch and continuous growth conditions. Finally, growth kinetics and INA of this bacterium was investigated in a 15 L bioreactor.

4.3.1 Investigations in Aerobic Shake Flasks

Single colonies of cit 7 cells from agar plates of King's B medium were used to inoculate 100 mL of sterile medium in 300 mL Erlenmeyer flasks. Cells were cultured aerobically for 48 h usually at 25° C, pH 7.0, at 200 RPM. At the end of this period, the P. syringae cells were harvested from the broth by centrifugation (8000 g, 15 min, SORVAL refrigerated centrifuge) and resuspended in phosphate buffer (PB) (0.05 M, pH 7.0).

4.3.1.1 Cell Concentration

P. syringae cit 7 cells grown on the SPM medium mentioned earlier, were resuspended in PB to 10^9 cfu per mL. This suspension was successively diluted to yield cell suspensions in the range of 10^3 - 10^8 cfu per mL. Each dilution was then tested for ice nucleation activity (INA).

4.3.1.2 Cooling Rate

All cooling rate studies were done using P. syringae cit 7 cells cultured as described above. The cells were resuspended in PB and the cell concentration of the suspension adjusted to 2.5 X 10^5 cfu/mL. Three successive samples of this bacterial concentration were placed in the cooling bath and subjected to cooling rates of 0.05° C, 0.20° C, and 1.0° C per min respectively. The INA of each sample was determined using the freezing drop method.

4.3.1.3 Investigation of INA of P. syringae cit 7 in Suspensions of Culture Medium, Phosphate Buffer, and Deionized Water

Cells were centrifuged at 10000 RPM for 15 min and resuspended in phosphate buffer(0.05M, pH 7.0). This step was repeated two more times, the second time the cells were resuspended in an equal volume of deionized water. Each time the cell concentration and INA were measured at a constant temperature and time of -4° C and 20 min. The INA of the bacteria free medium (which was the supernatant from step 1), sterile phosphate buffer and distilled water was also determined at -4° C for 20 min.

4.3.1.4 Comparison of P. syringae INA on a Petri Dish versus Aerobic, Shake Flask

Both solid and liquid samples were inoculated with a loopful of P. syringae cit7 culture and incubated for 7h, 24h, 45 h, and 58h at 25° C and pH 7.0. At the end of the incubation period, 5 mL of sterile SPM medium was poured onto 5 Petri plates and the lawn of growth extracted into solution using a sterile, bent Pasteur pipette. All cells (from both liquid and solid media) were resuspended in phosphate buffer (0.05M, pH 7.0). The $O.D_{600}$ for cells obtained from both solid and liquid phases was adjusted at 7 h to 0.10 (1×10^8) and at 24, 45 and 58 h to 0.9 (1×10^9 cells per mL). These suspensions were assayed for INA at a constant temperature of -4° C for 20 min.

4.3.1.5 INA of Different P. syringae Strains

P. syringae cit 7, PDDCC461, 5D4132, and 5D19 were cultured for 48 h at 25° C and pH 7.0. Re-suspensions of cells in phosphate buffer (0.05M and pH 7.0) were adjusted to a final concentration of 10^9 cells/mL (final $O.D_{600nm}$ of 0.9). These suspensions were immediately assayed for INA.

4.3.1.6 Growth Temperature, pH, and Aeration

Growth temperature studies were carried out by culturing cit7 cells in SPM medium at pH of 7.0 and at constant temperatures of 15° C, 25° C, 30° C, and 35° C. In each case, at the end of the growth phase,the cells were resuspended in PB and the $O.D_{600}$ of the suspension adjusted to 0.9. A similar procedure was

followed for pH and aeration studies. In pH studies, the medium pH was adjusted to 5.0, 6.0, 7.0, and 8.0 before inoculation with cit 7. In aeration studies, growth and INA production was investigated under microaerophylic, surface and forced aeration conditions.

4.3.2 Batch Growth Studies of P. syringae in a 1 L Bioreactor

A schematic diagram of the experimental set-up used is shown in Figure 4.1. The bioreactor consisted of a 1.6 L jacketed glass jar (Bellco) with two side ports and a stainless steel head-plate (316 SS) built at the U.W.O. mechanical shop. The bioreactor had a working volume of 1 L. The head-plate contained ports for dissolved oxygen and pH probes, as well as ports for acid /base /antifoam /inoculum introduction and a thermal well for temperature measurement. A condenser/air outlet was also provided in the head plate. The condenser for cooling outgoing air from the bioreactor was of the coil-in-jacket type with tap water circulating in the jacket to provide the cooling. The top of the condenser was packed with glass-wool and acted as a filter for the exhaust air.

Aeration was provided using the facility constant air supply. An inlet air filter made up of a 25 cm long glass tube assembly packed with glass wool fibres ensured that air supply entering the bioreactor was sterile. The air after passing through the inlet filter was introduced into the bioreactor via a sintered glass sparger. The contents of the bioreactor were stirred using a magnetic stirrer.

The dissolved oxygen level was monitored using a dissolved oxygen meter (Cole Palmer Instrument Co., Chicago, IL) connected to a polarographic oxygen

Figure 4.1. Schematic Diagram of the 1 L Bioreactor Used in Batch Cultivation of P. syringae cit 7

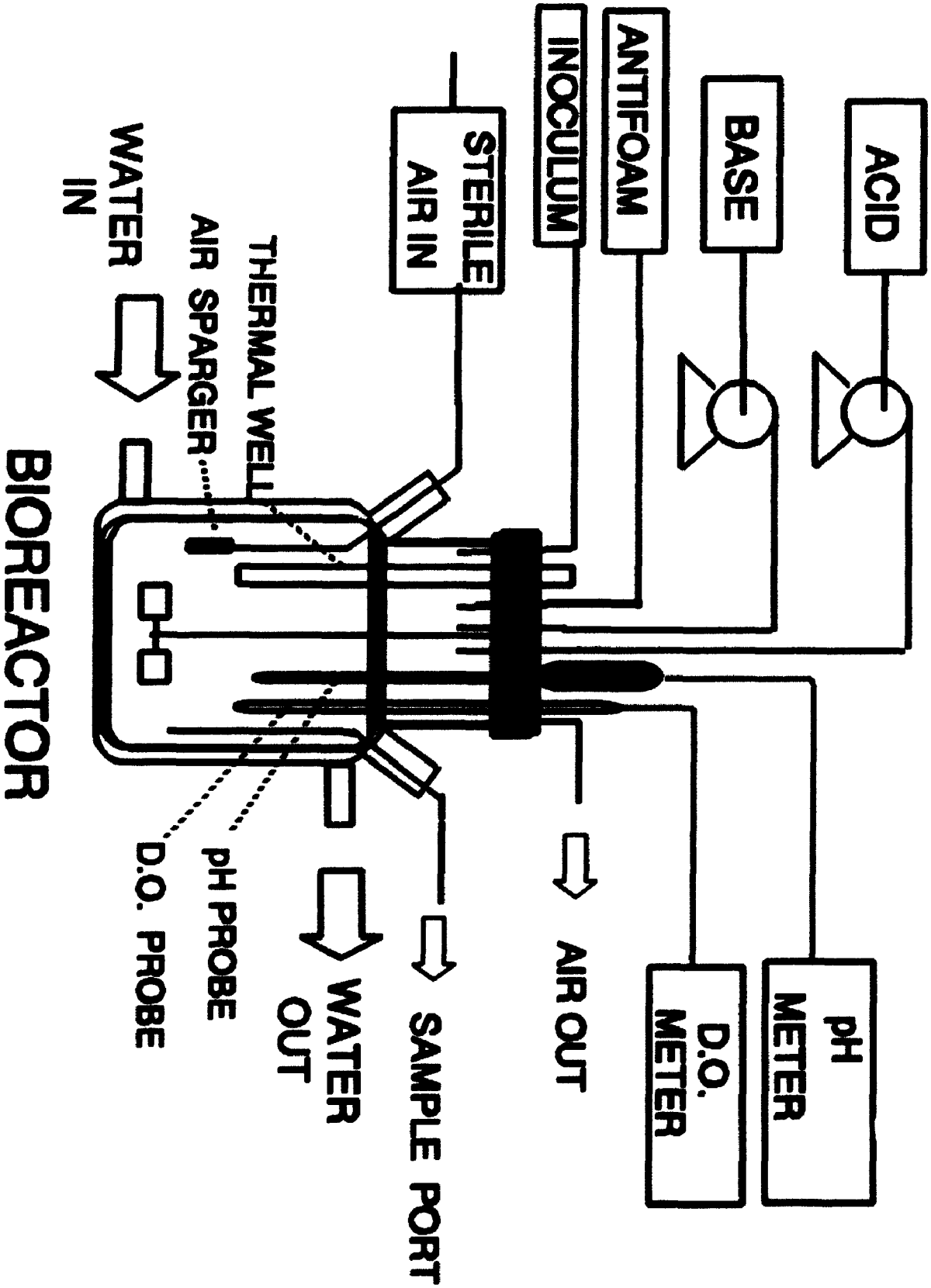
ACID
BASE
ANTIFOAM
INOCULUM
STERILE AIR IN
WATER IN
AIR SPARGER
THERMAL WELL
BIOREACTOR
D.O. PROBE
pH PROBE
WATER OUT
SAMPLE PORT
AIR OUT
pH METER
D.O. METER

probe (Cole Palmer Instrument Co., Chicago, IL.). Zero and one hundred percent saturation levels were calibrated after sterilizing the bioreactor contents and cooling to the desired fermentation temperature. Purging with oxygen free nitrogen (CANOX, London, Ont.) gave the zero percent saturation level. Aeration for 10 to 15 min gave the one hundred percent saturation level. Dissolved oxygen levels during the fermentation were maintained at greater than 10% of saturation by appropriately increasing the aeration rate.

The pH was monitored using a pH meter controller (New Brunswick Scientific, Edison, N.J.) connected to a Cole Palmer autoclavable pH probe. The probe was calibrated using pH 4, 7, or 10 colour key buffer solutions (BDH Chemical Ltd., Toronto, Ont.). The pH was controlled at 7.0 using 1 N HCl and 1 N NaOH solutions.

Antifoam was added to reduce excessive foaming which usually occurred during the late stationary phase of cell growth. A 1:5 volume mixture of antifoam B: HPLC grade water was supplied manually using a peristaltic pump connected to the bioreactor head-plate.

Temperature was controlled by circulating water from an aquarium at constant temperature. For temperatures below 25° C, the whole set-up (bioreactor + accessories) was placed in a constant temperature chamber (cold room) available at the Biochemical Engineering Research Laboratories at U.W.O. The temperature in the cold room environment could be accurately maintained (± 0.5° C) at temperatures ranging from 0° C to 25° C. In all studies, agitation in the bioreactor were maintained at 250 RPM.

4.3.2.1 Bioreactor Preparation and Sterilization Protocol

The protocol followed for preparing and sterilizing the bioreactor was as follows.

1) One litre of the growth medium was prepared as described previously.
2) Nine hundred and fifty mL of the prepared medium at pH 7.0 were then transferred to the 1 L bioreactor and the remaining 50 mL were transferred to a 300 mL Erlenmeyer flask to be used as inoculum.
3) The bioreactor was then fitted with all accessories including D.O. and pH probes and flasks for adding acid/base/antifoam/ and inoculum.
4) The bioreactor + contents + accessories were autoclaved at 121° C for 90 min.

4.3.2.2 Inoculum

Fifty mL of sterile medium was inoculated with a loopful of P. syringae culture from a KBA slant in a 300 mL Erlenmeyer flask. The flask was incubated at 25° C with shaking at 100 RPM on an orbital shaker under aerobic conditions for 24 h. At the end of this period, the cells were transferred to the 1 L bioreactor.

4.3.2.3 Sterility and Contamination Control

Checks for maintaining the growth of pure cultures were done in three ways: (i) Sterility plates: Before inoculation of medium, a sterile 2 mL sample was

withdrawn, and spread on a NAG Petri plate and incubated at 30° C for 48 h. The plate was checked at 24 h and 48 h for growth. Sterility was confirmed by no growth on the plates.

(ii) Streak plates: Using standard microbiological techniques, a streak plate was made at the end of each fermentation, to isolate bacterial colonies, and the plates were examined after incubation at 30° C, for 24 h and 48 h.

(iii) Microscopic examination and Gram stains: The sample of growing cells was examined microscopically and also by Gram staining to check for contaminating microorganisms.

4.3.3 Continuous Cultivation of P. syringae in the 1 L Bioreactor

Except for feed addition and product removal, the set-up was essentially as described in section 4.3.2. Due to the type of bioreactor configuration available, level control was achieved by using two peristaltic pumps, one each for the feed inflow and product outflow respectively, and a U- tube immersed in the bioreactor. Figure 4.2 illustrates how the continuous flow system operated to maintain a constant liquid level. The flow rate of the feed pump could be varied from 10 mL/h to 130 mL/h and accurately monitored. The product outflow pump always operated at a slightly higher flow rate than the feed inflow pump. When the level of the liquid in the bioreactor was higher than the neck of the U-tube, product flowed out through the U-tube. However, as soon as the level dropped below the U-tube, the outflow stopped until the feed inflow pump restored the liquid level once again to the top of the U-tube. Thus the feed pump controlled the product outflow through the bioreactor and maintained a constant level in the bioreactor.

Figure 4.2. Schematic Diagram of the Experimental Set-up Used for Continuous Cultivation of P. syringae cit 7 in the 1 L Bioreactor

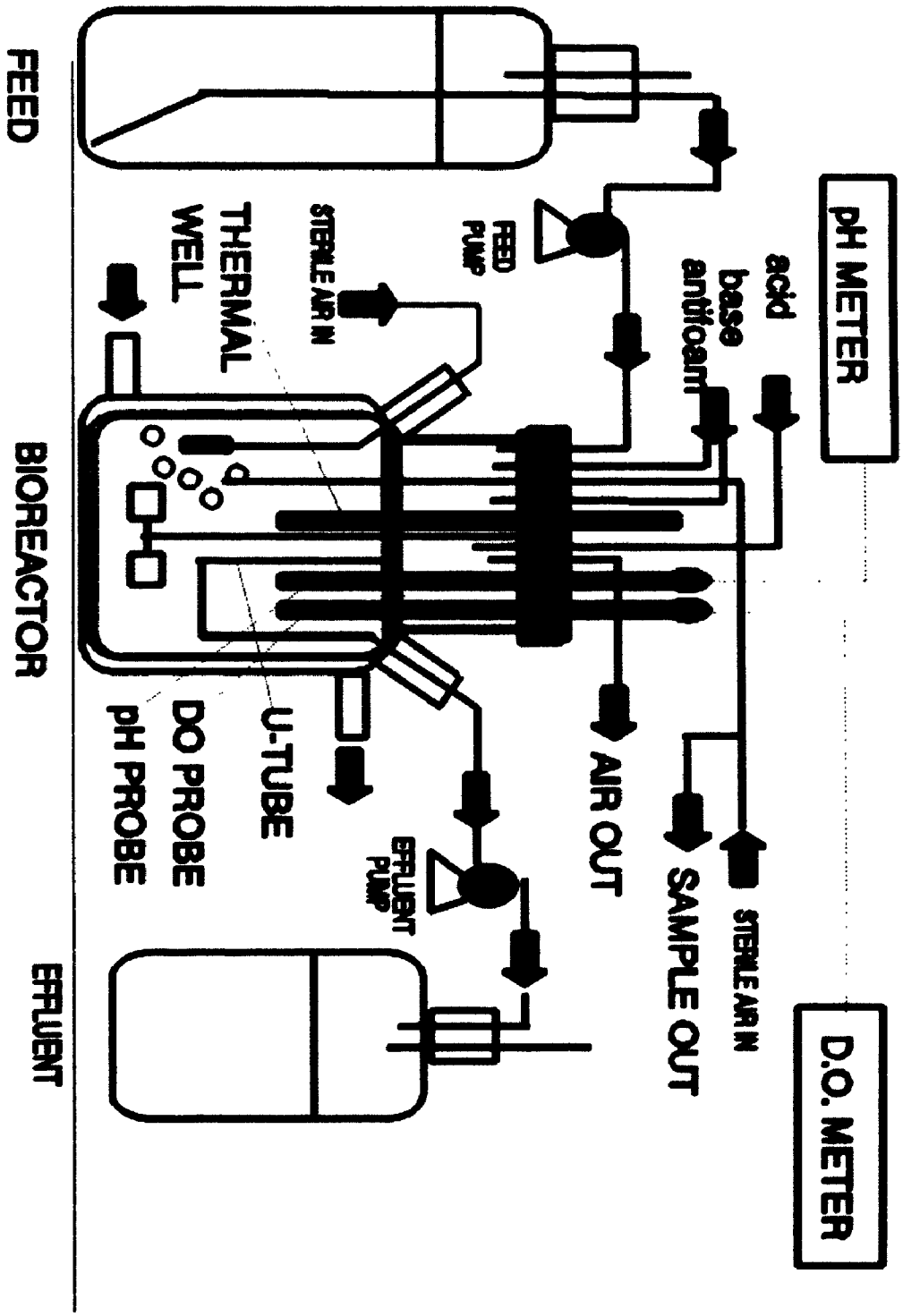
pH METER
D.O. METER
acid
base
antifoam
FEED PUMP
STERILE AIR IN
THERMAL WELL
AIR OUT
SAMPLE OUT
STERILE AIR IN
EFFLUENT PUMP
U-TUBE
DO PROBE
pH PROBE
FEED
BIOREACTOR
EFFLUENT

4.3.4 Batch studies in the 15 L bioreactor

The Biolafitte fermenter had a total volume of 15 L and a working volume of 12 L. A schematic diagram of the apparatus is shown in Figure 4.3. The fermenter vessel was mounted on a support module, the base of which carried the drive motor, (air) flowmeter, air inlet and outlet filters and a bank of valves for centralized distribution of steam, water, and air. The vessel and all components in contact with the culture medium were made of type 316 stainless steel. The vessel included a top flange with 6 swing bolts to secure the head-plate. Six standard (25 mm diameter) ports were included in the lower section of the vessel for temperature, pH, dissolved oxygen, and fluorosensor probes and sampling valves.

A rectangular viewing window was installed in the vessel front for convenient inspection of the contents. A pressure relief valve and graphite rupture disk were mounted on the upper wall of the vessel. The head-plate included a pressure gauge, and fittings for air inlet/outlet, antifoam/feed addition, and acid/base addition for pH control. A condenser was also provided on the air outlet line.

Filtration of air in/out was provided by sintered stainless steel cartridge filters, sterilizable in place by counter-flow of steam. The fermenter could be sterilized in place with steam. A control and monitoring unit coupled to an IBM-PC was used to monitor dissolved oxygen, and fluorescence signal as well as to monitor and control the pH, temperature, and RPM in the 15 L bioreactor. The BioChem Technology (Malvern, PA, U.S.A) fluorosensor was used to monitor cell NADH levels. The instrument was comprised of a steam sterilizable sensor unit

Figure 4.3. Schematic Diagram of Experimental Set-up for Batch Cultivation of P. syringae cit 7 Bacteria in the 15 L Bioreactor System

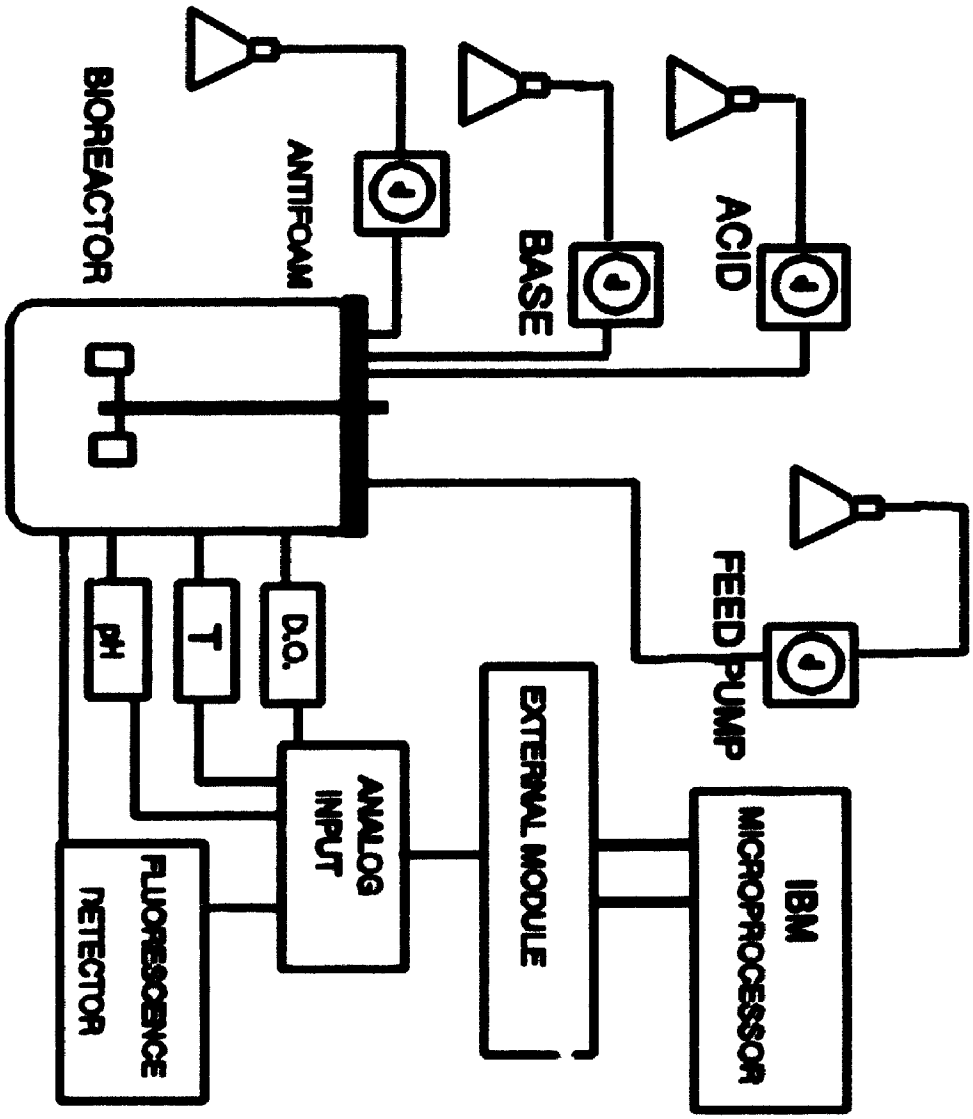
BIOREACTOR
ANTIFOAM
BASE
ACID
FEED PUMP
pH
T
D.O.
ANALOG INPUT
EXTERNAL MODULE
IBM MICROPROCESSOR
FLUORESCENCE DETECTOR

and came with standard fittings (25 mm i.d.) which allowed it to be easily attached to the bioreactor port. The optical head of the sensor unit was a thick quartz window which was in contact on one side with the fermentation broth. This window was held in place by a flange and could be subjected to in situ sterilization. The rest of the fluorosensor unit was placed into the bioreactor port after sterilization and cooling to the required temperature.

A loopful of P. syringae culture was introduced into 50 mL of pre-inoculum in a 300 mL Erlenmeyer flask. This was incubated for 48 h at 25° C. This pre-inoculum was added to 950 mL of sterile medium in a 2 L flask. This was incubated aerobically with shaking at 25° C for 36 h. Five hundred mL of this inoculum was then aseptically pumped to the bioreactor to initiate the fermentation.

4.4 Analytical Methods

The cell concentration pf P. syringae was determined as follows. Using sterilized pipettes, 0.1 mL of test sample was added to 0.9 mL of sterile phosphate buffer (0.1 M, pH 7.0) in a sterilized 10 mL capped tube. The contents were mixed using a vortex mixer. Similarly, further dilutions were made in the range of 10^{1} to 10^{9}. For each dilution, three 0.1 mL samples were spread on agar plates containing KMBA (King's Medium B Agar) using aseptic techniques. The agar plates were incubated for three days at 25° C and inspected for colonies between 30 - 300 per plate. Each cell formed a distinct colony in appropriately diluted samples. Thus the cell concentration for a given test sample could be estimated as: number of colony forming units (cfu) per mL X dilution factor.

Ten mL samples of fermentation broth were vacuum filtered through a 0.22 μm pore size filter disk which had been previously pre-dried and pre-weighed. The filter was then dried at 110° C for 24 h and reweighed. The bacterial dry weight was obtained by difference. A UV/VIS Perkin-Elmer Spectrophotometer was used to measure the optical density of fermentation broth at 600 nm.

Sucrose was estimated on a Waters HPLC using a Refractive Index Detector (Model 410) and a Carbohydrate Analysis Column (3.9 mm X 30 cm stainless steel column packed with amine-bonded, 10μ silica) (Waters #84038). The solvent used was Acetonitrile/Water (60:40 v/v) at a flow-rate of 1 mL/min. Sucrose was also estimated using the phenol-sulfuric acid method (Dubois et al., 1956). Two mL of test solution was placed in a 30 mL capped glass tube. One mL of 5% phenol (in water) and 5 mL of reagent grade, concentrated sulfuric acid was added and the contents were allowed to sit at room temperature for 30 min. At the end of this period, the absorbance at 488 nm was measured on a Phillips PU 8625 UV/VIS spectrophotometer. The blank used was 2 mL of distilled, deionized water + 1 mL 5% phenol + 5 mL conc. sulfuric acid. Standard curves for both techniques are included in Appendix IV.

4.5 Ice Nucleation Assay

The IN spectra of bacterial suspensions were measured using a procedure similar to that described by Vali (1971). A Neslab refrigerated bath containing as refrigerant a 50:50 mixture (by volume) of ethylene glycol and water was used. The temperature of the bath was either lowered at a constant rate or held constant at -

4° C for 20 min during which time the fraction of droplets frozen was recorded. The working surface for INA determination was provided by an aluminum dish (CanLab) floating in the bath. The surface was prepared by spraying it with a 1% w/v solution of paraffin in xylene and evaporating out the xylene. For INA measurement of growing cells, 5 mL samples from the bioreactor were resuspended in phosphate buffer (pH 7.0, 0.05M). Thirty drops of a suitable dilution of this cell suspension, 9.75 μL each, were placed on the Al surface for a constant time period of 20 min. After 20 min the fraction of droplets frozen, f, was recorded. An average of three repeats of f for each bioreactor sample was used to quantitatively estimate bacterial INA as described by Vali (1971). The results were expressed as cumulative ice nuclei concentration, η (ice nuclei per g cell DW) at -4° C where η is given by equation 3.24. Heat transfer from a single drop to the cooling bath was theoretically estimated. A schematic representation of the apparatus for the purpose of heat transfer calculations is shown in Figure 4.4.

The INA of the bacterial samples was reported as (a) the "droplet freezing spectrum" - a plot of fraction of droplets frozen, f, versus temperature of the cooling bath (θ° C); (b) the temperature at which all the droplets of a given cell suspension froze, θ_1 °C; or (c) the cumulative nucleus concentration, η using equation 4.1.

$$\eta = \frac{1}{V} \cdot \ln\left[\frac{1}{1-f}\right] \cdot \frac{1}{X} \qquad (4.1)$$

Figure 4.4. Schematic Diagram of the Drop Freezing Apparatus showing the Aluminum Dish in the Refrigerated Bath at a temperature of - θ ° C. Heat flow from a water drop 9.75 μL in volume, and initially at 25° C to the bath is shown.

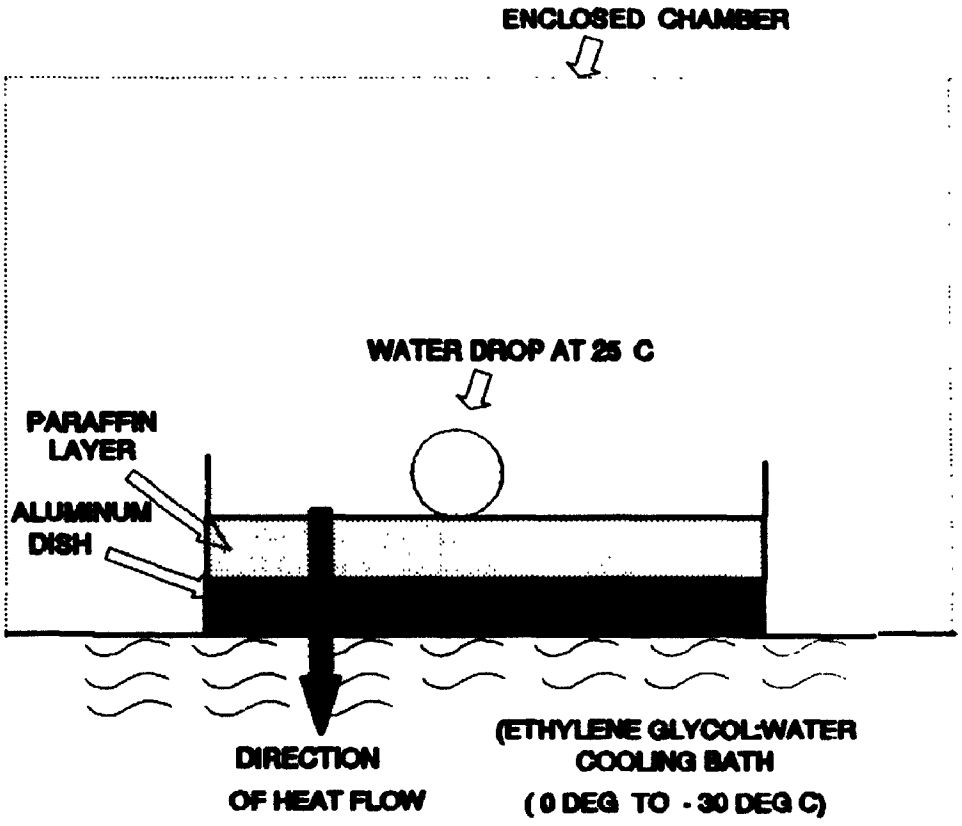
ENCLOSED CHAMBER
WATER DROP AT 25 C
PARAFFIN LAYER
ALUMINUM DISH
DIRECTION OF HEAT FLOW
(ETHYLENE GLYCOL:WATER COOLING BATH
(0 DEG TO - 30 DEG C)

where:

η = cumulative ice nuclei concentration (cumulative number of ice nuclei per g cell DW at -4° C)

f = fraction of droplets frozen

V = volume of an individual drop (9.75 μL)

X = cell concentration (g cell DW/L)

CHAPTER 5

RESULTS AND DISCUSSION

5.1 Introduction

Several experimental variables which can affect the freezing of drops containing ice nucleating (IN) bacteria were considered and are described in Section 5.2. The first series of experiments were done using aerobic shake-flasks to examine the effect of culture medium conditions on the ice nucleation activity (INA) of P. syringae, and are shown in section 5.3. In section 5.4, the results of batch and continuous cultivation of bacteria in a 1 L bioreactor are presented and analyzed. Batch growth in a 15 L bioreactor is also described in this section. Section 5.5 shows an unstructured, mechanistic model describing cell growth and INA in the 1 L bioreactor, and growth model simulations are also presented.

5.2 Variables Affecting Freezing of Drops containing Ice Nucleating (IN) Bacteria

In all experiments reported in this thesis, cells of P. syringae after cultivation on various growth media were always centrifuged, washed and resuspended in phosphate buffer (0.05 M, pH 7.0) before INA of the cells was measured using the drop freezing assay. Thus, the possible INA of spent media was excluded. Other possible variables which may affect the freezing of drops containing INA bacteria are the following:(a) phosphate buffer, and deionized, distilled water used; (b) heat transfer effects on water drops placed in the cooling bath; (c) cooling rate of the bath; (d) concentration of IN cells in a drop; and (e) the separation of cells from the growth media and their re-suspension into phosphate buffer. The effect of these variables on the freezing on drops containing IN bacteria are discussed below.

5.2.1 Ice Nucleation Activity (INA) of Phosphate Buffer and Deionized Water

INA of phosphate buffer and deionized, distilled water, was measured separately for the temperature range of interest in this thesis, i.e., 0° C to -10° C. Thirty drops each of phosphate buffer, and deionized, distilled water were exposed to temperatures of 0° C, -6° C, -8° C, and -10° C for a period of 20 min each on a paraffin coated, aluminum dish in a refrigerated bath as described in the Materials and Methods. Figure 5.1 shows that phosphate buffer and water drops did not freeze in the temperature range 0 to -10° C. However, freezing of phosphate buffer and water drops was observed at temperatures below -10° C. This is due to the

Figure 5.1. Test for the Freezing of Control Drops of Deionized Distilled Water and Phosphate Buffer (0.05 M, pH 7.0).

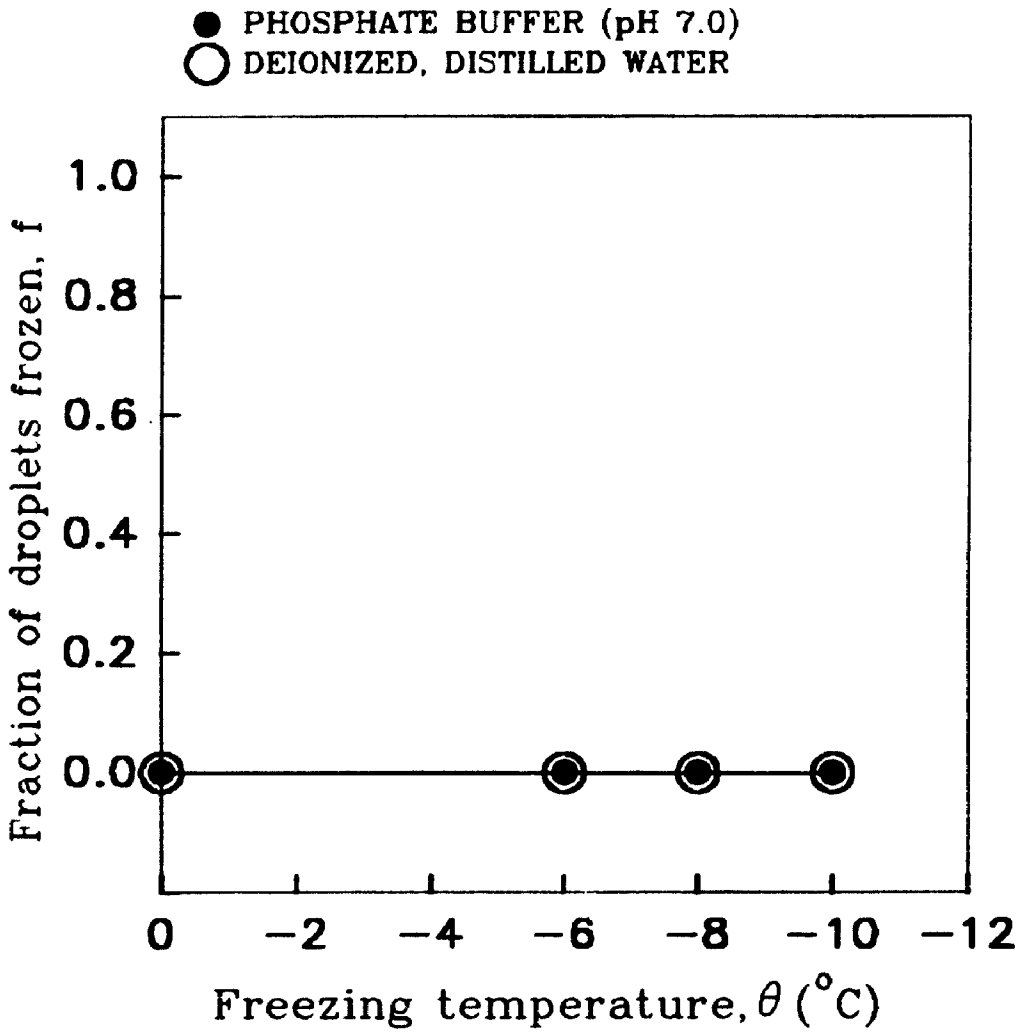
PHOSPHATE BUFFER (pH 7.0)
DEIONIZED, DISTILLED WATER
Fraction of droplets frozen, f
1.0
0.8
0.6
0.4
0.2
0.0
0
−2
−4
−6
−8
−10
−12
Freezing temperature, θ (°C)

fact that at temperature ranges below -10° C, many common heterogeneous ice nuclei become active, e.g., dust particles, which may initiate ice formation.

The use of a paraffin layer to coat the surface of the aluminum was necessary as the paraffin coating ensured a hydrophobic environment and prevented "travelling" ice which moves along minute cracks on the aluminum surface. Such moving ice crystals can travel from a frozen to an unfrozen drop and cause nucleation to take place.

5.2.2 Heat Transfer Effects During the Freezing of Water Drops Containing Ice Nucleating Bacteria

When drops containing IN P. syringae were placed on the surface of a paraffin coated, aluminum dish, and exposed to a low temperature θ° C, they were subject to freezing due to the presence of bacterial ice nuclei which were active at their characteristic temperature, θ° C. At a given constant temperature of θ° C, however, it was noted that the freezing of drops was time dependent. Some drops were observed to freeze almost immediately, while the remaining drops (of a total fraction, f, which froze at θ °C in 20 min) were observed to freeze on average in less than 5 min. However, there was no typical, observed time dependence pattern of freezing of water drops containing IN bacteria exposed to 20 min in a freezing bath at any constant temperature θ° C. It was reasoned therefore, that either (a) heat transfer effects on drops placed in the cooling bath or (b) actual physical limitations of orientation of the INP on the bacterial

membrane surface may have contributed to the above-mentioned observed freezing process.

A systematic perusal of the literature showed that no previous researchers have studied the effects of heat transfer rates on the freezing of water drops containing IN bacteria. In this study, an unsteady state, theoretical analysis of heat transfer was performed for the cooling of water drops containing IN bacteria, initially at 25° C (room temperature) and placed on a paraffin coated aluminum dish in a refrigerated bath at -4° C. The details of this analysis are provided in the Appendix B. The temperature of -4° C was chosen as this was a typical temperature in most measurements of bacterial INA. At temperatures lower than -4° C, faster heat transfer from the drops to the bath would occur due to a greater (temperature) gradient between the water drop and the infinite heat sink (refrigerated bath). The warmest ice nucleation temperature observed was -2.5° C and very few bacterial ice nuclei were active at this temperature.

A schematic of the drop freezing apparatus used as a basis for these heat transfer calculations is shown in Figure 4.4. The heat transfer calculations were performed assuming a single water drop, 9.75 μL in volume resting on a 0.13 mm (measured) thick paraffin layer.

The results of the heat transfer calculations indicated that the water drop containing INA bacteria, initially at 25° C, when placed in a cooling bath at -4° C, would reach the temperature of the bath in 30 sec or less. Therefore heat transfer from a small drop of volume 9.75 μL to a 5 L (infinite) heat sink at a constant,

controlled temperature of -4° C, was very rapid and heat transfer limitations on the freezing of water drops can be neglected.

Therefore, if heat transfer limitations are excluded, the observed time dependence of the freezing of drops at a constant temperature θ° C may be a function of (1) an asymmetric distribution of INA among various drops; (2) the orientation of the ice nucleation protein (INP) on the membrane surface; (3) orientation of bacteria in the drop; (4) physical location of the bacteria etc. All these factors may play a role in the observed freezing of drops at a constant temperature of θ° C. The analysis of the effect of these variables was beyond the scope of this thesis and is included as a recommendation for further studies.

5.2.3 Effect of Cooling Rate of the Bath on the Freezing of Drops containing INA Bacteria

Previously, the effect of bath cooling rate on the freezing of drops containing IN bacteria has not been investigated. If the temperature of the cooling bath changes at a rate which approaches the time required for heat transfer from the water drop, the temperature of the drop may lag the measured temperature. This may affect the results of the ice nucleation measurements.

In this study, the dependence of the drop freezing spectrum (i.e., a plot of fraction of drops freezing f vs. freezing temperature, θ° C) of P. syringae on the cooling rate of the bath was investigated. Figure 5.2 shows the effect of cooling rate of the refrigerated bath on the freezing of drops containing IN bacteria. An identical concentration of cells of IN P. syringae cit 7 was used for each cooling

Figure 5.2. Fraction of Drops Freezing, f, versus Freezing Temperature, θ° C, as a Function of the Cooling Rate of the Refrigerated Bath.

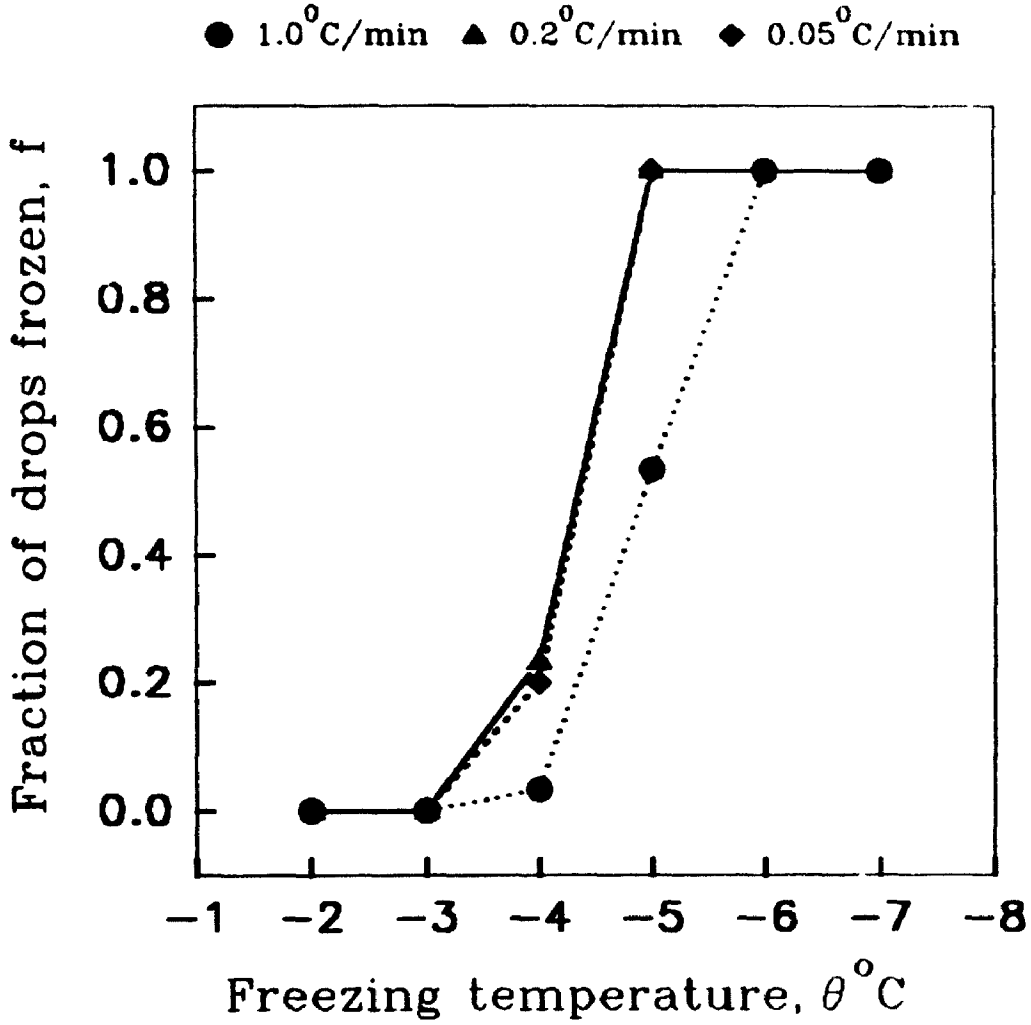
● 1.0°C/min ▲ 0.2°C/min ◆ 0.05°C/min
Fraction of drops frozen, f
1.0
0.8
0.6
0.4
0.2
0.0
−1 −2 −3 −4 −5 −6 −7 −8
Freezing temperature, θ °C

rate as described in Materials and Methods. Figure 5.2 shows that at a cooling rate of 1° C/min, there is a greater spread in the observed drop freezing spectrum, than at the other cooling rates. This is most likely due to the fact that the temperature of the drop may lag the temperature of the bath at a cooling rate of 1° C per min (or higher) at least in this apparatus used.

Thus Vali's assumption that the freezing of drops is independent of the time rate of change of temperature (Vali, 1971) is probably valid only if the cooling rate is sufficiently slow. In all subsequent investigations in this study, a constant cooling rate of 0.05° C/min or a constant temperature and time i.e. -4° C for 20 min, was used.

Previous reported studies of IN bacteria have been carried out using various cooling rates, e.g., (a) drops held at -9° C for 2 min (Govindarajan & Lindow, 1988a); (b) 1° C/min (Obata et al., 1989); (c) 0.05° K/s (Dubrovsky et al., 1990); 5° K/min (Sikyta et al., 1988); (e) drops held at -5° C or -9° C for 3 min (Orser et al., 1985); (f) 0.2° C/min (Govindarajan & Lindow, 1988b) etc. In light of the results obtained in this work, it is also important to take into account the cooling rate of the refrigerated bath when comparing results from separate studies of IN bacteria.

5.2.4 Effect of Cell Concentration

Increasing the concentration of IN bacteria in a drop of water would increase the number of ice nucleation sites, hence enhance the probability of freezing of the drop. Indeed, previous studies with different bacteria have indicated that the freezing of drops is a function of cell concentration (Obata et al., 1987, Stewert and Bear 1988, Maki et al., 1974 and Lindow, 1983a). On the other hand, Dubrovsky et al. (1989) reported that INA was concentration independent.

Figure 5.3 is a plot of the concentration of cells of P. syringae cit 7 in each water drop of a sample of drops placed on a paraffin coated, aluminum dish, versus θ_1 , i.e., the temperature (° C) at which all the drops in the sample froze. Figure 5.3 indicates that by increasing the concentration of cells in a drop from 10^3 to 10^6 cells/mL, θ_1 can be increased from -12° C to -4° C. However, a "saturation" effect is noted at cell concentration greater than 10^6 cells/mL where the freezing events are independent of cell concentration. Thus, depending on the number of cells in a given drop of water, the freezing events may or may not depend on cell concentration e.g., the concentration of cells used by Dubrovsky et al. (1989) in their procedure may have exceeded the saturation value.

On the basis of the above observations, a new term is proposed, called the "saturation ice nucleation point", which is characteristic of a given bacterial strain grown at a particular set of growth conditions. At the "saturation ice nucleation" point", two new measurable parameters are defined, namely the saturation cell concentration x_{sat}, and the corresponding saturation freezing temperature, θ_{sat}, for 100% freezing. In figure 5.3, $x_{sat} = 10^6$ cells/mL and $\theta_{sat} = -4°$ C.

Figure 5.3. Effect of Cell Concentration of P. syringae Cit 7 on θ_1, the Temperature for 100% Drop Freezing, i.e., at f = 1, where f is the fraction of drops freezing.

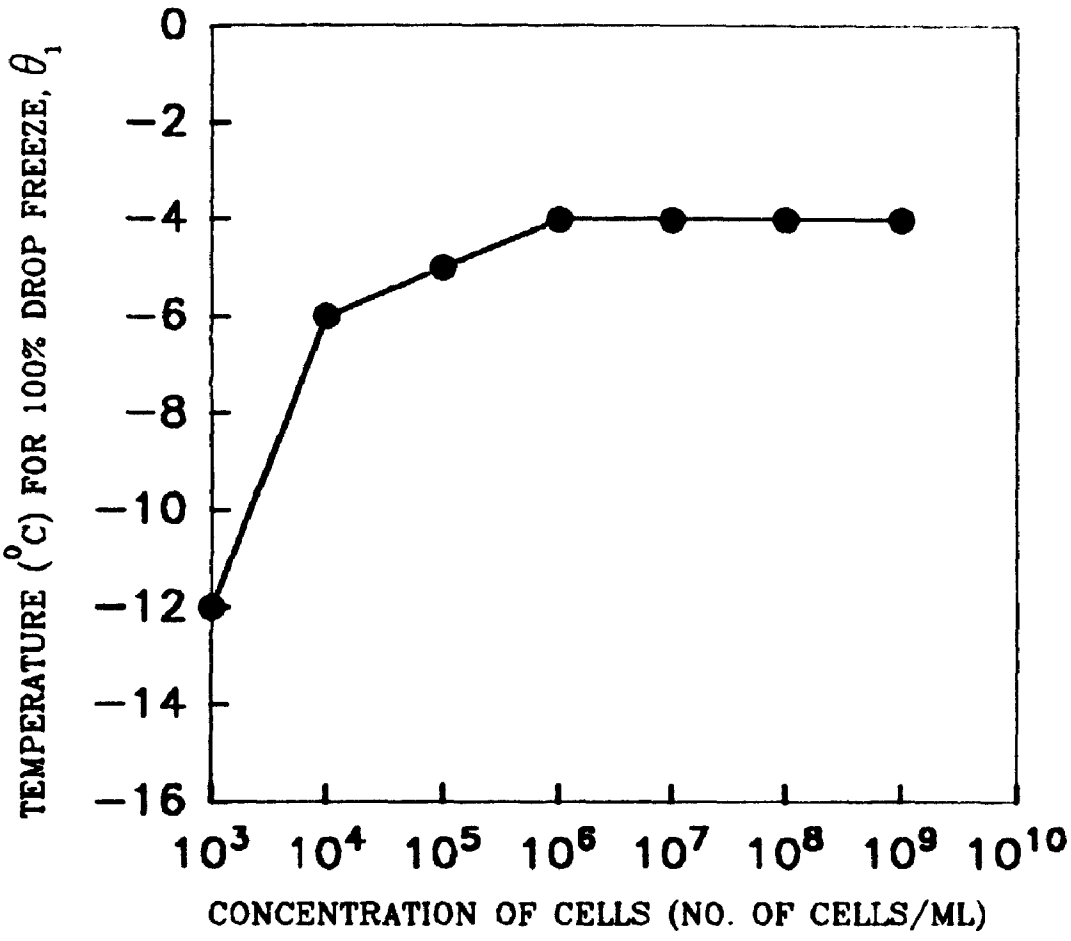
TEMPERATURE (°C) FOR 100% DROP FREEZE, θ_1
0
−2
−4
−6
−8
−10
−12
−14
−16
10^3 10^4 10^5 10^6 10^7 10^8 10^9 10^{10}
CONCENTRATION OF CELLS (NO. OF CELLS/ML)

At high concentrations in the drop, greater than θ_{sat}, the cells are closely packed, hence only a certain maximum number of ice nucleation sites can be exposed for interaction with water molecules. At concentrations less than the saturation value, x_{sat}, fewer active ice nuclei are available hence lower values of θ_1 are obtained.

The saturation value of $x_{sat} = 10^6$ cells /mL for P. syringae cit 7 (in Figure 5.3) may be used as a new criterion for optimum cell density in bacterial ice nucleation applications such as snow making. Thus, it would not make economical sense in snow making to use cell densities higher than x_{sat}, without further improvement in INA, i.e., further increases in the freezing temperatures of all drops.

5.2.5 Ice Nucleation Activity (INA) of P. syringae cit 7 in Suspensions of Culture Medium, Phosphate Buffer, and Deionized Water

INA of the P. syringae cit 7 cells was determined in culture medium, phosphate buffer (0.05 M, pH 7.0), and deionized water as described in Materials and Methods. INA of the bacteria-free medium, sterile phosphate buffer and distilled water was also determined at -4° C. Table 5.1 shows the comparison of INA of P. syringae cit 7 cells in culture medium, and in suspensions in 0.05 M phosphate buffer and deionized water. As seen in Table 5.1, no significant differences could be noted in INA of the bacteria in different suspensions. This investigation showed that INA only resided on the cells of P. syringae and was not due to the culture supernatant, phosphate buffer, or deionized water.

On the basis of the literature surveyed, there is no reported evidence that P. syringae releases the INP into the culture medium. The only bacterium which

Table 5.1. Ice Nucleation Activity (INA) of P. syringae cit7 in Suspensions of Culture Medium, Phosphate Buffer, and Deionized Water.

TEST CONDITION	CELL CONCENTRATION (CFU/ML)	BACTERIAL INA* (Ice nuclei per cell)
Cells in medium after 48 h of growth	2.33×10^9	1.13×10^7
Cell suspension in phosphate buffer (1st wash)	1.96×10^9	1.09×10^7
Cell suspension in phosphate buffer (2nd wash)	1.57×10^9	1.30×10^7
Cell suspensions in deionized water (3rd wash)	1.35×10^9	1.42×10^7
Cell free medium	0.00	0.00
Phosphate buffer (pH 7.0, 0.05 M)	0.00	0.00
Deionized water	0.00	0.00

*: INA defined here as $K(\theta)$/ cell concentration determined at -4° C for 20 min. Units: cumulative nos. ice nuclei per L/ cfu per L = cumulative nos. of ice nuclei per cfu.
$K(\theta)$ defined by Equation 3.23.

Growth conditions: P. syringae cit 7 grown on sucrose 5 g/L, ammonium sulfate 1.0 g/L, K_2HPO_4 3.5 g/L, KH_2PO_4 1.0 g/L, $MgSO_4.7H_2O$ 0.1 g/L, at 24° C, pH 7.0 for 48 h

is reported to shed membrane vesicles containing INA into the medium is Erwinia herbicola (Phelps, 1987). Break-up of the cell wall and cell lysis of P. syringae has been found to destroy INA in the bacterium (Warren, 1987). The non-release of the INP into the medium is a disadvantage in certain applications, e.g., in the food industry, because whole bacteria would then have to be used to initiate freezing. One application where whole but non-viable cells of P. syringae are used is grain preservation (by freeze killing of insect pests). This has been done using cells of P. syringae which were previously killed by UV radiation (Fields, 1991).

5.2.6 Summary

It was found in this study that phosphate buffer, and deionized distilled water used, had no effect on the freezing of drops containing IN cells of P. syringae. Heat transfer effects on water drops placed in the cooling bath can be ignored if the drops are held at a given freezing temperature θ °C for 20 min. The cooling rate of the bath was found to affect the drop freezing spectrum at cooling rates of 1° C per min but not at lower cooling rates investigated. At and above a cell concentration of 10^6 cells/mL of IN cells in a drop, INA was found to be independent of concentration. The separation of cells from the growth media and their re-suspension into phosphate buffer did not affect the measurement of bacterial INA.

5.3 Effect of Culture Conditions on INA of P. syringae

Several previous studies on the effect of culture conditions on bacterial INA have been reported (Obata et al. (1987); O'Brien and Lindow (1988); Yankofsky et al. (1981); Stewart and Bear (1988); Maki et al. (1974); Dubrovsky et al. (1989); Obata et al. (1989); Rogers et al. (1987); Lynn and Noto (1988); Hendricks et al. (1988); Mueller et al. (1990); Kozloff et al.(1983)). However, the factors influencing the expression of the IN phenotype are still not completely understood. In a culture of IN bacteria not all cells express the phenotype at any one time; each individual cell may display a different INA as indicated by its threshold temperature, θ_{th}, i.e., the highest temperature at which it can nucleate ice. INA of cells may also change with time, growth conditions or post-growth treatment (Rogers et al. 1987). INA is also a function of cell genotype, varying from one bacterium to another and from one sub-strain to another (Warren, 1987). In this section, the results of the effect of culture conditions on the expression of INA in the ice nucleation bacterial strain, P. syringae cit 7 are considered.

5.3.1 INA of different P. syringae strains.

INA expressed by different strains of P. syringae was evaluated. Figure 5.4 shows the drop freezing spectrum i.e., plot of fraction of drops frozen, f versus freezing temperature, θ ° C for cells of P. syringae cit 7, PDDCC461, 5D4132, and 5D19 respectively. It was observed from the drop freezing spectra obtained, that INA expression was not identical for the four strains of P. syringae. Each P. syringae strain has a specific temperature range over which it was active in

Figure 5.4. Fraction of Drops Freezing, f, versus Freezing Temperature, θ °C, as a Function of P.syringae Strain.

Conditions: P. syringae cells cultured on sucrose 5.0 g/L, peptone 1.0 g/L, K_2HPO_4 3.5 g/L, KH_2PO_4 1.0 g/L, $MgSO_4.7H_2O$ 0.1 g/L in 300 mL Erlenmeyer flasks containing 100 mL of medium. The flasks shaken aerobically at 200 RPM for 48 h, 25° C, pH 7.0. Cells resuspended in phosphate buffer (0.05 M, pH 7.0) and adjusted to an O.D. (600 nm) of 0.9 which corresponded to 10^9 cells per mL, and immediately assayed for INA.

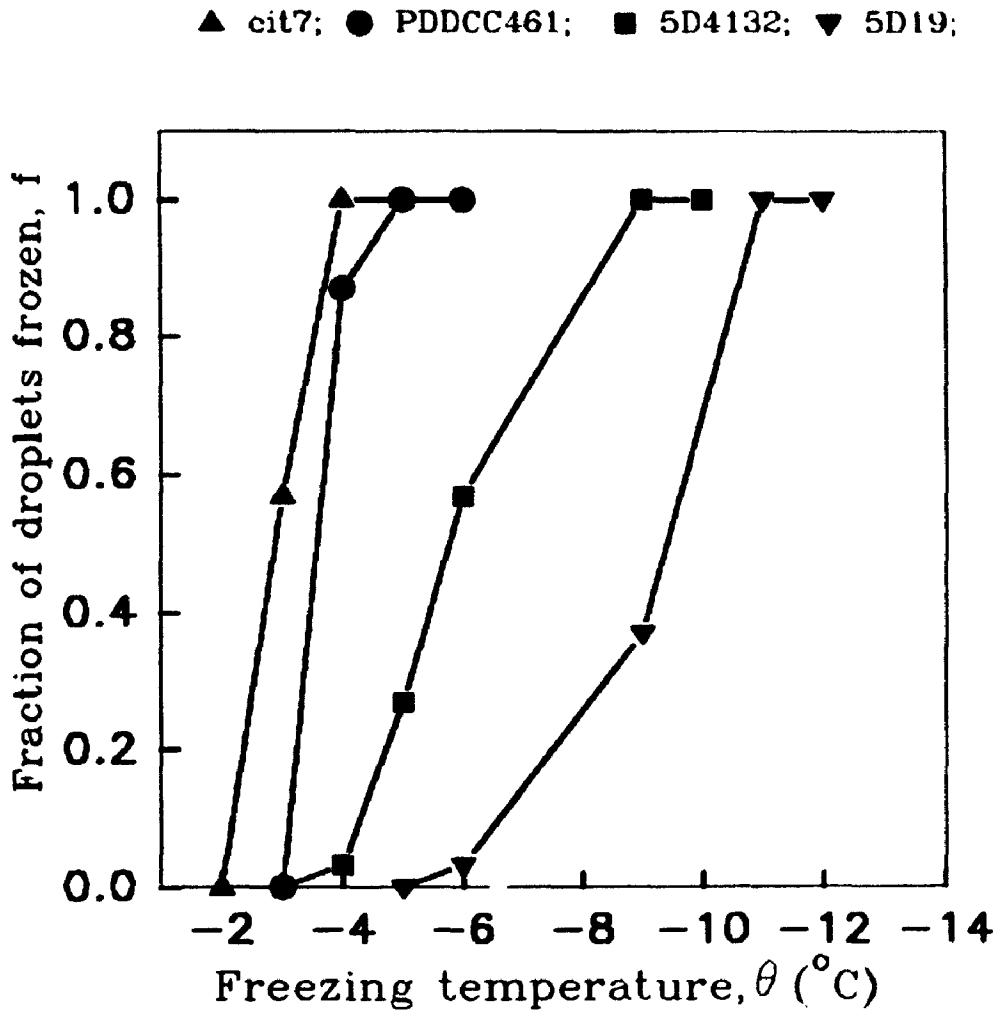
▲ cit7; ● PDDCC461; ■ 5D4132; ▼ 5D19;
Fraction of droplets frozen, f
1.0
0.8
0.6
0.4
0.2
0.0
−2
−4
−6
−8
−10
−12
−14
Freezing temperature, θ (°C)

initiating ice nucleation. In order of efficiency in promoting ice nucleation, the four strains are ranked as follows: cit 7 > PDDCC461 > 5D4132 > 5D19. Thus cit 7 was the most "efficient" in promoting ice nucleation, because it has INA in a higher freezing temperature range (-2° C to -3° C) compared to other strains. P. syringae 5D19 was only active in a temperature range of -5° C to -10° C. Differences in the ice nucleation gene may lead to variation in the expression of the INP. This may be a result of the diversity in terms of habitat and host plants where these bacteria are found P. syringae has been identified to have 41 different sub-groups (Dye et al., 1980). Not all of these 41 sub-groups possess INA. Thus a great heterogeneity in INA exists within P. syringae strains. In further studies reported in this thesis, only P. syringae cit 7 was used, due to its high level of INA expression.

5.3.2 Medium Composition

5.3.2.1 INA of P. syringae cit 7 Cells Grown on a Petri Dish versus Cells in Liquid Medium

INA of P. syringae cit 7 which had been cultivated on a Petri dish was compared with INA of these cells grown in aerobic shake flasks as described previously in the Materials and Methods. Figure 5.5 shows a plot of θ_1 (the temperature for 100% drop freezing) versus cell growth time in the shake-flask or Petri plate. The maximum INA was reached in 45 h and in all cases INA was higher in cells grown in liquid media than on a Petri dish. Thus growth on solid media does not result in higher INA than cell growth in aerobic shake flasks. The latter has additional advantages of providing accurate control of environmental

Figure 5.5. Temperature for 100% Drop Freezing, θ_1 °C, versus Growth Time, t, h, for P. syringae cit 7 Cells Growing in Aerobic Shake-Flasks or Petri Dish.

Conditions: P. syringae cit 7 cultured on sucrose 5.0 g/L, peptone 1.0 g/L, K_2HPO_4 3.5 g/L, KH_2PO_4 1.0 g/L, $MgSO_4.7H_2O$ 0.1 g/L in 300 mL Erlenmeyer flasks containing 100 mL of medium at 25° C, pH 7.0 and on Petri plates containing the above medium + 2% agar. Cells were resuspended in phosphate buffer (0.05 M, pH 7.0) and adjusted to 10^6 cells per mL at 7 h, and 10^9 cells per mL at 24, 45, and 58 h respectively. The cells were immediately assayed for INA.

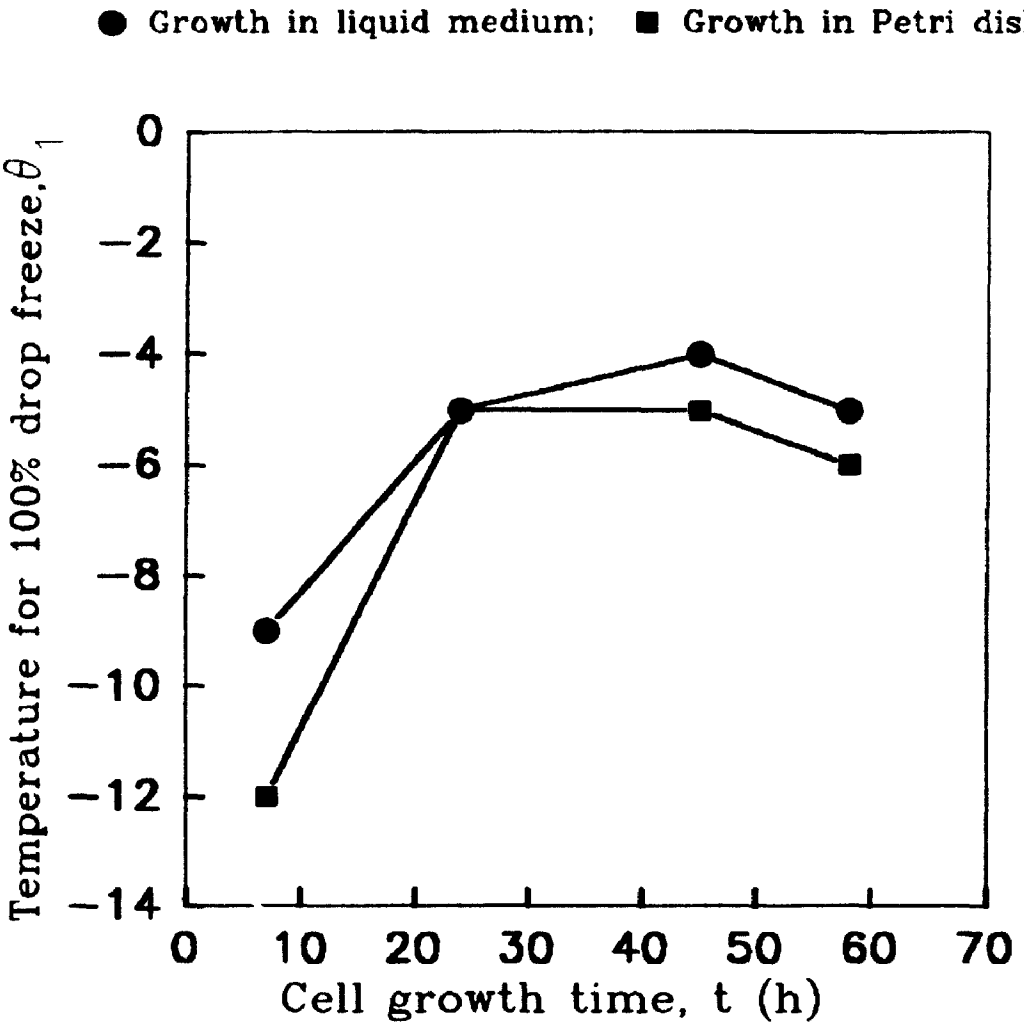
● Growth in liquid medium; ■ Growth in Petri dish
Temperature for 100% drop freeze, θ_1
0
−2
−4
−6
−8
−10
−12
−14
0
10
20
30
40
50
60
70
Cell growth time, t (h)

conditions as well as ease of scale-up to large scale bioreactors for the production of INA bacteria.

5.3.2.2 INA of P. syringae on Various Growth Media

A review of literature revealed that the components of the cell growth medium affect the expression of INA in bacteria (e.g. Maki et al., (1974); Lynn and Noto, (1988); Hendricks et al., (1988); Obata et al., (1987)). An evaluation for a suitable growth medium which promotes the production of INA in P. syringae cit 7, was therefore carried out. Cells were cultivated on glycerol, sorbitol, glucose, xylose, fructose, sucrose, sodium citrate and mannitol using ammonium sulfate, ammonium phosphate, Bacto-peptone and glutamic acid. Tables 5.2 to 5.5 describe the results of cultivating P. syringae cit 7 cells in various media.

The results are presented in three ways. First, threshold temperatures, θ_{th} are given, showing the temperature at which ice nucleation is induced by the most active nucleus in the culture. Thus higher values of θ_{th} indicate the presence of ice nuclei active at warmer temperatures. Second, the temperature at which all drops of a given sample freeze, θ_1 is given. Thirdly, the cumulative ice nuclei per g cell DW, η which are active at the threshold temperature, θ_{th} are reported. This value of η is calculated from the average of three measurements of fraction of drops freezing f, at the temperature θ_{th}.

In Table 5.2, the following carbon sources were investigated: glycerol (10.0 g/L); glucose (10.0 g/L); sodium citrate (16.0 g/L); fructose (10.0 g/L); sodium tart rate (37.5 g/L); xylose (10.0 g/L) and sodium acetate (22.0 g/L). These

Table 5.2. Effect of Carbon Sources in Growth Medium on the INA of P. syringae cit7 Using Ammonium Phosphate and Sulfate as the Nitrogen Sources

CARBON SOURCE (G/L)	θ_{th} (° C)	θ_1 (° C)	ICE NUCLEI PER G CELL DW, η, AT θ_{th}
Glycerol (10.0)	-4.0	-5.0	2.58×10^5
Glucose (10.0)	-4.0	-5.0	2.59×10^4
Sodium citrate (16.0)	-4.0	-6.0	4.83×10^3
Fructose (10.0)	-4.0	-6.0	1.74×10^4
Sodium tartarate (37.5)	-4.5	-6.0	1.22×10^4
Xylose (10.0)	-4.5	-9.0	8.48×10^3
Sodium Acetate (22.0)	-5.0	-12.0	6.95×10^3

θ_{th} = Threshold temperature at which freezing initiated

θ_1 = Temperature at which all droplets of the test sample froze

Constant components in the medium: Ammonium phosphate (2), $MgSO_4.7H_2O$ (0.1), $ZnSO_4.7H_2O$ (0.05), K_2HPO_4 (0.1), ammonium sulfate (0.1). All concentrations shown in brackets are in g/L.

CONDITIONS: P. syringae cit 7 cells grown for 48 h, 24° C at pH 7.0. Resuspended in phosphate buffer (0.05 M, pH 7.0) to an O.D. (600 nm) to same volume as original suspension in medium

Table 5.3. Effect of Carbon Sources in Growth Medium on the INA of P. syringae Cit7 with Ammonium Sulfate as Nitrogen Source

CARBON SOURCE (5 G/L)	θ_{th} (° C)	θ_t (° C)	ICE NUCLEI PER G CELL DW, η, AT θ_{th}
Sucrose	-3.5	-4.0	2.23×10^5
Glycerol	-4.0	-5.0	4.52×10^3
Sorbitol	-4.0	-5.0	1.37×10^6
Glucose	-4.0	-5.0	3.11×10^5
Sodium Citrate	-4.0	-5.0	4.24×10^4
Xylose	-4.0	-5.0	1.71×10^5
Fructose	-4.0	-5.0	6.78×10^6

θ_{th} = Threshold temperature at which freezing initiated

θ_1 = Temperature at which all droplets of the test sample froze

Constant components (g/L): Ammonium Sulfate (1), K_2HPO_4, (3.5), KH_2PO_4 (1), $MgSO_4.7H_2O$ (0.1)

CONDITIONS: P. syringae cit 7 cells grown for 48 h, 24° C at pH 7.0. Resuspended in phosphate buffer (0.05 M, pH 7.0) to an O.D. (600 nm) to same volume as original suspension in medium

Table 5.4. Effect of Carbon Sources in Growth Medium on the INA of P. syringae Cit7 with Bacto-peptone as the Nitrogen Source

CARBON SOURCE (5 G/L)	θ_{th} (° C)	θ_1 (° C)	ICE NUCLEI PER G CELL DW, η, AT θ_{th}
Sucrose	-2.5	-3.0	2.32×10^4
Sorbitol	-3.0	-4.0	5.35×10^3
Glucose	-3.5	-4.0	6.56×10^5
Fructose	-3.5	-4.0	9.45×10^5
Glycerol	-3.5	-4.0	9.50×10^4
Mannitol	-3.5	-4.0	3.63×10^4

θ_{th} = Threshold temperature at which freezing initiated

θ_1 = Temperature at which all droplets of the test sample froze

Constant components (g/L): Peptone 1.0,K_2HPO_4 3.5,KH_2PO_4 1.0,$MgSO_4.7H_2O$ 0.1,variable component 5 g/L

CONDITIONS: P. syringae cit 7 cells grown for 48 h, 24° C at pH 7.0. Resuspended in phosphate buffer (0.05 M, pH 7.0) to an O.D. (600 nm) to same volume as original suspension in medium

Table 5.5. Effect of Carbon Sources in Growth Medium on the INA of P. syringae cit7 with Glutamic Acid as Nitrogen Source

CARBON SOURCE (5 G/L)	θ_{th} (° C)	θ_1 (° C)	ICE NUCLEI PER G CELL DW, η, AT θ_{th}
Sucrose	-3.0	-4.0	5.23×10^4
Fructose	-3.0	-4.0	8.05×10^4
Sorbitol	-3.0	-4.0	6.18×10^4
Sodium citrate	-3.0	-4.0	3.49×10^4

θ_{th} = Threshold temperature at which freezing initiated

θ_1 = Temperature at which all droplets of the test sample froze

Constant components (g/L): Glutamic acid 2.0, K_2HPO_4 3.5, KH_2PO_4 1.0, $MgSO_4.7H_2O$ 0.1, carbon source 5 g/L

CONDITIONS: P. syringae cit 7 cells grown for 48 h, 24° C at pH 7.0. Resuspended in phosphate buffer (0.05 M, pH 7.0) to an O.D. (600 nm) to same volume as original suspension in medium

Table 5.6. Effect of Sucrose Concentration in Growth Medium on the INA of P. syringae Cit7

CARBON SOURCE (G/L)	θ_{th} (° C)	θ_1 (° C)	ICE NUCLEI PER G CELL DW, η, AT θ_{th}
Sucrose (3.0)	-2.5	-3.0	1.12×10^4
Sucrose (5.0)	-2.5	-3.0	7.09×10^3
Sucrose (7.0)	-2.5	-3.0	8.48×10^3
Sucrose (9.0)	-2.5	-3.0	1.19×10^4

θ_{th} = Threshold temperature at which freezing initiated

θ_1 = Temperature at which all droplets of the test sample froze

Constant components (g/L): Peptone 1.0, K_2HPO_4 3.5, KH_2PO_4 1.0, $MgSO_4.7H_2O$ 0.1 g/L

CONDITIONS: P. syringae cit 7 cells grown for 48 h, 24° C at pH 7.0. Resuspended in phosphate buffer (0.05 M, pH 7.0) to an O.D. (600 nm) to same volume as original suspension in medium

Table 5.7. Effect of Nitrogen Sources in Growth Medium on the INA of P. syringae Cit7 using Sucrose as the Carbon Source

NITROGEN SOURCE (1 G/L)	θ_{th} (° C)	θ_1 (° C)	ICE NUCLEI PER G CELL DW, η, AT θ_{th}
Yeast Extract	-3.0	-4.0	1.33×10^5
Malt Extract	-4.0	-5.0	3.21×10^5
Sodium Nitrate	-5.0	-12.0	8.70×10^5

θ_{th} = Threshold temperature at which freezing initiated

θ_1 = Temperature at which all droplets of the test sample froze

Constant components (g/L): Sucrose 5.0, K_2HPO_4 3.5, KH_2PO_4 1.0, $MgSO_4.7H_2O$ 0.1.

CONDITIONS: P. syringae cit 7 cells grown for 48 h, 24° C at pH 7.0. Resuspended in phosphate buffer (0.05 M, pH 7.0) to an O.D. (600 nm) to same volume as original suspension in medium

weight compositions reported for each carbon source corresponded to 0.325 M carbon in each medium investigated. Table 5.2 shows that P. syringae cit 7 cells grown on glycerol as the carbon source had the highest INA among the various media, with a higher threshold temperature, θ_{th} as well as higher value of η. Cells cultured on sodium citrate, xylose and sodium acetate did not express INA as well as cells grown on the other media.

In Table 5.3, 5 g/L of sucrose, glycerol, sorbitol, glucose, sodium citrate, xylose and fructose respectively were used to culture P. syringae cells with ammonium sulfate as the nitrogen source. Cells cultured on sucrose were found to have a threshold temperature of θ_{th} of -3.5° C, indicating some warm temperature ice nuclei were being produced. Cells grown on the remaining carbon sources showed a θ_{th} of -4° C. Cells cultured on fructose, xylose, glycerol or sorbitol nad a higher INA than cells cultured on glycerol or sodium citrate.

In Table 5.4, sucrose, sorbitol, glucose, fructose,glycerol, and mannitol at 5 g/L respectively were used to cultivate P. syringae cit 7 cells with Bacto-peptone as the nitrogen source. With sucrose, a highest threshold temperature, θ_{th}, of -2.5° C was detected. Bacto-peptone being a complex medium, may have components which have a synergistic effect on the development of cellular INA at least with this strain of the bacterium. Cells grown on sorbitol had a threshold of -3° C. Higher values of θ_1 were also observed for all growth media. Among media which produced cells with ice nuclei active at -3.5° C, glucose or fructose in combination with Bacto-peptone produced ice nuclei concentration of 656000 and 945000 per g cell DW respectively.

In Table 5.5, glutamic acid was used as the sole nitrogen source, and sucrose, fructose, sorbitol or sodium citrate were investigated as carbon sources. In this case, all combinations produced cells with identical θ_{th} values. Differences in INA expressed as η , ice nuclei per g cell DW, among the different media were also found to be insignificant.

Based on medium composition studies of Table 5.2 to 5.5, it was decided to choose sucrose as the carbon source for growing P. syringae cit 7 cells. Four different concentrations 3.0 g/L, 5.0 g/L, 7.0 g/L and 9.0 g/L of sucrose were investigated for the effect of initial sucrose concentration on INA production. However, no differences in INA were noted in the cells as seen in Table 5.6.

In Table 5.7, three nitrogen sources were compared for their effect on bacterial INA of P. syringae cit7 using sucrose as the carbon source. Cells cultured on sodium nitrate did not express INA as well as cells grown on yeast extract. However threshold temperatures lower than -2.5° C were obtained in all three cases.

5.3.2.3 Summary and Discussion of Medium Composition Effects

P. syringae cells produced active ice nuclei after growth on all the media investigated (Table 5.2 to 5.7). The most suitable carbon and nitrogen sources were found to be sucrose and Bacto-peptone. Cells cultured on these medium components expressed a threshold of -2.5 ° C which was the highest among all media considered. Other suitable combinations included fructose and glutamic acid

and fructose and Bacto-peptone. Cells expressed INA poorly when media included sodium acetate, tartrate, malt extract or sodium nitrate as components.

The ice nuclei of P. syringae and other bacteria which are active in the temperature range of 0 to -10° C have been classified as Type I: active between 0° C to -5° C; Type II: active between -5° C to -8° C; and Type III: active at temperatures lower than -8° C (Yankofsky et al. (1981). In terms of such a classification, P. syringae produced Type I ice nuclei on most of the media in Tables 5.2 to 5.7. Type II and III ice nuclei were only produced if sodium nitrate was the nitrogen source.

Two questions arise from the above mentioned medium composition studies. (a) Is it the concentration or the nature of a carbon source,a more significant factor in the expression of INA? and (b) Why do certain medium components affect INA?

Obata et al., (1987) investigated the effect of medium composition on INA of Pseudomonas strain KUIN. In their study, thirteen different media were prepared by replacing the carbon source in Koser citrate broth by each of 13 carbon sources. A constant weight composition of 2.0 g/L of carbon source was used every time. These authors found that the highest threshold temperatures, θ_{th} were produced by cells grown on glycerol, erythritol, or sodium citrate. Since a constant 2 g/L of carbon source was used by Obata et al., (1987), the actual molar concentration of carbon may have varied in the different media employed. The observed heterogeneity in the expression of INA by Pseudomonas KUIN can be due to either the nature of the carbon source or the concentration of available

carbon. In Table 5.2 in this thesis, as mentioned, a constant carbon composition of 0.325 M was used. A variation in expression of INA by P. syringae cells grown on different carbon sources was still observed. Hence, it is possible that the nature of the carbon source in the growth medium may be a determining factor in the expression of bacterial INA.

The species Pseudomonas is extremely versatile, e.g., P. multivorans can utilize 108 of 146 diverse organic compounds as growth substrates (Ornston, 1971). Within a single Pseudomonas strain, there may be a multitude of catabolic pathways of various degrees of complexity. These ubiquitous bacteria readily adapt to varying environments. This metabolic flexibility suggests the ability to form inducibly large quantities of enzymes capable of catalyzing unique reactions. It is possible therefore that components of the medium used to grow IN cells may influence INP metabolism by regulation of allosteric intermediates. Further research into the metabolism of INP production is an important challenge which must be addressed to answer the above questions in a fundamental way.

It is also important to consider environmental conditions existing on host plants which are the natural habitat of P. syringae. Levitt (1980) reported that concentration of carbon components in leaves (e.g., sucrose, glycerol, mannitol etc.) varied seasonally. In particular, sucrose was found to accumulate with the onset of cold temperatures. It is suggested therefore that sucrose may be an inducer to cause the bacteria to produce greater amounts of ice nuclei.

Based on this study, molasses, a source of sucrose can be investigated as a cheap substrate for large scale production of P. syringae cit 7. This study

illustrates the importance of choosing an appropriate medium for cell growth which can lead to an improved expression of INA.

5.3.3 Growth Temperature

The effect of cell growth temperature on INA of P. syringae cit 7 cells was investigated in aerobic shake flasks. Figure 5.6 shows the fraction of drops frozen, f, at decreasing freezing temperature θ °C, for cells grown separately at 15° C, 25° C, 30° C and 35° C. It is seen in this figure that cells cultured at growth temperatures of 30° C and 35° C had a significantly lower drop freezing spectrum compared to cells grown at 15° C or 25° C. While Pseudomonas species can grow in the range of 0° C to 40° C, the effects of low growth temperatures on INA have not been reported in the scientific literature. Obata et al., (1987) investigated the effects of growth temperature on INA of P. fluorescens. The authors found that cells cultured at 25° C had higher ice nucleation temperatures than cells cultured at 30° C. Similarly, P. viridiflava cells cultivated at 25° C nucleated ice at -4° C while cells cultivated at 30° C nucleated ice only below -4° C (Obata et al., 1989). Mueller et al., (1990) cultured r-DNA E. coli bacteria containing the ice nucleation gene at 15° C, 23° C and 37° C. The concentration of INP clusters on the bacterial surface was visualized using immuno-fluorescent staining techniques. Cells grown at 37° C were found to have very low concentrations of INP clusters compared to bacteria grown at 15° C or 23° C. Our research with P. syringae cit 7 as well as the above mentioned previous studies showed that the temperature was also a significant factor in determining the expression of bacterial INA.

Figure 5.6. Fraction of Drops Freezing, f, versus Freezing Temperature, θ °C, as a Function of Cell Growth Temperature.

Conditions: P.syringae cit 7 cells cultured on sucrose 5.0 g/L, peptone 1.0 g/L, K_2HPO_4 3.5 g/L, KH_2PO_4 1.0 g/L, $MgSO_4.7H_2O$ 0.1 g/L in 300 mL Erlenmeyer flasks containing 100 mL of medium. The flasks shaken aerobically at 200 RPM for 48 h, 15,25, 30, 35° C, pH 7.0. Cells resuspended in phosphate buffer (0.05 M, pH 7.0) and adjusted to an O.D. (600 nm) of 0.9 which corresponded to 10^9 cells per mL, and immediately assayed for INA.

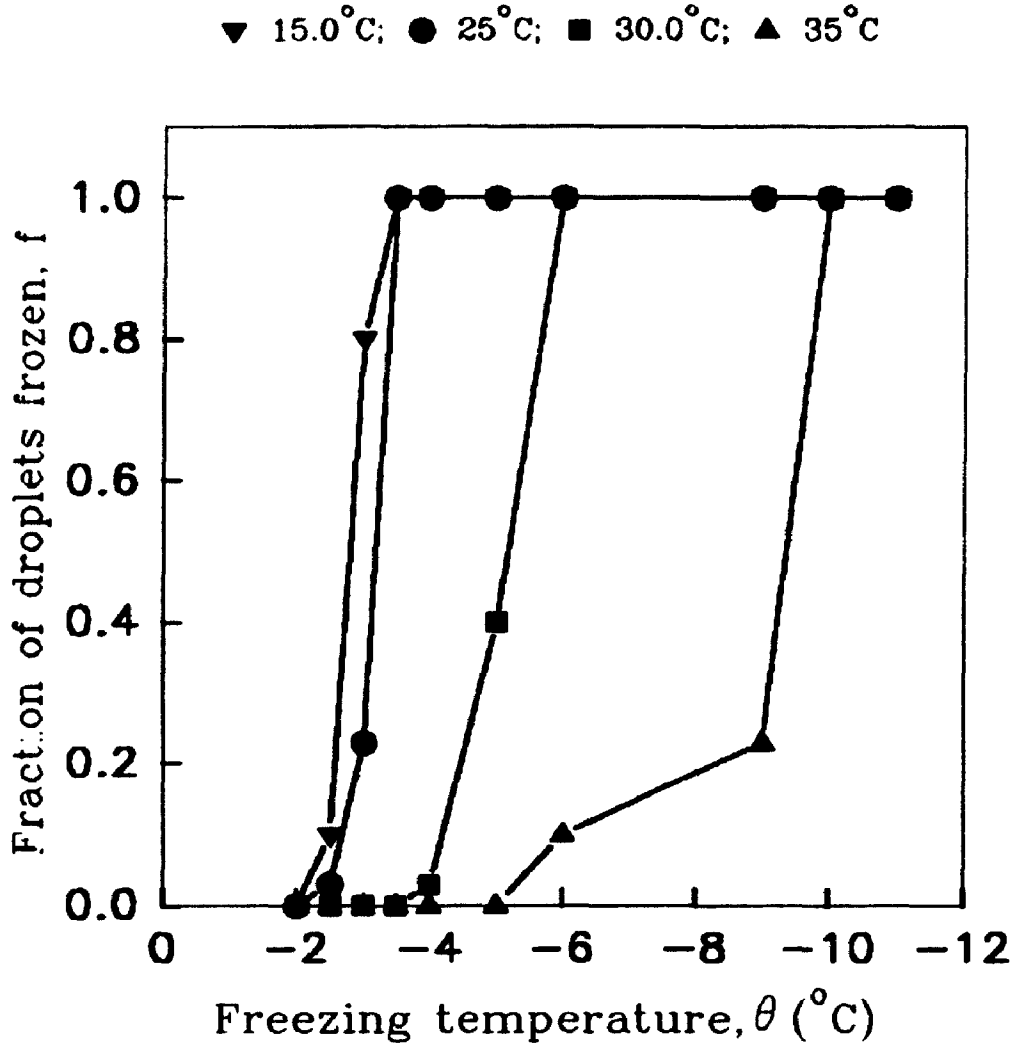
▼ 15.0°C; ● 25°C; ■ 30.0°C; ▲ 35°C
Fraction of droplets frozen, f
1.0
0.8
0.6
0.4
0.2
0.0
0
−2
−4
−6
−8
−10
−12
Freezing temperature, θ (°C)

5.3.4 pH

The effect of pH on INA of P. syringae cit 7 was investigated. Figure 5.7 shows a plot of f versus θ at different pH conditions. Cells grown at pH 8.0 had a lower level of INA than at pH 5.0, 6.0, or 7.0. Previously, Hendricks et al., (1988) identified an optimum pH range of 5.5 to 6.7 for producing P. syringae with a high expression of INA. Their reported results are similar to the results in Figure 5.7. Kozloff et al. (1983) also investigated the effect of pH on INA of P. syringae. These authors reported that a pH between 5.0 and 9.0 did not affect INA of bacterial cells. It should be noted however, that in their study the drop freezing tests for measurement of INA were conducted in a temperature range of -8° C to -12° C. At these low temperatures, other heterogeneous nuclei, e.g., dust particles may also initiate ice formation.

5.3.5 Aeration

Only one previous report has described the effect of aeration on INA. Ryder (1987) has found that changing the conditions from microaerophylic to surface aeration increased INA. The effect of aeration, therefore, was also considered in this study. Figure 5.8 shows the fraction of drops frozen, f, versus θ, for cells of P. syringae cit 7 grown under different aeration conditions. It can be seen that cit 7 cells grown under microaerophylic or surface aeration conditions had lower drop freezing spectra in the range of -3° C to -5° C compared to cit 7 cells cultured in flasks using forced aeration by bubbling air through the medium at two different

Figure 5.7. Fraction of Drops Freezing, f, versus Freezing Temperature, θ °C, as a Function of pH of the Medium.

Conditions: P.syringae cit 7 cells cultured on sucrose 5.0 g/L, peptone 1.0 g/L, K_2HPO_4 3.5 g/L, KH_2PO_4 1.0 g/L, $MgSO_4.7H_2O$ 0.1 g/L in 300 mL Erlenmeyer flasks containing 100 mL of medium. The flasks shaken aerobically at 200 RPM for 48 h, pH 5.0, 6.0, 7.0, 8.0 and at 25° C. Cells resuspended in phosphate buffer (0.05 M, pH 7.0) and adjusted to an O.D. (600 nm) of 0.9 which corresponded to 10^9 cells per mL, and immediately assayed for INA.

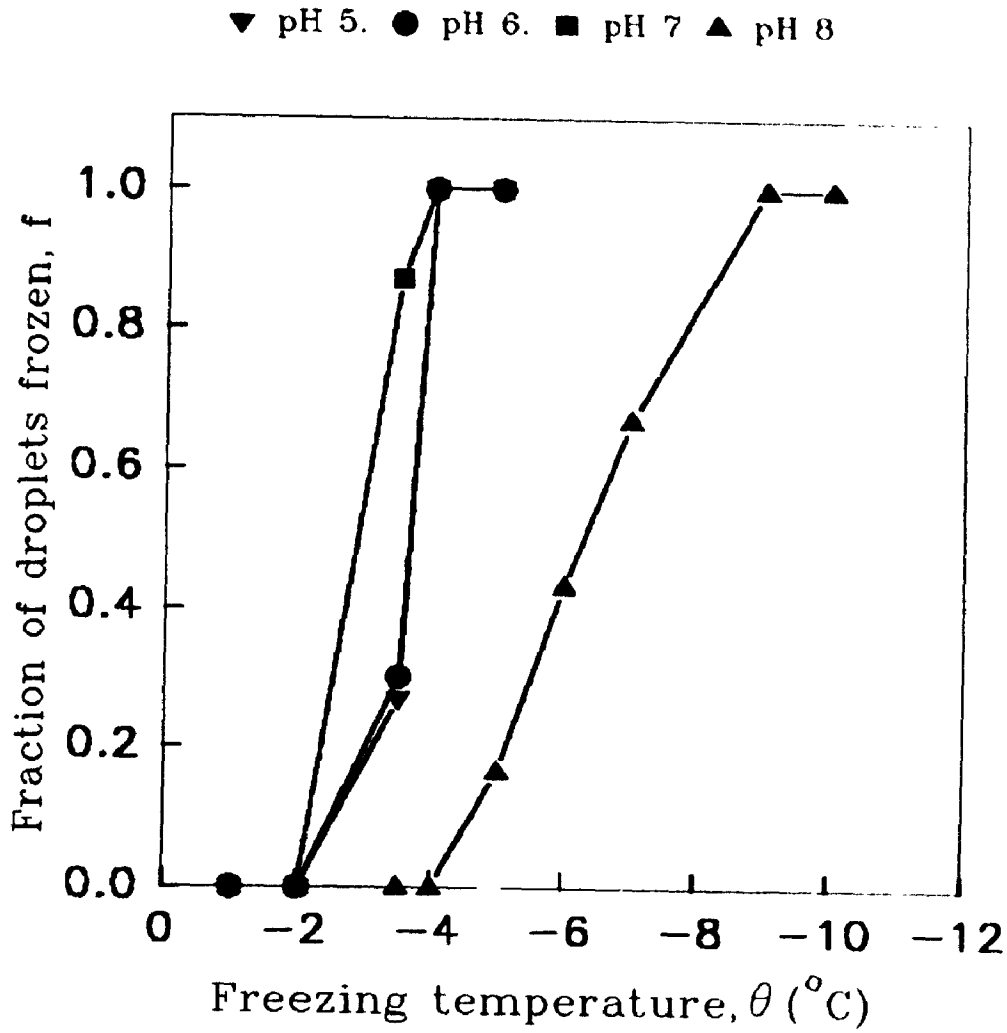
▼ pH 5. ● pH 6. ■ pH 7 ▲ pH 8
Fraction of droplets frozen, f
1.0
0.8
0.6
0.4
0.2
0.0
0
−2
−4
−6
−8
−10
−12
Freezing temperature, θ (°C)

Figure 5.8. Fraction of Drops Freezing, f, versus Freezing Temperature, θ °C, as a Function of Aeration Conditions.

Conditions: P.syringae cit 7 cells grown on sucrose 5.0 g/L, peptone 1.0 g/L, K_2HPO_4 3.5 g/L, KH_2PO_4 1.0 g/L, $MgSO_4.7H_2O$ 0.1 g/L in 300 mL Erlenmeyer flasks containing 100 mL of medium. The flasks shaken aerobically at 200 RPM for 48 h, under various aeration conditions and at 25° C and pH 7.0. Cells resuspended in phosphate buffer (0.05 M, pH 7.0) and adjusted to an O.D. (600 nm) of 0.9 which corresponded to 10^9 cells per mL, and immediately assayed for INA.

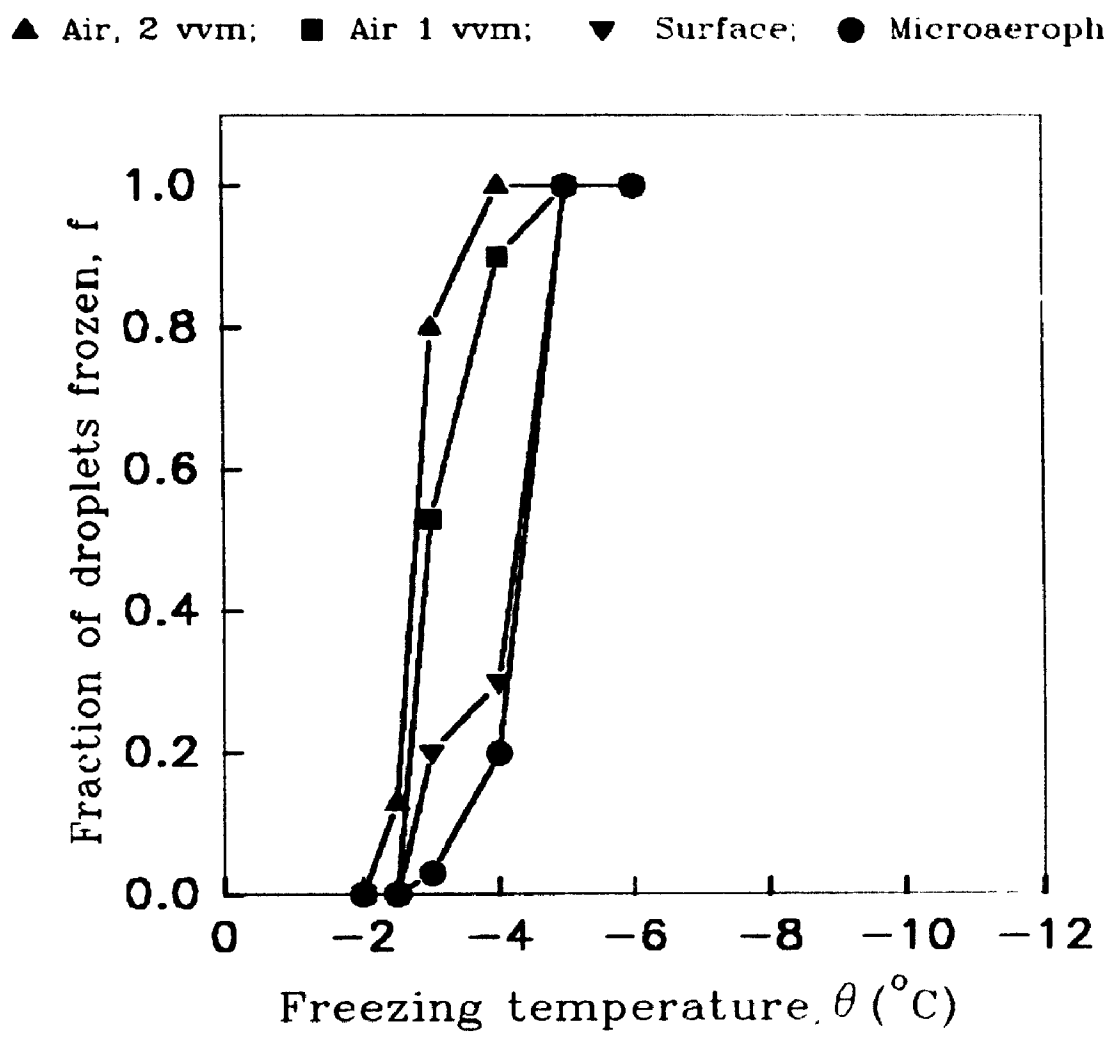
▲ Air, 2 vvm; ■ Air 1 vvm; ▼ Surface; ● Microaerophylic
Fraction of droplets frozen, f
1.0
0.8
0.6
0.4
0.2
0.0
0
−2
−4
−6
−8
−10
−12
Freezing temperature, θ (°C)

flow-rates (1, 2 vvm respectively). Thus aeration is another variable affecting INA of P. syringae.

5.3.6 Summary of Effect of Culture Conditions on INA of P. syringae cit 7.

The expression of INA in P. syringae cit 7 was found to be a function of medium composition, pH, growth temperature and aeration. A combination of sucrose and peptone in the growth medium gave the highest threshold temperature, θ_{th} of -2.5° C. P. syringae cell growth at temperatures exceeding 25° C decreased their INA. Similarly, growth of P. syringae at pH 8.0 also decreased INA compared with pH values between 5.0 and 7.0. Microaerophylic conditions also lowered INA in the P. syringae bacteria.

5.4 Batch and Continuous Bioreactor Studies of P. syringae cit 7

No previous study has been reported in the literature on the kinetics of growth and INA of P. syringae cit 7 during batch or continuous cultivation in bioreactors under controlled, measurable, experimental conditions. This microorganism can grow at temperatures ranging from 0° C to 40° C. however, there are no available data on the kinetics of growth at low temperatures. In this thesis, cell growth and INA of P. syringae cit 7 was examined in batch and continuous bioreactors at different temperatures and dilution rates. These represent the first original results in the area of bacterial ice nucleation.

5.4.1 Batch Growth Kinetics and INA of P. syringae cit 7 as a Function of Temperature.

Figures 5.9 to 5.15 describe the change in sucrose concentration (g/L), cell concentration (g DW/L), and INA, η, of P. syringae cit 7 as a function of batch growth time, t (h) in the 1 L bioreactor system shown in Figure 4.2.

Batch growth at 5.5° C

In Figure 5.9 it can be seen that the sucrose concentration, S, decreased from 5 g/L to 0.0 g/L in 250 h of cultivation. The cell concentration, X, increased to 1.50 g DW/L in the same time period. The ice nuclei per g cell DW, η, increased from an initial 10^3 at inoculation or zero time to 10^8 at the stationary phase of cell growth.

Figure 5.9. Batch Growth Kinetics and Ice Nucleation Activity of P. syringae cit7 in the 1 L Bioreactor, T = 5.5 ° C.

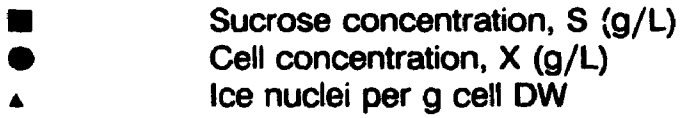

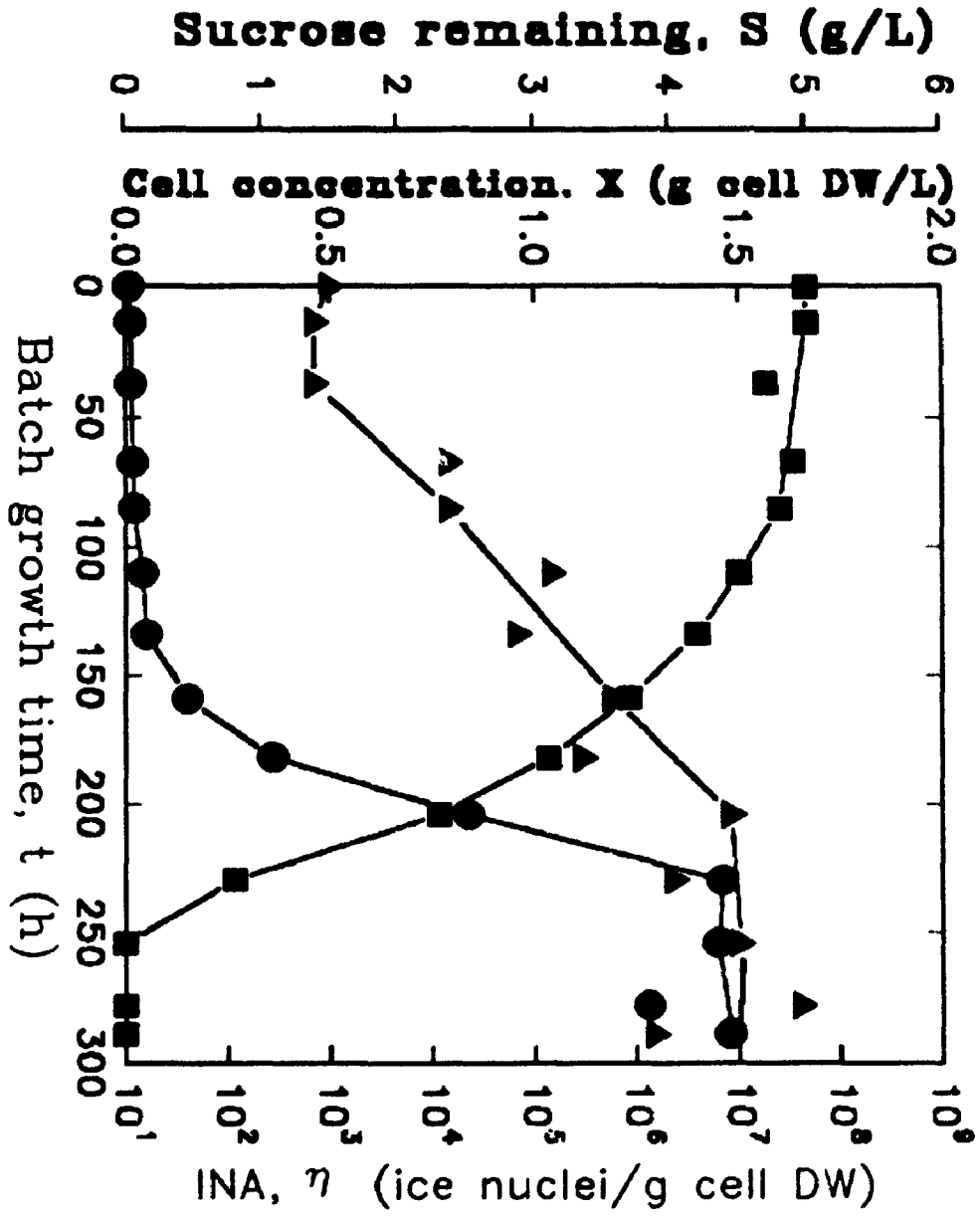
Sucrose remaining, S (g/L)
0
1
2
3
4
5
6
Cell concentration, X (g cell DW/L)
0.0
0.5
1.0
1.5
2.0
Batch growth time, t (h)
0
50
100
150
200
250
300
10^1
10^2
10^3
10^4
10^5
10^6
10^7
10^8
10^9
INA, η (ice nuclei/g cell DW)

Figure 5.10. Batch Growth Kinetics and Ice Nucleation Activity of P. syringae cit7 in the 1 L Bioreactor, T = 10.0 °C.

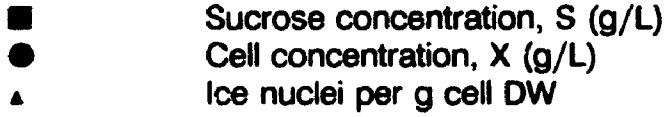

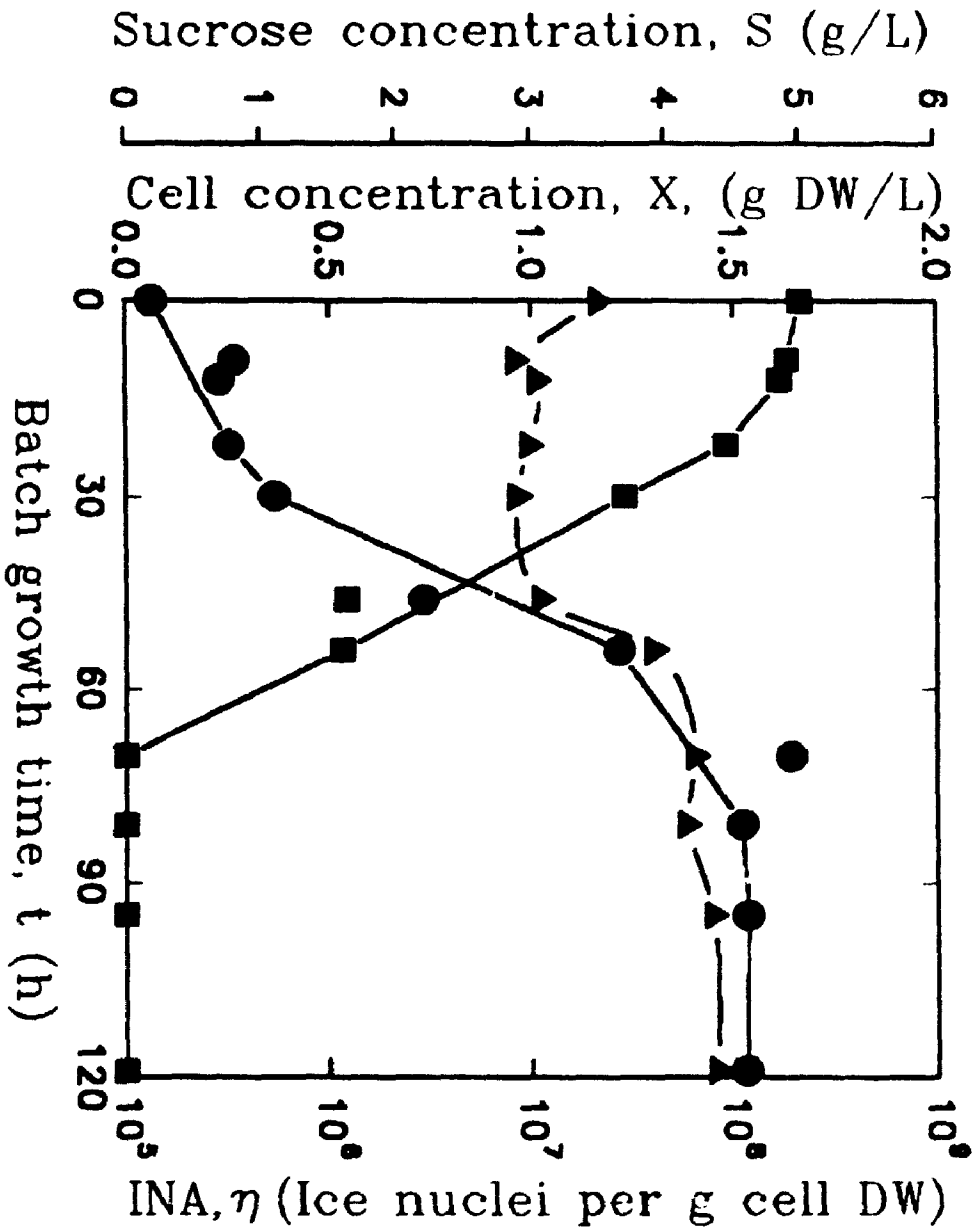
Sucrose concentration, S (g/L)
0
1
2
3
4
5
6
Cell concentration, X, (g DW/L)
0.0
0.5
1.0
1.5
2.0
Batch growth time, t (h)
0
30
60
90
120
10^5
10^6
10^7
10^8
10^9
INA, η (Ice nuclei per g cell DW)

Figure 5.11. Batch Growth Kinetics and Ice Nucleation Activity of P. syringae cit7 in the 1 L Bioreactor, T = 15.0° C.

■ Sucrose concentration, S (g/L)
● Cell concentration, X (g/L)
▲ Ice nuclei per g cell DW

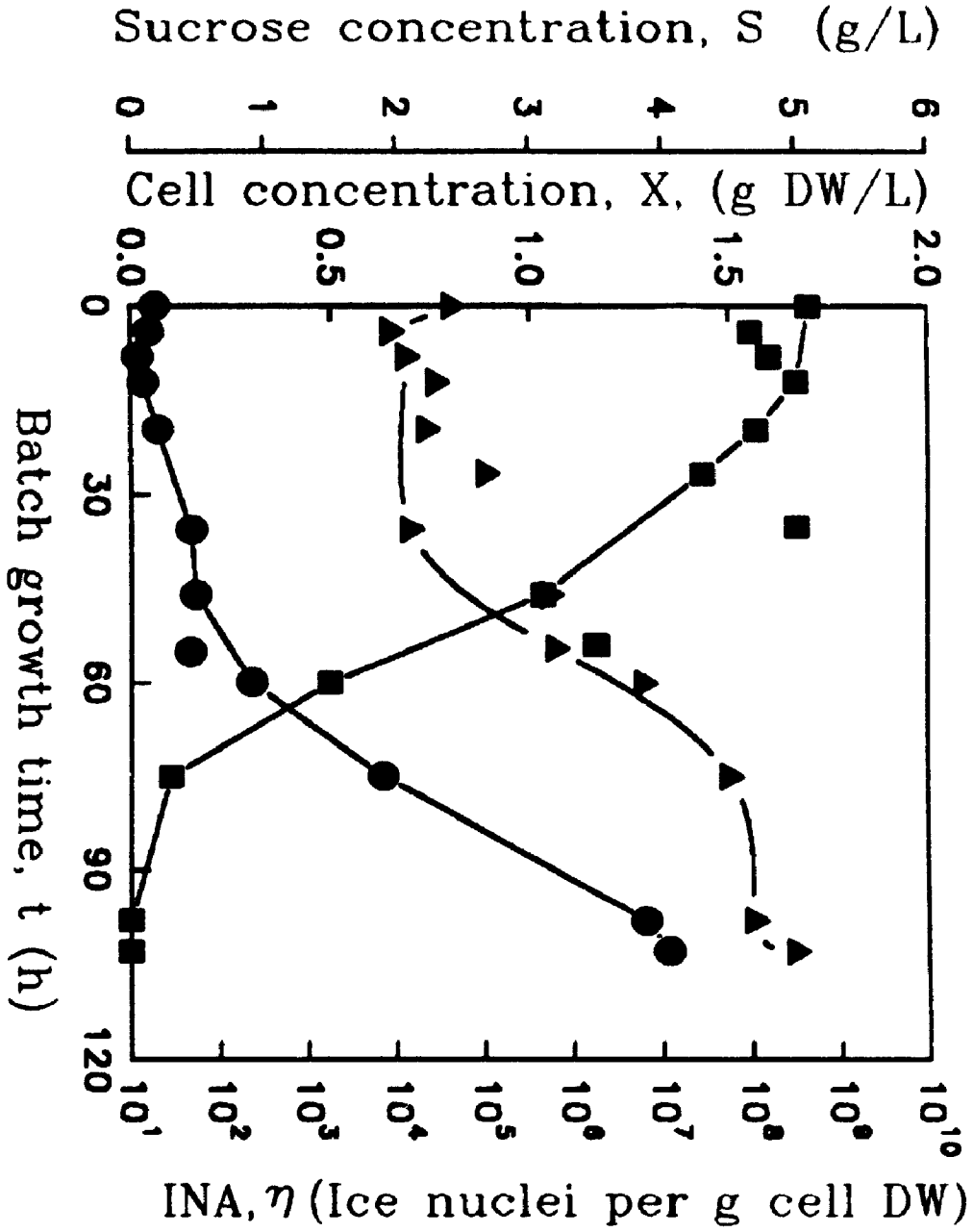
Sucrose concentration, S (g/L)
0
1
2
3
4
5
6
Cell concentration, X, (g DW/L)
0.0
0.5
1.0
1.5
2.0
Batch growth time, t (h)
0
30
60
90
120
10^1
10^2
10^3
10^4
10^5
10^6
10^7
10^8
10^9
10^{10}
INA, η (Ice nuclei per g cell DW)

Figure 5.12. Batch Growth Kinetics and Ice Nucleation Activity of P. syringae cit7 in the 1 L Bioreactor, T = 20.0° C.

■ Sucrose concentration, S (g/L)
● Cell concentration, X (g/L)
▲ Ice nuclei per g cell DW

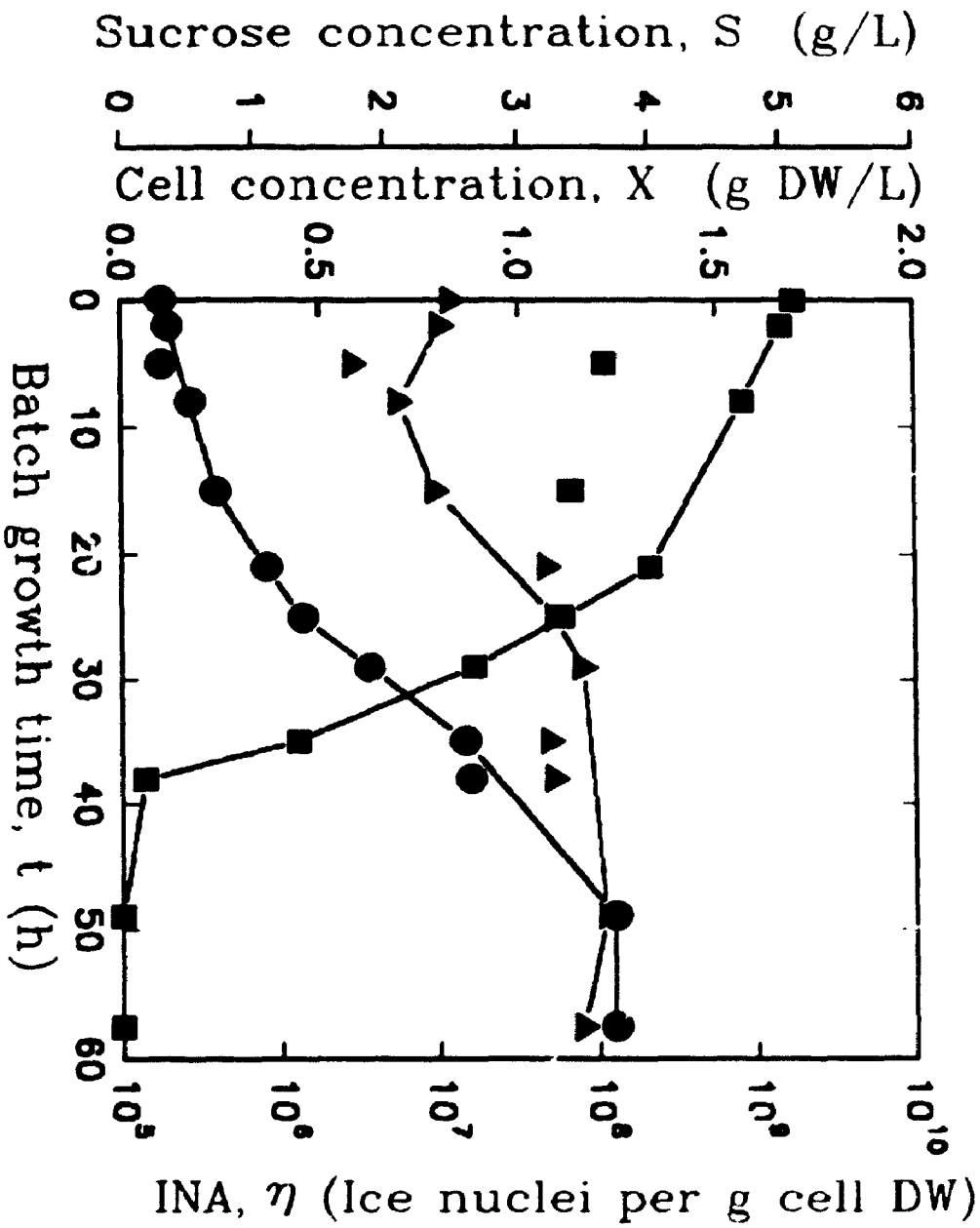
Sucrose concentration, S (g/L)
0
1
2
3
4
5
6
Cell concentration, X (g DW/L)
0.0
0.5
1.0
1.5
2.0
Batch growth time, t (h)
0
10
20
30
40
50
60
10^5
10^6
10^7
10^8
10^9
10^{10}
INA, η (Ice nuclei per g cell DW)

Figure 5.13. Batch Growth Kinetics and Ice Nucleation Activity of P. syringae cit7 in the 1 L Bioreactor, T = 25.0 • C.

■ Sucrcse concentration, S (g/L)
● Cell concentration, X (g/L)
▲ Ice nuclei per g cell DW

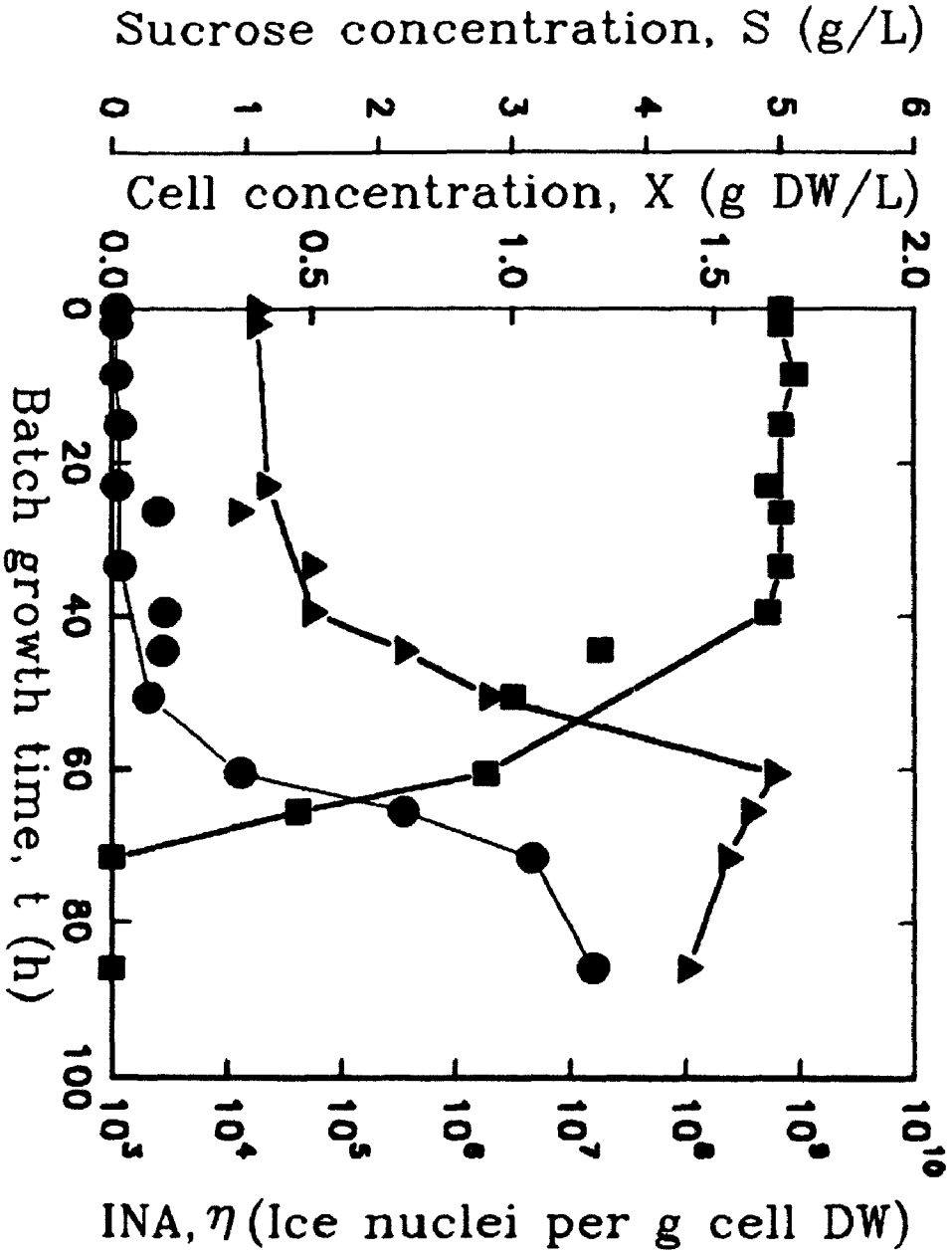
Sucrose concentration, S (g/L)
0
1
2
3
4
5
6
Cell concentration, X (g DW/L)
0.0
0.5
1.0
1.5
2.0
Batch growth time, t (h)
0
20
40
60
80
100
10^3
10^4
10^5
10^6
10^7
10^8
10^9
10^{10}
INA, η (Ice nuclei per g cell DW)

Figure 5.14. Batch Growth Kinetics and Ice Nucleation Activity of P. syringae cit7 in the 1 L Bioreactor, T = 28.0 ° C.

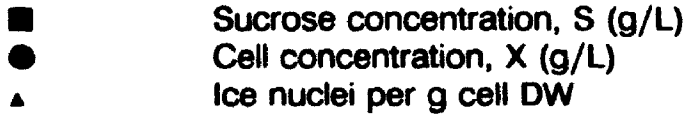

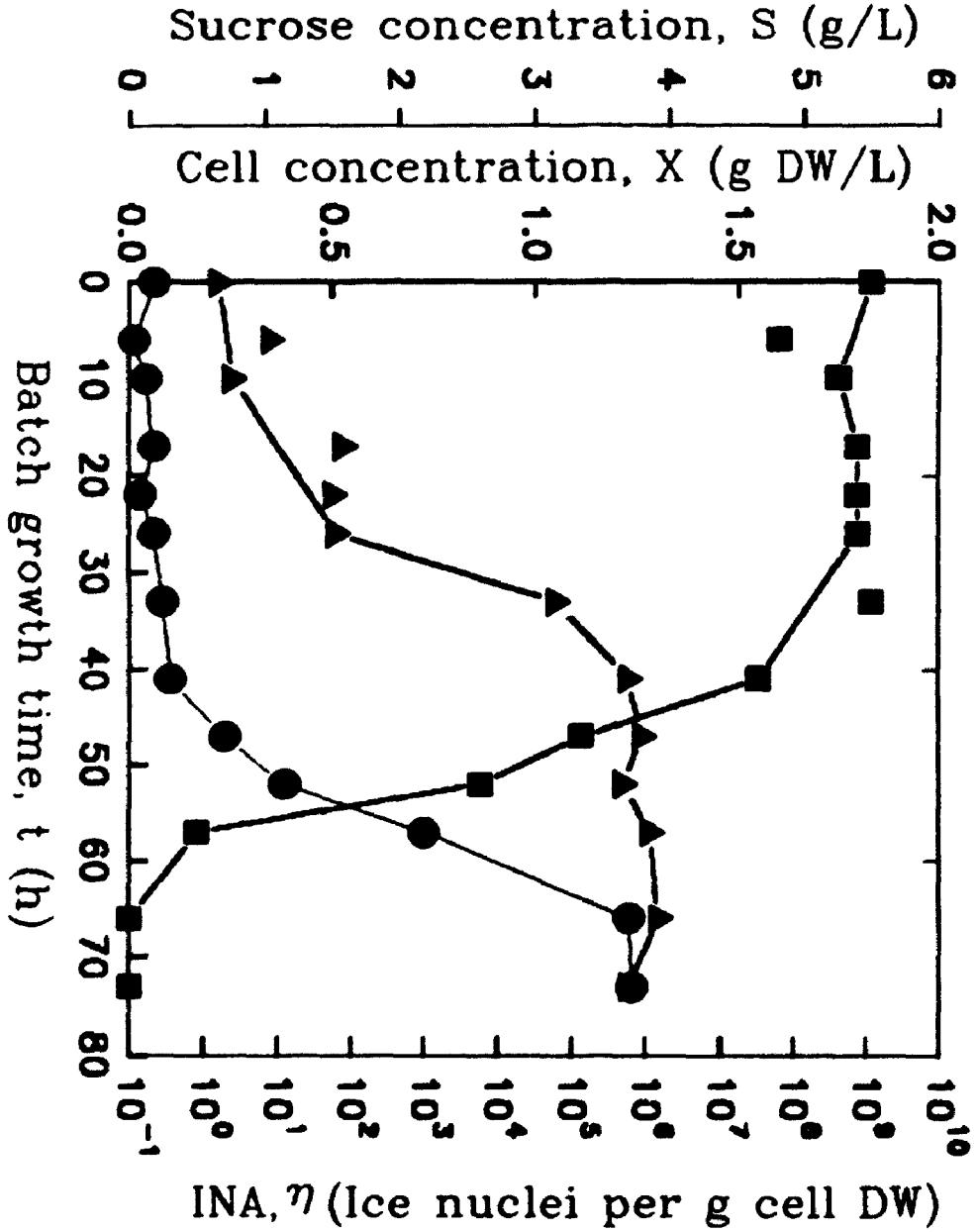
Sucrose concentration, S (g/L)
0
1
2
3
4
5
6
Cell concentration, X (g DW/L)
0.0
0.5
1.0
1.5
2.0
Batch growth time, t (h)
0
10
20
30
40
50
60
70
80
10^{-1}
10^{0}
10^{1}
10^{2}
10^{3}
10^{4}
10^{5}
10^{6}
10^{7}
10^{8}
10^{9}
10^{10}
INA, η (Ice nuclei per g cell DW)

Figure 5.15. Batch Growth Kinetics and Ice Nucleation Activity of P. syringae cit7 in the 1 L Bioreactor, T = 35.0 °C.

■ Sucrose concentration, S (g/L)
● Cell concentration, X (g/L)
▲ Ice nuclei per g cell DW

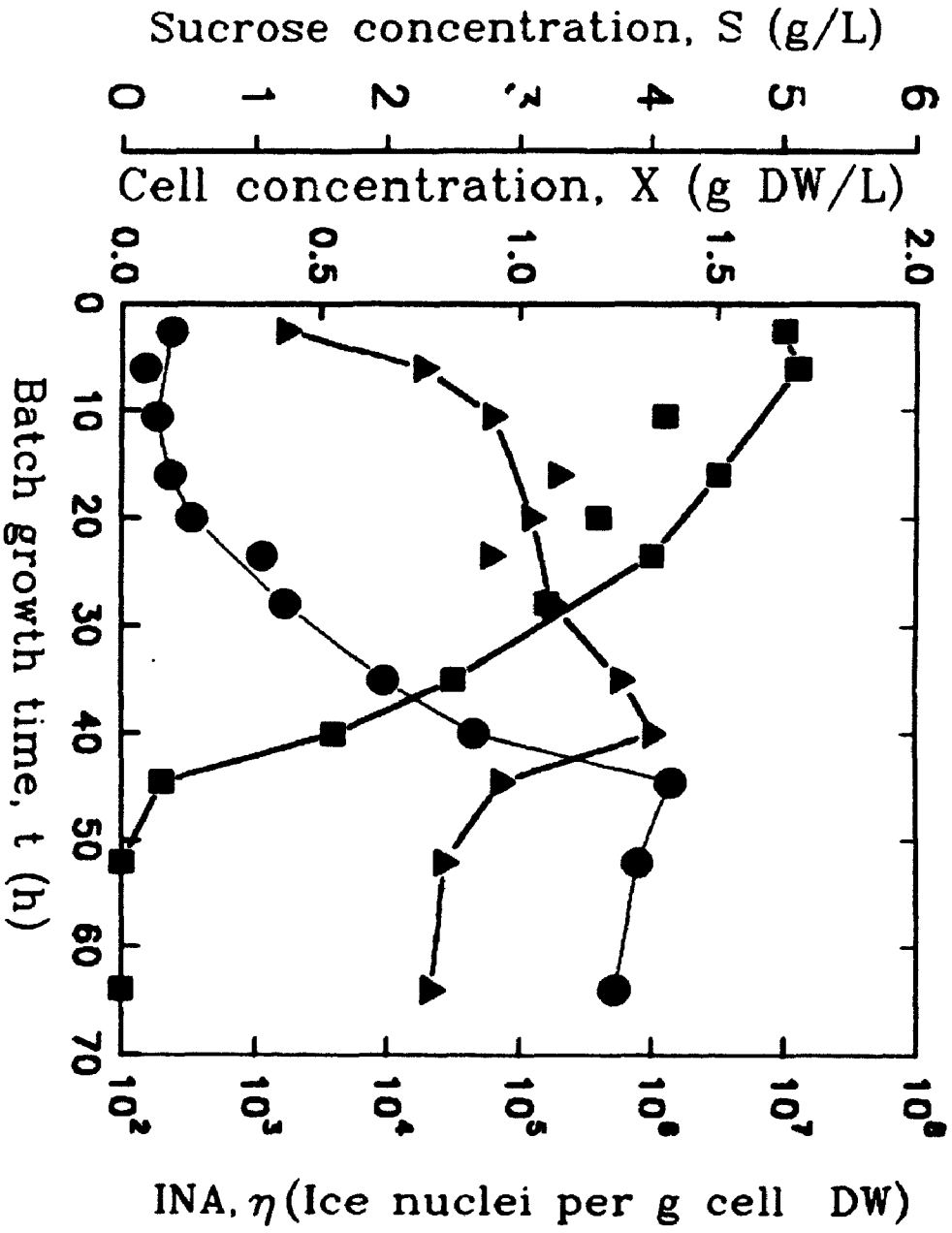
Sucrose concentration, S (g/L)
0
1
2
3
4
5
6
Cell concentration, X (g DW/L)
0.0
0.5
1.0
1.5
2.0
Batch growth time, t (h)
0
10
20
30
40
50
60
70
10^2
10^3
10^4
10^5
10^6
10^7
10^8
INA, η (Ice nuclei per g cell DW)

Batch growth at 10° C

In figure 5.10, the sucrose concentration, S, decreased from 5.0 g/L to 0.0 g/L in 70 h of cultivation at 10° C. The bacterial concentration, X, reached a final value of 1.5 g/L and INA increased from an initial 10^7 ice nuclei/g cell DW to 10^8 ice nuclei/g cell DW in the cultivation period.

Batch growth at 15° C

Figure 5.11 shows the growth kinetics at 15° C. As seen in the figure, the sucrose concentration dropped from 5.0 to 0.0 g/L in 90 h. The increase in cultivation time to reach stationary phase compared to the study at 10° C is due to a longer lag phase. The final cell concentration reached in this case was 1.4 g cell DW/L. INA increased from approximately 10^4 ice nuclei per g cell DW to 10^8 ice nuclei per g cell DW in the given time period.

Batch growth at 20° C

Figure 5.12 shows the growth kinetics at 20° C. The sucrose concentration declined from 5.0 to 0.0 g/L in 50 h. The final cell concentration reached in this case was 1.3 g cell DW/L. INA increased from approximately 10^7 ice nuclei per g cell DW to 10^8 ice nuclei per g cell DW in the given time period.

Batch growth at 25° C

Figure 5.13 shows the growth kinetics at 25° C. The sucrose concentration changed from 5.0 to 0.0 in 60 h of cultivation while the final bacterial concentration

reached was 1.2 g cell DW/L in the same period. INA increased from approximately 10^4 to 10^8 ice nuclei per g cell DW.

Batch growth at 28° C

Figure 5.14 shows the growth kinetics at 28° C. While sucrose was completely consumed in 70 h, the final bacterial DW was 1.3 g cell DW/L and INA increased from an initial value of 1 ice nuclei/g cell DW to 10^6 ice nuclei/g cell DW in the cultivation period.

Batch growth at 35° C

The growth kinetics at 35° C are depicted in Figure 5.15. Sucrose was completely consumed in 50 h with cell concentration reaching 1.4 g cell DW/L. A noted feature in this figure is a decrease in INA during the stationary phase of cell growth. INA decreased from a maximum of 10^6 ice nuclei per g cell DW at the end of the exponential phase of growth to approximately 10^4 ice nuclei per g cell DW.

5.4.2 Effect of Temperature on Maximum Specific Growth Rate, μ_{max} of P. syringae cit 7.

Figure 5.16 shows the maximum specific growth rate of P. syringae cit 7, μ_{max}, in the bioreactor as a function of cell growth temperature, (T ° C) in the 1 L bioreactor. It can be seen in this figure that starting at 5.5° C, the maximum specific growth rate approximately doubles for every 10° C temperature rise. The optimum

Figure 5.16. Maximum Specific Growth Rate, μ_{max} (h^{-1}) of P. syringae cit 7 as a Function of Temperature, (T° C).

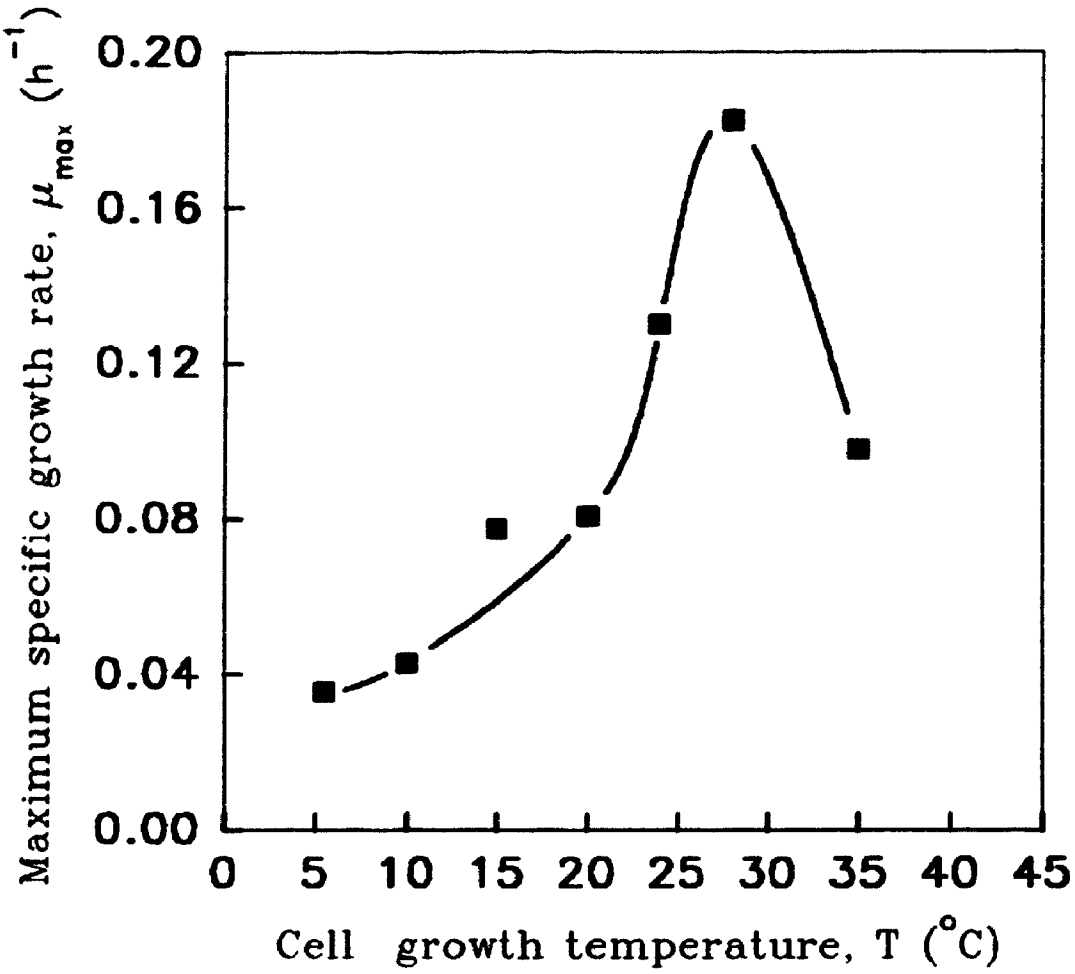
Maximum specific growth rate, μ_{max} (h^{-1})
0.20
0.16
0.12
0.08
0.04
0.00
0
5
10
15
20
25
30
35
40
45
Cell growth temperature, T (°C)

temperature for maximum growth was found to be 28° C. At 35° C, the cells multiply but at a reduced maximum specific growth rate.

Figure 5.17 shows the Arrhenius relationship for μ_{max} and 1/T of P. syringae cit 7. The values of the Arrhenius constants A^o, E_a can be calculated from figure 5.17. The cell temperature deactivation kinetics are not developed because only one high temperature (35° C) point is available. Thus the Arrhenius equation which describes the activation effect of temperature T (° K) on μ_{max} of P. syringae cit 7 in the temperature range of 5.5° C to 28° C is given by Equation 5.1.

$$\mu_{max} = e^{17.21}\, e^{-\frac{11400}{1.987T}} \qquad (5.1)$$

Lower μ_{max} at higher deactivating temperatures, e.g. 35° C or higher, is mainly due to thermal denaturation of enzymes and other biochemical constituents of P. syringae cells. Similarly, reduced growth rates at low temperatures may be caused by slower endocellular transport processes, including possible diffusional limitations of nutrients from the liquid environment to the cells.

5.4.3 Maximum INA, η_{max}, in the Bioreactor as a Function of Cell Growth Temperature.

INA of growing P. syringae cells in the bioreactor at any given temperature was found to be a function of batch (growth) time and reached a maximum value

Figure 5.17. Arrhenius Relationship of Maximum Specific Growth Rate, μ_{max} (h^{-1}) of P. syringae cit 7 versus Inverse Batch Growth Temperature, 1/T (° C).

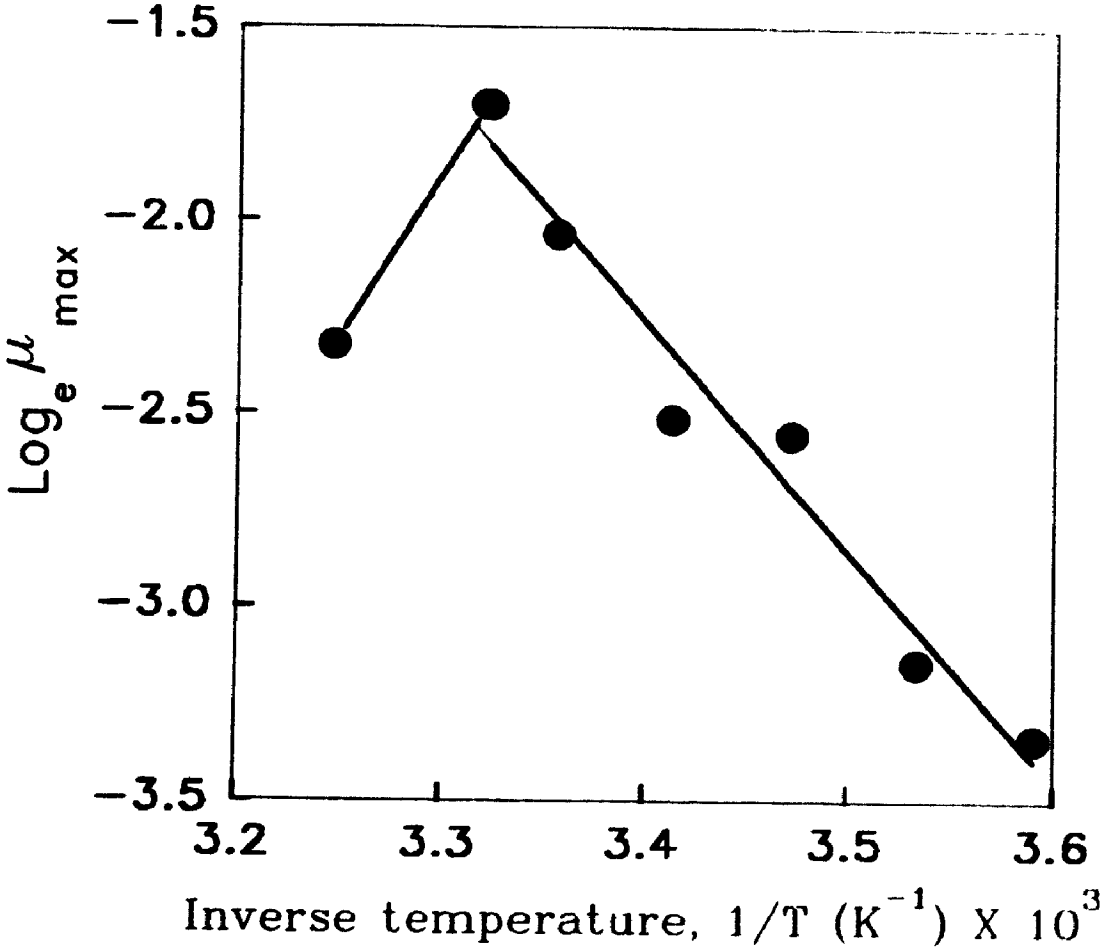
−1.5
−2.0
−2.5
−3.0
−3.5
$Log_e \mu_{max}$
3.2
3.3
3.4
3.5
3.6
Inverse temperature, 1/T (K^{-1}) X 10^3

at the end of the exponential phase. This value of maximum INA can be denoted as η_{max} (cumulative no. of ice nuclei per g cell DW). From an industrial perspective, η_{max}, the maximum INA achieved at a given cell growth temperature, can be a very important parameter that can be used to optimize the growth temperature in a bioreactor system used for commercial large scale production of IN bacteria of P. syringae. Figure 5.18 is a plot of the maximum INA in the bioreactor, η_{max} versus cell growth temperature from 5.5° C to 35° C. It can be seen that η_{max} reached a maximum at 25° C then significantly decreased. The maximum INA was thus found to be at 25° C even though the optimum cell growth temperature was 28° C. These results can be explained by the study of Mueller et al., (1990) mentioned earlier, where low growth temperatures were found to produce cells with higher INP clusters. In nature, the onset of colder temperatures may serve as a induction mechanism for IN cells to produce larger amounts of protein. This would enable them to invade the leaf tissue through frost damage and access nutrients within the leaf surface.

5.4.4 Effect of Temperature on Cell Yield.

Figure 5.19 shows the cell yield, $Y_{x/s}$, as g of cells formed per g of sucrose consumed as a function of batch growth temperature. Over the range of temperatures from 5.5° C to 35° C, the average cell growth yield, $Y_{x/s}$, was found to decrease slightly. Cell yields are a function of medium composition and growth conditions of P. syringae.

Figure 5.18. Maximum Ice Nucleation Activity, η_{max}, (ice nuclei/g cell DW) of P. syringae Cit 7 in the 1 L Bioreactor versus Batch Growth Temperature, T (° C).

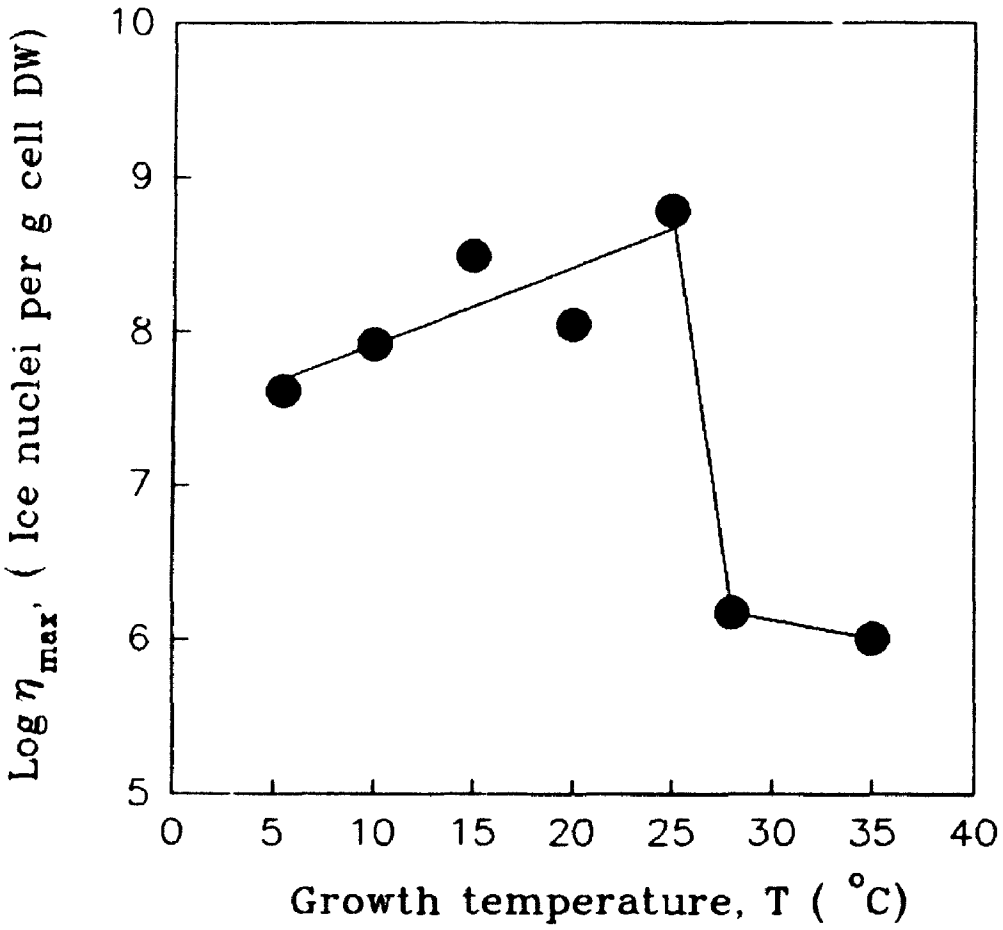
10
9
8
7
6
5
0
5
10
15
20
25
30
35
40
Log η_{max}, (Ice nuclei per g cell DW)
Growth temperature, T (°C)

Figure 5.19. Cell Yield, $Y_{x/s}$, g Cell DW per g Sucrose, for P. syringae Cit 7 as a Function of Batch Growth Temperature, T° C

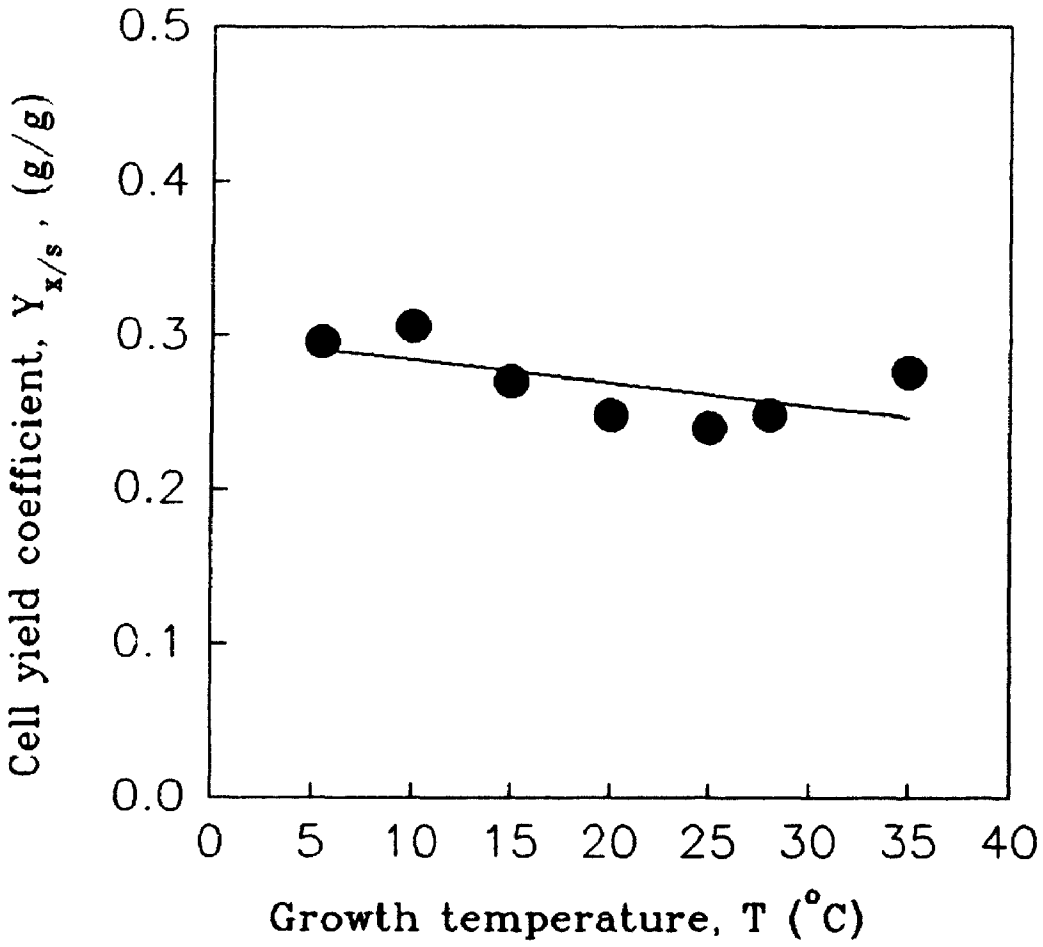
0.5
0.4
0.3
0.2
0.1
0.0
0
5
10
15
20
25
30
35
40
Cell yield coefficient, $Y_{x/s}$, (g/g)
Growth temperature, T (°C)

5.4.5 Effect of Temperature on Specific Batch INA Productivity.

From an economic point of view, it is important to calculate the specific cell productivity of ice nuclei formation during batch growth in bioreactors. In the 1 L bioreactor, the ice nuclei productivity, q_p (ice nuclei per g cell DW per h), was obtained as follows. First, the time required for exponential cell growth, t_{exp}, was found from batch growth data at a given temperature. Next the maximum number of ice nuclei formed per g cell DW, η_{max} was divided by t_{exp} and the results are shown in Table 5.8. Using this procedure, the maximum specific INA productivity, q_p, ice nuclei /g cell DW/h was found to be at 25° C. Table 5.8 also shows the bioreactor volumetric productivity of INA, q_v, expressed as the ice nuclei/L bioreactor volume/h. The value of q_v was calculated by dividing the ice nuclei concentration in the bioreactor which corresponded to η_{max} by the exponential growth time. Figure 5.20 shows both q_p and q_v as functions of batch growth temperature T (° C).

5.4.6 Summary and Discussion of Temperature Effects.

Kinetic studies at different temperatures in a 1 L batch bioreactor showed that the optimum cell growth temperature was 28° C. However, cells cultured at temperatures higher than 25° C had significantly lower levels of INA. The optimum temperature for INA production in the 1 L bioreactor was found to be 25° C where approximately 6.00 X 10^8 ice nuclei per g cell DW were obtained with a specific INA productivity, q_p of 1.08 X 10^7 ice nuclei/ g cell DW/h. The corresponding optimum volumetric productivity q_v was found to be 6.45 X 10^6 at 25° C.

Table 5.8. Specific INA Productivity of P. syringae cit7 for Different Growth Temperatures

Temperature (° C)	η_{max}	t_{exp}	q_p	q_v
5.5	4.09 X10^7	120	3.40 X10^5	4.33 X 10^5
10	8.31 X10^7	81	1.02 X10^6	1.56 X 10^6
15	3.10 X10^8	76	4.07 X10^6	5.49 X 10^6
20	1.10 X10^8	57.5	1.91 X10^6	2.37 X 10^6
25	6.09 X10^8	56	1.08 X10^7	3.45 X 10^6
28	1.51 X10^6	24	6.29 X10^4	7.75 X 10^4
35	1.01 X10^6	44	2.29 X10^4	2.03 X 10^4

t_{exp} = exponential growth time, h, in the 1 L working volume bioreactor for each growth temperature measured from a plot of cell concentration, X g cell DW/L versus time t h.

η_{max} = maximum INA, ice nuclei/g cell DW reached in the 1 L working volume bioreactor at different cell growth temperatures

q_p = batch specific INA productivity, ice nuclei/g cell DW/h = η_{max}/t_{exp}

q_v = batch volumetric INA productivity, ice nuclei/L bioreactor vol/h

Figure 5.20 Specific and Volumetric INA Productivity,i.e., q_p and q_v respectively in the 1 L Bioreactor versus Batch Growth Temperature, T° C

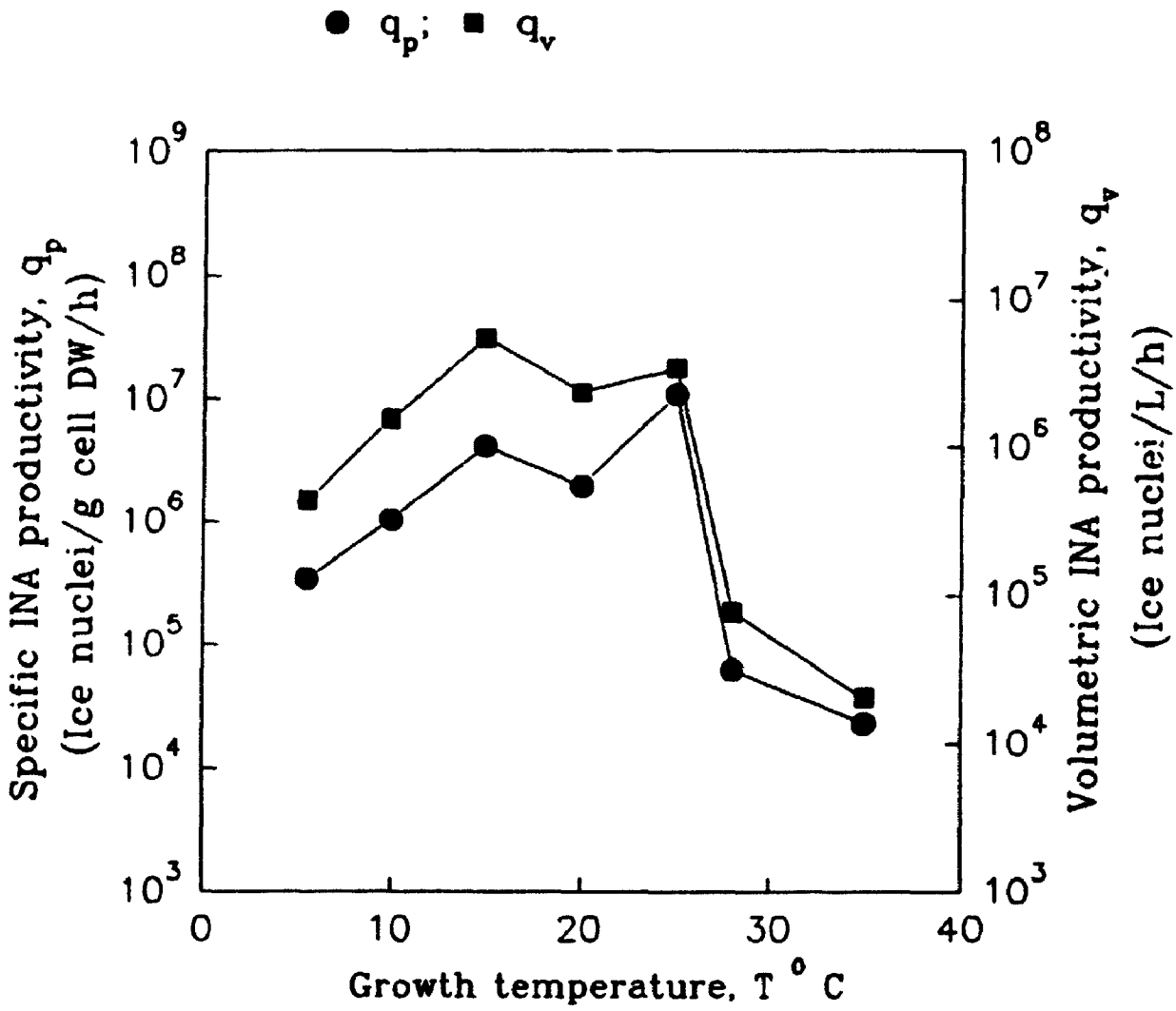
● q_p; ■ q_v
Specific INA productivity, q_p (Ice nuclei/g cell DW/h)
Volumetric INA productivity, q_v (Ice nuclei/L/h)
10^9
10^8
10^7
10^6
10^5
10^4
10^3
10^8
10^7
10^6
10^5
10^4
10^3
0
10
20
30
40
Growth temperature, T ^{0} C

Certain general conclusions can be drawn from growth studies of P. syringae cit 7 at different temperatures. (1) INA of P. syringae cit 7 develops during the lag and log phases of growth and is not considered a secondary metabolite. (2) INA of the cells develops rapidly in the late exponential phase. (3) INA of growing cells is a function of batch growth time and increases to a maximum value at the end of the exponential phase. (4) Final values of INA given by η_{max} do not exceed 10^9 ice nuclei per g cell DW at all temperatures. These results in the 1 L bioreactor were higher than those obtained in shake flasks, which reflects better mixing and aeration conditions in the 1 L bioreactor vessel compared with shake flasks.

For cell growth temperatures lower than 25° C, our studies in the 1 L bioreactor have demonstrated a continuous increase in INA with growth. For temperatures exceeding 25° C, an increase in INA during exponential cell growth and a subsequent decrease in the stationary phase was noted. This may mean that the process of ice nuclei formation in the cell membrane is a dynamic event. Post translations effects may be more pronounced at higher temperatures leading to deactivation of the IN protein and lowered INA.

Differences in INA due to growth temperatures may be attributed to either lower levels of ice nucleation protein or modification of the ice nucleation phenotype at higher temperatures e.g., at 28° C and 35° C. Because the ice nucleation protein is associated with the cell membrane, post translational factors including the stability of the protein, export efficiency, or conformation at the membrane surface may be affected by growth temperature. Changes in membrane

composition, e.g., lipid composition in response to change in growth temperature may also affect the ice nucleation productivity of P. syringae cells.

5.4.7 Continuous Cultivation of P. syringae cit 7 and Expression of INA

A systematic review of literature revealed that no previous reports have appeared on continuous cultivation of P. syringae cit 7 or any other ice nucleating bacteria. This thesis is the first report on continuous cultivation of ice nucleating bacteria. The advantages of continuous cultivation of IN bacteria are that since the ice nuclei formation occurs during the log phase of cell growth and not as a secondary metabolite, P. syringae cells can be economically produced on a large scale, in a continuous stirred tank bioreactor (CSTBR). The effect of dilution rate on INA production and cell growth needs to be examined. However, often the kinetics associated with continuous cultures vary markedly from batch growth conditions. All continuous flow, steady state experiments (at different dilution rates) in this investigation were conducted at 25° C and pH 7.0 and therefore, can only be compared with previous batch growth data at 25° C.

5.4.7.1 Effect of Increasing Dilution Rate

Figure 5.21 shows the change in P. syringae cit 7 steady state concentration, X (g cell DW/L), sucrose remaining, S (g/L) and INA of P. syringae cit7 (ice nuclei per g cell DW) with increasing dilution rates. In general, a progressive decrease in steady state cell concentration X from 0.84 to 0.19 g cell DW/L was noted as the flow rate through the system was increased from 16 mL/h to 91 mL/h which corresponded to a dilution rate range of 0.016 to 0.0.0910 h^{-1}. The corresponding steady state sucrose concentration increased from less than 0.3 g/L to 5.0 g/L. The bacterial INA decreased from approximately 5.50 X 10^6 ice

Figure 5.21. Change in Sucrose Concentration, S, Cell Concentration, X, and INA, η, of P. syringae cit7 in the CSTBR at Steady State Conditions, at 25° C and pH 7.0.

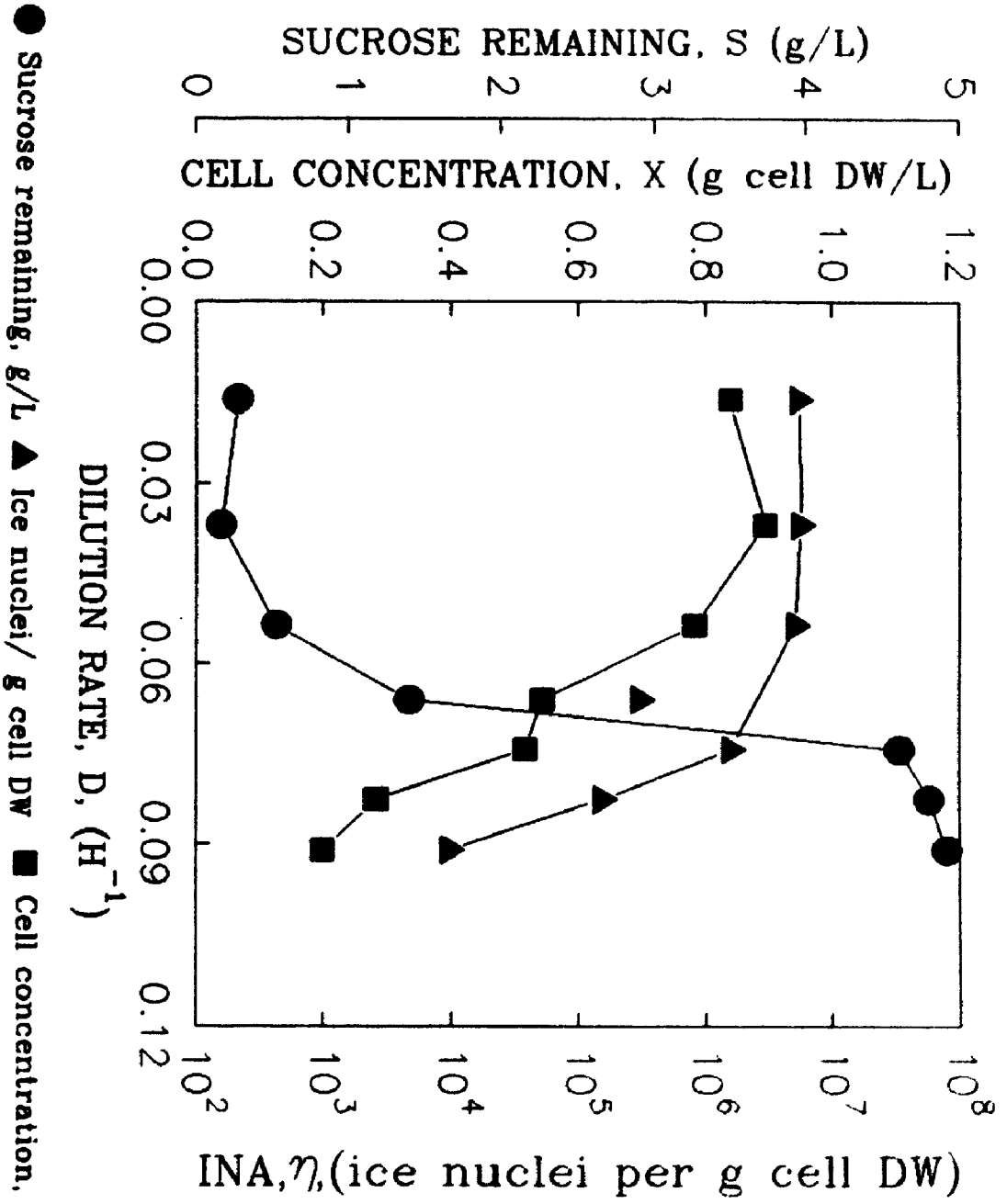

● Sucrose remaining, g/L ▲ Ice nuclei/ g cell DW ■ Cell concentration, g cell DW/L

nuclei/ g cell DW to 0.98 X 10^3 ice nuclei per g cell DW. INA was approximately constant until a dilution rate of 0.06 h^{-1}, and then rapidly decreased as the dilution rate approached μ_{max} at which washout occurs.

The change in the observed values of INA, η (ice nuclei per g cell DW) was similar to the trend observed in batch cultures. In batch growth at 25° C, INA was observed to be low in the early exponential phase compared to the value of INA in the late exponential phase of cell growth. The specific growth rate, μ (h^{-1}) is higher in the early exponential phase but starts to decrease in the latter phase of cell growth. Similarly, in the CSTBR it was seen that as dilution rate (specific growth rate increased), INA decreased. "Washout" conditions were observed at the flow rates exceeding 100 mL/h. The dilution rate at washout is numerically equal to the maximum specific growth rate of microorganisms, μ_{max}, under the given conditions of operation. This value is obtained from the Lineweaver-Burk plot which is shown later.

5.4.7.2 Calculation of Monod Constants, μ_{max} and K_s from Continuous Culture Data

As shown earlier in section 3.6, under continuous flow conditions at steady state, the dilution rate, D h^{-1} is equal to the specific growth rate, μ h^{-1} of the microorganism. This is seen from the cell mass balance around the bioreactor vessel:

$$\frac{dX}{dt} = \mu . X - D . X \qquad (5.2)$$

where X is the cell concentration, g cell DW/L, and t is growth time, h. Under steady flow conditions, dX/dt = 0, hence equation 5.2 reduces:

$$\mu = D \qquad (5.3)$$

Thus the Monod equation becomes:

$$D = \frac{\mu_{max} . S}{K_s + S} \qquad (5.4)$$

where S is the limiting substrate concentration, g/L and K_s is the substrate limitation constant g/L. Equation 5.4 can be rearranged in the classical Lineweaver-Burk form shown in equation 5.5.

$$\frac{1}{D} = \frac{K_s}{\mu_{max}} \cdot \frac{1}{S} + \frac{1}{\mu_{max}} \qquad (5.5)$$

Therefore equation 5.5 can be used to determine both the maximum specific growth rate, μ_{max}, and the substrate saturation constant, K_s, from a plot of 1/D versus 1/S. Figure 5.22 is a plot of 1/D versus 1/S from where K_s and μ_{max} can be calculated. The values of these constants obtained from equation 5.5 are:

$$\mu_{max} = 0.0814\ h^{-1}$$
$$K_s = 0.21\ g/L \qquad (5.6)$$

Atkinson and Mavituna, (1983) list values for μ_{max} for continuous cultures of Pseudomonas at 28° C and using ammonia as the nitrogen source. The conditions used in this thesis for continuous cultivation of P. syringae were somewhat similar to these conditions. The reported literature values for different Pseudomonas species, are μ_{max} = 0.03 to 0.40 h^{-1}. Thus this value of μ_{max} of 0.0814 h^{-1} is in the range of reported values in the literature for Pseudomonas. As shown earlier, for batch growth, a μ_{max} of 0.1300 h^{-1} was obtained at 25° C for P. syringae cit 7. However, since the batch (continuously changing) and steady state (constant) environments are very different the metabolism, morphology and adaptation of the bacteria to the different environments may vary between the

Figure 5.22. Lineweaver-Burk Plot for Continuous Cultivation of P. syringae cit7 in the CSTBR, at 25° C and pH = 7.0.

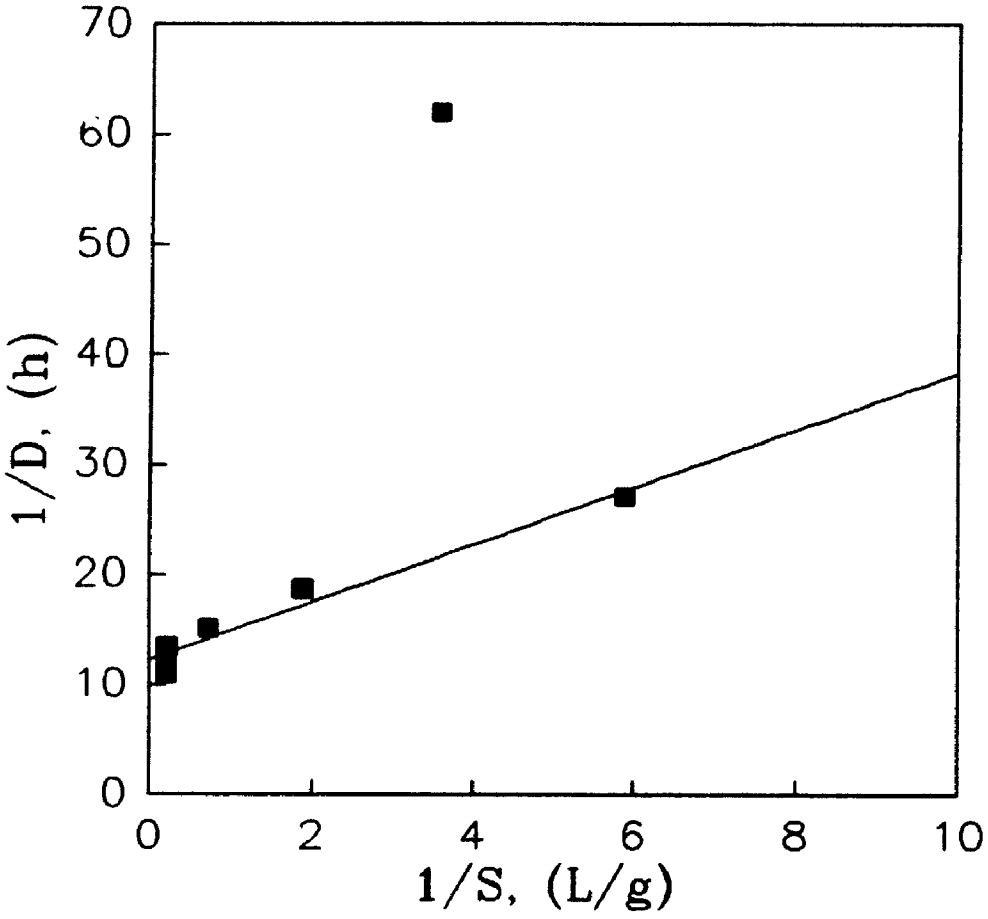
70
60
50
40
30
20
10
0
1/D, (h)
0
2
4
6
8
10
1/S, (L/g)

batch and continuous culture conditions. Another source of variation is the difficulty in actually obtaining "washout" conditions during actual operation of the CSTBR and maintaining steady state very close to washout.

5.4.7.3 Estimation of Growth Yield and Maintenance Coefficients from Continuous Culture Data

It is known that microorganisms need energy both for growth as well as for turnover of cell materials, maintenance of concentration gradients, motility etc. The substrate consumed by cells is therefore the sum of two components: cell growth and cell maintenance. It is possible that ATP may be generated and lost through its hydrolysis not being coupled to growth or maintenance functions, however this loss cannot be distinguished from maintenance energy. The total growth yield, Y_E can be written as:

$$Y_E = \frac{\Delta X}{\Delta S_E} = \frac{\Delta X}{\Delta S_G + \Delta S_M} \qquad (5.7)$$

where Y_E is the overall growth yield, $Y_{x/s}$ (g DW cell produced/g substrate used), where the substrate used is the energy source, ΔS_E, is total substrate consumed (g/L), ΔS_G, is substrate consumed for cell growth (g/L), ΔS_M is substrate consumed for cell maintenance, and ΔX is the amount of biomass produced.

When the maintenance energy is zero, $\Delta S_M = 0$, the overall growth yield, Y_E equals the growth yield, Y_{EG} (g/g) which is given by equation 5.7.

$$Y_{EG} = \frac{\Delta X}{\Delta S_G} \qquad (5.8)$$

Y_{EG} is therefore the maximum possible value of the growth yield from the substrate energy source. If we have one limiting substrate S, e.g., sucrose, in the bioreactor as the energy and carbon source, its distribution among various components is as follows:

$$\begin{matrix}\textit{total rate of} \\ \textit{substrate} \\ \textit{consumption}\end{matrix} = \begin{matrix}\textit{consumption} \\ \textit{for cell} \\ \textit{growth}\end{matrix} + \begin{matrix}\textit{consumption} \\ \textit{for cell} \\ \textit{maintenance}\end{matrix} + \begin{matrix}\textit{consumption} \\ \textit{for products} \\ \textit{formation}\end{matrix} \qquad (5.9)$$

Pirt (1975) described an equation utilizing the above relationship to measure the true growth yield and cell maintenance coefficient. Ignoring substrate utilization for product formation we can write:

$$\begin{matrix}\textit{total rate of} \\ \textit{substrate} \\ \textit{consumption}\end{matrix} = \begin{matrix}\textit{consumption} \\ \textit{for cell} \\ \textit{growth}\end{matrix} + \begin{matrix}\textit{consumption} \\ \textit{for cell} \\ \textit{maintenance}\end{matrix} \qquad (5.10)$$

that is:

$$\frac{\mu X}{Y_E} = \frac{\mu X}{Y_{EG}} + m.X \qquad (5.11)$$

hence:

$$\frac{1}{Y_E} = \frac{1}{Y_{EG}} + \frac{m}{\mu} \qquad (5.12)$$

Thus equation 5.12 may be used to estimate Y_{EG} and m by plotting $1/Y_{x/s}$ versus 1/D where D = μ under steady state continuous flow conditions which is shown in Figure 5.23, where $Y_{x/s}$ is equal to Y_E the overall growth yield for P.syringae cit 7. However, Figure 5.23 shows that the predicted linear correlation $1/Y_{x/s}$ versus 1/D is not satisfactory.

The values of Y_{EG} and m obtained by this technique are: Y_{EG} = 0.53 (g/g) and m = 0.0763 h^{-1}. Atkinson and Mavituna (1983) list values for Y_{EG}, and m for continuous cultures of Pseudomonas at 28° C and using ammonia as the nitrogen source as 0.29 g/g and 0.03 g/L respectively. Our experimentally obtained maintenance coefficient value, m = 0.0763 h^{-1}, was similar to the reported value. However, the yield coefficient is different because the carbon source used in the

Figure 5.23. Plot of Inverse Growth Yield ($1/Y_{x/s}$) versus Inverse Dilution Rate for Estimation of Y_{EG} (g/g) and Maintenance Coefficient, m (h^{-1}) of P. syringae cit 7 at 25° C and pH 7.0.

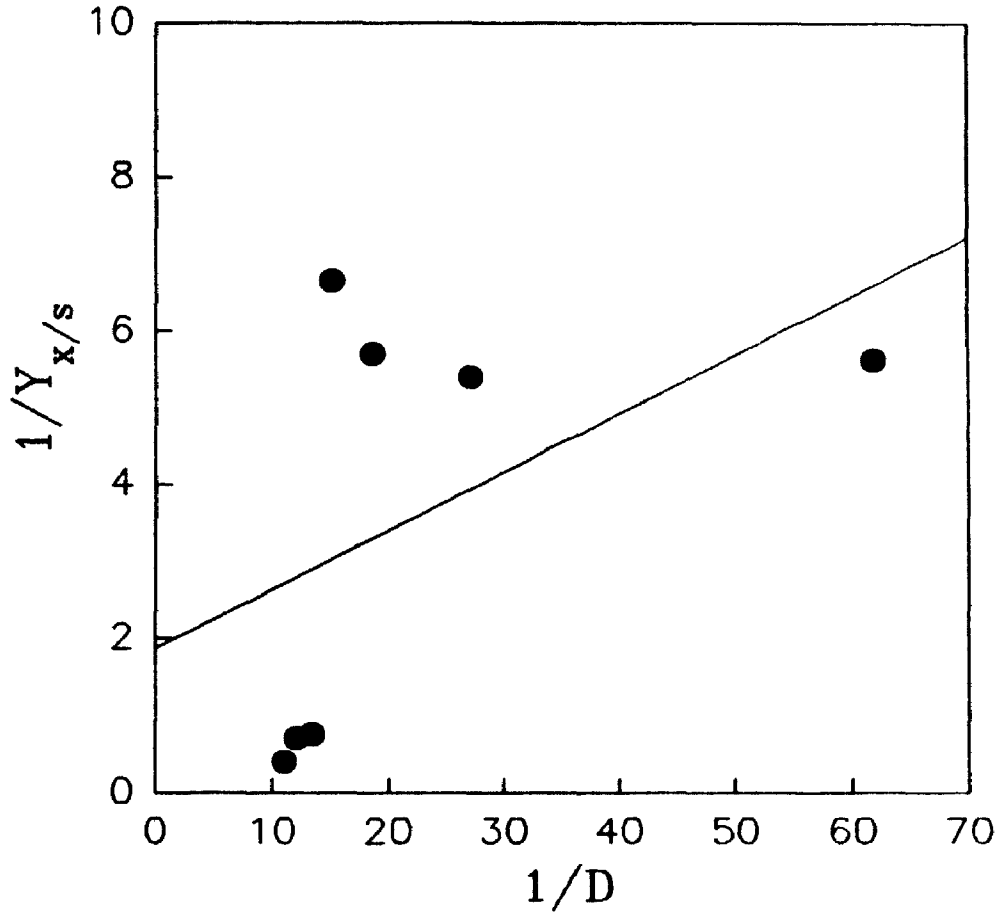
10
8
6
4
2
0
$1/Y_{x/s}$
0
10
20
30
40
50
60
70
1/D

literature value was formate and it is known that the energy and carbon content of different substrates is different for the same amount of substrate.

Also, it may be noted that the calculated yield and maintenance coefficient values obtained from Equation 5.12 are based on Equation 5.10. Since substrate utilization for all products and intermediates formed was ignored, Equation 5.12 may not be truly valid unless equation 5.9 and not equation 5.10 is used, i.e., a carbon balance is made in the bioreactor and all products and intermediates are accounted for. Practical and analytical considerations make this sometimes impossible, thus the effect of substrate consumed for product formation is often ignored in the above derivation. This may lead to non-linear plots of $1/Y_E$ versus $1/\mu$ especially if product profile changes with specific growth rate.

An additional, plausible explanation for the observed plot of Figure 5.23, is that since Equation 5.10 is based on Monod kinetics, the Monod equation may not be exactly followed in this case. Hence the reason for the observed scatter in the plot of Figure 5.23.

5.4.7.4 Cell and INA productivity of P. syringae cit 7 in the CSTBR

Cell productivity, q_x = g Dw cell/L bioreactor volume/h, is defined by equation 5.13.

$$q_x = D.X \qquad (5.13)$$

Equation 5.14 defines INA productivities in the bioreactor, namely, q_p = ice nuclei/g DW cell/h, and q_v = ice nuclei/ L bioreactor volume/ h, respectively.

$$q_p = D.\eta$$
$$q_v = D.X.\eta \qquad (5.14)$$

Figure 5.24 shows q_x as a function of dilution rate, D. The plots of ice specific and volumetric INA productivities, q_p and q_v versus dilution rate, D, are shown in Figure 5.25. respectively as a function of dilution rate. Cell productivity, q_x, reached a maximum at a dilution rate of 0.054 h^{-1}. It can be seen in Figure 5.25 that INA productivity, q_p was also maximum at a dilution rate of 0.054 h^{-1} and continuously decreased after a dilution rate of 0.06 h^{-1}. Figure 5.25 shows a maximum q_v = 2.19 X 10^5 ice nuclei/L bioreactor volume/h at a D of 0.054 h^{-1}.

5.4.8 Growth and INA of P. syringae cit 7 in a 15 L Bioreactor

P. syringae cit 7 was cultivated in a laboratory scale 15 L bioreactor. The objective was to determine the growth kinetics and INA of this microorganism in a larger bioreactor. It is known that scale-up can affect growth kinetics, due to

Figure 5.24. Cell Volumetric Productivity, q_x (g cell DW/L-h) of P. syringae Cit7 in the CSTBR at 25° C and pH = 7.0.

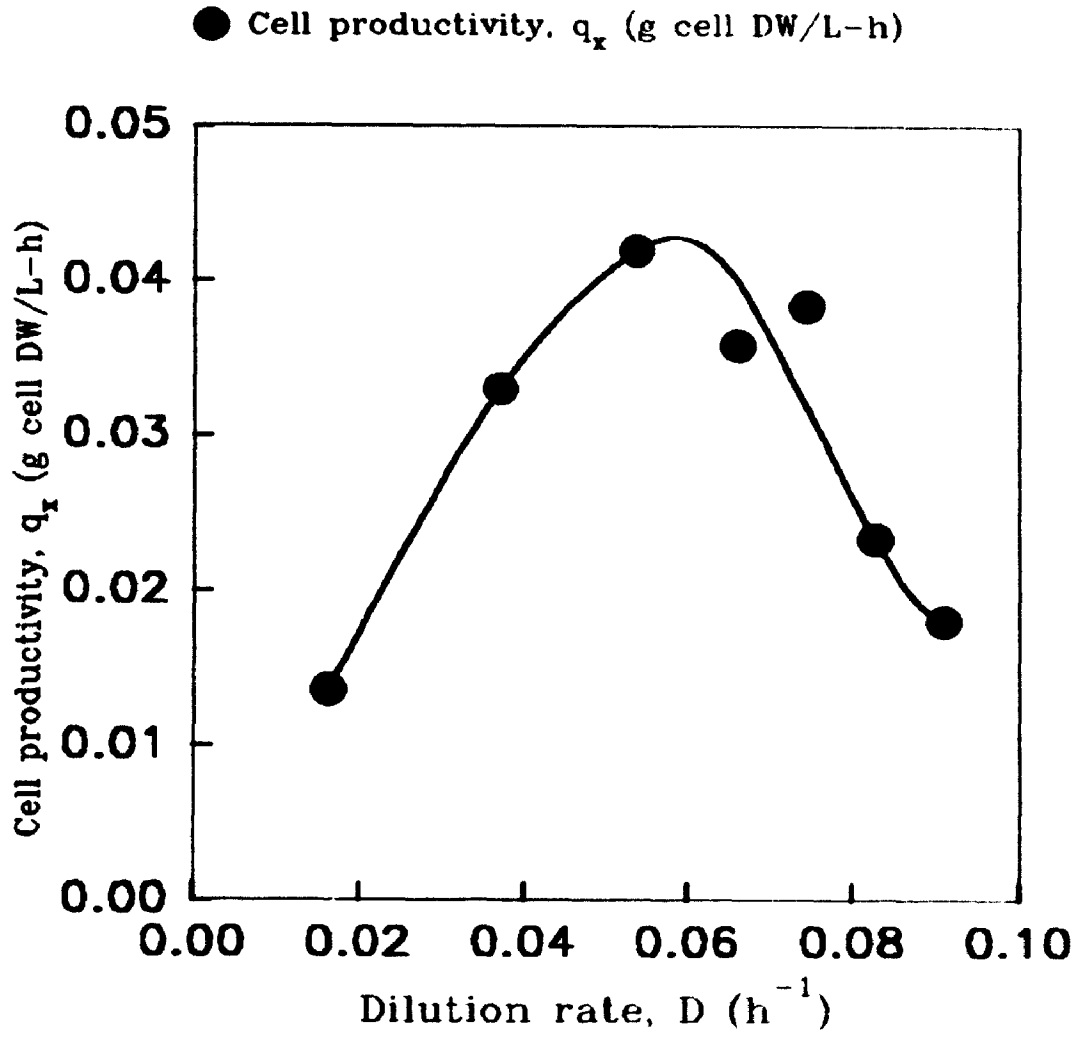
Cell productivity, q_x (g cell DW/L-h)
0.05
0.04
0.03
0.02
0.01
0.00
Cell productivity, q_x (g cell DW/L-h)
0.00
0.02
0.04
0.06
0.08
0.10
Dilution rate, D (h^{-1})

Figure 5.25. Specific INA Productivity, q_p (ice nuclei/g cell DW-h) and Volumetric INA productivty, q_v, ice nuclei/l bioreactor volume /h of P. syringae Cit7 in the CSTBR at 25° C and pH = 7.0.

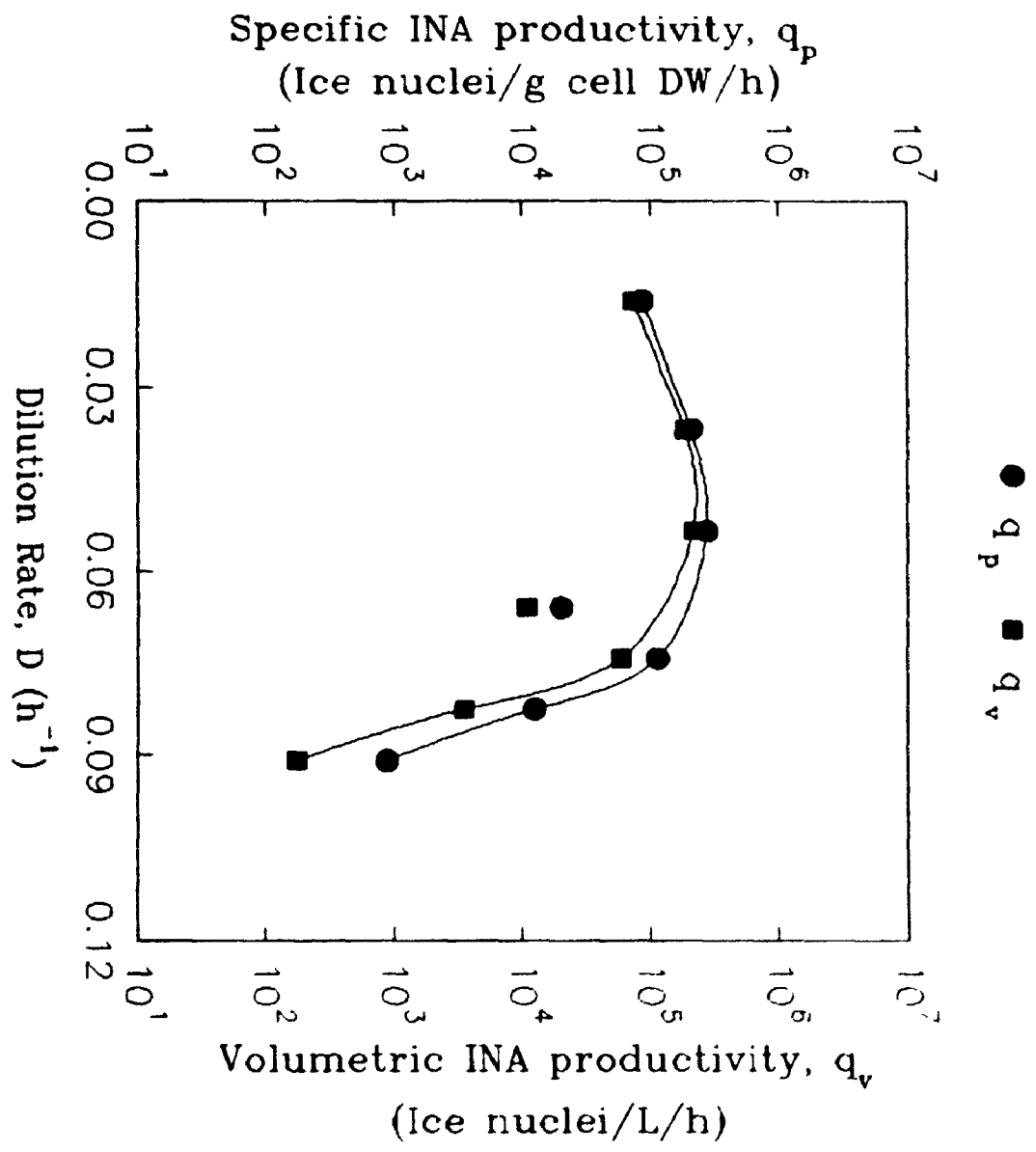
Specific INA productivity, q_p
(Ice nuclei/g cell DW/h)
10^1
10^2
10^3
10^4
10^5
10^6
10^7
0.00
0.03
0.06
0.09
0.12
Dilution Rate, D (h^{-1})
q_p
q_v
Volumetric INA productivity, q_v
(Ice nuclei/L/h)

mass transfer limitations of substrates resulting from the different hydrodynamic and oxygen mass transfer conditions existing in a larger scale reactor. Dead zones may exist in larger reactors which lead to poor mixing and accumulation of toxins which can inhibit growth. The optimized conditions developed in the 1 L bioreactor, i.e., temperature of 25° C, pH 7.0 were used to grow the cells as described in Materials and Methods.

Figure 5.26 shows the growth kinetics of P. syringae in the larger 15 L scale bioreactor. It can be seen that the sucrose concentration decreased from 5 g/L to 0.0 g/L in 82.0 h of cultivation. The cell concentration, X, increased to 1.24 g DW/L in the same time period. The ice nuclei per g cell DW, η, increased from an initial 10^4 at inoculation or zero time to approximately 7.0 X 10^6 at the stationary phase of cell growth. The results in the 15 L cultivation were similar to the results in the 1 L cultivation with INA found to develop in the lag as well as log phase of cell growth. However, the maximum level of INA in the 15 L bioreactor was found to be lower than INA obtained in the 1 L bioreactor. Thus growth of cells in the 15 L bioreactor seemed to affect INA of P. syringae cit 7. Since it was seen earlier that aeration may be a variable affecting the INA of P. syringae cit 7, one possibility is the poorer oxygen transfer in the 15 L bioreactor due to the presence of dead zones or stagnant regions. An aspect which needs to be considered in further studies is an appropriate criterion for scale-up of INA bacteria production. Since oxygen transfer may become of critical importance at larger scales, an appropriate criterion for scale-up of INA could be the maintenance of constant mass transfer coefficient, $K_L a$ (h^{-1}).

Figure 5.26. Batch Growth Kinetics and Ice Nucleation Activity of P. syringae Cit7 in the 15 L Bioreactor at 25.0° C

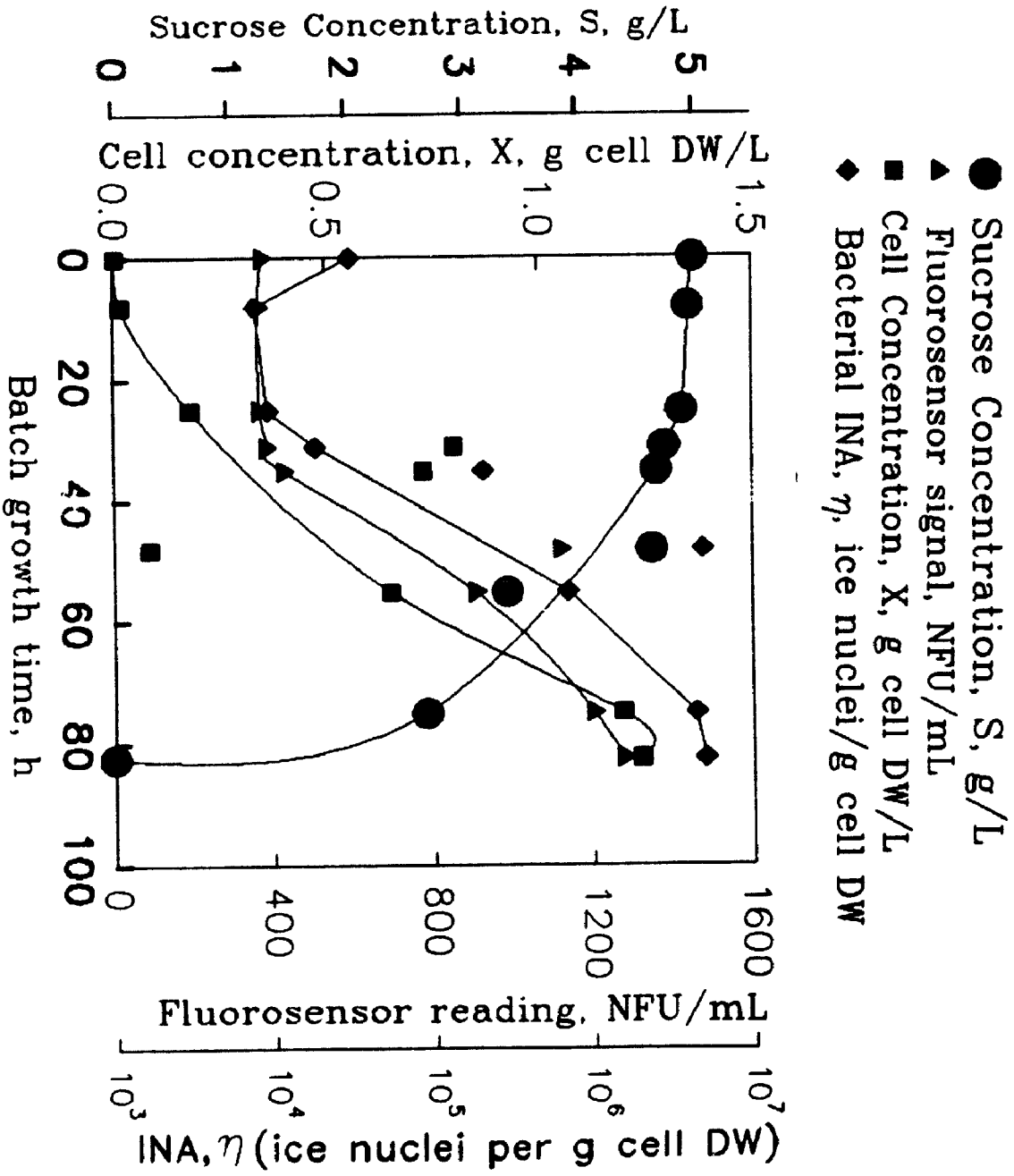
Sucrose Concentration, S, g/L
Fluorosensor signal, NFU/mL
Cell Concentration, X, g cell DW/L
Bacterial INA, η, ice nuclei/g cell DW
Sucrose Concentration, S, g/L
0
1
2
3
4
5
Cell concentration, X, g cell DW/L
0.0
0.5
1.0
1.5
Batch growth time, h
0
20
40
60
80
100
0
400
800
1200
1600
Fluorosensor reading, NFU/mL
10³
10⁴
10⁵
10⁶
10⁷
INA, η (ice nuclei per g cell DW)

5.5 Mathematical Modelling of Batch Growth of P. syringae and its INA in a 1 L Bioreactor System

In Chapter 3, an unstructured mechanistic model was proposed for representing P. syringae cit 7 cell growth and INA development with batch growth time in the 1 L bioreactor at different temperatures. In this section, the results of the model simulations are discussed.

Two important assumptions on which this model was based were described in Chapter 3.

(a) The model assumed that ice nuclei formation in the bioreactor occurred in the log phase of cell growth.

(b) The model assumed that ice nuclei formation was non-linearly related to cell concentration.

Both these assumptions were incorporated into the model through Equation 3.25 shown in Chapter 3. In order to use Equation 3.25 in the mathematical model, and still have $Y_{p/x}$ as a constant, the total cultivation period of cells in the bioreactor was divided into 4 phases, i.e., lag phase, early exponential, late exponential, and stationary phase respectively. $Y'_{p/x}$ was given different constant values over each of these phases of cell growth.

Figures 5.27 to 5.33 describe the model simulations for change in sucrose concentration S (g/L), cell concentration X (g/L) (shown by dotted line) and INA P (ice nuclei/L) in the 1 L bioreactor. The experimental data for sucrose, cells and

Figure 5.27. Batch Growth Kinetics and Ice Nucleation Activity of P. syringae cit7 in the 1 L Bioreactor at 5.5° C. Model Simulations versus Experimental Data. Solid points shown are experimental values of sucrose (●), cell concentration (○) and ice nuclei concentration (♦) per L of bioreactor volume. Simulations are given as: S-S-S (sucrose); P-P-P (ice nuclei concentration); ..... (cell concentration). The bars indicate the approximate 95% confidence limits of simulated versus experimental cell concentration data calculated through the non-linear regression program UWHAUS.

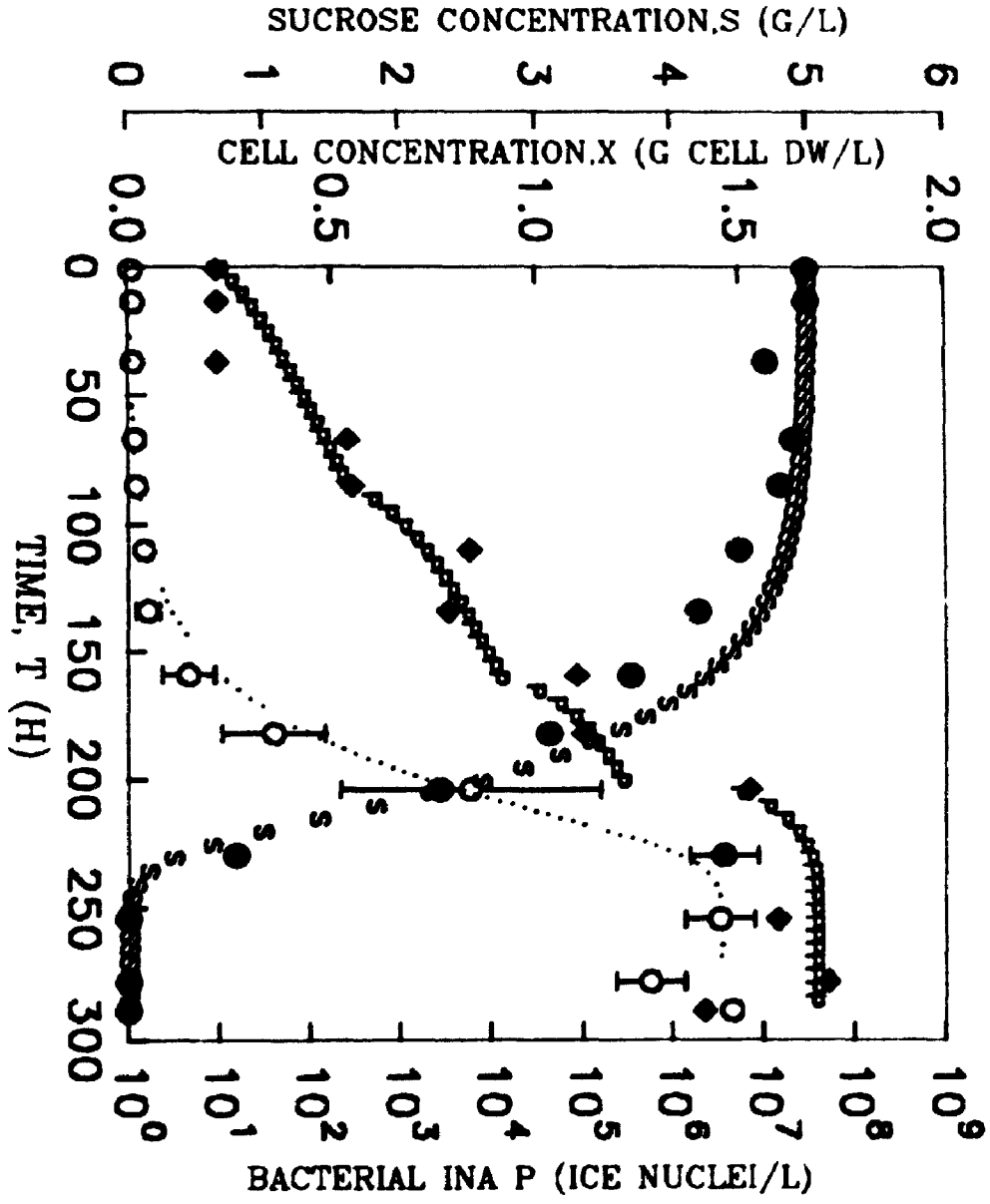
SUCROSE CONCENTRATION,S (G/L)
0
1
2
3
4
5
6
CELL CONCENTRATION,X (G CELL DW/L)
0.0
0.5
1.0
1.5
2.0
TIME, T (H)
0
50
100
150
200
250
300
BACTERIAL INA P (ICE NUCLEI/L)
10^0
10^1
10^2
10^3
10^4
10^5
10^6
10^7
10^8
10^9

Figure 5.28. Batch Growth Kinetics and Ice Nucleation Activity of P. syringae cit7 in the 1 L Bioreactor at 10.0 °C. Model Simulations versus Experimental Data. Solid points shown are experimental values of sucrose (●), cell concentration (○) and ice nuclei concentration (♦) per L of bioreactor volume. Simulations are given as: S-S-S (sucrose); P-P-P (ice nuclei concentration); ..... (cell concentration). The bars indicate the approximate 95% confidence limits of simulated versus experimental cell concentration data calculated through the non-linear regression program UWHAUS.

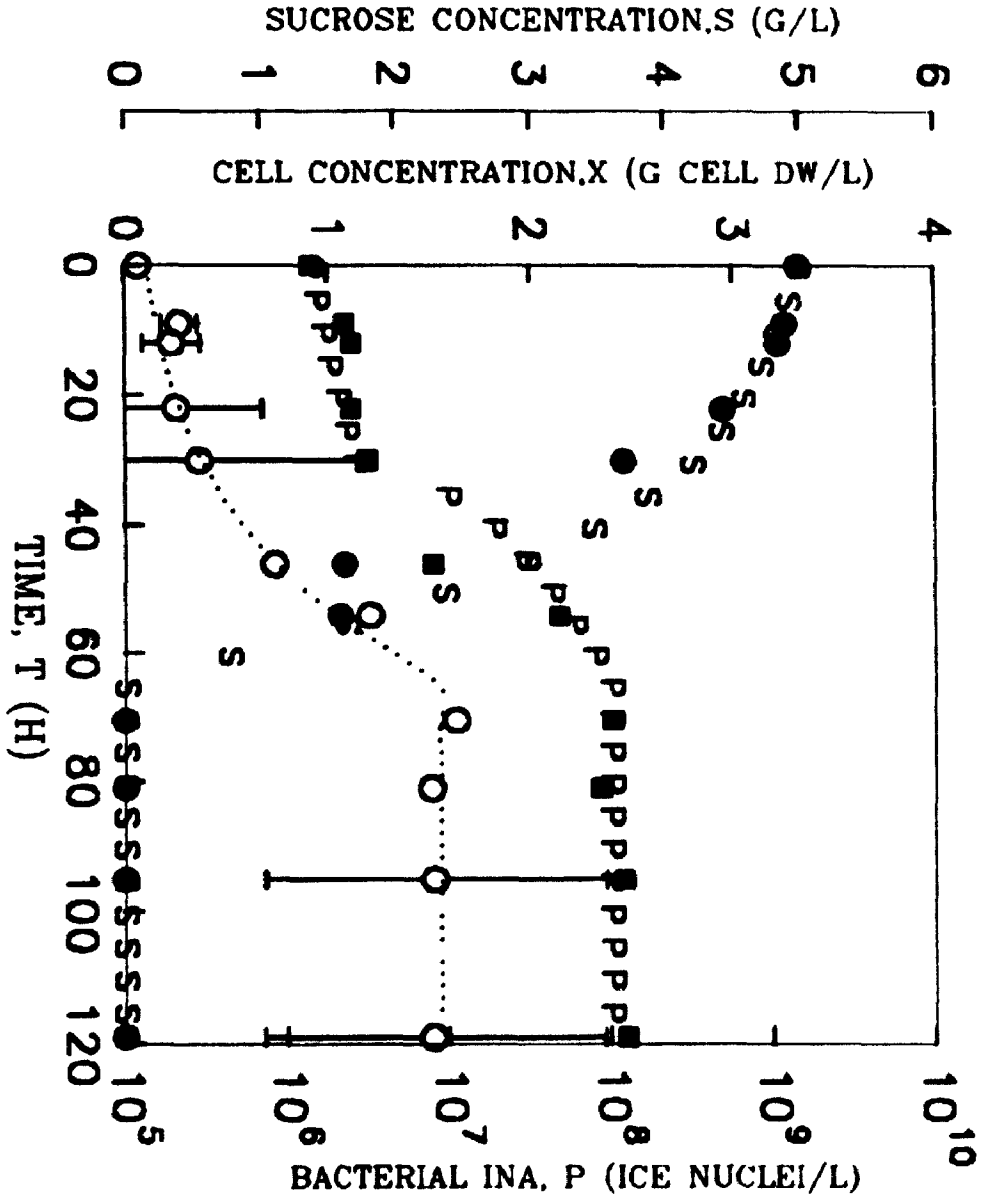
SUCROSE CONCENTRATION,S (G/L)
0
1
2
3
4
5
6
CELL CONCENTRATION,X (G CELL DW/L)
0
1
2
3
4
TIME, T (H)
0
20
40
60
80
100
120
BACTERIAL INA, P (ICE NUCLEI/L)
10^5
10^6
10^7
10^8
10^9
10^{10}

Figure 5.29. Batch Growth Kinetics and Ice Nucleation Activity of P. syringae cit7 in the 1 L Bioreactor at 15.0 °C. Model Simulations versus Experimental Data. Solid points shown are experimental values of sucrose (●), cell concentration (○) and ice nuclei concentration (♦) per L of bioreactor volume. Simulations are given as: S-S-S (sucrose); P-P-P (ice nuclei concentration); ..... (cell concentration). The bars indicate the approximate 95% confidence limits of simulated versus experimental cell concentration data calculated through the non-linear regression program UWHAUS.

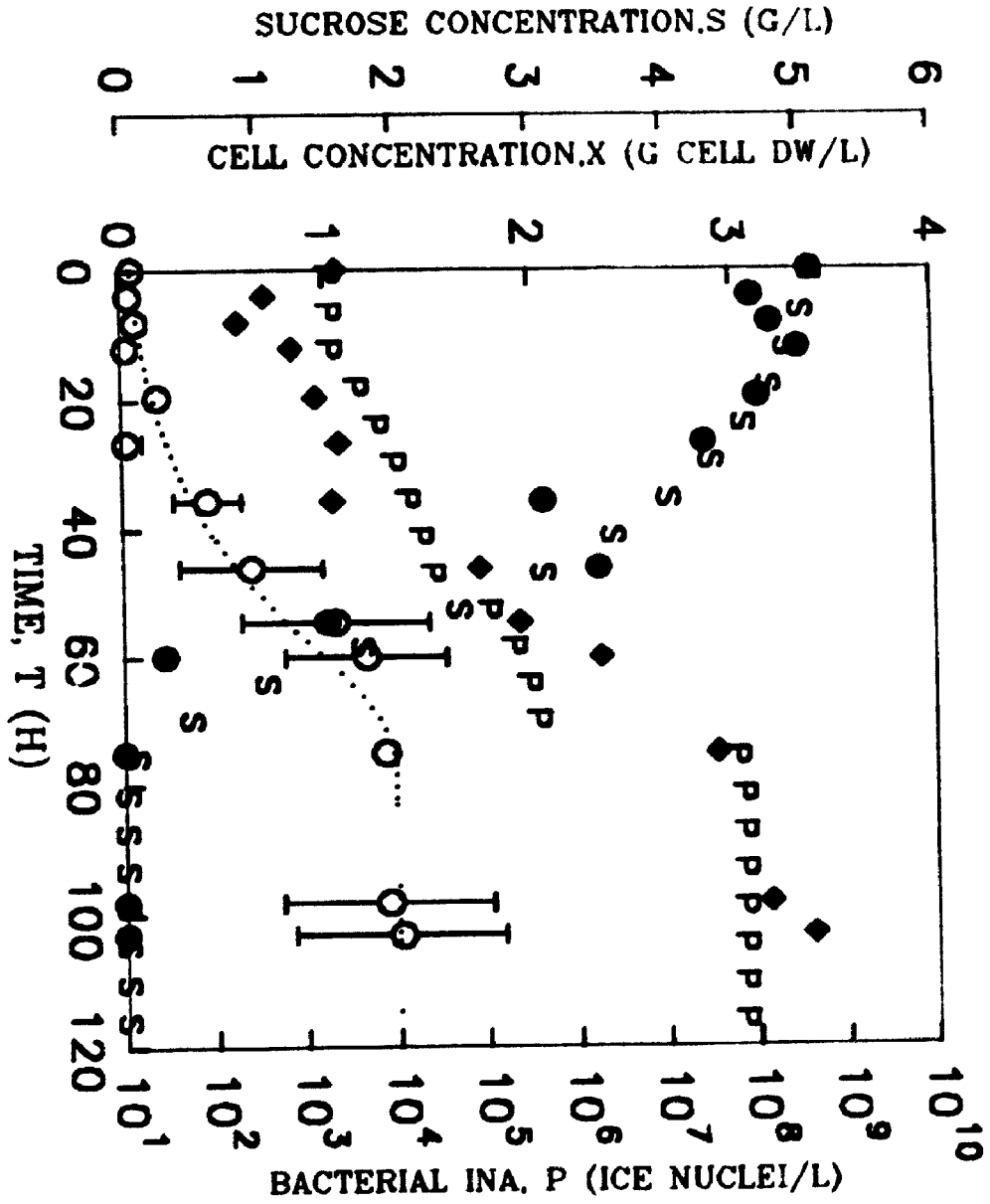
SUCROSE CONCENTRATION.S (G/L)
0
1
2
3
4
5
6
CELL CONCENTRATION.X (G CELL DW/L)
0
1
2
3
4
TIME, T (H)
0
20
40
60
80
100
120
10^1
10^2
10^3
10^4
10^5
10^6
10^7
10^8
10^9
10^{10}
BACTERIAL INA. P (ICE NUCLEI/L)

Figure 5.30. Batch Growth Kinetics and Ice Nucleation Activity of P. syringae cit7 in the 1 L Bioreactor at 20.0 °C. Model Simulations versus Experimental Data. Solid points shown are experimental values of sucrose (●), cell concentration (○) and ice nuclei concentration (♦) per L of bioreactor volume. Simulations are given as: S-S-S (sucrose); P-P-P (ice nuclei concentration); ..... (cell concentration). The bars indicate the approximate 95% confidence limits of simulated versus experimental cell concentration data calculated through the non-linear regression program UWHAUS.

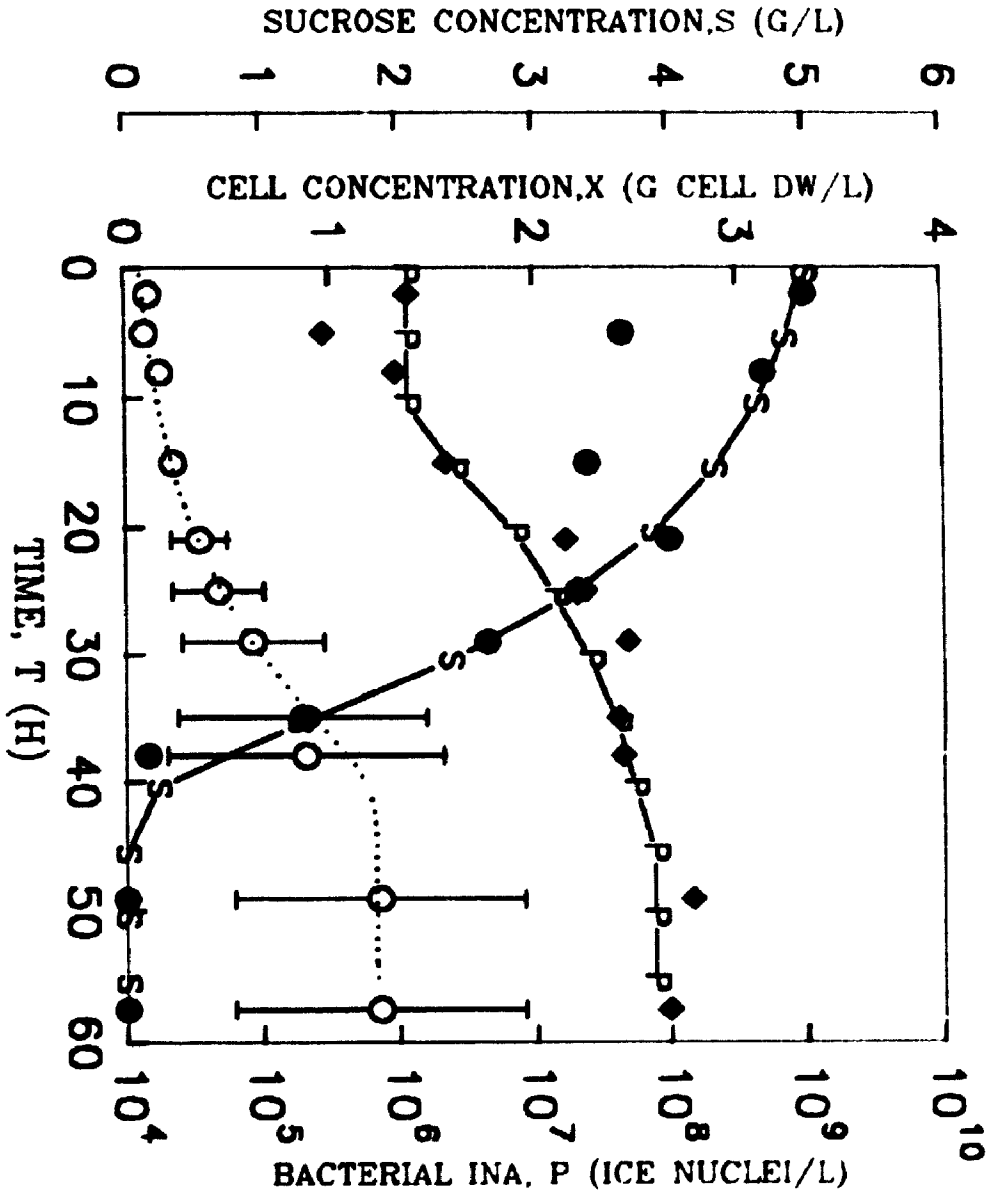
SUCROSE CONCENTRATION,S (G/L)
0
1
2
3
4
5
6
CELL CONCENTRATION,X (G CELL DW/L)
0
1
2
3
4
TIME, T (H)
0
10
20
30
40
50
60
10^4
10^5
10^6
10^7
10^8
10^9
10^{10}
BACTERIAL INA, P (ICE NUCLEI/L)

Figure 5.31. Batch Growth Kinetics and Ice Nucleation Activity of P. syringae cit7 in the 1 L Bioreactor at 25.0 °C. Model Simulations versus Experimental Data. Solid points shown are experimental values of sucrose (●), cell concentration (○) and ice nuclei concentration (♦) per L of bioreactor volume. Simulations are given as: S-S-S (sucrose); P-P-P (ice nuclei concentration); ..... (cell concentration). The bars indicate the approximate 95% confidence limits of simulated versus experimental cell concentration data calculated through the non-linear regression program UWHAUS.

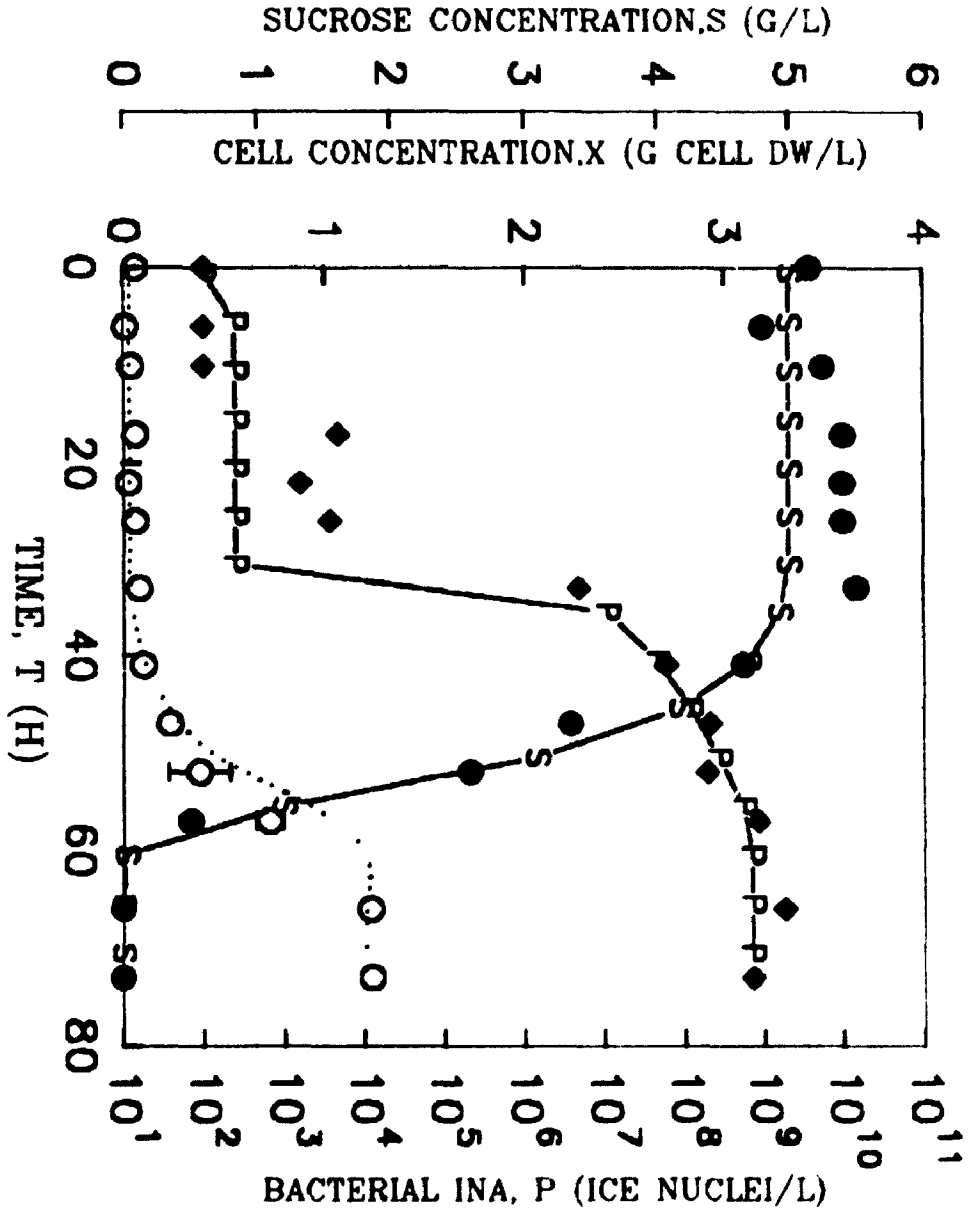
SUCROSE CONCENTRATION,S (G/L)
0
1
2
3
4
5
6
CELL CONCENTRATION,X (G CELL DW/L)
0
1
2
3
4
TIME, T (H)
0
20
40
60
80
10^1
10^2
10^3
10^4
10^5
10^6
10^7
10^8
10^9
10^{10}
10^{11}
BACTERIAL INA, P (ICE NUCLEI/L)

Figure 5.32. Batch Growth Kinetics and Ice Nucleation Activity of P. syringae cit7 in the 1 L Bioreactor at 28.0 °C. Model Simulations versus Experimental Data. Solid points shown are experimental values of sucrose (●), cell concentration (○) and ice nuclei concentration (♦) per L of bioreactor volume. Simulations are given as: S-S-S (sucrose); P-P-P (ice nuclei concentration); ..... (cell concentration). The bars indicate the approximate 95% confidence limits of simulated versus experimental cell concentration data calculated through the non-linear regression program UWHAUS.

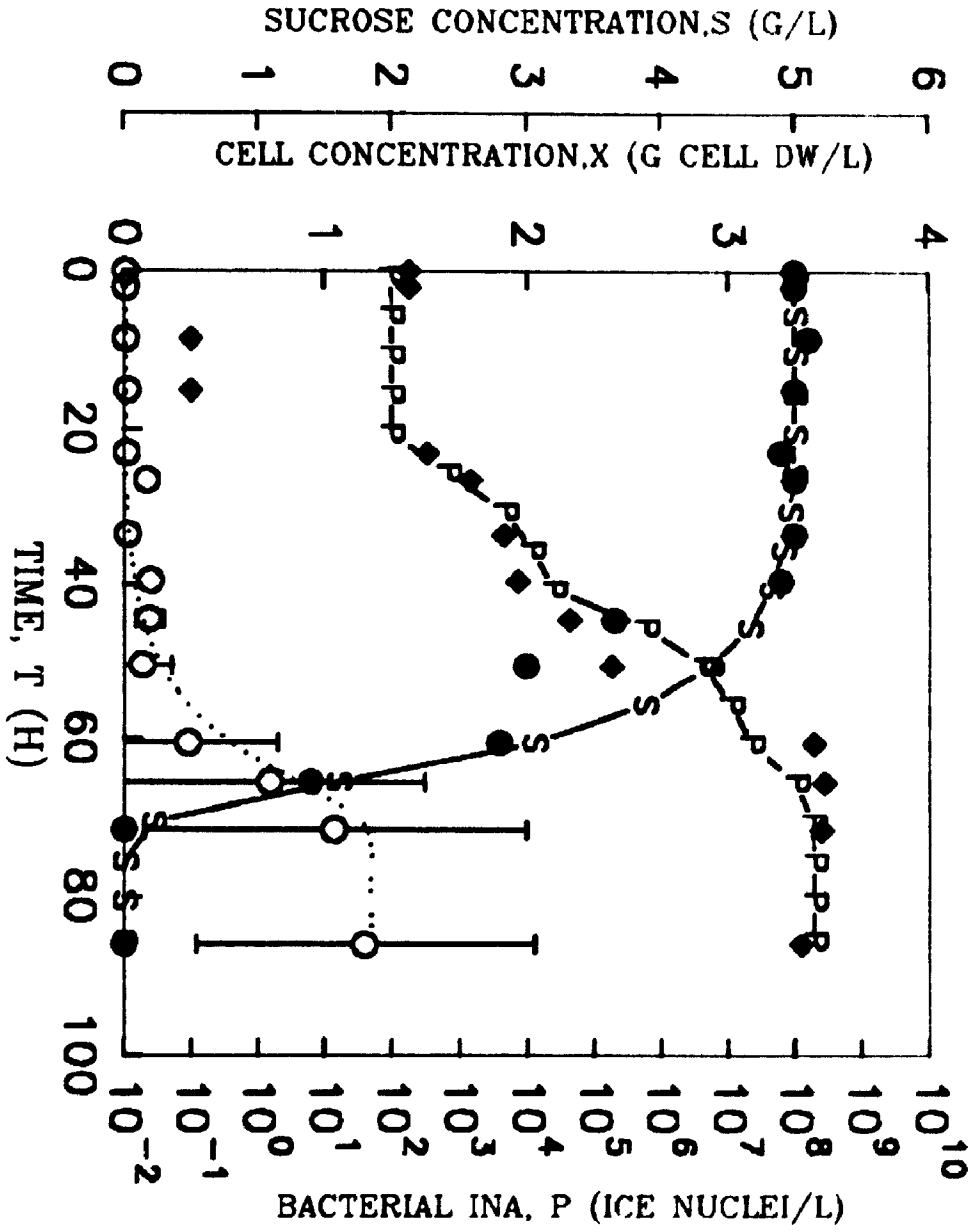
SUCROSE CONCENTRATION,S (G/L)
0
1
2
3
4
5
6
CELL CONCENTRATION,X (G CELL DW/L)
0
1
2
3
4
TIME, T (H)
0
20
40
60
80
100
10^{-2}
10^{-1}
10^{0}
10^{1}
10^{2}
10^{3}
10^{4}
10^{5}
10^{6}
10^{7}
10^{8}
10^{9}
10^{10}
BACTERIAL INA, P (ICE NUCLEI/L)

Figure 5.33. Batch Growth Kinetics and Ice Nucleation Activity of P. syringae cit7 in the 1 L Bioreactor at 35.0 °C. Model Simulations versus Experimental Data. Solid points shown are experimental values of sucrose (●), cell concentration (○) and ice nuclei concentration (♦) per L of bioreactor volume. Simulations are given as: S-S-S (sucrose); P-P-P (ice nuclei concentration); ..... (cell concentration). The bars indicate the approximate 95% confidence limits of simulated versus experimental cell concentration data calculated through the non-linear regression program UWHAUS.

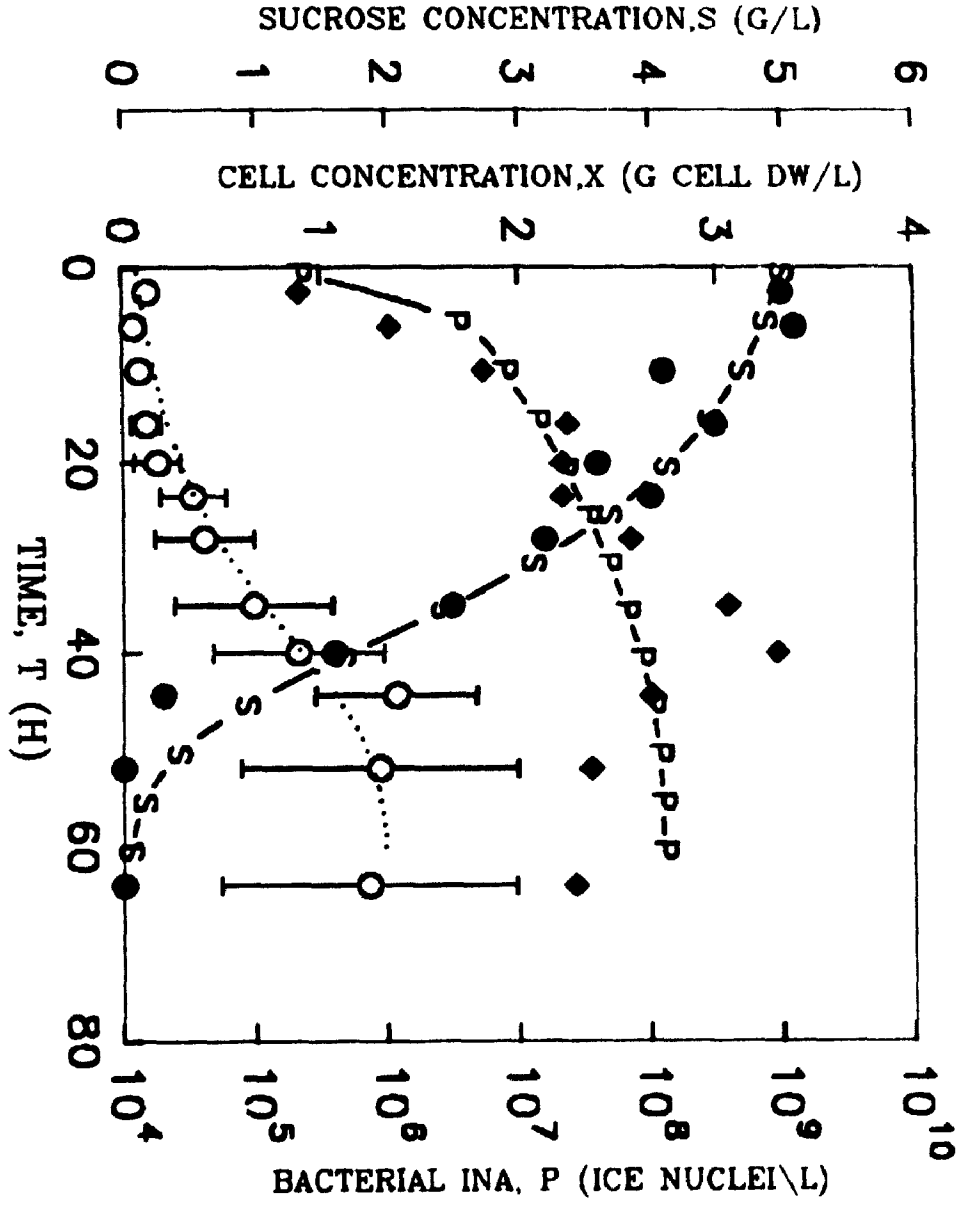
SUCROSE CONCENTRATION,S (G/L)
0
1
2
3
4
5
6
CELL CONCENTRATION,X (G CELL DW/L)
0
1
2
3
4
TIME, T (H)
0
20
40
60
80
S
P
BACTERIAL INA, P (ICE NUCLEI\L)
10^4
10^5
10^6
10^7
10^8
10^9
10^{10}

INA (given by $K(\theta)$ cumulative ice nuclei per L) are also shown in these figures as solid points.

Using model parameters obtained from least squares fitting of cell concentration simulations with experimentally available values of X g cell DW/L, the change in S and P versus time t was obtained (Figures 5.27 to 5.33). It is seen that the model simulations adequately represented the experimental data for sucrose, cells and INA at different temperatures. The least squares estimates of the parameters used are listed in Table 5.9.

It is recognized here that even though the model adequately simulates the cell growth kinetics and INA development, it is difficult to assign physical validity to the constants obtained in Table 5.9. A systematic review of literature revealed that experimental values of K_s for P. syringae cit 7 at the different growth temperatures are not available. Thus, separate experimental verification needs to be carried out by growing P. syringae cells at a given temperature but with increasing initial substrate concentration. Such a procedure will yield representative data of the specific growth rate, μ as a function of initial substrate concentration, S, from where K_s and μ_{max} may be calculated. The constant B also needs to be determined experimentally. This can be done through the use of defining equation of B (Equation 3.29) and a complete carbon balance on the bioreactor to account for all products formed (e.g., closed carbon balance). If experimental values of the constants B and K_s become available, the remaining constants m and $Y'_{p/x}$ can be easily calculated using the model developed in this thesis.

Table 5.9 Least square estimates of model parameters

T (°C)	μ_{max}	B	K_s	m
5.5	0.0355	3.45	0.853	0.000063
10.0	0.0431	3.36	0.090	0.00010
15.0	0.0777	4.57	1.600	0.00010
20.0	0.0808	4.66	0.500	0.00010
25.0	0.1303	4.04	0.800	0.00010
28.0	0.1825	4.06	0.300	0.00010
35.0	0.0980	4.51	2.200	0.00010

The simulation program used had a tendency to move towards the local optimum on the parameter response surface. Thus very accurate initial guesses for the parameters are needed since a number of optima can result using 4 variable parameters.

Even with the above mentioned limitations, the mechanistic model which was proposed, proved to be useful for the batch growth kinetics of P. syringae cit 7. The model provides an insight into the mechanism of INA development since it was based on assumptions which could be generalized to different temperatures. It can also provide a basis for further improvement with the availability of more experimental data and can also be tested for the growth and INA production of other ice nucleating bacteria.

CHAPTER 6

CONCLUSIONS AND RECOMMENDATIONS

In this research, the kinetics of growth and ice nucleation activity of P. syringae bacteria was investigated at different nutrient and culture conditions, and under batch and continuous bioreactor conditions. Important conclusions of this thesis are summarized here.

The measurement of bacterial ice nucleation using the droplet freezing assay was first investigated thoroughly. In the range of 0° C to -10° C, effects of phosphate buffer and deionized water on initiating ice nucleation in drops were discounted. Separation of cells from the culture free medium also did not affect its INA. An unsteady state analysis of heat transfer from the drop to the cooling bath proved heat transfer was very rapid. Drop freezing was a function of cell numbers in the drop. It was shown in this thesis that beyond a certain "saturation" cell concentration, the INA of bacteria becomes independent of concentration. In the case of P. syringae, this value is 10^6 cells per mL of broth. This "saturation" value may be used as an optimum cell concentration for snow making applications.

The objective of aerobic, shake-flask studies was to broadly examine various environmental factors for their effect on the activity of the ice nucleating Pseudomonas syringae bacteria. These factors included growth temperature, pH, aeration, medium composition, cell concentration as well as bacterial strain used.

Since all these factors were found to affect INA, the expression of INA in P. syringae cit 7 appears to be a complex function of environmental conditions e.g., temperature, medium composition. pH, aeration.

Cells grown in liquid medium appear to have greater IN efficiencies than on solid media and INA is maximum in the late exponential phase of cell growth. Type I ice nuclei (i.e. which initiate freezing between -2° C to -5° C) were produced by P. syringae cit 7 when it was cultured on sucrose, glucose, fructose, glycerol, sorbitol, as the carbon source. However, some components of the medium, e.g. sodium nitrate did not produce cells with high INA. The ice nucleation sites of the P. syringae bacteria were also found to be thermo-sensitive with growth of the cells over 25° C leading to a decrease in INA. Growth at pH of 8.0 also decreased INA and microaerophylic conditions in shake flasks were found to lower INA in the bacteria.

Cells grown on sucrose as a carbon source had high levels of INA. Previously, glucose, glycerol, sodium citrate have been the common carbon sources used for cultivating INA bacteria. A previous study of sugar accumulation on plant leaves showed that sucrose concentrations increased during winter (Levitt, 1980). The increased concentration of sucrose and a combination of other conditions including low temperatures may induce the bacteria to produce large amounts of the ice nucleation protein. An indirect evidence of this hypothesis was seen in this investigation, where the INA of bacteria was found to be dependent

on growth conditions.

Cell growth studies in the bioreactor were conducted in a range of temperatures from 5.5° C to 35° C. The maximum INA of P. syringae cit 7 as well as the maximum INA productivity (ice nuclei/ g cell DW.h) was found at 25° C. An Arrhenius relationship for cell growth as a function of temperature was also established in this study. The optimum cell growth temperature for P. syringae was found to be 28° C.

Continuous cultivation of P. syringae cit 7 cells in the 1 L bioreactor revealed that high values of INA can be maintained at relatively low dilution rates with specific growth rates close to the values in late exponential phase of cell growth.

A mechanistic model was developed which was based on two key assumptions, i.e., (1) INA is developed during the lag and log phases of cell growth but not as a secondary metabolite, and (2) the product yield coefficient, $Y'_{p/x}$, was constant with different values in different phases of cell growth. With these assumptions, and using the Monod equation to represent the kinetics of cell growth of P. syringae cit 7, the mathematical model was found to adequately fit the data.

More fundamental studies need to be done to elucidate the biochemical pathways involved in the production of the ice nucleation protein. Such studies could explain why medium composition, included the nature of the carbon source can affect INA. Studies are also needed on the kinetics of growth and INA on the natural environment of the plant leaf since this may be the optimum environment for the bacteria to develop ice nucleation activity. However, this is only possible if

controlled experiments are designed which may prove to be difficult.

The effect of pH or aeration was not examined in detail. Further studies in this direction are needed to establish more closely the optimum pH and aeration for producing cells with high INA. Several other variables need to be examined, e.g., the effect of removal of the outer cell membrane on the INA of the bacteria, the effect of proteases, and lysozyme on bacterial INA. The killing of whole cells, without disrupting the structure of the cells (by using radiation for example) would be an ideal technique to provide highly efficient, non-viable ice nuclei for applications in the food industry. Thus further research needs to focus on the development of efficient techniques to achieve this objective. In this study, the optimum conditions of growth of P. syringae cells in a bioreactor were established. Specific growth rates and INA productivities as well as cell yields were determined as a function of temperature as well as dilution rate. Scaling up the production of the ice nucleation bacteria to 150 L reactors would be the next step in this direction. Further studies can also examine various novel applications of INA bacteria, e.g., to separate wastes using freeze concentration. A difficult question to be answered concerns the nature of the selection for evolution and maintenance of microbial ice-nucleating sites. A variety of explanations have been advanced, including opportunistic plant-pathogenesis (via frost damage) to increased adsorption of water vapour; none can be tested easily. Thus this enigma of bacterial ice nucleation will continue to be focus of much research for molecular biologists, biochemical engineers and applied microbiologists in the near future.

REFERENCES

Arai, S., and Watanabe, M., "Freeze texturing of food materials by ice nucleation with the bacterium Erwinia ananas", Agric. Biol. Chem. **50(1)**, pp. 169 - 175 (1986).

Atkinson, M.M., and Bakur, J.C., "Association of host plasma membrane K^+/H^+ exchange with multiplication of Pseudomonas syringae pv. syringae in Phaseolus vulgaris", Phytopathol.**77(9)**, pp. 1273-1279 (1987).

Atkinson, B., and Mavituna, F., Biochemical Engineering and Biotechnology Handbook, The Nature Press, MacMillan, N.Y. (1983)

Bailey, J.E., and Ollis, D.F., Biochemical Engg. Fund. , 2nd ed. McGraw Hill (N.Y) pp. 373-454 (1986).

Barthakur, N., and Maybank, J., "Anomalous behaviour of some amino acids as ice nucleators", Nature **200**, pp. 866-868 (1963).

Bigg, E.K., "The supercooling of water", Proc. Phys. Sci. **b66**, pp. 688-694(1953).

Bigg, E.K., and Miles, G.T., "The results of large scale measurement of natural ice nuclei. J. Atmos. Sci., **211**, pp. 396-403 (1964).

Biotechnology news report, "Field tests conducted", Biotechnol. news. **8(1)** (1988).

Breed, R.S., Murray, E.G., and Hitchens, A.P., Bergey's Manual of Determin. ive Bacteriology, 6th ed., Williams and Wilkins Co., Baltimore, pp. 189 (1948).

Bruce, I., "Concerning drops", Am. J. Phys., **52(12)**, pp. 1102-1105 (1984)

Burke, M.J., and Lindow, S.E., "Surface properties and size of the ice nucleation site in ice nucleation active bacteria: theoretical considerations", Cyrobiol. **26**, pp. 80-84 (1990).

Chen, J., and Kevorkian, V., "Heat and mass transfer in making snow", Ind. Eng. Chem. Proc. Des. Develop. **10(1)**, pp. 75-78 (1971).

Chowdhury, J., "CPI warm up to freeze concentration", Chem. Engg. April 25, pp. 24 - 31 (1988).

Cody, Y.S., Gross, D.C., Proebsting Jr., E.L., and Spotts, R.A., "Suppression of ice nucleation active Pseudomonas syringae by antagonistic bacteria in fruit tree orchards and evaluations of frost control", Phytopathol. **77(7)**, pp. 1036 - 1044 (1987).

Corroto, L.V., Wolber, P.K., and Warren, G.J., "Ice nucleation activity of Pseudomonas fluorescens: mutagenesis, complementation analysis and identification of a gene product", EMBO J. **5,** pp. 231 - 236 (1986).

Deninger, C.A., Mueller, G.D., and Wolber, P.K., "Immunological characterization of ice nucleation proteins from Pseudomonas syringae, Pseudomonas fluorescens, and Erwinia herbicola", J. Bacteriol. **170(2),** pp. 669 - 675 (1988).

Dubois, M., Gilles, K.A>, Hamilton, J.K., Rebers, P.A., and Smith, F., "Colorimetric method for the determination of sugars and related substances", Anal. Chem. **28(3),** pp. 350-356 (1956).

Dubrovsky, M., Petera, V., Sikyta, B., Hegerova, H., "Measurement of the ice nucleation activity of Pseudomonas syringae CCM 4073", Biotechnol. Techniques **3(3),** pp. 173-178 (1989).

Duman, J.G., Morris, J.P., and Castellino, F.J., "Purification and composition of the ice nucleation protein from queens of the hornet Vespula masculata", J. Comp. Physiol. B, **154,** pp. 79-83 (1984).

Dye, D.W., Bradbury, J.F., Goto, M., Hayward, A.C., Lelliot, R.A., and Schroth, M.N., "International standards for naming pathovars of phytopathogenic bacteria and a list of pathovar names and pathotype strains", Rev. Plant Pathol. **59(4),** pp. 153-168 (1980).

Environmental Protection Agency Experimental Use Permit Documents Ref Nos. 55269-EUP-2,54306-EUD-1, 54306-EUP-2 (1988).

Feeney, R.E., and Yeh, Y., "Antifreeze proteins from fish bloods" Adv. Protein Chem. **32,** pp. 191-282 (1978)

Fennema, O.R., Powrie, W.D., and Marth, E.H., Low temperature preservation of foods and living matter, Marcel Dekker, N.Y., pp. 153-155 (1973).

Fields, P., "Cold-hardiness of Cryptolestes Ferrugineus: The use of ice nucleation active bacteria as a cold synergist", Proc. Fifth Int. Working Conf. Stored Prod. Protect. Bordeaux, France, pp. 1-9, (1991).

Fletcher, N.H. The Chemical Physics of Ice, Cambridge Univ. Pr. pp. 85 (1970).

Franks, F., Biophysics and biochemistry at low temperatures, Cambridge Univ. Press, (1985).

Fukuta, N., and Mason, B.J., "Epitaxial growth of ice on organic crystals", J. Phys. Chem. Solids, pp. 715-718 (1963).

Garten, V.A., and Head, R.B., "A theoretical basis of ice nucleation by organic crystals", Nature **205,** pp.160-162 (1965).

Govindarajan, A.G., and Lindow, S.E., "Phospholipid requirements for expression of ice nuclei in bacterial membranes in vitro", Plant Physiol. **75,** pp. 143 (abstr.) (1984).

Govindarajan, A.G., and Lindow, S.E. "Phospholipid requirement for expression of ice nuclei in Pseudomonas syringae and in vitro" J. Biol. Chem. **263**, pp. 9333-9338 (1988a).

Govindarajan, A.G., and Lindow, S.E., "Size of bacterial ice nucleation sites measured in situ by radiation inactivation analysis", Proc. Natl. Acad. Sci. U.S.A. **85,** pp. 1334-1338 (1988b).

Green, R.L., Corotto, L.V., and Warren, G.J., "Deletion mutagenesis of the ice nucleation gene from Pseudomonas syringae S203", MGG Mol. Gen. Genet., **215(1),** pp. 165-172 (1988).

Green, R.L., and Warren, G.J. "Physical and functional repetition in a bacterial ice nucleation gene", Nature **317(17),** pp. 645-648 (1985).

Haefele, D.M., and Lindow, S.E., "Flagellar motility confers epiphytic fitness advantages upon Pseudomonas syringae", Appl. Environ. Microbiol. **53(10),** pp. 2528 - 2533 (1987).

Hartland, S., and Hartley, R.W., Axisymmetric Fluid-Liquid Interfaces, Elsevier Scientific, pp. 24. (1976)

Head, R.B., "Steroids as ice nucleators", Nature **191,** pp. 1058-1059 (1961).

Head, R.B., "Ice nucleation by α - Phenazine", Nature **196,** pp. 736-738 (1962).

Hendricks, D.M., Orrego, S.A., Ward, P.J., "Production of microorganisms with high ice nucleating activity" European Patent **EP 0261624** pub Mar 30 (1988).

Himmelblau, D.M., Process Analysis by Statistical Methods, Chap. 6, John Wiley and Sons Inc. N.Y., pp. 176-207 (1970).

Hirano, S S., "Ecology and physiology of Pseudomonas syringae", Bio/Technology **3(12),** pp. 1073 - 1078 (1987).

Hirano, S.S., Nordheim, E.V., Arny, D.C., and Upper, C.D., "Lognormal distributions of epiphytic bacterial populations on leaf surfaces", Appl. Environ. Microb. **44(3),** pp. 605 - 700 (1982).

Hoel, P.G., Introduction to Mathematical Statistics, 3rd ed., N.Y., Wiley, pp. 427-428.

Jutan, A. "Process Analysis and Statistical Methods in Chemical Engineering", University of Western Ontario, London (1987)

Incropera, F.P., and DeWitt, D.P., Introduction to Heat Transfer: 2nd Ed., John Wiley & Sons, N.Y., Appendix A (1990)

Kieft, T.L., "Ice nucleation activity in lichen", Appl. Environ. Microbiol. **54(7),** pp. 1678 -1681 (1988).

Kim, H.K., Orser, C., Lindow, S.E., Sands, D.C., "Xanthomonas campestris pv. transluscens strains active in ice nucleation", Plant Dis. **71(11),** pp. 994 - 997 (1987).

King, E.O., Ward, M.K, Raney, D.E. "Two simple media for the demonstration of pyocyanin and fluorescein", J. Lab. Clin Med. **44**, pp. 301-307 (1954).

Kocak, R., and Van Gemert, H., "Man-made snow: biotechnology assisting the snow making industry", J. Biotechnol. **2(1),** pp. 37 -38 (1988).

Kozloff, L.M., Schofield, M.A., and Lute, M., "Ice nucleation activity of Pseudomonas syringae and Erwinia herbicola", J.Bacteriol. **153(1)**, pp. 222-231 (1983).

Kozloff, L.M., Lute, M., Westway, D., "Phosphotidylinositol as a component of the ice nucleating site of Pseudomonas syringae and Erwinia herbicola", Science **226,** pp. 845 -846 (1984).

Lamer, V.K., "Nucleation in phase transitions", Ind. Eng. Chem. **44(6)** pp. 1270-1273 (1952).

Levitt, J., Responses of plants to environmental stress VI: Chilling, Freezing, High Temperature Stress 2nd Ed. Acad. Press. N.Y. pp. 163-223 (1980).

Liao, J.C., and Ng, K.C., "Effect of ice nucleators on snow making and spray freezing", Ind. Eng. Chem. Res. **29**, pp. 361-366 (1990).

Lindemann, J., Constandine, H.A., Barchet, W.R., and Upper, C.D., "Plants as sources of airborne bacteria including ice nucleation bacteria", Appl. Environ. Microbiol. **44,** pp. 1059 (1982).

Lindemann, J., and Suslow, T.V., "Characteristics relevant to the question of environmental fate of genetically engineered INA⁻ deletion mutant strain of Pseudomonas", Proc. 6th Int. Conf. Plant Path. Bacteria, Maryland, June 2-7, 1985, Civerolo, E.L., Collmer, A., Davis, R.E., and Gillaspie, A.G., Eds., Martinus Nijhoff Publishers, (1987).

Lindow, S.E., "Population dynamics of epiphytic ice nucleation active bacteria on frost sensitive plants and frost control by means of antagonistic bacteria", Plants Cold Hardiness ed. P.H. LI, A. Sakai, Acad. Press. N.Y. pp. 395-416 (1982).

Lindow, S.E., "The role of bacterial ice nucleation in frost injury to plants", Ann. Rev. Phytopathol. **21,** pp. 363 - 384 (1983a).

Lindow, S.E., "Biological control of frost injury to tomato with non-ice nucleation active epiphytic bacteria", (Abstr.) in Proc. IVth Int. Cong. Plant Pathol. Melbourne, Aust., pp. 23 (1983b).

Lindow, S.E., "Ecology of Pseudomonas syringae relevant to the field use of ice-minus deletion mutants constructed in vitro for plant frost control, in Engineered organisms in the environment: scientific issues, H.O. Halvorson, D. Pramer, and M. Rogul (eds.) ASM Washington D.C., pp. 23 -35 (1985).

Lindow, S.E., "Lack of correlation of in vitro antibiosis with antagonism of ice nucleation active bacteria on leaf surfaces by non ice nucleation active bacteria", Phytopathol. **78(4),** pp. 444 - 450 (1988).

Lindow, S.E., Arny, D.C., and Upper, C.D., "Distribution of ice nucleation active bacteria on plants in nature", Appl. Environ. Microbiol., **36,** pp. 831 (1978).

Lindow, S.E., Arny, D.C., and Upper, C.D., "Bacterial ice nucleation: a factor in frost injury to plants in nature", Appl. Environ. Microbiol. **36**, pp. 831-838 (1983).

Lindow, S.E., Lahue, E., Govindarajan, A.G., Panapoulos, N.J., and Gies, D., "Localization of ice nucleation activity and the iceC gene product in Pseudomonas syringae and Escherichia coli", Mol. Plant Microb. Interact. **2(5)**, pp. 262-272 (1989).

Low, M., "Glycosyl-phosphatidylinositol: a versatile anchor for cell surface proteins", The FASEB J. **3**, pp. 1600-1608 (1989).

Lucas, J.W., "Supercooling and ice nucleation in lemons", Pl. Physiol., **29**, pp. 245-251 (1954)

Lynn, S.Y., and Noto, G.D., "Fermentation of microorganisms having high ice nucleating activity using a defined medium", European patent EP 0272669 Pub. 29 June, (1988).

Maki, L.R., Galyan, E.L., Chang-Chien, M., and Caldwell, D.R.,"Ice nucleation induced by Pseudomonas syringae",Appl. Microbiol. **28(3)**, pp. 456-459 (1974).

Maki, L.R., and Willoughby, K.J., "Bacteria as biogenic sources of freezing nuclei", J. Appl. Meterol. **17**, pp. 1049-1053 (1978).

Margaritis, A., and Bassi, A.S., "Principles and biotechnological applications of bacterial ice nucleation", CRC Critical Rev. Biotechnol. **11(3)** pp. 277-295 (1991)

McElroy, G., "Supercritical extraction of cyclosporin A from the fungus B. nivea", M.Sc. Thesis, Dept. Chem. Biochem.Engg., University of Western Ontario, London, Ontario, 1992.

Marquardt, D.L., "An algorithm for least squares estimation of non-linear parameters", J. Soc. Ind. Appld. Math. **2** pp. 1964 (1944).

Mason, B.J., "The growth of snow crystals", Sci. Amer. **204(1)**, pp. 120-131 (1961).

Monod, J., "The growth of bacterial cultures", Ann. Rev. Microbiol., **3**, pp. 371-394 (1942).

Mueller, G.M., Wolber, P.K., and Warren, G.J., "Clustering of ice nucleation protein correlates with ice nucleation activity",Cryobiol. **27**, pp. 416-422 (1990)

Neegaard, P., in Seeds V.I and II, MacMillan Press, Great Britain, (1977).

O'Brien, R.D., and Lindow, S.E., "Effect of plant species and environmental conditions on ice nucleation activity of Pseudomonas syringae on leaves", Appl. Environ. Microbiol. **54(9)**, pp. 2281 -2286 (1988).

Obata, H., Saeki, Y., Tanishita, J., Tokuyama, T., "Ice nucleation activity of Pseudomonas fluorescens", J. Ferment. Technol. **65** pp. 693-698 (1987).

Obata, H., Nakai, T., Tanashita, J., and Tokuyama, T., "Identification of an ice nucleating bacterium and its ice nucleation properties", J. Ferm. Bioengg. **67(3)**, pp. 143-147 (1989).

Ornston, L.N., "Regulation of catabolic pathways in Pseudomonas", Bacteriol. Rev., **35(2)**, pp. 87-116 (1971).

Orser, C., Staskawicz, B.J., Loper, J., Panopoulos, N.J., Dahlbeck, D., Lindow, S.E., and Schroth, M.N., "Cloning of genes involved in bacterial ice nucleation and fluorescent pigment/ siderophore production", Molecular Genetics of Bacterial Plant Interaction, A. Pühler Ed., Springer-Verlag, New York, pp. 353 - 361 (1983).

Orser, C.S., Lotstein, R., Lahuew, E., Willis, D.K., and Panopolous, N.J., "Structural and functional analysis of Pseudomonas syringae pv. syringae ice region and construction of ice deletion mutants", Phytopathol. **74**, pp. 798 (Abstr.) (1984).

Orser, C., Staskawicz, B.J., Panopolous, N.J., Dahlbeck, D., Lindow, S.E., "Cloning and expression of bacterial ice nucleation genes in E. coli", J. Bacteriol. **164(1)**, pp. 359 - 366 (1985).

Phelps, P., "The expression of ice nucleation activity in bacteria and the structure of the ice nucleation site", Ph.D Thesis, Univ. of Colorado, Boulder, (1987)

Phelps, P., Giddings, T.H., Prochoda, M., and Fall, R., "Release of cell free ice nuclei by Erwinia herbicola", J. Bacteriol. **167**, pp. 496 - 502 (1986).

Pirt, S.J., Principles of Microbe and Cell Cultivation, John Wiley, New York (1975).

Pooley, L., and Brown, T.A., "Effect of culture conditions on expression of the ice nucleation phenotype of Pseudomonas syringae", FEMS Microbiol. Letts., **77**, pp. 229-232 (1991).

Power, B.A., and Power, R.F., "Some amino acids as ice nucleators", Nature **194**, pp. 1170-1171 (1970).

Rogers, J.S., Stall, R.E., and Burke, M.J., "Low temperature conditioning of the ice nucleation active bacterium" Erwinia herbicola, Cryobiol. **24**, pp. 270-279 (1987)

Rohsenow, W.M., and Hartnett, J.P., Handbook of Heat Transfer, pp.3-41, pp. 3-59, McGraw Hill, N.Y. (1973).

Ryder, J.M., "Biogenic ice nuclei in the freezing of fish", PhD thesis Univ. of Rhode Island (1987).

Sands, D.C., Scharen, A.L., Carpenter, E., Caple, J., and Snider, J.R., "A hypothetical bio-precipitation cycle involving ice-nucleation and dew condensing bacteria, plants and rainfall", Proc. 6th Int. Conf. Plant Path. Bacteria, MaryLand, June 2-7, 1985, Civerolo, E.L., Collmer, A., Davis, R.E., and Gillaspie, A.G., Eds., Martinus Nijhoff Publishers, (1987).

Schnell, R.C., and Vali, G., "Atmospheric ice nuclei from decomposing vegetation", Nature **236**, pp. 163-165 (1973).

Scott, P.T., "Altered and enhanced iodargyrite with bismuth thioiodide for use in precipitation enhancement operations", Gov. Rep. Announce Index (U.S.) **88(3)** ,nos 806,362 (1988).

Seemüller, E., and Arnold, M., "Pathogenicity, syringomycin production and other

characteristics of pseudomonad strains isolated from deciduous fruit trees", Proc. 4th Int. Conf. Plant Path. Bacteria Aug. (Station de P⁻thologie, eds) pp. 703-710 (1978).

Sikyta, B., Hegerova, H., and Kudela, V., Czech. Patent. Appl., pp. 1875-1888 (1988)

Slater, J.H., Comprehensive Biotechnology, 1 Chap. 11, M.Moo-Young (ed.) Pergamon Pr., N.Y. pp. 201 - 202 (1985).

Soulage, G., " Atmospheric ice nuclei", Ann. Geophys., **13**, pp. 103-134.

Southworth, M.W., Wolber, P.K., and Warren, G.J., "Nonlinear relationship between concentration and activity of a bacterial ice nucleation protein", J. Biol. Chem., **263**, pp. 15211-15216 (1988).

Sprang, M.L., and Lindow, S.E., "Subcellular localization and partial characterization of ice nucleation activity of Pseudomonas syringae and Erwinia herbicola", Phytopathol. **71**, pp. 256 (abstr.) (1981).

Stanier, R.Y., Adelberg, E.A., and Ingraham, J., The Microbial World, 4th ed. Prentice Hall, Englewood Cliffs, New Jersey (1976).

Stansbury, E.J., "Stochastic freezing", McGill Univ., Stormy Weather Group, Sci. Rep. MW-35, 43-52 (1961).

Stewert, W.E., and Bear, L.L., "Concentration effects of ice nucleation active bacteria on water nucleation temperature", Proc. 23rd InterSoc. Energy Conv. Eng. Conf. July 31-Aug 5, Denver, Colorado, D. Yogi Goswami Ed. ASME, N.Y. 2, pp. 147-149 (1988).

Suslow, T.V., Lindow, S.E., and Dix, H., "Enhancement of snow production by ice nucleation active bacteria in air:water systems", Proc. 6th Int. Conf. Plant Path. Bacteria, MaryLand, June 2-7, (1985) Civerolo, E.L., Collmer, A., Davis, R.E., and Gillaspie, A.G., Eds., Martinus Nijhoff Publishers, (1987).

Thangaraj, K., Palanisamy, M., Gobinathan, R., and Ramasamy, P., "Substrate foreign atoms and ice nucleation activity", J. Colloid. Interface Sci. **126(2)**, pp. 463 - 468 (1988).

Turnbull, D. and Vonnegut, B., "Nucleation catalysts", Ind. Eng. Chem. **44(6)**, pp. 1292-1297 (1952).

Vali, G., "Quantitative evaluation of experimental results on the heterogeneous freezing of supercooled liquids", J. Atmos. Sci. **28**, pp. 402-409 (1971).

Vali, G., and Stansbury, E.J., "Time dependent characteristics of the heterogeneous nucleation of ice", Can. J. Phys. **44**, pp. 477-502 (1966).

Van Brunt, J., "Environmental release: A portrait of opinion and opposition", Bio/Technology **5(6)**, pp. 558-563 (1987).

Warren, G.J., "Bacterial ice nucleation: molecular biology and applications", Biotechnol Genet. Eng. Rev. **5**, pp.107-135 (1987).

Warren, G., Wolber, P., and Green, R., "Functional significance of oligo nucleotide repeats in a bacterial ice nucleation gene", Proc. 6th Int. conf. Plant Path. Bacteria, Maryland, June 2-7, , Civerolo, E.L., Collmer, A., Davis, R.E., and Gillaspie, A.G., (eds.), Martinus Nijhoff publishers, 1987, pp. 1013-1017 (1985).

Warren, G.J., Corotto, L., and Wobler, P.,"Conserved repeats in diverged ice nucleation structural genes from two species of Pseudomonas", Nucleic Acids Res. **14**, pp. 8047-8060 (1986).

Warren, G.J., and Wolber, P.K., "Ice nucleation immunoassay", U.S. patent **4, 784,943** (1989).

Warren, G.J., Lindemann, J., Suslow, T.V., and Green, R.L., "Ice nucleation deficient bacteria as frost protection agents", in Biotechnology in Agricultural Chemistry, ACS Symposium series, **334**, H.M. LeBaron, R.O. Mumma, R.C. Honeycutt, and J.H. Duesing, Eds., American Chemical Society Books, Washington D.C., pp. 215 - 227 (1987).

Watanabe, M., and Arai, S., "Freezing of water in the presence of the ice nucleation active bacterium, Erwinia ananas and its application for the efficient freeze drying of foods", Agric. Biol. Chem. **51(2)**, pp. 557 -563 (1987).

Watanabe, M., Watabe, S., and Soichi, A., "Interaction of an anti-nucleating chemical and an ice nucleating bacterium: a case study with n- octyl benzyldimethyl ammonium salt and Erwinia ananas", Agric. Biol. Chem. **52(8)**, pp. 1869-1871 (1988).

Wolber, P.K., and Green, R.L., "Detection of bacteria by transduction of ice nucleation genes", TIBTECH **8**, pp. 276-279 (1990).

Wolber, P.K., Deininger, C.A., Southworth, M.W., Vandwkerchove, J., Montagu, M.V., and Warren, G.J., "Identification and purification of a bacterial ice nucleation protein", Proc. Nat. Acad. Sci. U.S.A. **83**, pp. 7256-7260 (1986).

Wolber, P.K., and Warren, G.J., "Structural modelling of the ice nucleation protein of Pseudomonas syringae", Biophys. J. **49**, pp. 293a (abstr.) (1986).

Wolber, P.K., and Warren, G., "Bacterial ice nucleation proteins", Trends Biochem. Sci., **14**, pp. 179-182 (1989).

Worthy, W., "Bacteria assay exploits ice nucleation research", Chem Eng. News Jan 8, pp. 23 (1990).

Yankofsky, S.A., Levin, Z., Bertold, T., and Sandlerman, N., "Some basic characteristics of bacterial freezing nuclei", J. Appl. Meteorol. **20**, pp. 1013-1019 (1981).

Zhao, J. L., and Orser, C.S., "Conserved repetition in the ice nucleation gene inaX from Xanthomonas campestris pv. translucens", MGG, Mol. Gen. Genet. **223(1)**, pp. 163-166 (1990).

APPENDIX A

STANDARD CURVES FOR SUCROSE ESTIMATION

Figure A-1. Standard Curve for Determination of Sucrose Using Phenol-Sulfuric Acid Method of Dubois et al. (1956).

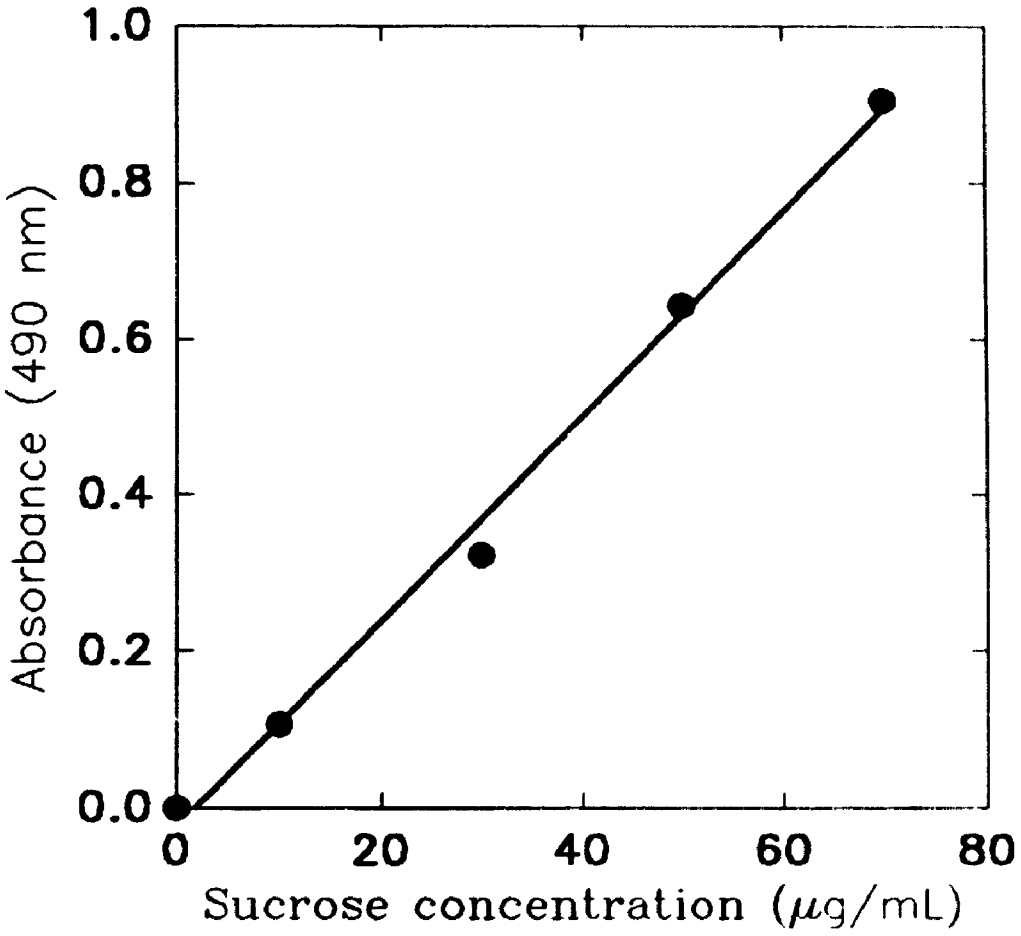
1.0
0.8
0.6
0.4
0.2
0.0
Absorbance (490 nm)
0
20
40
60
80
Sucrose concentration (μg/mL)

Figure A-2. Standard Curve for Determination of Sucrose using HPLC Method.

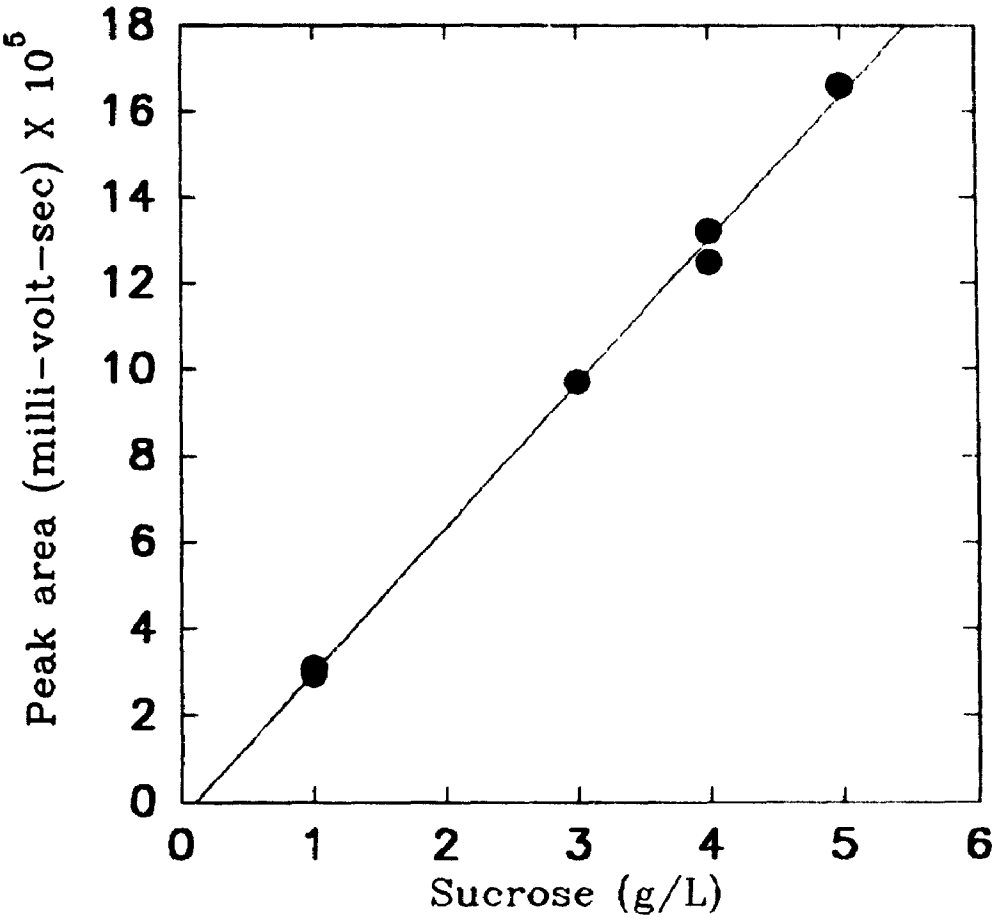
Peak area (milli-volt-sec) X 10^5
18
16
14
12
10
8
6
4
2
0
0
1
2
3
4
5
6
Sucrose (g/L)

APPENDIX B

CALCULATION OF TIME REQUIRED TO COOL A SINGLE WATER DROP ON A HYDROPHOBIC SURFACE FROM 25° C TO A COOLING BATH TEMPERATURE OF -4° C

Objective: To Estimate the Time Required to Cool a Single Water Drop Placed on a Hydrophobic Surface from 25° C to -4° C

Procedure:

(1) As shown in Figure 4.4, a water drop 9.75 μL in volume was placed on the surface of a paraffin coated (hydrophobic), aluminum foil dish.

(2) The aluminum foil dish is first placed in the cooling bath for at least 30 min before the drops containing ice nucleating bacteria are introduced. The bath is covered from the top with a close fitting lid hence convection of air is minimized.

(3) The heat transfer problem is therefore divided into two parts:

(a) Calculate the time required for the surface of the paraffin coated aluminum dish to reach a temperature of -4° C.

(b) Calculate the time required for a single drop placed on a surface (at -4° C) to reach the temperature of the surface.

Part (a): Calculation of time required for the surface of the paraffin coated aluminum dish to reach a temperature of -4° C

Description: Figure B-1 is a schematic representation of heat flow in a double layer (aluminum + paraffin) placed on a refrigerated bath at -4° C. t_0 denotes the temperature at the surface of the paraffin layer; t_0 = 25° C is the initial temperature of the surface of the dish. t_a denotes the temperature at the base of the dish and is the temperature of the bath assuming perfect contact between the aluminum base and the well stirred refrigerated bath (infinite heat sink). t_a = -4° C is a constant.

Figure B-1. Schematic Representation of a Paraffin Coated Aluminum Dish Floating on a Ethylene glycol-Water Cooling Bath Showing Direction of Heat Flow. The symbol t_0 (° C), is the initial temperature of the paraffin surface as soon as the dish is placed in the cooling bath and t_a is the temperature (° C) at the base of the dish and is equal to the temperature of the cooling bath.

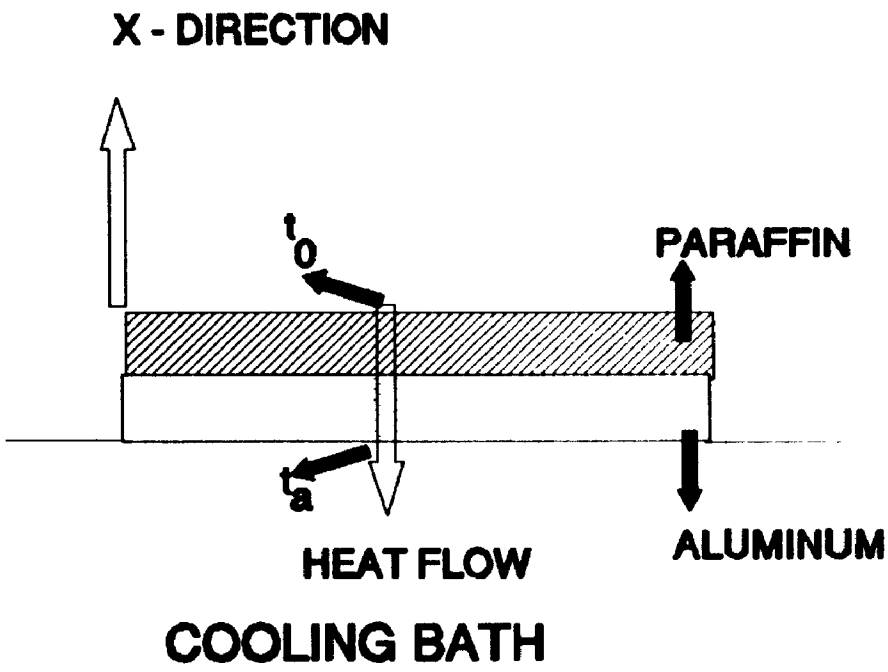
X - DIRECTION
t_0
PARAFFIN
t_a
HEAT FLOW
ALUMINUM
COOLING BATH

Assumptions for part (a) calculations:

(1) Heat flows in one dimension (i.e., vertically in the x-direction from the top of the paraffin coated aluminum dish, through the dish and to the heat sink).

(2) The base of the dish is in complete contact with the heat sink. Thus $t_s = -4°C$ is a constant.

(3) The surface of the dish is in contact with a layer of stagnant air and hence heat flow from the surface to the air is neglected. The air is at a lower temperature than the surface of the dish.

With the above assumptions, the problem of part (a) reduces to transient, heat flow in an infinite plate, with one side insulated.

Required Data: The material of the dish may be considered composite. The lower section is aluminum (Al) with a relatively high thermal conductivity, and thermal diffusivity while the top layer is paraffin (Pa) with much lower values of thermal conductivity and thermal diffusivity. These values are obtained from literature (Incropera and DeWitt, 1990) and are as follows:

Thermal Diffusivity of Al = $\alpha_{Al} = (k/\rho C_p)_{Al} = 97.0 \times 10^{-6}\ m^2/s$ at 300° K

Thermal Diffusivity of Pa = $\alpha_{Pa} = (k/\rho C_p)_{Pa} = 9.23 \times 10^{-8}\ m^2/s$ at 300° K

Since the thermal diffusivity of paraffin is lower than the thermal diffusivity of aluminum, for the problem in part (a) we assume that the whole dish is made up of paraffin with a thermal diffusivity, $\alpha_{Pa} = 9.23 \times 10^{-8}\ m^2/s$.

Using vernier callipers, the actual measured thickness of aluminum dish + paraffin was: 0.1143 mm.

For problem estimation therefore:

Thermal diffusivity, $\alpha_{Pa} = 9.23 \times 10^{-8}$ m^2/s

Plate thickness, δ = 0.12 mm of paraffin

Let t = the temperature of the surface of the dish at any time θ, after exposure to the cooling temperature of -4° C.

Let $Y = (t-t_0)/(t_a - t_0)$ be the dimensionless temperature change from an initial temperature of t_0. Let $Z = \alpha\theta/\delta^2$ be the dimensionless time of exposure.

In order to estimate the required time, Figure B-2 is used. This figure from the Handbook of Heat Transfer (Rohsenow and Hartnett, 1973) is a plot of Y versus Z defined as above and gives the temperature response of a thick plate with insulated rear face for a range of Biot numbers after sudden exposure to a uniform convective environment at t_a.

The Biot number defined as $Bi = h.\delta/k$ is the ratio of heat transfer at the base of the dish to heat transfer within the layers of the dish. The heat transfer at the base of the dish is equivalent to turbulent flow over a flat plate. However, the problem can be generalized by considering a whole range of Bi numbers from Bi = 0.1 to Bi = 1000. Hence considering the two extreme cases:

- Bi = 0.1 and

Figure B-2. Temperature Response of a Thick Plate ($0 \leq x \leq \delta$) with Insulated Rear Face $x = \delta$, after Sudden Exposure to a Uniform Convective Environment t_a at $x = 0$ and for $x/\delta = 1$ (Rohsenow and Hartnett, 1973).

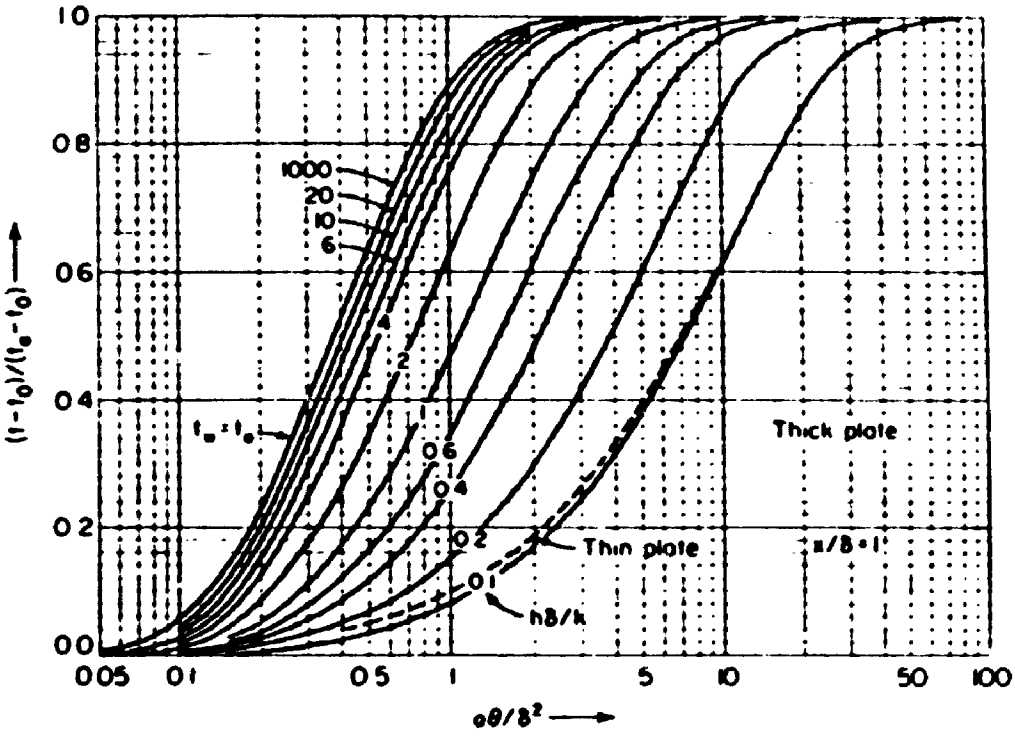
10
08
06
04
02
00
005
01
05
1
5
10
50
100
1000
20
10
6
4
2
1
0·6
0·4
0·2
0·1
$t_w = t_0$
Thick plate
Thin plate
$x/\delta = 1$
$h\delta/k$
$(t-t_0)/(t_0-t_0)$
$\alpha\theta/\delta^2$

- Bi = 1000.0

Case 1: Bi = 0.1

For Bi = 0.1 and a final temperature at the surface of the dish, t = -4° C, we have:

$Y = (-4 - 25)/(-4-25) = 1.0$

From Figure B-2 at Y = 1, and Bi = 0.1 we have:

$Z = \alpha.\theta/\delta^2 = 80$

Now $\delta = 0.12 \times 10^{-3}$ m $= 1.2 \times 10^{-4}$

Therefore: $\alpha.\theta = 80 \times (1.2 \times 10^{-4})^2 = 1.152 \times 10^{-6}$

$\alpha = 9.23 \times 10^{-8}$ m^2/s (assumed)

Therefore $\theta = 1.152 \times 10^{-6}/9.23 \times 10^{-8} = 12.48$ s

Case 2: Bi = 1000

For Bi = 1000 and a final temperature at the surface of the dish, t = -4° C, we have:

$Y = (-4 - 25)/(-4-25) = 1.0$

From Figure B-2 at Y = 1, and Bi = 1000.0 we have:

$Z = \alpha.\theta/\delta^2 = 3.0$

Now $\delta = 0.12 \times 10^{-3}$ m $= 1.2 \times 10^{-4}$

Therefore: $\alpha.\theta = 3.0 \times (1.2 \times 10^{-4})^2 = 4.32 \times 10^{-8}$

$\alpha = 9.23 \times 10^{-8}$ m^2/s (assumed)

Therefore $\theta = 4.32 \times 10^{-8}/9.23 \times 10^{-8} = 0.46$ s

Considering the larger number of 12.48 s we can say that it will take less than 20 s for the surface of the Al foil dish to reach -4° C. Thus for a range of Bi numbers

of 0.1 to 1000, the surface of the Al foil dish reaches -4° C in less than 20 s. Therefore, we have very fast heat transfer between the cooling bath and the aluminum dish coated with paraffin. The paraffin surface reaches the temperature of the cooling bath within a maximum of 20 s. In our experiments we allowed 30 min for equilibration which is more than enough compared to 20 s required.

Part (b) Heat transfer from a single drop to the paraffin surface at -4° C

A single water drop is shown in Figure B-3 placed on a hydrophobic surface at -4 °C. The spherical drop of radius R makes a small circle of contact with the hydrophobic surface. This small circle of contact has a radius of x_D and a contact area for heat transfer equal to $\pi.(x_D)^2$.

The surface tension of a water drop in contact with a layer of paraffin is given by σ = 66.2 dyn/cm (Bruce, 1984).

If the surface tension is known, Hartland and Hartley (1976) have proposed a formula for calculating the radius x_D from properties of the small drop. This formula is shown in equation B.1.

$$x_D = R^2 \left(\frac{2}{3}\frac{\rho g}{\sigma}\right)^{\frac{1}{2}} \qquad \text{(B-1)}$$

Figure B-3. Schematic Representation of a Water Drop of radius R Placed on a Paraffin Layer at -4° C. $2r_D$ is the diameter of the contact area for heat transfer.

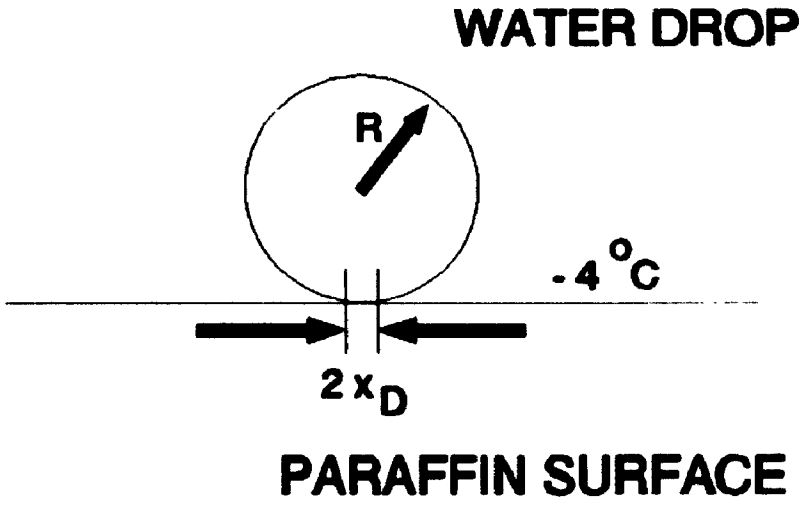
WATER DROP
R
-4 °C
2 x D
PARAFFIN SURFACE

Volume of drop = 9.75×10^{3} cm^3

Radius of the drop = 0.132 cm

σ = 66.2 dyne/cm

Density of water = 1.0 g/cm^3

Therefore: $x_D = (0.13253)^2 \times [(2/3) \times (1 \times 980)/66.2]^{(1/2)}$

From where x_D = 0.055 cm = 0.56 mm

In actual practice, after testing the 30 drops containing ice nucleating cells in the cooling bath, the dish was taken out and left to stand at room temperature. This allowed the water drops to evaporate, leaving small circular imprints on the dish. The diameter of these circles after evaporation of the drops could be approximately measured. This diameter was found to be smaller than 2 mm. Hence the experimental value of x_D should be less than 1 mm. This is quite similar to the value of x_D obtained from theoretical calculations in Equation B-1. Therefore, the value of x_D calculated by Equation B-1 was taken as the radius of the circle for the purpose of calculating heat transfer.

Assumptions for part (b) calculations:

(1) Heat flows in one dimension (i.e., vertically in the x-direction from the drop to the surface of the paraffin.

(2) The base of the drop is in complete contact with the surface of the paraffin.

(3) The drop is in contact with a layer of stagnant air.

(4) The presence of ice nucleating bacteria does not affect the heat transfer characteristics of the drop. This is a valid assumption because the cells are

themselves composed of > 80% water.

In order to calculate heat transfer from the drop to the surface of the paraffin layer at -4° C, we use Figure B-4 from the Handbook of Heat Transfer (Rohsenow and Hartnett, 1973). This is a plot of Y versus Z defined as above and gives the temperature response at the centre of thick bodies after a sudden change in surface temperature for a range of Biot numbers after sudden exposure to a uniform convective environment at t_w. However, since heat is only transferred from a small contact circle of radius x_D, we have to replace the spherical drop by a cylinder of equivalent volume and having heat transfer from one end with radius x_D. The volume of a cylinder with radius x_D = 0.56 mm and thickness = 9.9 mm for the same volume as the spherical drop of 9.75 μL.

From Figure B-4, for the case of a short cylinder (f) and a final temperature t = -4° C, we have:

$Y = (-4 - 25)/(-4-25) = 1.0$

From Figure B-2 at Y = 1, and curve f we have:

$Z = \alpha\theta/\delta^2 = 0.9$

Now $\delta = 0.99 \times 10^{-3}$ m $= 9.9 \times 10^{-4}$

Therefore: $\alpha\theta = 0.9 \times (9.9 \times 10^{-4})^2 = 8.821 \times 10^{-7}$

The thermal diffusivity of water $\alpha_{water} = 1.32 \times 10^{-7}$ m^2/s

Therefore $\theta = 8.821 \times 10^{-7}/1.32 \times 10^{-7} = 6.68$ s

Hence heat transfer from the water drop to the heat sink is very rapid.

Figure B-4. Temperature Response of the Centre of Thick Bodies after Sudden Change in Surface Temperature from t_0 initially to t_w for $\theta \geq 0$: (a) infinite plate (thickness 2δ) (b) infinite elliptical rod (b = δ) (c) infinite square rod (side = 2δ) (d) infinite cylinder (radius = δ) (e) cube (side = 2δ) (f) short cylinder (radius = δ) (g) sphere (radius = δ) (Rohsenow and Hartnett, 1973).

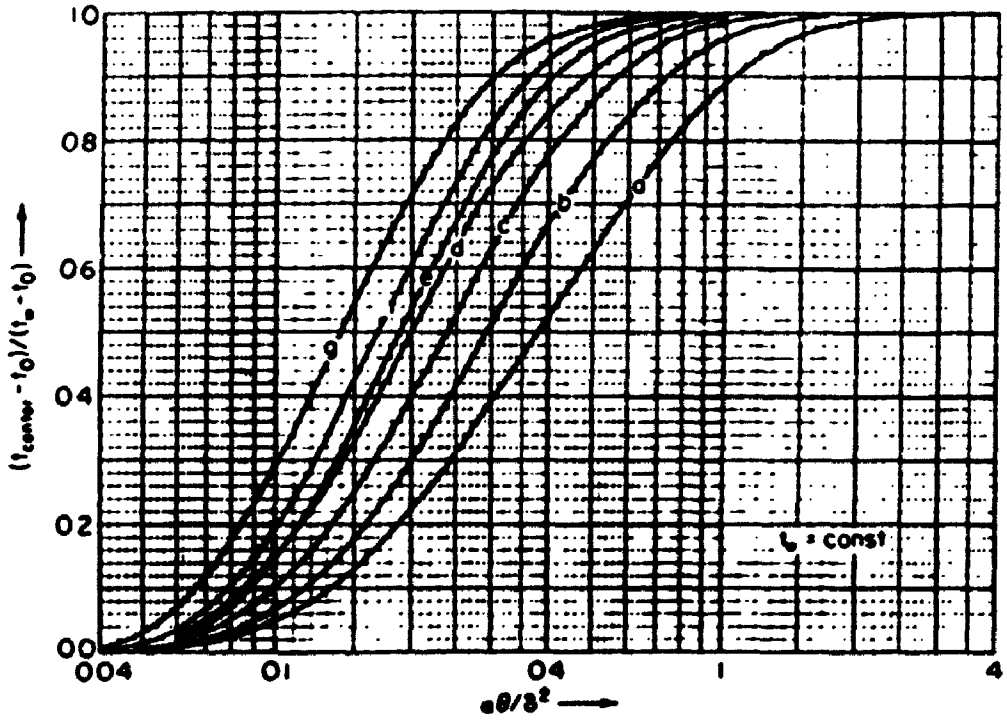
10
08
06
04
02
00
004
01
04
1
4
$(t_{center} - t_0)/(t_b - t_0)$ ⟶
$\alpha\theta/s^2$ ⟶
t_b = const

Conclusion: It takes less than 20 s for the surface of the aluminum dish to reach -4° C and approximately 10 s for the water drop placed on the paraffin coated, aluminum foil dish to reach -4° C. Thus in a total time of less than 30 s, the 9.75 μL water drop containing ice nucleating bacteria is brought down to -4° C from the original room temperature of 25° C, after the drop is placed on the paraffin coated surface of the aluminum dish. Therefore, for all drop freezing tests reported in this thesis to determine INA, the 30 water drops placed on the hydrophobic surface of the aluminum dish reached thermal equilibrium with the cooling bath temperature almost "instantaneously". The drops were exposed for a total of 20 min time on the aluminum dish after which the number of frozen drops were counted. This time of 20 min is much greater than the thermal equilibration time of less than 30 s. The thermal equilibrium time will be much shorter (much less than 30 s) when the bath is at -10° C. The thermal calculations shown above, can be used as a basis to explain why it is important to choose a "slow" enough cooling rate of the bath, so that the water drops are always in thermal equilibrium with the cooling bath temperature. This also explains why it is difficult to compare literature data on INA among researchers using different cooling rates during the drop freezing test.

APPENDIX C

SAMPLE COMPUTER PROGRAM FOR ONE TEMPERATURE - 25° C

```
c       BATCH SIMULATION OF ICE NUCLEATING BACTERIA IN A 1 L
        BIOREACTOR
C
$debug
      dimension x(55),y(55),scrat(100),signs(3),diff(3),th(3)
c
c      common/xx/x
      external model
c
      open(5,file='Xx.dat')
      open(6,file='uw.res')
      open(65,file='uwrs.dat')
c
c     Read the data from the data file, fname
c
      np=3
      nob=14
c

      do 10 i=1,nob
      read(5,*) x(i),y(i)
 10     continue
c
c     Declare the parameters in the routine
c
      signs(1)=1.0
      signs(2)=1.0
      signs(3)=1.0
      diff(1)=.001
      diff(2)=.001
      diff(3)=.0001
      eps1=.0001
      eps2=.0001
      mit=20
c
      write(*,992)
 992    format(' Please enter an initial value for lamda: ',\)
      read(*,*) flam
        fnu=10.
c
c
      write(*,*)'ks  = th(1); yps  = th(2); m  = th(3)'
      do 11,i=1,np
      write(*,100) i
 100    format(' Please enter your initial guess for theta',I2,':  ',\)
 11     read(*,*) th(i)
```

```
      call uwhaus(1,model,nob,y,np,th,diff,signs,eps1,eps2,
     1 mit,flam,fnu,scrat)
      close(5)
      close(6)
      close(65)
      stop
      end
c
c
      subroutine model(nprob,th,yrs,nob,np)
      dimension th(*),yrs(*),
     1 S(1000), P(1000), X(1000), Y(4), XK(4,4),
     1  YY(4), BB(55),TT(55),D(1000),  yxx(55),txt(55),
     1  yss(55), ypp(55), yexx(55), yess(55), yepp(55)
        REAL  MUMAX, KS, MC

C
C       OPEN FILES
C
       OPEN(UNIT = 10, FILE ='BAT1.DAT')
        OPEN(UNIT = 20, FILE ='X.DAT')
        open(unit = 30, file ='s.dat')
        open(unit = 40, file ='p.dat')
       OPEN(UNIT =50, FILE ='PAR.DAT')

C
C       N DEFINES NUMBER OF FUNCTIONS
C
       N = 4
        NP = 3
        NPROB=1
C       NOB DEFINES NUMBER OF DATA POINTS

        NOB  = 14
C
C       ENTER CONSTANTS
C
       H = 0.50
        MUMAX = 0.1303
        mc = TH(3)
        YPS = TH(2)
        KS = TH(1)
        YXS = 0.28
        ypx1 = 0.002
        ypx2 = 0.002
        ypx3 = 200.0
```

```
      ypx4 = 250.0
C
C     ENTER INITIAL VALUES OF S,P,X
C
      S0 = 5.0
      P0 = 0.0001
      X0 = 0.011
      D0 = 0.0001
C     MAIN PROGRAM BEGINS
C
      II = 1
      SUM = 0.0
      SUM1 = 0.0
      SUM2 = 0.0

      S(II) = S0
      P(II) = P0
      X(II) = X0
      D(II) = D0

      H2 = H/2.0
      H6 = H/6.0

      IMAX = 86.0/H
      DO 53 M = 1, IMAX
C      Y(1) = D(II)
C      Y(2) = X(II)
C      Y(3) = P(II)
C     Y(4) = S(II)
c     LAG PHASE- CHANGE IN T ONLY
      IF(II.GE.50) GO TO 666
      GO TO 667
c 666 WRITE(*,*) NNUM =50
 666  Y(1) = D(II)
      Y(2) = X(II)
      Y(3) = P(II)
      Y(4) = S(II)
      XX = X(II)
      SS = S(II)
      GO TO 668

 667  Y(1) = D(1)
      Y(2) = X(1)
      Y(3) = P(1)
      Y(4) = S(1)
      XX = X(1)
```

```
      SS = S(1)

C      XX = X(II)
C      SS = S(II)
 668  T1 = II*H

      IF(T1.LE.23.0) go to 534
      if(t1.le.44.0) go to 434
      if(t1.le.60.0) go to 536
      ypx = ypx4
      go to 165
 534  YPX = YPX1
      go to 165
 434  ypx = ypx2
      go to 165
 536  YPX = ypx3
 165   DO 34 K = 1,4
      DO 6 J = 1,N
      IF(J.EQ.1) GO TO 60
      IF(J.EQ.2) GO TO 61
      IF(J.EQ.3) GO TO 62
      IF(J.EQ.4) GO TO 63
 60    XK(K,J) = (MUMAX*SS)/(KS+SS)
      IF(K.EQ.4) go  to 79
      GO TO 6
 79    YY(J) =(1.0/6.0)*(XK(1,J) + 2*(XK(2,J) +XK(3,J))+XK(4,J))
      GO TO 6
 61    XK(K,J) = (MUMAX*SS*XX)/(KS + SS)
      GO TO 64
 62    XK(K,J) =  YPX*(MUMAX*SS)/(KS+SS)*XX
      GO TO  64
 63    XK(K,J) = -((MUMAX*SS*XX)/((KS + SS)*YXS)
   1  +(YPX*((MUMAX*SS)/(KS+SS))*XX)/YPS + MC*XX)
 64    IF(K.EQ.1) GO TO 12
      IF(K.EQ.2) GO TO 12
      IF(K.EQ.3) GO TO 13
      IF(K.EQ.4) GO TO 14
 12    YY(J) = Y(J) + H2*XK(K,J)
      GO TO 6
 13    YY(J) = Y(J) + H*XK(K,J)
      GO TO 6
 14    YY(J) = Y(J)+H6*(XK(1,J)+2*(XK(2,J)+XK(3,J))+XK(4,J))
 6     CONTINUE
      XX = YY(2)
      SS = YY(4)
 34    CONTINUE
```

```
C       IMAX = II

        II = II + 1

       D(II) = YY(1)
       X(II) = YY(2)
       P(II) = YY(3)
       S(II) = YY(4)

        IF(S(II).LE.0.0) THEN
        S(II) = 0.0
C       GO TO 52
        ENDIF

C       WRITE(*,*)  II, S(ii), P(ii), X(ii),D(II)
 53     CONTINUE

 52     DM = 1.0

        DO 55 J =1, NOB

        READ(20,*) TT(J), BB(J)
        read(30,*) tt(j), yess(j)
        read(40,*) tt(j), yepp(j)
       Z = TT(J)/H
        IZ = INT(Z)
       IF(IZ.EQ.0)THEN
       IZ = 1
       ENDIF
c       if(j.le.nob/3) go to 111
c       IF(J.LE.2*NOB/3.0) GO TO 112
c       GO TO 113
c111   YRS(J)        = X(IZ)
        yrs(j)  = x(iz)
        txt(j)  =  tt(j)
        yxx(j)  = x(iz)
        yexx(j) =  bb(j)
        RDF1 = X(IZ) - BB(J)
        SUM = SUM + RDF1*RDF1

c       GO TO 114
c112   YRS(J)        = S(IZ)
c       mz = j - 14
        yss(j) = s(iz)
c       yess(mz) = bb(j)
        RDF2 = S(IZ) - yess(J)
```

```
      SUM1 = SUM1 + RDF2*RDF2

c     go to 114
c 113 YRS(J)       = 0.01*P(IZ)
c      mz = j - 28
       ypp(j) = p(iz)
c      yepp(mz) = bb(j)*100.0
       RDF3 = p(iz) - yepp(J)
      SUM2 = SUM2 + RDF3*RDF3

      SUMT = SUM + SUM1 + 0.0001*SUM2
 55   CONTINUE
      do 4 jjk =  1, nob
      write(*,446) tt(jjk),yxx(jjk), bb(jjk),
     1 yss(jjk),yess(jjk),
     1 ypp(jjk),yepp(jjk)
446   format(f8.1,3x,f6.2,3x,f6.2,3x,f6.2,3x,f6.2,3x,f8.4,4x,f8.4)
4     continue
      DO 54 I = 1, IMAX, 10

      T =DM/IMAX * 119.0
c     WRITE (*,*) I, T, S(I), X(I), P(I),D(I)
      WRITE(10,*) I, T, S(I), X(I), p(I)
      DM = DM + 10.0
 54   CONTINUE
      WRITE(50,*) mumax, yxs, ypx1,ypx2, ypx3, ypx4, th(1),
     1  th(2), th(3), SUM, SUM1, SUM2,SUMT
       WRITE(*,199) th(1),
     1  th(2), th(3), SUM, SUM1, SUM2, SUMT
199   format(f7.3,3x,f8.2,3x,f9.5,2x,f8.4, 2x,f8.4,2x, f12.2,2x,f8.4)
      CLOSE(10)
       CLOSE(20)
       close(30)
       close(40)
       CLOSE(50)

    RETURN
    END

  SUBROUTINE UWHAUS(NPROB,MODEL,NOB,Y,NP,TH,DIFF,SIGNS,EPS1,EPS2,
     1 MIT, FLAM, FNU, SCRAT)
       external model
    DIMENSION SCRAT(1)
    IA = 1
    IB = IA + NP
    IC = IB + NP
```

```
      ID=IC+NP
      IE=ID+NP
      IF=IE+NP
      IG=IF+NOB
      IH=IG+NOB
      II = IH + NP * NOB
      IJ = IH
      CALL  HAUS59 (NPROB,
     1  MODEL,NOB,Y,NP,TH,DIFF,SIGNS,EPS1,EPS2,MIT
     1  ,FLAM,FNU,SCRAT(IA), SCRAT(IB), SCRAT(IC), SCRAT(ID),
     2  SCRAT(IE), SCRAT(IF), SCRAT(IG), SCRAT(IH), SCRAT(II),
     3  SCRAT(IJ) )
      RETURN
      END

          SUBROUTINE  HAUS59(NPRBO,  MODEL,  NBO,
Y,NQ,TH,DIFZ,SIGNS,EP1S,EP2S,
     1MIT,FLAM,FNU,   Q,P,E,PHI,TB,F,R,A,D,DELZ)
C                FORTRAN II VERSION
C                H. J. WERTZ
C     ADAPTED FOR THE CDC 6400  (J. F. MACGREGOR)
C
C     DIMENSION TH(NQ), DIFZ(NQ), SIGNS(NQ), Y(NBO)
C     DIMENSION Q(NQ), P(NQ), E(NQ), PHI(NQ), TB(NQ)
C     DIMENSION F(NBO), R(NBO)
C     DIMENSION A(NQ,NQ), D(NQ,NQ), DELZ(NBO,NQ)
      DIMENSION TH(1), DIFZ(1), SIGNS(1), Y(1), Q(1), P(1), E(1),
     1   PHI(1), TB(1), F(1), R(1), A(1), D(1), DELZ(1),
     1   fd1(60), fd2(60), fd3(60)
      ACOS(X) = ATAN(SQRT(1.0/X**2 - 1.0))
      NP = NQ
      NPROB = NPRBO
      NOB = NBO
      EPS1 = EP1S
      EPS2 = EP2S
      NPSQ = NP * NP
       NSCRAC = 5*NP+NPSQ +2*NOB+NP*NOB
      WRITE (06,1000) NPROB,NOB,NP,NSCRAC
      WRITE (06,1001)
       CALL GASS60(1, NP, TH, TEMP, TMEP)
      WRITE (06,1002)
       CALL GASS60(1, NP, DIFZ, TEMP, TEMP)
      IF(MIN0(NP-1,50-NP,NOB-NP,MIT-1,999-MIT))99,15,15
 15   IF(FNU-1.0)99, 99, 16
 16   CONTINUE
      DO 19 I=1,NP
```

```
      TEMP = ABS(DIFZ(I))
      IF(AMIN1(1.0-TEMP, ABS(TH(I))))99, 99, 19
 19   CONTINUE
      GA = FLAM
      NIT = 1
      LAOS = 0
      IF(EPS1) 5,70,70
 5    EPS1 = 0
 70   SSQ = 0
      CALL MODEL(NPROB, TH, F, NOB, NP)
      DO 90 I = 1, NOB
      R(I) = Y(I) - F(I)
 90   SSQ=SSQ+R(I)*R(I)
      WRITE (06,1003) SSQ
C
C                                        BEGIN ITERATION
C
 100  GA = GA / FNU
      INTCNT = 0
      WRITE(06,1004)  NIT
 101  JS = 1 - NOB
      DO 130 J=1,NP
      TEMP = TH(J)
      P(J)=DIFZ(J)*TH(J)
      TH(J)= TH(J)+P(J)
        Q(J)=0
c       Q(J) = 0
       JS = JS + NOB
      CALL MODEL(NPROB, TH, DELZ(JS), NOB, NP)
      II = JS-1
      DO 120 I = 1, NOB
      IJ = IJ + 1
      DELZ(IJ) = DELZ(IJ) - F(I)
 120  Q(J) = Q(J) + DELZ(IJ) * R(I)
      Q(J)= Q(J)/P(J)
C                                  Q=XT*R (STEEPEST DESCENT)
 130  TH(J) = TEMP
      IF(LAOS) 131,131,414
 131  DO 150 I = 1, NP
      DO 151 J=1,I
      SUM = 0
      KJ = NOB*(J-1)
      KI = NOB*(I-1)
      DO 160 K = 1, NOB
      KI = KI + 1
      KJ = KJ + 1
```

```
160  SUM = SUM + DELZ(KI) * DELZ(KJ)
     TEMP= SUM/(P(I)*P(J))
     JI = J + NP*(I-1)
     D(JI) = TEMP
     IJ = I + NP*(J-1)
151  D(IJ) = TEMP
150  E(I) = SQRT(D(JI))
666  CONTINUE
     DO 153  I = 1, NP
     IJ = I-NP
     DO 153 J=1,I
     IJ = IJ + NP
     A(IJ) = D(IJ) / (E(I)*E(J))

     JI = J + NP*(I-1)
153  A(JI) = A(IJ)
C                                   A= SCALED MOMENT MATRIX
     II = - NP
     DO 155 I=1,NP
     P(I)=Q(I)/E(I)
     PHI(I)=P(I)
     II = NP + 1 + II
155  A(II) = A(II) + GA
C
     I=1
      CALL MATIN(A, NP, P, I, DET)
C                                   P/E = CORRECTION VECTOR
      STEP=1.0
     SUM1=0.
     SUM2=0.
     SUM3=0.
     DO 231 I=1,NP
     SUM1=P(I)*PHI(I)+SUM1
     SUM2=P(I)*P(I)+SUM2
     SUM3= PHI(I) * PHI(I) + SUM3
231  PHI(I) = P(I)
      TEMP = SUM1/SQRT(SUM2*SUM3)
     TEMP = AMIN1(TEMP, 1.0)
     TEMP = 57.295*ACOS(TEMP)
     WRITE(06,1041)  DET,TEMP
170  DO 220 I = 1, NP
     P(I) = PHI(I) *STEP / E(I)
     TB(I) = TH(I) + P(I)
220  CONTINUE
     WRITE(06,7000)
7000 FORMAT(30H TEST POINT PARAMETER VALUES     )
```

```
      WRITE(06,2006)  (TB(I),I=1,NP)
      DO 221 I = 1, NP
      IF(SIGNS(I)) 221, 221, 222
  222 IF(SIGN(1.0,TH(I))*SIGN(1.0,TB(I))) 663, 221, 221
  221 CONTINUE
      SUMB=0
      CALL MODEL(NPROB, TB, F, NOB, NP)
      DO 230 I=1,NOB
      R(I)=Y(I)-F(I)
  230  SUMB=SUMB+R(I)*R(I)
      WRITE(06,1043)  SUMB
      IF(SUMB - (1.0+EPS1)*SSQ) 662, 662, 663
  663 IF( AMIN1(TEMP-30.0, GA)) 665, 665, 664
  665  STEP=STEP/2.0
      INTCNT = INTCNT + 1
      IF(INTCNT - 36) 170, 2700, 2700
  664 GA=GA*FNU
      INTCNT = INTCNT + 1
      IF(INTCNT - 36) 666, 2700, 2700
  662 WRITE(06,1007)
      DO 669 I=1,NP
  669  TH(I)=TB(I)
       CALL GASS60(1, NP, TH, TEMP, TEMP)
      WRITE(06,1040)  GA,SUMB
      IF(EPS2) 229,229,225
  229 IF(EPS1) 270,270,265
  225  DO 240 I = 1, NP
      IF(ABS(P(I))/(1.E-20+ABS(TH(I)))-EPS2) 240, 240, 241
  241 IF(EPS1) 270,270,265
  240 CONTINUE
      WRITE(06,1009)  EPS2
      GO TO 280
  265  IF(ABS(SUMB - SSQ) - EPS1*SSQ) 266, 266, 270
  266 WRITE(06,1010)  EPS1
      GO TO 280
  270  SSQ=SUMB
      NIT=NIT+1
        IF(NIT - MIT) 100, 100, 280
 2700  WRITE(6,2710)
 2710 FORMAT(//,'**** THE SUM OF SQUARES CANNOT BE REDUCED TO
THE SUM
     1OF SQUARES AT THE END OF THE LAST ITERATION - ITER STOPS ',/)
C


C                                   END ITERATION
```

```
C
  280 WRITE(06,1011)
      WRITE(06,2001) (F(I),I=1,NOB)
      WRITE(06,1012)
      WRITE(06,2001) (R(I),I=1,NOB)
      WRITE(06,1017)
      CALL GASS60(4,NP,TEMP,TEMP,D)
 1017 FORMAT(////16H XPRIME-X MATRIX)
      SSQ=SUMB
      IDF=NOB-NP
      WRITE(06,1015)
      I=0
       CALL MATIN(D, NP, P, I, DET)
      DO 7692 I=1,NP
      II = I + NP*(I-1)
 7692 E(I) = SQRT(D(II))
      DO 340 I=1,NP
      JI = I + NP*(I-1) - 1
      IJ = I + NP*(I-2)
      DO 340 J = I, NP
      JI = JI + 1
      A(JI) = D(JI) / (E(I)*E(J))
      IJ = IJ + NP
  340  A(IJ) = A(JI)
       CALL GASS60(3, NP, TEMP, TEMP, A)
      IF(IDF) 341, 410, 341
  341 SDEV = SSQ/FLOAT(IDF)
      WRITE(06,1014) SDEV,IDF
       SDEV = SQRT(SDEV)
      DO 391 I  1,NP
      P(I)=TH(I)+2.0*E(I)*SDEV
  391  TB(I)=TH(I)-2.0*E(I)*SDEV
      WRITE(06,1039)
       CALL GASS60(2, NP, TB, P, TEMP)
      LAOS = 1
      GO TO 101
  414 DO 415 K = 1, NOB
      TEMP = 0
      DO 420 I=1,NP
      DO 420 J=1,NP
      ISUB = K+NOB*(I-1)
      DEBUG1 = DELZ(ISUB)
C     DEBUG1 = DELZ(K + NOB*(I-1))
      ISUB = K+NOB*(J-1)
      DEBUG2 = DELZ(ISUB)
C     DEBUG2 = DELZ(K + NOB*(J-1))
```

```
      IJ = I + NP*(J-1)
      DEBUG3 = D(IJ)/(DIFZ(I)*TH(I)*DIFZ(J)*TH(J))
  420 TEMP = TEMP + DEBUG1 * DEBUG2 * DEBUG3
      TEMP = 2.0*SQRT(TEMP)*SDEV
      R(K)=F(K)+TEMP
  415 F(K)=F(K)-TEMP
      fd3(k) = f(k)
      WRITE(06,1008)
      IE=0
      DO 425 I=1,NOB,14
      IE=IE+14
      IF(NOB-IE) 430,435,435
  430 IE=NOB
  435 WRITE(06,*) (R(J),J=1,IE)

  425 WRITE(06,*) (F(J),J=1,IE)


  410 WRITE(06,1033) NPROB
      RETURN
   99 WRITE(06,1034)
      GO TO 410
 1000 FORMAT('NON-LINEAR ESTIMATION, PROBLEM NUMBER....', I3,// I5,
     1 'OBSERVATIONS', I5, 'PARAMETERS', I14,'SCRATCH REQUIRED')
 1001 FORMAT(/'INITIAL PARAMETER VALUES'      )
 1002 FORMAT(/'PROPORTIONS USED IN CALCULATING DIFFERENCE
QUOTIENTS')
 1003 FORMAT(/'INITIAL SUM OF SQUARES =',E12.4)
 1004 FORMAT(/////45X,' ITERATION NO.', I4)
 1007 FORMAT(/'PARAMETER VALUES VIA REGRESSION'        )
 1008 FORMAT(////'APPROXIMATE CONFIDENCE LIMITS FOR CELL CONC.')
 1009 FORMAT(/ ' ITERATION STOPS - RELATIVE CHANGE IN EACH
PARAMETER LE
     1SS THAN', E12.4)
 1010 FORMAT(/,' ITERATION STOPS - RELATIVE CHANGE IN SUM OF
SQUARES LE
     1SS THAN',  E12.4)
 1011 FORMAT(' FINAL FUNCTION VALUES')
 1012 FORMAT(////'RESIDUALS'  )
 1014 FORMAT(//'VARIANCE OF RESIDUALS =       ',E12.4,1H,I4,
     1 'DEGREES OF FREEDOM' )
 1015 FORMAT(////'CORRELATION MATRIX')
 1033 FORMAT(//'END OF PROBLEM NO.',I3)
 1034 FORMAT(/'PARAMETER ERROR ')
 1039 FORMAT(/'INDIVIDUAL CONFIDENCE LIMITS FOR EACH PARAMETER
(ON LI
```

```
     1NEAR HYPOTHESIS)')
1040      FORMAT(/,' LAMDA=',E10.3,40X,' SUM OF SQUARES AFTER
REGRESSION =',
     1 E15.7)
1041  FORMAT('DETERMINANT =  E12.4', 6X, 'ANGLE IN SCALED COORD. =',
     1  F5.2,'DEGREES')
 1043 FORMAT('TEST POINT SUM OF SQUARES =',    E12.4)
 2001 FORMAT(/10E12.4)
 2006 FORMAT(10E12.4)
      END

      SUBROUTINE MATIN(A, NVAR, B, NB, DET)
      DIMENSION A(NVAR, 1), B(NVAR, 1)
      PIVOTM = A(1,1)
      DET = 1.0
      DO 550 ICOL = 1, NVAR
      PIVOT = A(ICOL, ICOL)
      PIVOTM = AMIN1(PIVOT, PIVOTM)
      DET = PIVOT * DET
C
C     DIVIDE PIVOT ROW BY PIVOT ELEMENT
C
      A(ICOL, ICOL) = 1.0
      PIVOT = AMAX1(PIVOT, 1.E-20)

      PIVOT = A(ICOL, ICOL)/PIVOT
      DO 350 L=1,NVAR
 350  A(ICOL, L) = A(ICOL, L)*PIVOT
      IF (NB) 371,371,372
  372 DO 370 L=1,NB
 370  B(ICOL, L) = B(ICOL, L)*PIVOT
C
C     REDUCE NON-PIVOT ROWS
 371  DO 550 L1=1,NVAR
      IF (L1-ICOL) 551,550,551
  551 T = A(L1, ICOL)
      A(L1, ICOL) = 0.
      DO 450 L=1,NVAR
 450  A(L1, L) = A(L1, L) - A(ICOL, L)*T
      IF (NB) 552,550,552
  552 DO 500 L=1,NB
 500  B(L1, L) = B(L1, L)-B(ICOL,L)*T
  550 CONTINUE
      RETURN
      END
```

```
      SUBROUTINE GASS60(ITYPE, NQ, A, B, C)
      DIMENSION A(NQ),B(NQ),C(NQ,NQ)
       NP = NQ
       NR = NP/10
       LOW = 1
       LUP = 10
10    IF( NR )15,20,30
15    RETURN
20    LUP=NP
      IF (LOW-LUP) 30,30,15
 30 WRITE(06,500) (J,J=LOW,LUP)
      GO TO (40,60,80,80), ITYPE
 40 WRITE(06,600) (A(J),J=LOW,LUP)
      GO TO 100
 60 WRITE(06,600) (B(J),J=LOW,LUP)
      GO TO 40
 80 IF(ITYPE.EQ.4) GO TO 70
      DO 90 I=LOW,LUP
 90 WRITE(06,720) I,(C(J,I),J=LOW,I)
      GO TO 71
 70 DO 72 I=LOW,LUP
 72 WRITE(06,721) I,(C(I,J),J=LOW,I)
 71 CONTINUE
      LOW2=LUP+1
      IF (LOW2-NP) 96,96,100
 96 IF (ITYPE.EQ.4) GO TO 97
      DO 95 I=LOW2,NP
 95 WRITE(06,720) I,(C(J,I),J=LOW,LUP)
      GO TO 100
 97 DO 98 I=LOW2,NP
 98 WRITE(06,721) I,(C(I,J),J=LOW,LUP)
100    LOW = LOW + 10
       LUP = LUP + 10
       NR = NR - 1
       GO TO 10
500   FORMAT(/I8,9I12)
600   FORMAT(10E12.4)
720   FORMAT(1H ,I3,1X,F7.4,9F12.4)
721   FORMAT(1H ,I3,1X,E10.4,9E12.4)
 1    CONTINUE
      RETURN
      END
```

APPENDIX D

EXPERIMENTAL DATA

EFFECT OF CELL CONCENTRATION ON TEMPERATURE FOR 100% DROP FREEZE

CELL CONCENTRATION (NOS OF CELLS/ML)	TEMPERATURE FOR 100% DROP FREEZE
1.0×10^3	-12.0
1.0×10^4	-6.0
1.0×10^5	-5.0
1.0×10^6	-4.0
1.0×10^7	-4.0
1.0×10^8	-4.0
1.0×10^9	-4.0

EFFECT OF CELL CONCENTRATION ON FRACTION OF DROPLETS FREEZING AT DIFFERENT TEMPERATURES

Freezing Temperature (° C)	CELL CONCENTRATION (CFU/ML)						
	10^3	10^4	10^5	10^6	10^7	10^8	10^9
-1.00	0.00	0.00	0.00	0.00	0.00	0.00	0.00
-2.00	0.00	0.00	0.00	0.00	0.00	0.00	0.00
-3.00	0.067	0.00	0.00	0.00	0.00	0.00	0.00
-4.00	1.00	1.00	1.00	1.00	0.87	0.40	0.10
-5.00	1.00	1.00	1.00	1.00	1.00	0.90	0.13
-6.00	1.00	1.00	1.00	1.00	1.00	1.00	0.27
-7.00	1.00	1.00	1.00	1.00	1.00	1.00	0.30
-8.00	1.00	1.00	1.00	1.00	1.00	1.00	0.30
-10.0	1.00	1.00	1.00	1.00	1.00	1.00	0.57
-12.0	1.00	1.00	1.00	1.00	1.00	1.00	1.00
-15.0	1.00	1.00	1.00	1.00	1.00	1.00	1.00

FRACTION OF DROPLETS FREEZING VERSUS COOLING RATE OF REFRIGERATED BATH

FREEZING TEMPERATURE (° C)	0.05° C/MIN	0.2° C/MIN	1.0° C/MIN
-2.00	0.00	0.00	0.00
-3.00	0.00	0.00	0.00
-4.00	0.20	0.23	0.03
-5.00	1.00	1.00	0.53
-6.00	1.00	1.00	1.00
-7.00	1.00	1.00	1.00

FRACTION OF DROPLETS FREEZING AS A FUNCTION OF BACTERIAL STRAIN

FREEZING TEMPERATURE (° C)	FRACTION OF DROPS FROZEN			
	CIT7	PDDCC461	5D4132	5D19
-2.0	0.0	0.0	0.0	0.0
-3.0	0.57	0.0	0.0	0.0
-4.0	1.0	0.87	0.0	0.0
-5.0	1.0	1.0	0.0	0.0
-6.0	1.0	1.0	0.033	0.033
-9.0	1.0	1.0	0.27	0.37
-11.0	1.0	1.0	0.57	1.0
-12.0	1.0	1.0	1.0	1.0

TEMPERATURE FOR 100% DROP FREEZE VERSUS GROWTH TIME FOR P. SYRINGAE CIT 7 CELLS GROWN ON SOLID VERSUS LIQUID MEDIUM

TIME (H)	LIQUID MEDIUM FREEZING TEMPERATURE	SOILD MEDIUM
7.0	-9.0	-12.0
24.0	-5.0	-5.0
45.0	-4.0	-5.0
58.0	-5.0	-6.0

FRACTION OF DROPLETS FREEZING AS A FUNCTION OF pH

FREEZING TEMPERATURE (° C)	FRACTION OF DROPS FROZEN			
	5.0	6.0	7.0	8.0
-1.0	0.0	0.0	0.0	0.0
-2.0	0.0	0.0	0.0	0.0
-3.5	0.3	0.27	0.87	0.0
-4.0	1.0	1.0	1.0	0.0
-5.0	1.0	1.0	1.0	0.167
-6.0	1.0	1.0	1.0	0.433
-7.0	1.0	1.0	1.0	0.670
-9.0	1.0	1.0	1.0	1.0
-10.0	1.0	1.0	1.0	1.0

FRACTION OF DROPLETS FREEZING AS A FUNCTION OF AERATION

FREEZING TEMPERATURE (°C)	FRACTION OF DROPS FROZEN			
	SEALED FLASK	SURFACE AERATION	AIR (1VVM)	AIR (2VVM)
-2.5	0.0	0.2	0.0	0.13
-3.0	0.03	0.3	0.53	0.80
-4.0	0.2	1.0	0.90	1.0
-5.0	1.0	1.0	1.0	1.0
-6.0	1.0	1.0	1.0	1.0

FRACTION OF DROPLETS FREEZING AS A FUNCTION OF TEMPERATURE

FREEZING TEMPERATURE (° C)	FRACTION OF DROPS FROZEN			
	15° C	25° C	30° C	35° C
-2.0	0.0	0.0	0.0	0.0
-2.5	0.03	0.1	0.0	0.0
-3.0	0.23	0.8	0.0	0.0
-3.5	1.0	1.0	0.0	0.0
-4.0	1.0	1.0	0.03	0.0
-5.0	1.0	1.0	0.4	0.0
-6.0	1.0	1.0	1.0	0.1
-9.0	1.0	1.0	1.0	0.23
-10.0	1.0	1.0	1.0	1.0
-11.0	1.0	1.0	1.0	1.0

BATCH FERMENTATION AT 5.5° C

TIME t (H)	SUCROSE S (G/L)	CELL CONC. X (G CELL DW/L)	INA ICE NUCLEI/L K(θ)	CELL COUNT (CFU/ ML X 10^6)	O.D. (600 NM)
0.0	5.0	0.010	0.10	1.86	0.004
13.5	5.0	0.014	0.11	0.36	0.006
37.0	4.7	0.014	0.01	2.60	0.008
67.0	4.9	0.018	0.00027	26.30	0.024
85.0	4.8	0.020	0.00030	10.00	0.045
110.0	4.5	0.040	0.0059	440.00	0.075
134.0	4.2	0.050	0.0035	468.00	0.175
159.0	3.7	0.150	0.089	300.00	0.0395
182.0	3.1	0.360	0.108	4770.00	0.892
204.0	2.3	0.840	7.08	8200.00	1.598
229.5	0.8	1.460	3.48	27100.00	2.134
254.0	0.0	1.450	14.70	5460.00	2.214
278.0	0.0	1.280	52.40	7250.00	2.176
289.0	0.0	1.480	2.29	7900.00	2.172

BATCH FERMENTATION AT 10.0° C

TIME t (H)	SUCROSE S (G/L)	CELL CONC. X (G CELL DW/L)	INA ICE NUCLEI/L ($X 10^6$) K(θ)	CELL COUNT (CFU/ ML $X 10^6$)	O.D. (600 NM)
0.0	5.00	0.0650	1.421	100.0	0.109
9.0	4.90	0.2705	2.288	740.0	0.225
12.0	4.85	0.2310	2.505	780.0	0.259
22.0	4.40	0.2550	2.505	985.0	0.332
30.0	3.70	0.3670	3.181	4760.0	0.420
46.0	1.65	0.7362	8.209	4250.0	1.250
54.0	1.60	1.2167	49.300	2500.0	1.612
70.5	0.00	1.6415	105.000	16000.0	2.080
81.0	0.00	1.5185	88.200	19600.0	2.133
95.0	0.00	1.5333	121.000	12300.0	2.131
119.0	0.00	1.5286	127.000	13400.0	2.093

BATCH FERMENTATION AT 15.0° C

TIME t (H)	SUCROSE S (G/L)	CELL CONC. X (G CELL DW/L)	INA ICE NUCLEI/L ($X\ 10^6$) K(θ)	CELL COUNT (CFU/ ML $X\ 10^6$)	O.D. (600 NM)
0.0	5.1	0.0600	0.00243	1.39	.015
4.0	4.7	0.0460	0.00040	6.55	.022
8.0	4.8	0.0160	0.00020	5.95	.012
12.0	5.0	0.0290	0.00079	26.50	.014
19.5	4.7	0.0670	0.00142	18.90	.016
26.5	4.3	0.0250	0.00252	106.00	.027
35.5	3.1	0.0150	0.00210	50.00	.053
46.0	3.5	0.1615	0.08753	378.00	.122
54.5	1.5	0.3928	0.24018	190.00	.242
60.0	0.3	0.3030	1.87	1920.00	.373
75.0	0.0	0.6315	36.00	5100.00	1.073
98.0	0.0	1.2920	138.00	43000.00	2.101
103.0	0.0	1.3500	419.00	30000.00	2.093

BATCH FERMENTATION AT 20° C

TIME t (H)	SUCROSE S (G/L)	CELL CONC. X (G CELL DW/L)	INA ICE NUCLEI/L (X 10^6)	CELL COUNT (CFU/ ML X 10^6)	O.D. (600 NM)
0.0	5.0	0.100	0.004	150.0	0.100
2.0	5.0	0.117	1.209	644.0	0.137
5.0	3.7	0.100	0.289	400.0	0.211
8.0	4.7	0.174	0.980	190.0	0.237
15.0	3.4	0.238	2.288	400.0	0.386
21.0	4.0	0.365	17.300	262.0	0.665
25.0	3.3	0.456	24.400	5100.0	0.924
29.0	2.7	0.625	49.800	19800.0	1.204
35.0	1.3	0.866	42.400	4500.0	1.462
38.0	0.2	0.880	45.900	20000.0	1.615
49.0	0.0	1.240	98.000	28000.0	2.008
57.5	0.0	1.240	147.000	28000.0	2.010

BATCH FERMENTATION AT 25.0° C

TIME t (H)	SUCROSE S (G/L)	CELL CONC. X (G CELL DW/L)	INA ICE NUCLEI/L ($X 10^6$) K(θ)	CELL COUNT (CFU/ ML $X 10^6$)	O.D. (600 NM)
0.0	5.00	0.010	0.000185	0.26	0.047
2.0	5.00	0.010	0.000185	0.12	0.094
8.5	5.10	0.010	0.000100	1.57	0.046
15.0	5.00	0.019	0.000100	1.37	0.044
23.0	4.90	0.152	0.000348	2.00	0.046
26.5	5.00	0.115	0.001476	4.00	0.046
33.5	5.00	0.019	0.004685	2.00	0.051
39.5	4.90	0.131	0.007457	2.70	0.062
44.5	3.65	0.125	0.044070	52.00	0.087
50.5	3.00	0.092	0.183770	360.00	0.178
60.5	2.80	0.320	195.00	3000.00	0.730
65.5	1.40	0.729	278.00	4600.00	1.401
71.5	0.00	1.051	251.00	11700.00	1.761
86.0	0.00	1.200	127.00	18500.00	2.011

BATCH FERMENTATION AT 28.0° C

TIME t (H)	SUCROSE S (G/L)	CELL CONC. X (G CELL DW/L)	INA ICE NUCLEI/L (X 10^3) K(θ)	CELL COUNT (CFU/ ML X 10^6)	O.D. (600 NM)
0.0	5.2	.0610	0.0001	1.33	0.018
6.0	4.8	.0125	0.0001	6.00	0.018
10.0	5.2	.0400	0.0028	1.33	0.014
17.0	5.4	.0600	.00473	5.33	0.018
22.0	5.4	.0210	.00160	25.00	0.018
26.0	5.4	.0600	.00370	50.00	0.022
33.0	5.5	.0800	4.933	80.00	0.027
41.0	4.6	.1000	58.805	60.00	0.062
47.0	3.3	.2342	212.96	866.00	0.186
52.0	2.6	.3819	193.42	5533.00	0.497
57.0	0.5	.7288	850.51	1500.00	1.151
66.0	0.0	1.2325	1856.52	5800.00	2.021
73.0	0.0	1.2414	743.48	55000.00	2.229

BATCH FERMENTATION AT 35.0° C

TIME t (H)	SUCROSE S (G/L)	CELL CONC. X (G CELL DW/L)	INA ICE NUCLEI/L ($X 10^{3}$) K(θ)	CELL COUNT (CFU/ ML $X 10^{6}$)	O.D. (600 NM)
2.5	5.0	0.1250	0.22	10.0	0.074
6.0	5.1	0.0570	1.07	172.0	0.104
10.5	4.1	0.0869	5.53	581.0	0.177
16.0	4.5	0.1205	23.96	1230.0	0.285
20.0	3.6	0.1747	21.60	2030.0	0.410
23.5	4.0	0.3536	21.60	3190.0	0.576
28.0	3.2	0.4094	71.09	5050.0	0.814
35.0	2.5	0.6591	84.30	10500.0	1.387
40.0	1.6	0.8854	897.90	13700.0	1.676
44.5	0.3	1.3831	101.46	15700.0	1.840
52.0	0.0	1.297	35.36	18100.0	2.028
64.0	0.0	1.241	26.69	17000.0	1.948

EFFECT OF TEMPERATURE ON THE MAXIMUM SPECIFIC GROWTH RATE OF Pseudomonas syringae cit7

Growth temperature, T (° C)	Maximum specific growth rate, μ_{max}	LN μ_{MAX}	1/T
5.5	0.0355	-3.338	0.1818
10.0	0.0431	-3.144	0.1
15.0	0.0777	-2.555	0.0667
20.0	0.0808	-2.516	0.05
25.0	0.1303	-2.038	0.04
28.0	0.1825	-1.701	0.036
35.0	0.0980	-2.323	0.028

RESULTS OF CONTINUOUS FERMENTATION

PUMP SETTING	FLOW-RATE (ML/H)	DILUTION RATE (H^{-1})	SUCROSE CONC. (G/L)	CELL CONC. (G/L)	ICE NUCLEI PER G CELL DW
4	16.155	0.0161	0.28	0.8400	5.49×10^6
9	36.946	0.0369	0.17	0.8947	5.68×10^6
13	53.579	0.0535	0.53	0.7835	5.21×10^6
16	66.054	0.0660	1.39	0.5428	3.07×10^5
18	74.370	0.0743	4.61	0.5161	1.58×10^6
20	82.687	0.0826	4.80	0.2823	1.53×10^5
22	91.002	0.0910	4.92	0.1985	9.80×10^3

CELL AND ICE NUCLEI PRODUCTIVITY UNDER CONTINUOUS FLOW CONDITIONS

DILUTION RATE, H^{1}	CELL PRODUCTIVITY, (G CELL/H-L)	INA PRODUCTIVITY, (ICE NUCLEI/H-L)
0.0161	0.0135	8.84×10^{4}
0.0369	0.0330	2.09×10^{5}
0.0535	0.0419	2.78×10^{5}
0.0660	0.0358	2.03×10^{4}
0.0743	0.0383	1.17×10^{5}
0.0826	0.0233	1.26×10^{4}
0.0910	0.0181	8.92×10^{2}

BATCH FERMENTATION IN THE 15 L BIOREACTOR

TIME (H)	SUCROSE REMAINING (G/L)	CELL CONCENTRATION (G DW/L)	INA (ICE NUCLEI/L)	CELL COUNT (CFU/ML)	FLUORO - SCENCE UNITS	O.D. (600 NM)
0.0	5.0	0.005	1.52×10^{2}	8.0×10^{6}	375.34	0.070
8.0	4.9	0.1897	1.47×10^{2}	2.67×10^{7}	365.80	0.057
25.0	4.75	0.1833	1.72×10^{3}	4.60×10^{7}	367.30	0.455
31.0	4.68	0.800	1.47×10^{4}	1.03×10^{8}	385.88	0.844
35.0	4.64	0.7267	1.5×10^{5}	2.30×10^{8}	427.05	1.215
48.0	3.39	0.0848	4.16×10^{5}	4.90×10^{8}	1120.20	2.295
55.0	2.69	0.65	4.56×10^{5}	3.30×10^{8}	906.04	2.293
75.0	0.0	1.196	5.29×10^{6}	8.0×10^{8}	1200.76	2.205
82.5	0.0	1.240	6.27×10^{6}	1.23×10^{9}	1276.57	2.200

APPENDIX E

PHOTOGRAPHIC PLATES

Plate E-1. Photograph of the 1 L Bioreactor Used

Plate E-2. Photograph of the Bioreactor Set up for Continuous Operation

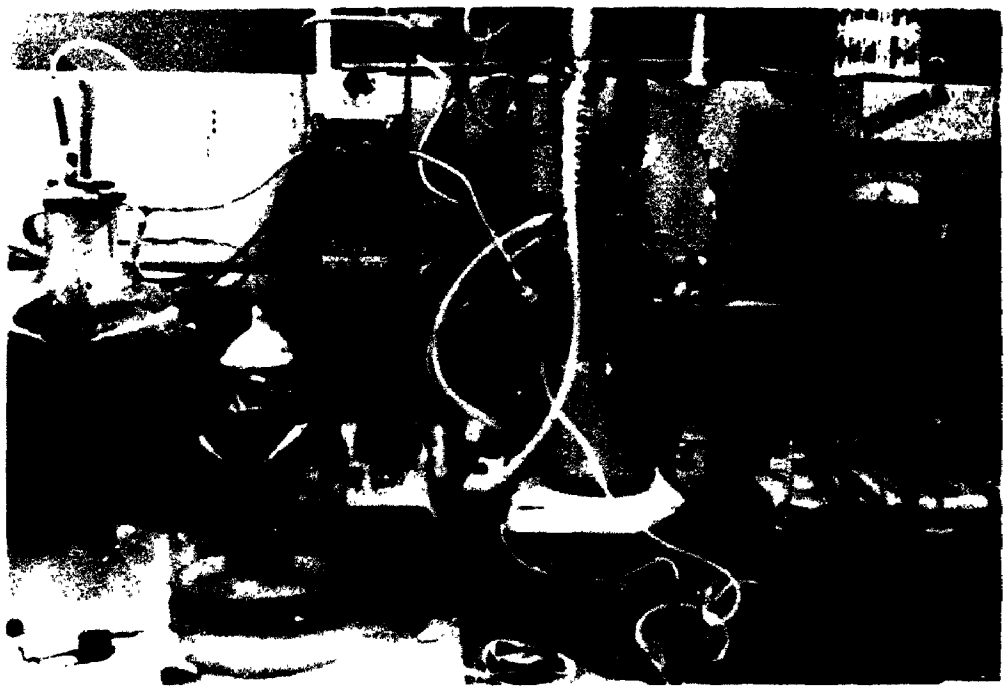

Plate E-3. Pseudomonas syringae on a Microscopic Slide (X 1500 Magnification) using Oil-Immersion Lens